Three-Body Hadron Dynamics from Lattice QCD: A Non-Relativistic Effective Field Theory Approach

Dissertation
zur
Erlangung des Doktorgrades (Dr. rer. nat.)
der
Mathematisch-Naturwissenschaftlichen Fakultät
der
Rheinischen Friedrich-Wilhelms-Universität Bonn

von
Fabian Müller
aus
Köln

Bonn, 2024

Angefertigt mit Genehmigung der Mathematisch-Naturwissenschaftlichen Fakultät der Rheinischen Friedrich-Wilhelms-Universität Bonn

Gutachter / Betreuer:	PD Dr. Akaki Rusetsky
Gutachter:	Prof. Dr. Dr. h. c. Ulf-G. Meißner
Tag der Promotion:	03.09.2024
Erscheinungsjahr:	2024

Abstract

Presently, lattice quantum chromodynamics is the only available tool that allows for the calculation of hadron properties in terms of their constituents, quarks and gluons, incorporating the non-perturbative nature of the strong interaction in the low-energy regime. However, information about few-hadron dynamics is not directly accessible. Instead, the finite-volume energy spectra, determined in lattice calculations, have to be related to the infinite-volume scattering- and decay-amplitudes.

In this thesis, by application of non-relativistic effective field theory techniques, methods for the analysis of data from lattice quantum chromodynamics are developed that allow for the extraction of three-body scattering- and decay properties. The fundamental concepts of lattice quantum chromodynamics, focusing on the methods of hadron spectroscopy, are outlined. The framework of non-relativistic effective field theories is introduced and the role of relativistic invariance is discussed.

A relation between finite volume decay matrix elements and infinite volume decay amplitudes is derived at the leading order in the non-relativistic effective field theory power counting for the weak decay of a scalar particle into three identical likewise scalar particles. This equation establishes a generalization of the Lellouch-Lüscher formalism to the three-body sector.

Furthermore, a novel formulation of the non-relativistic effective field theory formalism is suggested, which is devoid of some shortcomings of the existing approaches related to the explicit non-covariance of the three-particle propagator. The three-particle quantization condition, relating the finite-volume energy spectra to the infinite-volume scattering matrix elements, is written down in a manifestly relativistic-invariant form within this modified formalism, such that data from different moving frames can be combined in a global analysis.

Finally, the three-body analog of the Lellouch-Lüscher equation is generalized to higher orders and the systematic inclusion of higher partial waves is discussed. In contrast to the leading order expression derived in an earlier chapter, it is expressed in a manifestly relativistic-invariant form. This setup is of particular importance, since in practice the extraction of weak decay amplitudes from lattice calculations requires the inclusion of data from different moving frames.

List of Publications

This thesis contains three chapters that are based on the following articles that have been published in peer-reviewed journals:

- F. Müller and A. Rusetsky, *On the three-particle analog of the Lellouch-Lüscher formula*, JHEP **03** (2021) 152, arXiv: 2012.13957 [hep-lat]
- F. Müller, J.-Y. Pang, A. Rusetsky and J.-J. Wu, *Relativistic-invariant formulation of the NREFT three-particle quantization condition*, JHEP **02** (2022) 158, arXiv: 2110.09351 [hep-lat]
- F. Müller, J.-Y. Pang, A. Rusetsky and J.-J. Wu, *Three-particle Lellouch-Lüscher formalism in moving frames*, JHEP **02** (2023) 214, arXiv: 2211.10126 [hep-lat]

In addition, the following articles have been published in peer-reviewed journals during the research project:

- F. Müller, T. Yu and A. Rusetsky, *Finite-volume energy shift of the three-pion ground state*, Phys. Rev. D **103**.5 (2021) 054506, arXiv: 2011.14178 [hep-lat]
- J.-Y. Pang, M. Ebert, H.-W. Hammer, F. Müller, A. Rusetsky and J.-J. Wu, *Spurious poles in a finite volume*, JHEP **07** (2022) 019, arXiv: 2204.04807 [hep-lat]
- R. Bubna, F. Müller and A. Rusetsky, *Finite-volume energy shift of the three-nucleon ground state*, Phys. Rev. D **108**.1 (2023) 014518, arXiv: 2304.13635 [hep-lat]

Furthermore, the following article has been published recently on the arXiv preprint server:

- J.-Y. Pang, R. Bubna, F. Müller, A. Rusetsky and J.-J. Wu, *Lellouch-Lüscher factor for the $K \to 3\pi$ decays*, (2023), arXiv: 2312.04391 [hep-lat]

Finally, the following article is in preparation:

- R. Bubna, H.-W. Hammer, F. Müller, J.-Y. Pang, A. Rusetsky and J.-J. Wu, *Lüscher equation with the long-range forces*, (in preparation)

Contents

CHAPTER 1

Introduction

History of the Strong Interaction With the discovery that nuclei consist of protons and neutrons, the presence of a strong force was postulated, compensating the electromagnetic repulsion and allowing the formation of bound states. Experiments in the 1950s revealed a variety of particles subject to the strong interaction, called *hadrons*. Due to the sheer amount of newly discovered particles, not all of these could be fundamental. In the *Eightfold Way*, Ne'eman and Gell-Mann [9, 10] systematically organized hadrons, having similar properties such as mass, in groups. The emerging patterns resembled the representations of an underlying approximate SU(3) symmetry. Considering the breaking of this symmetry perturbatively the mass splitting in the multiplets [10, 11] could be explained. This led to the prediction of the mass of the, up-to-then, unknown Ω^--particle, which was confirmed a fey years after [12].

In 1964 Gell-Mann [13] and Zweig [14] proposed the existence of spin-1/2 constituent particles occurring in three flavors, the *quarks*. The observed baryons, hadrons of half-integer spin, are described as bound states of three quarks, while mesons, the bosonic hadrons, are formed by a quark-antiquark pair. However, the wave functions of some baryons, constructed within the quark constituent model, seemed to violate the spin-statistics theorem. For example, the wave function of the Ω^- baryon, composed out of three strange quarks with parallel spin, would be completely symmetric, in contradiction to the Pauli exclusion principle. The problem was resolved by introducing an additional SU(3) symmetry, such that the quarks occur in one of three states. This new quantum number was later referred to as *color*.

Although free quarks could never be observed directly, the deep inelastic scattering experiments of the late 1960s and early 1970s [15–17], probing the short-range structure of hadrons, provided an experimental evidence for their existence. The measured cross sections, compared to the Mott cross section, display an approximate *scale invariance*, i.e. do not depend on the transferred momentum. As pointed out by Bjorken [18], this feature should be observed if the nucleons contain point-like particles. Further analysis confirmed that these constituents carry the postulated spin of the quarks [19], as well as their fractional charge [20]. On the other hand, the experiments could rule out a simple three-quark model of the proton, but showed consistency with more elaborate models [21], including a "sea" of quark-antiquark pairs and neutral *gluons* that mediate the force.

In 1973, Politzer [22] and independently Gross and Wilczek [23], demonstrated that Yang-Mills theories obey *asymptotic freedom*, causing the interaction to become weaker at higher energies and leading to a scaling behavior consistent with the deep inelastic scattering experiments. Fritzsch,

Leutwyler and Gell-Mann considered this as an argument in favor of describing the strong interactions by promoting the SU(3)-color group to a non-abelian gauge symmetry [24], a concept that has already been discussed earlier by Han and Nambu [25, 26]. This theory, referred to as *Quantum Chromodynamics* (QCD), became an essential component of the Standard Model. QCD exhibits a fundamental difference to the electroweak theory, as its degrees of freedom, quarks and gluons, are not present in the observable spectrum. They are subject to *color confinement*, the phenomenon that color-charged particles can not be isolated. Nevertheless, using the fact that the strong coupling constant α_s is small at high energies allows for application of perturbative techniques. This provides a rich testing ground for QCD. Several experiments quantitatively support QCD as underlying field theoretic description of the strong interactions [27].

However, in the infrared regime, i.e. at low energies, the coupling strength increases such that perturbation theory is not reliable anymore. In order to gain access to a description of processes at the hadronic scale, where perturbation theory breaks down, alternative techniques are required. This thesis will focus on two of these methods: the formulation of *Effective Field Theories* (EFTs) and *Lattice QCD* (LQCD). Within the scope of this thesis, a EFT framework will be established, that allows for the interpretation of LQCD data in the three-particle sector. In particular, a formalism will be derived that enables to determine three-body decay amplitudes from LQCD transition matrix elements.

Lattice Quantum Chromodynamics Lattice QCD is a non-perturbative approach, based on the path integral formulation of QCD in finite, discretized Euclidean space-time. In its simplest realization this space-time lattice is a (four-dimensional) hypercube of length L and spacing a, the distance between neighboring lattice sites. This discretization naturally introduces an ultraviolet (UV) cutoff $\Lambda \sim 1/a$, while the finite volume leads to a quantization of momenta. Thus the path integral indeed reduces to a finite-, but tremendously high-dimensional usual integral, rendering an explicit evaluation impossible. Instead, correlation functions are calculated using numerical methods, such as *Markov chain Monte Carlo*, generating samples of (gauge) field configurations according to the probability distribution determined by the path integral.

Establishing a relation of these correlators, contaminated by discretization and other artifacts, to real continuum QCD observables is a highly non-trivial task. Essentially, three limits have to be taken: the continuum limit, $a \to 0$, the thermodynamic limit, $L \to \infty$, as well as an extrapolation to physical quark masses. In order to reduce computational cost, lattice calculations are often performed at much higher than physical quark masses. Although at present LQCD calculations are practicable at physical quark masses also in the multi-particle sectors [28, 29], simulations beyond the physical point, performing the chiral extrapolation subsequently, might remain beneficial in certain cases as discussed in [30].

Although hadron masses, space-like form factors and similar observables can be obtained straightforwardly, the extraction of scattering information from LQCD turns out to be rather obscure at a first glance. For example, while scattering amplitudes acquire a non-zero imaginary part above threshold, correlation functions calculated in Euclidean space-time are entirely real. Indeed, as proven by Maiani and Testa [31], in general it is not possible to simply recover on-shell amplitudes, defined in Minkowski-space-time, from infinite-volume Euclidean space-time correlation functions, which are dominated by off-shell contributions. Nevertheless, LQCD still provides access to physical scattering amplitudes. It turns out, that the volume dependence of the correlation functions does not only

represent an unpleasant relic of lattice regularization, but rather a key to the extraction of scattering properties. As shown by Lüscher [32, 33], the finite-volume dependence of the two-particle spectrum, obtained from the four point correlation function, encodes information of the infinite-volume scattering amplitude. The method developed by Lüscher allows for the a direct calculation of the scattering phase shift from two-particle energy levels in the finite volume. With subsequent generalizations to moving frame [34, 35], non-identical particles with spin [36–38] and coupled channel interactions [39–42] this method developed into a well established formalism that has been extensively applied to various systems, see the following reviews [43, 44].

Lüscher and Lellouch [45], further extended this formalism in order to relate two-particle weak decay amplitudes to the corresponding finite-volume transition matrix elements, obtained from lattice calculations (see also [35, 41, 46–48] for generalizations). Finally, with the inclusion of external currents [47–54], the two-particle sector is well understood.

The results above rely on the fact that, utilizing unitarity, a closed form of the two-particle scattering amplitude can be found. On the contrary, in the three-particle sector, such a remarkable simple relation between spectra and observables is not to be expected. Nevertheless, after it was shown that also the finite-volume three-particle spectrum can be solely determined by S-matrix elements [55, 56], the last decade has seen a lot of progress in the derivation of an analog of Lüschers method in the three-body sector. Currently three different frameworks have been developed: the *Relativistic Field Theory* (RFT) [57, 58], *Finite Volume Unitarity* (FVU) [59] and *Non-relativistic Field Theory* (NREFT) [60, 61] approaches. Within all these conceptually equivalent formalism, a *quantization condition* is derived, allowing to fix certain parameters by a fit to the finite-volume spectrum in the three-particle sector. In return, infinite-volume observables can be calculated by solving pertinent integral equations using these parameters in a second step. Equivalence between these formalisms was shown in specific setups [61–64]. Both, the RFT and FVU quantization conditions have been applied to $\pi^+\pi^+\pi^+$-scattering from LQCD data [28, 65, 66]. The RFT formalism has been also applied to the $\pi\pi K$- and $KK\pi$-systems [67], while the FVU approach was used for the analysis of the KKK-system [29]. Furthermore, the pole position and branching ratio of the $a_1(1260)$ resonance has been determined using the FVU approach [68]. An empirical comparison of these two formalisms was carried in a study of lattice φ^4-theory, showing good agreement for various coupling strength [69].

The lack of applications of the NREFT formalism for the study of LQCD data in the three-body sector can be also traced back to the absence of explicit Lorentz-invariance. Preferably, data from various spectra that were measured with different values of total three-momentum each, referred to as different *moving frames*, should be analyzed together. In order to derive a quantization condition capable of performing a global fit to spectra in different moving frames, a Lorentz-invariant setup is required. Thus, a major aim of the research project, that has been partially summarized in this thesis, is the derivation of a Lorentz invariant formulation of the NREFT approach in the three-body sector.

However, it should be pointed out that rendering the quantization condition relativistically invariant is a subtle issue in all different formulations. The reason is that, in order to yield a relation to physical observables, infinite-volume amplitudes and their finite-volume counterparts, entering the quantization condition, must be on-shell. As a consequence, the integral equations for the amplitudes in the infinite volume and similarly the quantization condition are inherently three-dimensional. Obtaining an explicit Lorentz-invariant form thus requires additional effort. A solution to this problem was proposed in the RFT formalism and could be straightforwardly adapted. On the other hand, achieving manifest relativistic invariance in such a way is not unproblematic. As will be shown later, the modifications applied in this framework lead to a violation of unitarity in the infinite- and spurious energy levels in a

finite volume. Therefore, a different procedure has been developed during the research project that is free from these issues.

Furthermore, despite growing interest of studying electroweak three-particle decays on the lattice, an analog of the Lellouch-Lüscher formula has not been available for a long time. Another aim of the research project was to close this gap. Here, once again, a relativistic-invariant setup proves to be essential.

Effective Field Theory Effective Field Theories serve as an approximation of their underlying model in the low-energy regime. By utilizing the separation of low- and high-energy scales, EFTs only include those degrees of freedom which are relevant at the chosen scale. The short distance effects on the other hand are absorbed in the EFTs parameters, the *Low-Energy Constants* (LECs). Instead of quarks and gluons, effective theories of QCD are formulated in terms of baryons and mesons directly. An EFT contains all possible operators, constructed out of the fields corresponding to the relevant degrees of freedom, obeying the same symmetries as the underlying model. In principle, there is an infinite number of those terms, which seems to render actual calculations impossible. On the other hand, employing an ordering scheme, that identifies the relevance of the individual contributions, allows for an perturbative procedure, that can be improved systematically. This scheme is referred to as *power counting*. A pedagogical and comprehensive introduction into effective field theories can be found in [70].

Probably the most prominent example of an EFT for low-energy hadron dynamics is chiral perturbation theory (ChPT) [71–73]. It is constructed based on the global $\mathrm{SU}(N_f)_L \times \mathrm{SU}(N_f)_R$ chiral symmetry of QCD in the limit of vanishing N_f quark masses. Indeed the three lightest quarks are almost massless. The observed spectrum of hadrons on the other hand, implies that invariance under the subgroup of axial $\mathrm{SU}(N_f)_A$ transformations, is not realized in the QCD vacuum. This indicates spontaneous symmetry breaking of $\mathrm{SU}(N_f)_L \times \mathrm{SU}(N_f)_R \to \mathrm{SU}(N_f)_V$, noting that the $\mathrm{SU}(N_f)_V$ subgroup is protected by the Vafa-Witten theorem [74]. According to Goldstone's theorem [75, 76], there are eight massless pseudoscalar particles, corresponding to the number of broken generators, that can be identified with the low lying octet mesons. In reality, the lightest quark masses are small but non-zero. Chiral symmetry is approximate but explicitly broken, such that the Goldstone bosons acquire a mass, that can be related to the quark masses using the Gell-Mann-Oakes-Renner relation [77]. Chiral perturbation theory is formulated in terms of the Goldstone boson fields, such that the resulting Lagrangian obeys all symmetries of QCD, including the spontaneously broken chiral symmetry. Explicit breaking of chiral symmetry due to the nonzero quark masses can be systematically included in this approach. A general construction of effective Lagrangians in the presence of spontaneous symmetry breaking, based on group-theoretical consideration, was developed by Callan, Coleman, Wess and Zumino (CCWZ) [78, 79]. The momentum $p \sim M_\pi \sim 140\,\mathrm{MeV}$ of the low lying octet mesons provides a soft scale compared to $\Lambda_\chi \sim 1\,\mathrm{GeV}$, the scale of the next heavier hadrons. Expansion of observables in p/Λ_χ thus yields a reliable power counting scheme.

Nucleons can be straightforwardly included, following the construction by CCWZ. In contrary to the pure mesonic sector, a power counting scheme as described above is invalid, as the nucleon mass, which is of the order of the hard scale, appears explicitly. One approach to define an consistent power counting is given by heavy baryon ChPT [80, 81], where the nucleon momentum is split into a large, of the order of the nucleon mass, and small residual component. The components of the field, corresponding to the large momentum, are integrated out, while for the residual components one can

impose a power counting scheme in terms of the small momenta. A similar strategy was applied to render the NREFT formalism in the three-body sector Lorentz-invariant. Other approaches that solve the power counting problem are given by, e.g. the *infrared regularization* [82] and *extended on-mass-shell scheme* [83, 84].

Chiral perturbation theory also plays an important role in the analysis of LQCD data. As pointed out above, results of lattice calculations can not directly be related to real QCD observables due to finite volume and lattice spacing effects, as well as unphysical large quark masses. As the quark masses represent input parameters of ChPT, it allows to study the pion mass dependence of observables[1]. Thus ChPT serves as a framework in order to study the chiral extrapolation to physical quark masses in LQCD. This is only true naively as ChPT is formulated in the continuum limit. On the other hand, it is possible to account for non-zero lattice spacing effects using modified version of ChPT [85–87]. Moreover, also volume dependence can be studied [88–90]. In return, the parameters in the chiral Lagrangian, can be extracted by fitting to lattice data, see Ref. [91] for a review of recent results.

Studying nuclear processes with all external momenta well below the mass of the pion, it is advantageous to consider an EFT without pions. In this regime the nucleon can be treated non-relativistically. Guided by the proposal of obtaining nuclear forces from chiral Lagrangians [92, 93], non-relativistic pionless EFTs have been elaborated that describe nucleon-nucleon scattering [94–96]. A major advantage of non-relativistic EFTs is that the contributions to the four-point function can be summed up to all orders, such that one arrives at a closed form for the scattering amplitude. This allows for an direct matching of the low-energy constants to the effective range expansion parameters, which are physical observables.

The framework was subsequently extended to the study of three-nucleon and -boson systems [97–100] and allowed for a quantitative description of neutron-deuteron scattering. An analysis of the volume dependence of the three-body bound state spectrum was carried out in [101–104] by solving the scattering equations, obtained in the EFT formalism, numerically. These studies paved the way for the NREFT approach to the three-particle quantization condition.

Outline This thesis is devoted to a development of a systematic approach to analyze LQCD data in the three-particle sector, based on the use of NREFT methods. In particular the relativistic invariance of the NREFT is addressed. An important result is the derivation of a three-body analog of the relativistic-invariant Lellouch-Lüscher equation.

The thesis is organized as follows: Chapter 2 and 3 provide a short introduction into the methods of LQCD and the NREFT formalism. Here the role of relativistic invariance will be discussed in detail. In Chapter 4 a three-body analog of the Lellouch-Lüscher formalism, restricted to the rest frame, is derived within the covariant NREFT framework at the leading order. Chapter 5 pays special attention to the relativistic-invariance of the NREFT quantization condition. A modified version is established that is valid in moving frames. Chapter 6 represents a generalization of the relativist-invariant NREFT quantization condition to arbitrary partial waves. Lorentz invariance is proven explicitly. Finally a three-body analog of the Lellouch-Lüscher formula in moving frames is derived.

[1] Note that the the quark masses can not be tuned arbitrary large as the applicability of ChPT has to be guaranteed.

CHAPTER 2

Lattice Quantum Chromodynamics

In this chapter the features of quantum chromodynamics will be discussed. Outlining the necessity of a non-perturbative treatment, the basic concepts of lattice quantum chromodynamics will be presented. Special attention will be paid to *hadron spectroscopy*, the framework to extract physical properties of hadrons from LQCD. While it turns out to be quite simple to determine quantities of stable particles, accessing scattering and resonance properties represents a non-trivial task. Therefore a major part of this chapter will focus on the relation between the finite-volume two-body energy spectra, measured in LQCD and infinite-volume S-matrix elements. The generalization to the three-body sector is discussed briefly.

2.1 Continuum QCD

Quantum Chromodynamics is a quantum field theoretical description of the strong interaction in terms of quarks and gluons. It is formulated as a SU(3)-gauge theory, defined by the Lagrangian[1]

$$\mathcal{L}_{\mathrm{QCD}} = -\frac{1}{2g^2}\,\mathrm{Tr}\left[F_{\mu\nu}F^{\mu\nu}\right] + \sum_f \bar{\psi}_f \left(\mathrm{i}\gamma^\mu D_\mu - m_f\right)\psi_f\,, \tag{2.1}$$

where the spinors $\psi_f(x)$ represent the quark fields, that couple to the gluon field $A_\mu(x)$ via the gauge-covariant derivative

$$D_\mu = \partial_\mu + \mathrm{i}A_\mu\,. \tag{2.2}$$

Furthermore, $F_{\mu\nu}$ is the field strength tensor of the gluon field:

$$F_{\mu\nu} = \partial_\mu A_\nu - \partial_\nu A_\mu + \mathrm{i}[A_\mu, A_\nu]\,. \tag{2.3}$$

While for each flavor $f = 1, \ldots, N$, the quark field consists of a SU(3) triplet, with charges referred to as *colors*, the gluon field transforms according to the adjoint representation. The Lagrangian is

[1] The Lagrangian displayed here does not contain the θ-term and gauge-fixing terms, which are not relevant for the following discussion.

invariant under local SU(3) gauge-transformations of the fields:

$$\begin{aligned}\psi(x) &\to \psi'(x) = \Omega(x)\psi(x),\\ \bar{\psi}(x) &\to \bar{\psi}'(x) = \bar{\psi}(x)\Omega^{\dagger}(x),\\ A_\mu(x) &\to A'_\mu(x) = \Omega(x)A_\mu(x)\Omega^{\dagger}(x) + \mathrm{i}(\partial_\mu\Omega(x))\Omega^{\dagger}(x),\end{aligned} \tag{2.4}$$

where $\Omega(x) \in \mathrm{SU}(3)$.

For vanishing quark masses $m_f = 0$, $f = 1, \ldots, N$, the Lagrangian contains a single dimensionless parameter, the strong coupling g or equivalently $\alpha_s = g^2/4\pi$. On the other hand, the *renormalization* procedure required to remove ultraviolet divergences arising from loop integrals in the perturbative expansion, introduces an artificial scale μ. As a consequence, physical observables, calculated in perturbation theory, explicitly depend on the renormalization scale μ. Consider a dimensionless observable $\mathcal{R}$, describing a process at some energy scale Q. By dimensional analysis, $\mathcal{R} \equiv \mathcal{R}(Q^2/\mu^2, \alpha_s)$ only depends on the ratio Q^2/μ^2 and the dimensionless quantity α_s. As the renormalization scale was added by hand, $\mathcal{R}$ indeed must be independed of μ. Thus, the coupling must be scale dependent, such that the explicit μ-dependence of $\mathcal{R}$ gets canceled:

$$0 = \mu\frac{d}{d\mu}\mathcal{R}(Q^2/\mu^2, \alpha_s) = \left(\mu\frac{\partial}{\partial\mu} + \mu\frac{d\alpha_s}{d\mu}\frac{\partial}{\partial\alpha_s}\right)\mathcal{R}(Q^2/\mu^2, \alpha_s)\,. \tag{2.5}$$

This scale dependence of the *running coupling* $\alpha_s(\mu)$ is described by the β-function which, at one-loop level, is given by [105]:

$$\mu\frac{d\alpha_s}{d\mu} = \beta(\alpha_s) = -\beta_0\frac{\alpha_s^2}{2\pi}, \quad \beta_0 = \left(\frac{11}{3}N_c - \frac{2}{3}N\right), \tag{2.6}$$

where $N_c = 3$ denotes the number of colors. For the observed number of quark flavors, $N = 6$, the β-function is negative, crucial for asymptotic freedom. Increasing the energy scale leads to a reduction of the coupling strength. Solving the differential equation above, and choosing $\mu = Q$, at the energy scale of the process considered:

$$\alpha_s(Q) = \frac{2\pi}{\beta_0 \ln(Q/\Lambda_{\mathrm{QCD}})}, \quad \Lambda_{\mathrm{QCD}} = \mu\exp\left(-\frac{1}{\beta_0}\frac{2\pi}{\alpha_s(\mu)}\right). \tag{2.7}$$

The quantity Λ_{QCD} introduced above is the *QCD scale*[2]. It describes the energy, at which the coupling diverges. The emergence of a intrinsic, dimensionful parameter from a scaleless theory is known as *dimensional transmutation*. Perturbation theory is only reliable at energies well above this scale[3]. Due to the non-perturbative nature of QCD in the low-energy regime, analytic access to properties of hadrons is very limited. However, lattice QCD provides an approach to study the low energy region directly from first principles of QCD.

Furthermore QCD is subject to color confinement. Quarks and gluons are not observed as isolated particles, but rather form color neutral bound states, the hadrons. This is in contrast to the electroweak

[2] Note that Λ_{QCD} is indeed scale independent.

[3] The value of Λ_{QCD} is depending on the renormalization scheme and the number of quarks. In the $\overline{\mathrm{MS}}$-scheme for $N = 3$ one finds $\Lambda_{\mathrm{QCD}} = (332 \pm 17)\,\mathrm{MeV}$ [105]

interaction, where leptons and gauge-bosons represent the fundamental degrees of freedom which appear in the measurable spectrum at the same time.

As can be seen from the Lagrangian, QCD possesses a global $\mathrm{SU}(N_f)$ flavor symmetry if the masses of a certain group of quarks is equal, $m_f = m$ for $f = 1, \ldots, N_f$. That is, the Lagrangian is invariant under the transformation

$$\psi = (\psi_1, \ldots, \psi_{N_f})^T\,, \quad \psi \to U\psi\,, \quad U \in \mathrm{SU}(N_f)\,. \tag{2.8}$$

In nature the masses of u- and d-quark are close to zero[4], such that an approximate SU(2) symmetry, referred to as *isospin symmetry*, emerges. Despite the complicated nature of the interaction of quarks and gluons, this symmetry should be inherited to the hadronic level. The observed hadronic spectrum should be classifiable by irreducible representations (irreps) of the isospin symmetry group. Furthermore, one may also include the s-quark as it is much lighter than the typical scale of hadronic masses enlarging the symmetry group to SU(3). Indeed such a classification in terms of SU(3) multiplets turned out to be successful, actually predating the formulation of the strong interactions in terms of QCD as described in the introductory part. Moreover, predictions of scattering properties, such as ratios of cross sections, using these symmetry arguments are in a good agreement with experiments. Including isospin-breaking effects, the Gell-Mann-Okubo formula [10, 11] explains the mass splitting of hadrons within a multiplet and reproduces the measured values on the percentage level.

Another important property of QCD is the invariance under a global *chiral symmetry* in case of massless quarks. Organizing the N quarks in a field $\psi = (\psi_1, \ldots, \psi_N)^T$ and decomposing into left- and right-handed components

$$\psi_{L/R} = P_{L/R}\psi\,, \quad P_{L/R} = \frac{1}{2}(1 \mp \gamma_5), \quad P_{L/R}^2 = P_{L/R}\,, \quad P_L + P_R = 1\,, \tag{2.9}$$

the fermionic Lagrangian can be rewritten as:

$$\mathcal{L}_f = \bar{\psi}_L \left(\mathrm{i}\gamma^\mu D_\mu\right)\psi_L + \bar{\psi}_R \left(\mathrm{i}\gamma^\mu D_\mu\right)\psi_R - \bar{\psi}_L\, M\, \psi_R - \bar{\psi}_R\, M\, \psi_L\,, \tag{2.10}$$

where $M = \mathrm{diag}(m_1, \ldots, m_N)$ is the quark mass matrix. For N_f vanishing quark masses, the Lagrangian is invariant under a global $\mathrm{U}_L(N_f) \times \mathrm{U}_R(N_f)$ symmetry:

$$\psi_{L/R} \to g_{L/R}\psi_{L/R}\,, \quad g_{L/R} \in \mathrm{U}_{L/R}(N_f)\,. \tag{2.11}$$

This seems to be a reasonable assumption for the $u-$, $d-$ and $s-$quarks, such that $N_f = 3$ in nature. The corresponding left- and right-handed currents might be decomposed into axial- and vector-components. While the singlet vector current gives rise to the conservation of baryon number density, it can be shown that the conservation of the singlet axial current is violated by the axial anomaly. Moreover, the observed spectrum of hadrons implies that the non-singlet axial symmetry can not be realized on the ground state. Otherwise meson and baryon multiplets would come in pairs with opposite parity. Thus, QCD is subject to spontaneous symmetry breaking[5] $\mathrm{SU}(N_f)_L \times \mathrm{SU}(N_f)_R \to \mathrm{SU}(N_f)_V$,

[4] As compared to the mass scale of hadrons, which, in the chiral limit $m_f \to 0$ is determined solely by Λ_{QCD}.

[5] The $\mathrm{SU}(N_f)_V$ subgroup is protected by the Vafa-Witten theorem [74] under certain assumptions.

where the residual vector subgroup $SU(N_f)_V$ corresponds to the flavor symmetry discussed in the preceding paragraph. This process results in the appearance of $N_f^2 - 1$ massless Goldstone modes. In nature these can be identified with the members of the lightest meson octet, pions, kaons and the eta-particle. Due to the explicit symmetry breaking effects of non-zero quark masses, these pseudo Goldstone bosons do not remain massless. The construction of an effective field theory in terms of these particles, also coupling to other hadrons and sources, is known as chiral perturbation theory and serves as a low-energy description of QCD dynamics for hadrons.

Since spontaneous symmetry breaking requires a non-perturbative treatment, this once again indicates that lattice methods are necessary for a description of hadronic interaction in terms of its fundamental components, quarks and gluons. However, it should be pointed out that in contrast to the long-ranged nature of the interaction between quarks and gluons, the interaction of hadrons, the nuclear force, is naturally short-ranged. Qualitatively, the reason is that hadrons are colorless bound states, preventing them to couple via the strong force of quarks and gluons at large separations. Only in close proximity, at the scale of a few femtometer, a residual effect of the interacting quarks and gluons can be observed. This is in analogy to van der Waals forces that emerge between neutral atoms or molecules via interactions of their charged constituents.

As pointed out above, in order to study QCD in terms of its fundamental building blocks, a non-perturbative treatment such as lattice QCD is required. Lattice QCD is based on the path integral formulation of QCD. After performing analytic continuation to Euclidean space-time by a Wick rotation, within this approach vacuum expectation values of operators O are calculated according to

$$\langle O \rangle = \frac{1}{Z} \int \mathcal{D}\psi \mathcal{D}\bar{\psi} \mathcal{D}A \, O[\psi, \bar{\psi}, A] \, \mathrm{e}^{-S_E[\psi,\bar{\psi},A]}, \quad Z = \int \mathcal{D}\psi \mathcal{D}\bar{\psi} \mathcal{D}A \, \mathrm{e}^{-S_E[\psi,\bar{\psi},A]} \tag{2.12}$$

where S_E is the Euclidean QCD action[6]:

$$S_E = \int d^4x \left\{ \frac{1}{2g^2} \mathrm{Tr}\left[F_{\mu\nu}(x) F_{\mu\nu}(x)\right] + \sum_f \bar{\psi}_f(x) \left(\gamma_\mu D_\mu + m_f\right) \psi_f(x) \right\} . \tag{2.13}$$

In principle the reconstruction of physical observables by analytical continuation of Euclidean correlation function, obtained form Eq. (2.12), back to Minkowski space is guaranteed [106, 107]. Indeed Eq. (2.12) is related to a stochastic process with probability weight factor $\exp\{-S_E\}$ and can be evaluated by numerical methods. Nevertheless, the path integral is ill-defined if no regularization is imposed. In the perturbative regime, the exponential is expanded in powers of the small coupling constant. The resulting functional integration leads to divergent loop integral which can be tamed, using *dimensional regularization* for example. Lattice regularization provides a different approach, which allows for the application of Monte Carlo methods. This scheme will be discussed in the following.

[6] For the sake of compact notation subscripts denoting Euclidean quantities are dropped. The Euclidean metric is given by $\delta_{\mu\nu} = \mathrm{diag}(1, 1, 1, 1)$, so that raising and lowering of indices is trivial. The gamma matrices obey the relation $\{\gamma_\mu, \gamma_\nu\} = 2\delta_{\mu\nu}$.

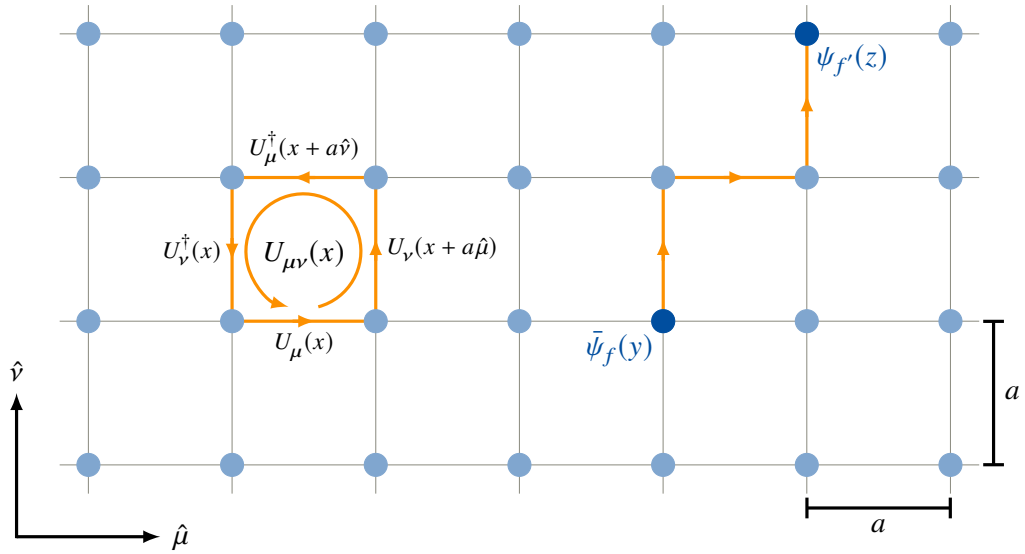

Figure 2.1: Plaquette operator $U_{\mu\nu}(x)$, as given in Eq. (2.22), and parallel transporter connecting the fermion fields $\bar{\psi}_f(y)$ and $\psi_f(z)$, Eq. (2.20), on a lattice with spacing a. The blue dots represent the lattice points, while the gray lines connect neighboring sites. The yellow arrows denote a link field in the directions defined by the unit vectors in the lower left corner.

2.2 Discretization of the Euclidean Path Integral

In lattice regularization the Euclidean space-time is usually discretized in a hypercubic lattice of spatial and temporal extend, $L = aN$ and $T = aN_T$ respectively. Here, a denotes the lattice spacing between neighboring sites which is considered to be the same in all directions for simplicity, while N and N_T denote the number of lattice sites in spatial and temporal directions, respectively. Also note that elongation of different spatial direction can be considered. On the other hand, when studying the effects of the finite spatial volume in the subsequent chapters, a uniform extent will be assumed. The set of lattice sites can then be written as

$$\Lambda = \left\{ x \in \mathbb{R}^4 \,\middle|\, x_\mu = a n_\mu \,, \quad n_\mu = 0, 1, \ldots, N_\mu - 1 \,, \quad \mu = 1, 2, 3, 4 \right\} , \tag{2.14}$$

where $N_4 \equiv N_T$ and $N_i \equiv N$ for $i = 1, 2, 3$. Quark fields ψ_f and $\bar{\psi}_f$ are placed only on these lattice sites and transform according to Eq. (2.4). The fields placed on the lattice are subject to a certain boundary condition. A common choice is given by periodic boundary conditions, where the endpoints of the lattice are identified, forming a 4-torus.

Maintaining gauge invariance is crucial when lattice regularization is used. Note that in the continuum theory, as the coordinates in color space are position dependent, the gauge field emerges necessarily. It accounts for the change of the inherently different gauge reference frames of fields $\psi_f(x)$ and $\psi_f(x + \varepsilon)$, with $\varepsilon \to 0$, when taking the derivative. In general, "comparing" quark fields at different space-time points, x and y, requires *parallel transport* of the field $\psi_f(x)$ to the gauge frame

at y along a path $\gamma_{x,y}$ connecting these two points:

$$\psi_f(y) = \Gamma(\gamma_{x,y})\psi_f(x), \quad \Gamma(\gamma_{x,y}) = P\exp\left(-\mathrm{i}\int_{\gamma_{x,y}} A\cdot ds\right). \tag{2.15}$$

Here $\Gamma \in \mathrm{SU}(3)$ is called *parallel transporter* and P denotes the path ordered product. With the transformation properties of the parallel transporter

$$\Gamma(\gamma_{x,y}) \to \Gamma'(\gamma_{x,y}) = \Omega(y)\Gamma(\gamma_{x,y})\Omega(x)^\dagger, \tag{2.16}$$

indeed the field $\psi_f(y) = \Gamma(\gamma_{x,y})\psi_f(x) \to \Omega(y)\psi_f(y)$ transforms according to a field located at y. As due to lattice regularization the notion of arbitrary close space-time points is abandoned, instead of gauge fields lattice QCD is formulated in terms of *link variables* $U_\mu(x)$ given as parallel transporter of neighboring sites in the direction of the unit vector $\hat{\mu}$:

$$U_\mu(x) = \Gamma(\gamma_{x+a\hat{\mu},x}) = P\exp\left(\mathrm{i}\int_0^a A(x+t\hat{\mu})dt\right). \tag{2.17}$$

According to Eq. (2.16) the link variables transform as

$$U_\mu(x) \to U'_\mu(x) = \Omega(x)U_\mu(x)\Omega(x+a\hat{\mu})^\dagger. \tag{2.18}$$

In lattice regularization the path integral measure reduces to a well-defined integration over a finite set of field variables

$$\int \mathcal{D}\psi\mathcal{D}\bar{\psi}\mathcal{D}A \to \int \prod_{x\in\Lambda} d\psi(x)\, d\bar{\psi}(x) \prod_\mu dU_\mu(x), \tag{2.19}$$

where dU denotes the invariant Haar-measure of SU(3). Since SU(3) is compact, integration over link variables $U_\mu(x) \in \mathrm{SU}(3)$ makes gauge fixing unnecessary when determining physical obervables.

2.2.1 Discretization of the Gauge Action

The remaining steps address the discretization of the Euclidean action. This is a rather non-trivial task as the use of link variables prevents a direct relation to the continuum version. The fundamental building blocks, used to assemble a lattice version of the QCD action, need to be gauge invariant. Due to the transformation properties of the gauge links and quark fields, there are only two distinct invariant quantities. The former consist out of gauge links connecting two quark fields, forming a lattice version of the gauge transporter:

$$\bar{\psi}_f(x_1)P_\gamma[U]\psi_{f'}(x_2) = \bar{\psi}_f(x_1)\left[\prod_{(y,\mu)\in\gamma} U_\mu(y)\right]\psi_{f'}(x_2), \tag{2.20}$$

where γ describes a path from x_2 to x_1. The latter is given by a trace over link variables along a closed loop:

$$L_\ell[U] = \mathrm{Tr}\left[\prod_{(y,\mu)\in\ell} U_\mu(y)\right], \tag{2.21}$$

where ℓ is a closed path. The simplest version of this quantity is the *plaquette*:

$$U_{\mu\nu}(x) = U_\mu(x)U_\nu(x+a\hat{\mu})U_\mu^\dagger(x+a\hat{\nu})U_\nu^\dagger(x)\,. \tag{2.22}$$

Schematically the plaquette, as well as the lattice version of the gauge transporter as defined in Eq. (2.20), are depicted in Fig. 2.1.

A suitable lattice version of the pure gauge part of the Euclidean action is given by [108]

$$S_G = -\frac{2}{g^2}\sum_{x\in\Lambda}\sum_{\mu<\nu}\mathrm{Re}\,\mathrm{Tr}\left[U_{\mu\nu}(x)\right]\,. \tag{2.23}$$

Inserting $U_\mu(x) = \exp(iaA_\mu(x))$, equivalent to Eq. (2.17) up to $O(a)$ (up to an irrelevant constant), the continuum action can be recovered when taking the limit $a \to 0$:[7]

$$S_G = \frac{a^4}{2g^2}\sum_{x\in\Lambda}\sum_{\mu,\nu}\mathrm{Tr}\left[F_{\mu\nu}(x)^2\right] + O(a^2) \quad \overset{a\to 0}{\longrightarrow} \quad \frac{1}{2g^2}\int d^4x\,\mathrm{Tr}\left[F_{\mu\nu}(x)^2\right]\,. \tag{2.24}$$

2.2.2 Fermions on the Lattice

In an naive approach, the fermionic action could be discretized according to

$$S_F = a^4\sum_{x\in\Lambda}\sum_f \bar{\psi}_f(x)\left(D[U]+m_f\right)\psi_f(x), \quad D[U] = \frac{1}{2}\gamma_\mu(\nabla_\mu+\nabla_\mu^*) \tag{2.25}$$

where ∇_μ and ∇_μ^* denote the covariant forward and backward difference operators respectively:

$$a\nabla_\mu\psi_f(x) = U_\mu(x)\psi_f(x+a\hat{\mu}) - \psi_f(x), \quad a\nabla_\mu^*\psi_f(x) = \psi_f(x) - U_\mu^\dagger(x-a\hat{\mu})\psi_f(x-a\hat{\mu})\,. \tag{2.26}$$

Indeed the continuum action is obtained up to discretization effects of $O(a^2)$. However this lattice action leads to an inflation of the number of quark states. These *doublers* appear as, due to periodicity, the lattice version of the free quark propagator has additional poles apart from the physical one. Fermion doubling inevitably arises in lattice regularization of theories that possess "continuum-like" chiral symmetry, if locality, translation invariance and hermiticity are imposed [109]. Removing the unphysical doublers one necessarily has to violate one of these assumptions. This leads to a variety of different formulations.

Wilson fermions [108] explicitly break chiral symmetry by adding an extra term to the naive action, that decouples the fermion doublers in the continuum limit. The Dirac operator in the naive

[7] Note that the left-hand side explicitly displays the sum over indices μ and ν, which is taken implicit on the right-hand side in the summation convention.

discretization is replaced with the Wilson-Dirac operator:

$$D[U] \longrightarrow D_W[U](x) = D[U] - a\frac{r}{2}\nabla_\mu^*\nabla_\mu\,, \tag{2.27}$$

where r is the Wilson parameter. While the physical pole in the propagator stays unaffected, the doublers acquire a mass of $2r/a$. In the continuum limit they become infinitely heavy, such that they decouple. Note that due to the extra term, discretization effects enter at $O(a)$.

Besides staggered fermions [110, 111], other prominent approaches are overlap [112, 113] and domain-wall discretization [114, 115]. In the latter two, the corresponding Dirac operator obeys the Ginsparg-Wilson relation

$$\{\gamma_5, D[U]\} = a\, D[U]\gamma_5 D[U]\,.$$

Chiral symmetry again is explicitly broken in order to evade fermion doubling. However, the relation implies the existence of a lattice version of chiral transformations [116] that reduce to the continuum symmetry in the limit $a \to 0$. Moreover the measure of Girnsparg-Wilson fermions explicitly breaks the lattice axial singlet transformation, resembling the axial anomaly.

2.2.3 Improved Action

As pointed out above, the lattice regularized action is subject to discretization effects. LQCD calculation thus require a continuum extrapolation, typically achieved by performing multiple simulations on lattices with decreasing spacing. In order to keep the volume constant, it is necessary to increase the number of lattice points, thus making calculations numerically expensive. On the other hand, the *Symanzik improvement program* [117, 118] provides a way to systematically reduce discretization effects.

In order to achieve the improvement one considers a continuum effective field theory of the lattice action. Here the inverse spacing naturally serves as a momentum cutoff. The operators entering the effective action are then multiplied by orders of powers of a according to their mass dimension. This yields a systematic way to organize the effective theory into powers of the lattice spacing. Adding suitable counterterms to the lattice action these correction terms can be canceled exactly, leading to an improvement in terms of the spacing. For an order $O(a)$ improvement of the Wilson fermion action S_W it is sufficient to add a single operator [119]:

$$S_{W'} = S_W + c_{\mathrm{sw}}a^5 \sum_{x\in\Lambda}\sum_{\mu<\nu}\sum_f \bar\psi_f(x)\frac{\sigma_{\mu\nu}}{2}\hat F_{\mu\nu}(x)\psi_f(x)\,, \tag{2.28}$$

where $\sigma_{\mu\nu} = -i[\gamma_\mu, \gamma_\nu]/2$ and $\hat F_{\mu\nu}(x)$ is defined in terms plaquettes as

$$\begin{aligned}\hat F_{\mu\nu}(x) &= -\frac{i}{8a^2}(Q_{\mu\nu}(x) - Q_{\nu\mu}(x))\,,\\ Q_{\mu\nu}(x) &= U_{\mu\nu}(x) + U_{\nu,-\mu}(x) + U_{-\mu,-\nu}(x) + U_{-\nu,\mu}(x)\,.\end{aligned} \tag{2.29}$$

The Sheikoleslami-Wohlert coefficient c_{sw} must be tuned appropriately [120–122].

Furthermore, an $O(a^2)$ improvement of the pure gluonic action can be achieved by adjusting S_G

according to [123–125]

$$S_{G'} = -\frac{2}{g^2}\sum_{x\in\Lambda}\left(b_0\sum_{\mu<\nu}\mathrm{Re\,Tr}\left[U_{\mu\nu}(x)\right] + b_1\sum_{\mu\neq\nu}\mathrm{Re\,Tr}\left[U^{1\times2}_{\mu\nu}(x)\right]\right). \tag{2.30}$$

Above $U^{1\times2}_{\mu\nu}(x)$ denotes a 1×2 loop in the μ and ν directions respectively, analogous to the definition of the plaquette. Explicit values of b_0 and b_1 can be found in, for example [123, 126]. While this procedure is already sufficient for an improvement of on-shell quantities, in general also interpolating operators have to be adjusted.

2.3 Hadron Spectroscopy

After having outlined the lattice regularization of QCD, the following section will focus on the extraction of physical properties of hadrons from LQCD. Access to observables is gained from calculating correlation functions of suitable *interpolating fields*, owing the quantum numbers of the hadrons of interest. For example, a choice of interpolators having non-zero overlap with the pion states is given by

$$\begin{aligned}\pi^+(x) &= \bar{d}(x)\gamma_5 u(x),\\ \pi^-(x) &= \bar{u}(x)\gamma_5 d(x),\\ \pi^0(x) &= \frac{1}{\sqrt{2}}\left(\bar{u}(x)\gamma_5 u(x) - \bar{d}(x)\gamma_5 d(x)\right),\end{aligned} \tag{2.31}$$

where $q(x) \equiv \psi_q(x)$ and $\bar{q}(x) \equiv \bar{\psi}_q(x)$ for quarks of flavor $f = q$ in favor of compact notion. Correlation functions are then calculated according to the lattice regularized version of Eq. (2.12). For $O \equiv O[\psi,\bar{\psi},U]$, applying Wick's theorem

$$\langle O\rangle = \frac{1}{Z}\int \mathcal{D}U\,\langle O\rangle_F[U]\,\mathrm{e}^{-S_G[U]}\det D[U], \quad Z = \int \mathcal{D}U\,\mathrm{e}^{-S_G[U]}\det D[U], \tag{2.32}$$

where $\det D[U] = \prod_f \det D_f[U]$ is the determinant of the lattice Dirac operator and $\mathcal{D}U = \prod_{x\in\Lambda}\prod_\mu dU_\mu(x)$ for abbreviation. Furthermore $\langle O\rangle_F$ denotes the Wick contraction of the operator O, which is the sum of all possible partitionings into pairs of quark- antiquark-fields with each pairing replaced by its corresponding Dirac propagator. Note that some of these partitionings might trivially vanish, as the Dirac propagator is diagonal in flavor space.

If $\det D[U] = \prod_f \det D_f[U] > 0$ is positive definite

$$dP[U] = \frac{1}{Z}\mathrm{e}^{-S_G[U]}\det D[U]\mathcal{D}U, \tag{2.33}$$

defines a probability measure and the integration in Eq. (2.32) can be performed using Monte Carlo methods. Expectation values are estimated by averaging over N independent samples

$$\langle O\rangle = \frac{1}{N}\sum_i^N \langle O\rangle_F[U_i] + O(N^{-1/2}), \tag{2.34}$$

Figure 2.2: Left: connected contribution to the π^+ two-point function. Right: disconnected contribution to the π^0 two-point function as in the third line of Eq. (2.38). The lines with arrows depict quark propagators.

where gauge configurations U_i are drawn according to the distribution defined by Eq. (2.33) using *importance sampling*. Modern LQCD calculations typically apply *Hybrid Monte Carlo* [127], which is a Markov chain Monte Carlo method that combines Hamiltonian dynamics with a subsequent Metropolis-Hastings accept-reject step [128, 129].

In hadron spectroscopy O usually is given by a product of hadron interpolators. For example, the mass of the positively charged pion, see section 2.3.1, can be obtained from the expectation value

$$\langle O_{\pi^+}(x,y)\rangle = \langle \pi^+(x)(\pi^+(y))^\dagger\rangle = \langle \pi^+(x)\pi^-(y)\rangle\,, \tag{2.35}$$

with interpolators given as in Eq. (2.31). Performing the Wick contractions

$$\langle O_{\pi^+}(x,y)\rangle_F[U] = -\mathrm{Tr}\left[\gamma_5 D_u^{-1}[U](x,y)\gamma_5 D_d^{-1}[U](y,x)\right]\,, \tag{2.36}$$

where $D_f^{-1}[U](x,y)$ is the quark propagator with flavor f, given by the inverse of the corresponding Dirac operator. If instead the expectation value

$$\langle O_{\pi^0}(x,y)\rangle = \langle \pi^0(x)(\pi^0(y))^\dagger\rangle \tag{2.37}$$

is considered, there exist more (non-trivial) contractions as O_{π^0} contains quarks and anti-quarks of the same flavor:

$$\begin{aligned}\langle O_{\pi^0}(x,y)\rangle_F[U] = &-\frac{1}{2}\mathrm{Tr}\left[\gamma_5 D_u^{-1}[U](x,y)\gamma_5 D_u^{-1}[U](y,x)\right]\\ &+\frac{1}{2}\mathrm{Tr}\left[\gamma_5 D_u^{-1}[U](x,x)\right]\mathrm{Tr}\left[\gamma_5 D_u^{-1}[U](y,y)\right]\\ &-\frac{1}{2}\mathrm{Tr}\left[\gamma_5 D_u^{-1}[U](x,x)\right]\mathrm{Tr}\left[\gamma_5 D_d^{-1}[U](y,y)\right] + u\leftrightarrow d\,.\end{aligned} \tag{2.38}$$

In contrast to the *connected contributions* in the first line, here additional types of contractions in the second and third line are referred to as *disconnected*, diagrammatically displayed in Fig. 2.2. Calculation of the latter typically demand much more numerical effort and higher statistics. On the other hand, in the isospin symmetric case $m_u = m_d$, the disconnected pieces in Eq. (2.38) cancel and the correlator reduces to that of the charged pions. This implies the degeneracy of the isospin triplet pion states. Nevertheless, the full spectrum of hadrons also include isospin singlet states such as the η meson that require the calculation of disconnected pieces even in the isospin limit.

2.3.1 Spectrum of Stable Hadrons

One of the most easily accessible quantities is the spectrum of stable hadrons, i.e. those that do not decay within the strong interactions. For $N_f = 3$, these include the light octet pseudoscalars π and K, the octet baryons N, Λ, Σ and Ξ as well as the Ω particle of the baryon decuplet. The masses of these particles can be obtained by considering two-point functions of the pertinent interpolating fields. With suitable interpolators O_h the correlator for the hadron h is given by, assuming $t > 0$:

$$C_h(t) = \frac{1}{L^3} \sum_{\mathbf{x}} \langle 0 | O_h(t, \mathbf{x}) O_h^\dagger(0, \mathbf{0}) | 0 \rangle \,. \tag{2.39}$$

Here and in the following a lattice with an infinite temporal extend, $T \to \infty$, is considered. Actual calculations on the other hand are performed at finite T. Imposing periodic boundary conditions this leads to pollution by *thermal states*[8] [130] that vanish in the limit $T \to \infty$.

Inserting a full set of eigenstates of the lattice Hamiltonian in the expression above and using translation invariance the correlation function is given by

$$C_h(t) = \sum_n \frac{Z_n}{2E_n(\mathbf{0})} \mathrm{e}^{-E_n(\mathbf{0})t} \,, \tag{2.40}$$

where $Z_n = |\langle 0 | O_h(\mathbf{0}, 0) | n \rangle|^2 \equiv |\langle 0 | O_h | n \rangle|^2$ is the probability that the state $|n\rangle$ is created by the operator O_h and $E_n(\mathbf{0})$ is the energy of this state with total momentum $\mathbf{p}_n = \mathbf{0}$. The stable hadron corresponds to the lightest state, denoted by $n = 0$, the interpolator has overlap with. Since $E_0 < E_1 < \ldots$, the contribution of exited states die out exponentially in time. In order to extract the mass of the hadron one defines the *effective mass*:

$$aM_{\mathrm{eff}}(t) = \log\left(\frac{C_h(t)}{C_h(t+a)}\right) , \tag{2.41}$$

reducing to the ground state energy for large values of time, $M_{\mathrm{eff}}(t) \to E_0(\mathbf{0})$ for $t \gg a$. Plotting $M_{\mathrm{eff}}(t)$ as a function of time, the mass of the stable hadron is obtained by a constant fit to the region where the data shows a plateau. The fit range, $[t_{\mathrm{min}}, t_{\mathrm{max}}]$, can be quite narrow mainly due to two effects. Usually t_{max} is limited by a low signal-to-noise ratio at large times [131, 132]. On the other hand, t_{min} is determined by the excited state contamination to the correlation function.

An improvement can be achieved if the interpolating fields are chosen such that the overlap to the ground state is maximized. Thus, in practice, rather than using the naive operators in Eq. (2.31) directly, *smearing* is applied to the quark fields. Here an average over spatially separated quarks is taken, intuitively corresponding to a more realistic spatial wave function. One of the most wildly used techniques is Gaussian or Jacobi smearing [133–135]. Moreover the noise can be reduced by smoothing the gauge configurations, typically subject to violent UV fluctuations. Prominent algorithms are provided by APE- [136], HYP- [137] and stout smearing [138].

In order to extract the energies of exited states a variational analysis can be deployed. In this

[8] In this case the expectation value in the correlator would not only contain the vacuum state $|0\rangle$ as in Eq. (2.39). Rather a sum over all lattice Hamiltonian eigenstates $|n\rangle$ has to be taken into account. Using the time evolution of the operator $O_h(t, \mathbf{x}) = \mathrm{e}^{-H(T-t)} O_h(0, \mathbf{x}) \mathrm{e}^{-Ht}$ the contribution of exited states $|n\rangle \neq |0\rangle$ vanishes as $\exp(-E_n(T-t))$ for $T \to \infty$. However, these thermal states can lead non-negligible artifacts in general (multi-particle) correlation functions.

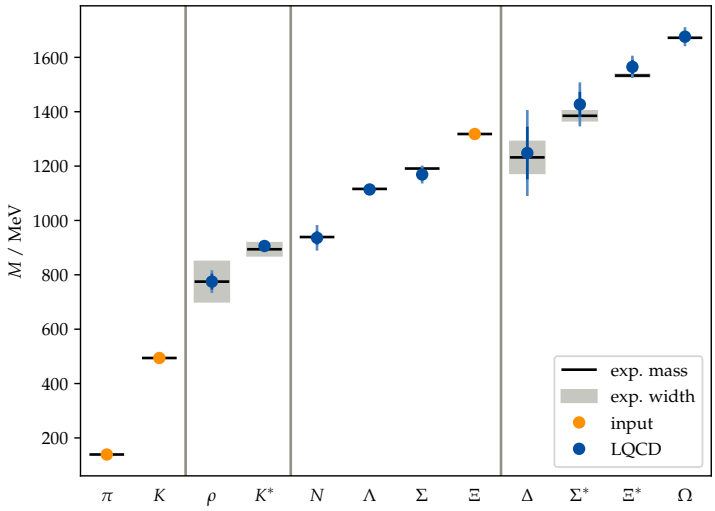

Figure 2.3: Masses of the light hadrons from LQCD compared to experimental values from [105]. Data (blue dots) is taken from [140], where dark and light blue bars denote statistical and systematic errors respectively. Yellow dots indicate the particles that were used as input. Black horizontal bars represent experimental values, with gray boxes specifying the width of resonances. Long gray vertical line separate different mutiplets.

approach a basis of different interpolators for the same hadron is constructed and the matrix of correlators is calculated. The energies can be determined by solving the generalized eigenvalue problem (GEVP) [139]: $C(t)\mathbf{v}_n = \lambda_n(t)C(t_0)\mathbf{v}_n$, where $C(t)$ denotes the correlator matrix and $\lambda_n(t) = \exp(-E_n t)(1 + O(\exp(-\Delta E_n t)))$ with $\Delta E_n = \min_{m\neq n}|E_n - E_m|$.

Fig. 2.3 shows the hadron spectrum obtained by the BMW collaboration [140] for $N_f = 2 + 1$ flavors, i.e. approximate physical strange quark and degenerate light quark masses extrapolated to the physical point of $M_\pi \approx 135\,\text{MeV}$. Simulations were performed using a stout averaged, Symanzik improved gauge action and Wilson fermions. Finite-volume effects to the stable hadron masses M, resulting from virtual pion exchange [141], were taken into account by fitting

$$M_L = M + \frac{c}{(M_\pi L)^{3/2}} \exp\left(-M_\pi L\right) \tag{2.42}$$

to the measured masses M_L, for three different box length L. In order to determine the masses of resonances, also displayed within the plot, a more elaborate formalism is needed, that will be discussed in the following section.

2.3.2 Two-Particle Scattering and Resonance Properties from Lattice QCD

The previous section showed that the masses of stable hadrons can be determined by a calculation of two-point functions on the lattice, extracting the lowest energy levels. As shown by Lüscher [32] their volume dependence is *regular*, i.e. coincides with the infinite-volume masses up to exponentially suppressed corrections. This method can be generalized in order to extract more complicated quantities

as long as the corresponding infinite-volume S-matrix elements contain a single particle in the in- and out states only. Prominent examples are the space-like electromagnetic form factors of various hadrons.

On the other hand, the method fails when applied to processes that involve more in- and outgoing particles, such as scattering. This statement is formulated in the Maiani-Testa no-go theorem, that was first proven in the context of time-like form factors [31] and will be outlined in the following paragraph with respect to two-particle scattering.

The Maiani-Testa No-Go Theorem

Considering the process $\pi^+(p_1)\pi^+(p_2) \to \pi^+(q_1)\pi^+(q_2)$ in infinite Euclidean space-time, the scattering amplitude is related to the four-point function

$$C_{\mathbf{p}_1,\mathbf{p}_2;\mathbf{q}_1,\mathbf{q}_2}(x_1^0, x_2^0; y_2^0, y_1^0) = \langle 0|\pi^+_{\mathbf{q}_1}(x_1^0)\pi^+_{\mathbf{q}_2}(x_2^0)\pi^-_{\mathbf{p}_2}(y_2^0)\pi^-_{\mathbf{p}_1}(y_1^0)|0\rangle\,, \tag{2.43}$$

where the limits $x_i^0 \to \infty$ and $y_i^0 \to -\infty$ are implicit assuming $x_1^0 \gg x_2^0$ and $y_1^0 \ll y_2^0$. The pion interpolators are momentum-projected according to

$$\pi^\pm_{\mathbf{k}}(x^0) = \int d^3\mathbf{x}\, \mathrm{e}^{\pm i\mathbf{k}\mathbf{x}}\, \pi^\pm(x^0, \mathbf{x})\,. \tag{2.44}$$

Taking the limits for x_1^0 and y_1^0 first, the correlation function is given by

$$C_{\mathbf{p}_1,\mathbf{p}_2;\mathbf{q}_1,\mathbf{q}_2}(x_1^0, x_2^0; y_2^0, y_1^0) = \frac{Z_\pi}{2E_\pi(\mathbf{p}_1)2E_\pi(\mathbf{q}_1)}\, \mathrm{e}^{-E_\pi(\mathbf{q}_1)x_1^0 + E_\pi(\mathbf{p}_1)y_1^0}\tilde{C}_{\mathbf{p}_1,\mathbf{p}_2;\mathbf{q}_1,\mathbf{q}_2}(x_2^0; y_2^0)\,, \tag{2.45}$$

where, with $|\mathbf{k}\rangle$ denoting a π^+-state with momentum $\mathbf{k}$,

$$\begin{aligned}\tilde{C}_{\mathbf{p}_1,\mathbf{p}_2;\mathbf{q}_1,\mathbf{q}_2}(x_2^0; y_2^0) &= \langle \mathbf{q}_1|\pi^+_{\mathbf{q}_2}(x_2^0)\pi^-_{\mathbf{p}_2}(y_2^0)|\mathbf{p}_1\rangle \\ &= \sum_{n,m} \frac{\langle \mathbf{q}_1|\pi^+_{\mathbf{q}_2}(0)|n;\mathrm{out}\rangle\langle m;\mathrm{in}|\pi^-_{\mathbf{p}_2}(0)|\mathbf{p}_1\rangle}{2E_n(\mathbf{Q}_n)2E_m(\mathbf{P}_m)}\, \mathrm{e}^{-(E_n(\mathbf{Q}_n)-E_\pi(\mathbf{q}_1))x_2^0}\, \mathrm{e}^{-(E_\pi(\mathbf{p}_1)-E_m(\mathbf{P}_m))y_2^0} \\ &\qquad \times (2\pi)^3\delta^3(\mathbf{q}_1+\mathbf{q}_2-\mathbf{Q}_n)(2\pi)^3\delta^3(\mathbf{p}_1+\mathbf{p}_2-\mathbf{P}_m)\,\langle n;\mathrm{out}|m;\mathrm{in}\rangle\,. \end{aligned} \tag{2.46}$$

Here full set of in- and out eigenstates have been inserted, according to the boundary conditions $x_2^0 \to \infty$ and $y_2^0 \to -\infty$. In Eq. (2.46) the matrix element $\langle n;\mathrm{out}|m;\mathrm{in}\rangle$ is the amplitude to be extracted. Now since $x_2^0 \to \infty$ and $y_2^0 \to -\infty$, the states with the lowest energy will dominate the sum. As can be read off from the matrix elements $\langle \mathbf{q}_1|\pi^+_{\mathbf{q}_2}(0)|n;\mathrm{out}\rangle$ and $\langle m;\mathrm{in}|\pi^-_{\mathbf{p}_2}(0)|\mathbf{p}_1\rangle$, these are the $\pi^+\pi^+$ states with total momenta $\mathbf{Q}_n = \mathbf{q}_1 + \mathbf{q}_2$ and $\mathbf{P}_m = \mathbf{p}_1 + \mathbf{p}_2$ respectively. For the sake of simplicity let $\mathbf{q}_1 + \mathbf{q}_2 = \mathbf{0} = \mathbf{p}_1 + \mathbf{p}_2$. While the energy of the in- and outgoing pion pairs considered in the scattering process is equal to $2E_\pi(\mathbf{p}_1)$, the lowest contributing intermediate states correspond to the two-pion states at rest, $E_n(\mathbf{Q}_n) = E_m(\mathbf{P}_m) = 2M_\pi$. Thus, the correlation function is dominated by matrix elements, $\langle n;\mathrm{out}|m;\mathrm{in}\rangle$, that do not correspond to the on-shell scattering process. Only at threshold, where all momenta vanish, a direct relation can be established.

Lüscher's Method

The preceding paragraph showed that a simple extraction of scattering parameters, thus also resonance properties and similarly decay amplitudes from Euclidean correlation functions remains flawed due to off-shell contributions[9]. That is, the correlation functions are dominated by matrix elements that do not correspond to the physical scattering process as described above. This statement is only strictly true in the infinite volume, where a continuum of intermediate states exists above threshold. In a finite box of length L with periodic boundary conditions, on the other hand, the momentum is quantized according to

$$\mathbf{p} = \frac{2\pi}{L}\mathbf{n}, \quad \mathbf{n} \in \mathbb{Z}^3 \,. \tag{2.47}$$

Therefore, the energy spectrum is discrete. For example, the non-interacting two-pion energies in the rest frame, as considered above, are given by

$$E_n = 2\sqrt{M_\pi^2 + \frac{4\pi^2}{L^2}\mathbf{n}^2}, \quad \mathbf{n} \in \mathbb{Z}^3 \,. \tag{2.48}$$

Due to interactions, these energies will be shifted. The existence of such a discrete energy spectrum in principle allows for the extraction of on-shell amplitudes from the correlation function in Eqs. (2.45) and (2.46) if sufficiently high energy levels are reached. However, singling out the correct matrix element remains a difficult task.

Nevertheless, the discrete energy spectrum of the finite-volume enables access to scattering parameters. With the pioneering perturbative calculations [143, 144] of the finite-volume energy shift of the n-Bosons ground state, the scattering length could be obtained by a fit to the energy spectrum. Proceeding work [32, 33] by Lüscher showed that the two-particle finite-volume energy spectrum is uniquely determined by on-shell S-matrix elements, when corrections that are exponentially small in the box length L are neglected. This framework, coined as *Lüscher method*, is formulated in terms of a quantization condition, relating the finite-volume energy levels E_n to the infinite-volume phase shifts $\delta_\ell(s)$. In the particular case of two identical bosons of mass M, it takes the form

$$\begin{aligned} &\det A = 0\,, \\ &A_{\ell m,\ell' m'} = \delta_{\ell\ell'}\delta_{mm'} \cot\delta_\ell(s) - \mathcal{M}_{\ell m,\ell' m'}(s,\mathbf{P};L)\,, \end{aligned} \tag{2.49}$$

where $\ell m, \ell' m'$ denotes the angular momentum space, over which the determinant is taken. The matrix $\mathcal{M}$ depends on the total momentum $\mathbf{P}$ of the center of mass system (CMS) explicitly, as well as due to $s = E^2 - \mathbf{P}^2$, where E is the energy. Furthermore $\mathcal{M}$ does not depend on the short-ranged interactions.

[9] Note that with the method described in [142], amplitudes above threshold can be extracted by measuring the proposed modified Euclidean correlators and fitting them for large but finite times.

These are completely described by the phase shift. Components of the matrix $\mathcal{M}$ are given by

$$\mathcal{M}_{\ell m,\ell' m'}(s,\mathbf{P};L) = \frac{(-1)^\ell}{\pi^{3/2}\gamma}\sum_{j=|\ell-\ell'|}^{\ell+\ell'}\sum_{s=-j}^{j}\frac{i^j}{\eta^{j+1}}C_{\ell m,js,\ell' m'}Z^{\mathbf{d}}_{js}(1;s),$$
$$C_{\ell m,js,\ell' m'} = (-1)^{m'}i^{\ell-j+\ell'}\sqrt{(2\ell+1)(2j+1)(2\ell'+1)}\begin{pmatrix}\ell & j & \ell'\\ m & s & -m'\end{pmatrix}\begin{pmatrix}\ell & j & \ell'\\ 0 & 0 & 0\end{pmatrix}, \tag{2.50}$$

where

$$\mathbf{d} = \frac{L}{2\pi}\mathbf{P}, \quad \eta = \frac{L}{2\pi}q^*, \quad \gamma = \frac{E}{\sqrt{s}} \tag{2.51}$$

with $q^* = \sqrt{s/4 - M^2}$ the relative momentum in the CMS and

$$Z^{\mathbf{d}}_{\ell m}(1;s) = \sum_{\mathbf{r}\in P_{\mathbf{d}}}\frac{\mathcal{Y}_{\ell m}(\mathbf{r})}{r^2-\eta^2}, \quad P_{\mathbf{d}} = \left\{\mathbf{r}\in\mathbb{R}^3\middle|\, r_\parallel = \gamma^{-1}(n_\parallel - |\mathbf{d}|/2),\ \mathbf{r}_\perp = \mathbf{n}_\perp,\ \mathbf{n}\in\mathbb{Z}^3\right\} \tag{2.52}$$

is the Lüscher Zeta-function. The parallel and perpendicular components in the sum are taken with respect to the CMS momentum. The functions $\mathcal{Y}_{\ell m}(\mathbf{k}) = |\mathbf{k}|^\ell Y_{\ell m}(\hat{\mathbf{k}})$ are related to the usual spherical harmonics. The appearance of the Lüscher Zeta-function leads to an *irregular*, i.e. non-exponential, L dependence of the finite-volume energy spectrum. Diagrammatically such contributions emerge from loops where the particles can go on-shell. A derivation of the quantization condition within the non-relativistic field theory approach will be given in section 3.2.2.

Solutions $E = E_n$ that satisfy Eq. (2.49) yield the finite-volume energy spectrum for given input phase shifts $\delta_\ell(s)$. These are related to the infinite-volume scattering amplitude $T_\ell(s)$ in the partial wave ℓ due to unitarity:

$$T(s,\cos\theta) = \sum_{\ell=0}^{\infty}(2\ell+1)P_\ell(\cos\theta)T_\ell(s), \quad T_\ell(s) = \frac{16\pi\sqrt{s}}{q^*\cot\delta_\ell(s) - iq^*}. \tag{2.53}$$

Here, $T(s,\cos\theta)$ is the total scattering amplitude and θ denotes the CMS angle. The formula above is only valid below the first inelastic threshold, which thus defines an upper bound for the validity of Lüscher's method in this simple form. Generalizations to coupled two-particle channels were provided by [37, 39–42], such that the range of applicability can be extended up to the three- or more[10]-particle threshold.

Of course, in order to determine scattering amplitudes from LQCD, the direction is reversed. The lattice energy spectra for given volumes in various frames with total momentum characterized by $\mathbf{d}$ are determined from suitable correlation functions. Then one uses the quantization condition Eq. (2.49) in order to perform a fit to these energy spectra, such that the optimal parameters of $\cot\delta_\ell(s)$ are found that minimize the residual sum of squares. Parameterizing the phase shift is a subtle issue, there exist several forms. For example, in case of short-range interactions, using that in the vicinity of the elastic threshold $(q^*)^2 = 0$, the function $(q^*)^{2\ell+1}\cot\delta_\ell(s)$ is analytic and, by unitarity, real above the

[10] Certain symmetries may restrict the possible interactions. For example, the process $\pi\pi \to \pi\pi\pi$ is forbidden by G-parity.

threshold, leads to the *effective-range expansion* (ERE) [145]:

$$(q^*)^{2\ell+1} \cot \delta_\ell(s) = -\frac{1}{a_\ell} + \frac{1}{2} r_\ell (q^*)^2 + O(q^{*4}), \tag{2.54}$$

with the coefficients a_ℓ and r_ℓ are referred to as *scattering length* and *effective range* respectively. It should be pointed out that the generalization of Lüscher's method, originally formulated for the two-particle system at rest, to moving frames represents a big advantage, as numerically expensive calculations in large volumes can be avoided while keeping the number of extracted energy levels fixed.

2.3.3 Symmetries of the Finite Volume

Rotational invariance is explicitly broken in a finite-volume box. As a consequence the quantization condition as displayed in Eq. (2.49) is non-diagonal in angular momentum and different partial waves are mixed. Formally the matrix A is infinite-dimensional since all partial waves contribute[11] and it is necessary to impose an angular momentum cutoff. Such a truncation can be justified as $T_\ell(s) \sim (q^*)^{2\ell}$ in the vicinity of threshold, provides a hierarchy of partial waves in the expansion as displayed in Eq. (2.53).

As rotational invariance, $\mathrm{O}(3) \cong \mathrm{SO}(3) \times \mathbb{Z}_2$, is not broken completely in a finite volume, further simplification can be achieved by partially diagonalizing the quantization condition into the irreps of the residual symmetry group. In case of a cubic lattice with vanishing total momentum $\mathbf{d} = \mathbf{0}$ this group corresponds to the octahedral group[12] O_h, containing the symmetry transformations of a cube. The group O_h contains 48 elements in total, build from 24 proper rotations and space inversion. Elements that are combinations of rotation and space inversion will be referred to as *improper rotations* in the following.

In contrast to the infinite volume, where infinitely many irreps of O(3) exists, labeled by angular momentum and parity[13] ℓ^P ($\ell \in \mathbb{N}$, $P = \pm$), there is only a finite number of irreps of the octahedral group. These are denoted by $\Gamma = A_1^\pm, A_2^\pm, E^\pm, T_1^\pm, T_2^\pm$ and are of dimensions 1, 1, 2, 3, 3 respectively. The superscript denotes the behavior under space inversion. Explicitly the matrix representations $T^\Gamma(g)$ for each group element $g \in O_h$ are given in [146, 147]. For example, A_1^+ labels the trivial representation, $T^{A_1^+}(g) = 1$ for all $g \in O_h$, while A_1^- acts as $T^{A_1^-}(g) = \pm 1$ if g is in a proper (+1) or improper (−1) rotation. Since O_h is a subgroup of O(3), all angular momentum representations ℓ^P of the infinite volume split into linear combinations of the ten irreps of the octahedral group. Applying the orthogonality of characters[14], the decomposition of representations ℓ^P into the irreps of the octahedral group can be performed as displayed up to $\ell = 4$ in Tab. 2.1. The mixing of partial waves is evident now: while $\ell^P = 0^\pm$ is completely described by the representation $A_1^\pm$, the latter is

[11] If rotational symmetry were exact, still all partial waves contribute, but the matrix A would be diagonal in ℓ and m, such that the quantization condition reduces to a product of one dimensional equations for each angular momentum separately.

[12] Taking into account fermions, in the infinite volume one considers the double cover SU(2) of the rotation group SO(3). Similarly in a finite volume the double cover of the octahedral group ${}^2O_h$ should be considered.

[13] The parity of a physical states is determined by its internal parity and the parity of the angular momentum state $P_\ell = (-1)^\ell$. For example, while a system of three scalar particles in $\ell = 0$ has parity $P = +$, for three pseudoscalar particles in $\ell = 0$ one has $P = -$.

[14] The relevant character tables can be found in [36]

Table 2.1: Decomposition of irreps of O(3) into irreps of O_h and C_{4v}. In the decomposition into irreps of C_{4v} the occurrence of A_1 and A_2 depend on the parity. Below, the notation $A_{i/j}$ is used, where for $P = 1$ ($P = -1$) $A_{i/j} = A_i$ ($A_{i/j} = A_j$).

ℓ^P	decomposition into irreps of	
	O_h	C_{4v}
$0^\pm$	$A_1^\pm$	$A_{1/2}$
$1^\pm$	$T_1^\pm$	$A_{2/1} \oplus E$
$2^\pm$	$E^\pm \oplus T_2^\pm$	$A_{1/2} \oplus B_1 \oplus B_2 \oplus E$
$3^\pm$	$A_2^\pm \oplus T_1^\pm \oplus T_2^\pm$	$A_{2/1} \oplus B_1 \oplus B_2 \oplus 2E$
$4^\pm$	$A_1^\pm \oplus E^\pm \oplus T_1^\pm \oplus T_2^\pm$	$2A_{1/2} \oplus A_{2/1} \oplus B_1 \oplus B_2 \oplus 2E$

Table 2.2: Contributions of irreps of O_h and C_{4v} to irreps of O(3). Note the irreps A_1 and A_2 of C_{4v} both contribute to 4^+ as well as 4^-, other than the pattern of alternating parties may suggest.

irreps of O_h	contribution to ℓ^P
$A_1^\pm$	$0^\pm, 4^\pm, 6^\pm, 8^\pm, \ldots$
$A_2^\pm$	$3^\pm, 6^\pm, 7^\pm, 9^\pm, \ldots$
$E^\pm$	$2^\pm, 4^\pm, 5^\pm, 6^\pm, \ldots$
$T_1^\pm$	$1^\pm, 3^\pm, 4^\pm, 5^\pm, \ldots$
$T_2^\pm$	$2^\pm, 3^\pm, 4^\pm, 5^\pm, \ldots$

irreps of C_{4v}	contribution to ℓ^P
A_1	$0^+, 1^-, 2^+, 3^-, \ldots$
A_2	$0^-, 1^+, 2^-, 3^+, \ldots$
B_1	$2^\pm, 3^\pm, 4^\pm, 5^\pm, \ldots$
B_2	$2^\pm, 3^\pm, 4^\pm, 5^\pm, \ldots$
E	$1^\pm, 2^\pm, 3^\pm, 4^\pm, \ldots$

also contained within the decomposition of the $\ell^P = 4^\pm$ state. Tab. 2.2 shows the contributions of the different irreps of O_h to various angular momenta.

For moving frames, the symmetry is further reduced to the stabilizer group $\mathcal{G}$ of the total momentum $\mathbf{d} \neq 0$:

$$\mathcal{G} = \left\{ g \in O_h \mid g\mathbf{d} = \mathbf{d} \right\} . \tag{2.55}$$

For example, for $\mathbf{d} = (0, 0, 1)$ the stabilizer group C_{4v} contains 8 elements, corresponding to transformations leaving an oriented rectangular prism invariant. Note that space inversion is not a symmetry anymore as it reverses the direction of $\mathbf{d}$. The irreps of C_{4v} are labeled by $\Gamma = A_1, A_2, B_1, B_2, E$ and are of dimensions $1, 1, 1, 1, 2$ respectively. Decomposition of angular momentum representations ℓ^P into these irreps as well as the inverse problem can be found in Tabs. 2.1 and 2.2.

In order to ease the notation, in the following states without internal parity will be considered. Partial diagonalization of the quantization condition is achieved if it is expanded in the basis of the irreducible representations of the symmetry group $\mathcal{G}$. For a given representation Γ of dimension d_Γ, these basis vectors will be denoted by $|\Gamma_t, \ell, \alpha\rangle$, where $\alpha = 1, \ldots, d_\Gamma$. Furthermore, $t = 1, \ldots, N_\Gamma$ denotes the multiplicity of the irrep Γ for a given angular momentum ℓ. These basis states can be expressed as a linear combination of angular momentum states:

$$|\Gamma_t, \ell, \alpha\rangle = \sum_{m=-\ell}^{\ell} c_{\ell,m}^{\Gamma_t \alpha} |\ell m\rangle . \tag{2.56}$$

The coefficients $c_{\ell,m}^{\Gamma_t \alpha}$ are tabulated in [36, 147, 148] for low values of ℓ. They can be found by letting the operator

$$\Pi_\alpha^\Gamma = \frac{d_\Gamma}{G} \sum_{g \in \mathcal{G}} \left(T_{\alpha\alpha}^\Gamma(g) \right)^* g \tag{2.57}$$

act on the angular momentum states $|\ell m\rangle$, projecting them on the invariant subspaces of the irreducible representations. Here $T_{ij}(g)^\Gamma$ denotes the matrix representations of the element g in the irrep Γ and $G = |\mathcal{G}|$ is the order of the stabilizer group. Furthermore, the action of the group element g on the state $|\ell m\rangle$ is given by

$$g|\ell m\rangle = \sum_{m'=-\ell}^{\ell} D_{m'm}^{(\ell)}(g) |\ell m'\rangle \,, \tag{2.58}$$

where $D^{(\ell)}$ denote the Wigner-matrices. The resulting rows and columns of matrices $\langle \ell m' | \Pi_\alpha^\Gamma | \ell m \rangle$ contain the (unnormalized) basis vectors $|\Gamma_t, \ell, \alpha\rangle$ as a linear combination of $|\ell m\rangle$. The rank of the matrix corresponds to the multiplicity t of the irrep Γ.

The operator A in the quantization condition can then be expressed as

$$A_{\ell\alpha,\ell'\alpha'}^{\Gamma_t,\Gamma'_{t'}} = \langle \Gamma_t, \ell, \alpha | A | \Gamma'_{t'}, \ell', \alpha' \rangle = \sum_{m=-\ell}^{\ell} \sum_{m'=-\ell'}^{\ell'} \left(c_{\ell,m}^{\Gamma_t \alpha} \right)^* c_{\ell',m'}^{\Gamma'_{t'} \alpha'} A_{\ell m, \ell' m'} \,. \tag{2.59}$$

Since the operator A transforms trivially under the symmetry group $\mathcal{G}$, according to the orthogonality of irreps it follows that

$$A_{\ell\alpha,\ell'\alpha'}^{\Gamma_t,\Gamma'_{t'}} = \langle \Gamma_t, \ell, \alpha | A | \Gamma'_{t'}, \ell', \alpha' \rangle = \delta_{\Gamma\Gamma'} \delta_{\alpha\alpha'} A_{\ell t, \ell' t'}^\Gamma \,. \tag{2.60}$$

Therefore the quantization condition $\det A = 0$ falls apart into separate conditions for each irrep Γ:

$$\begin{aligned} &\det A^\Gamma = 0 \,, \\ &A_{\ell t, \ell' t'}^\Gamma = \delta_{\ell\ell'} \delta_{tt'} \cot \delta_\ell(s) - \mathcal{M}_{\ell t, \ell' t'}^\Gamma(s, \mathbf{P}; L) \,, \\ &\mathcal{M}_{\ell t, \ell' t'}^\Gamma(s, \mathbf{P}; L) = \sum_{m=-\ell}^{\ell} \sum_{m'=-\ell'}^{\ell'} \left(c_{\ell,m}^{\Gamma_t \alpha} \right)^* c_{\ell',m'}^{\Gamma_{t'} \alpha} \mathcal{M}_{\ell m, \ell' m'} \,. \end{aligned} \tag{2.61}$$

This represents a practical advantage, as the dimensions of matrices entering the quantization condition are drastically reduced.

At the end of this paragraph, the quantization condition will be used to generate the finite-volume spectra in two toy models. Considering $\ell = 0$, only the $A_1^{(+)}$ representation contributes in the rest frame as well as the frame with $\mathbf{d} = (0, 0, 1)$. The determinant equation simplifies to a usual one:

$$\cot \delta_0(s) - \frac{1}{\pi^{3/2} \gamma \eta} Z_{00}^{\mathbf{d}}(1, s) = 0 \,. \tag{2.62}$$

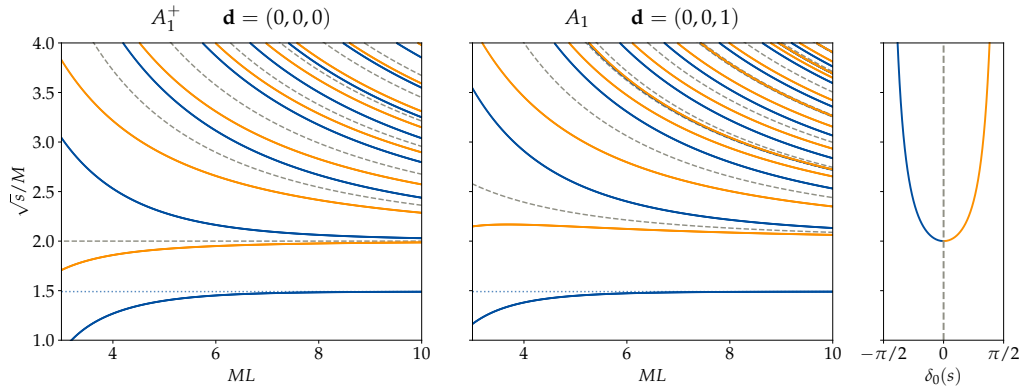

Figure 2.4: Finite-volume CMS energy spectra in the rest frame and moving frame irrep for elastic S-wave scattering. Non-interacting levels are indicated by gray dashed lines. Yellow lines denote the energy spectrum for attractive interaction ($a < 0$). In case of repulsive interaction ($a > 0$), represented by blue lines, a bound state exists with infinite-volume energy indicated by the dotted blue line. The left and middle panel show the spectrum in the A_1^+ irrep in the rest frame and A_1 irrep in a moving frame, with $\mathbf{d} = (0, 0, 1)$, respectively. The right panel shows the phase shift $\delta_0(s)$, with $q^* \cot \delta_0(s) = -1/a$, as a function of $\sqrt{s}$ for $a < 0$ (yellow line) and $a > 0$ (blue line). Note that here the $\sqrt{s}$-axis is vertical.

The first model considers elastic S-wave scattering of two identical bosons of mass M, described by

$$q^* \cot \delta_0(s) = -\frac{1}{a} \tag{2.63}$$

to lowest order in the effective range expansion. Choosing $a = \pm 1.5M$ (in natural units) the quantization in Eq. (2.62) can be used to produce the energy spectra in the $A_1^{(+)}$ representations of the rest and $\mathbf{d} = (0, 0, 1)$ frame. These are shown in Fig. 2.4 for the case of attractive ($a < 0$) and repulsive ($a > 0$) interaction and compared to the non-interacting levels. For convenience the CMS energies $\sqrt{s} = \sqrt{E_n^2 - \mathbf{P}^2}$ are plotted. In the attractive case the energy levels are shifted downwards as compared to the non-interacting levels, while in the repulsive case they are shifted upwards[15]. Note that for $a > 0$ a bound state exists, the corresponding binding energy in the infinite volume is indicated by the blue dotted line.

The second model considers a S-wave resonance. It can be described by a Breit-Wigner phase shift

$$q^* \cot \delta_0(s) = \frac{6\pi}{g^2} \frac{\sqrt{s}}{M_R^2} (M_R^2 - s), \tag{2.64}$$

where M_R denotes the mass of the resonance and g controls its coupling. Choosing $M_R = 3M$ and $g = 1.333$ the energy spectra in the rest and moving frames for the $A_1^{(+)}$ irreps are depicted in Fig. 2.5. The energy of the resonance is indicated by a yellow line. It can be seen that the energies closely follow the non-interacting levels, but bend away to the next one in the vicinity of the resonance crossing a level. This phenomenon is known as *avoided level crossing* [149].

[15] In the moving frame some non-interacting levels are close to each other, such that the energy level of the repulsive potential might almost overlap with the next energy level of the attractive potential in the figure.

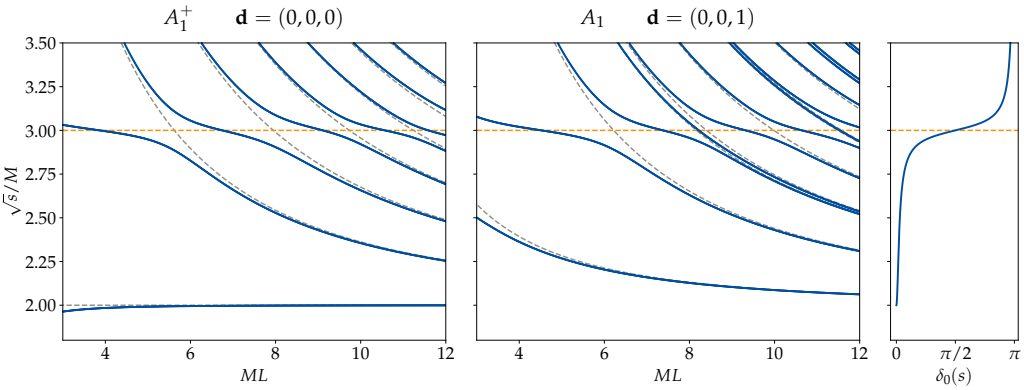

Figure 2.5: Finite-volume CMS energy spectra in the rest frame and moving frame irrep for a S-wave resonance. Non-interacting levels are indicated by gray dashed lines, while the resonance energy is represented by a yellow dashed line. The left and middle panel show the spectrum in the A_1^+ irrep in the rest frame and A_1 irrep in a moving frame, with $\mathbf{d} = (0,0,1)$, respectively. The right panel shows the resonance phase shift $\delta_0(s)$ as a function of $\sqrt{s}$. Note that here the $\sqrt{s}$-axis is vertical.

An important remark is in order. This concerns the levels that lie in between two narrowly separated non-interacting energies that appear in the moving frame[16]. An example of such an occurrence can be observed in Fig. 2.5 between the third and fourth non-interacting levels[17]. The small gap between such neighboring non-interacting energies can be attributed to relativistic effects, the levels are degenerate in the non-relativistic limit. For example, the third and fourth non-interacting levels in the middle panel of Fig. 2.5 correspond to pairs of particles with momenta (representatives[18]) $\mathbf{p}_1 = 2\pi/L\,(0,0,2)$, $\mathbf{p}_2 = 2\pi/L\,(0,0,-1)$ and $\mathbf{p}_1 = 2\pi/L\,(1,1,1)$, $\mathbf{p}_2 = 2\pi/L\,(-1,-1,0)$ respectively. In the interacting case, there will always lie a "pinched" level in between such two non-interacting energies. The problem with these energy level arises when considering the non-relativistic limit, in which the two non-interacting energies approach and from a degenerate level. Naively one would expect that the "pinched" level thus turns into an unphysical solution which lies exactly at the non-interacting energy. On the other hand, as shown in App. A.1, the residue of such a "pinched" level vanishes in the non-relativistic limit, such that the expected unphysical solution indeed disappears from the spectrum.

Furthermore, for practical applications of the Lüscher method one should treat "pinched" energy levels with caution as these are rather insensitive to changes of the form and strength of the interactions. Moreover, fitting the quantization condition to the finite-volume spectrum in order to determine the parameters of the phase shift, error bands on the energies of the extracted "pinched" levels result in extremely large error bands on the phase shift, due to the steep form of the Lüscher Zeta-function in that region. A similar discussion can also be found in [150] where states of the same characteristic, appearing in finite volumes subject to elongation, have been observed.

[16] Such levels can also be seen in the toy model spectra of Ref. [43], where the figures above have been inspired from.

[17] The same behavior can be found in Fig. 2.4 but due to cluttered presentation identifying these levels might be difficult.

[18] The energy level corresponds to the state, build from these momenta, that transforms in the A_1 irrep. It can be obtained by applying the projection operator Eq. (2.57) on the state $|\mathbf{p}_1, \mathbf{p}_2\rangle$, where the group element acts as $g|\mathbf{p}_1, \mathbf{p}_2\rangle = |g\mathbf{p}_1, g\mathbf{p}_2\rangle$.

2.3.4 Determination of Two-Particle Energy Spectra

As discusses in the preceding paragraphs, scattering information in the two-particle sector can be determined from the corresponding energy spectrum. The extraction of two-particle energy levels proceeds similarly as described in Sec. 2.3.1. First one has to find a suitable choice of interpolators. Application of Lüscher's method in moving frames $\mathbf{P} = 2\pi/L\mathbf{d}$ as stated in Eq. (2.61) requires operators that only have non-vanishing overlap with states $|\mathbf{P}; \Gamma, \alpha\rangle$ in a irreducible representation Γ of the stabilizer group of $\mathbf{P}$. Focusing on the S-wave scattering of two positively charged pions again provides a simple example that can be generalized easily.

An operator that has overlap with a two π^+-state with total momentum $\mathbf{P}$ is given by

$$O_{\pi\pi}(\mathbf{P}, \mathbf{q}; t) = \pi^+_{\mathbf{P}-\mathbf{q}}(t)\pi^+_{\mathbf{q}}(t)\,, \tag{2.65}$$

where

$$\pi^+_{\mathbf{k}}(t) = \sum_{\mathbf{x}} \mathrm{e}^{\mathrm{i}\mathbf{k}\mathbf{x}}\, \pi^+(\mathbf{x}, t)\,. \tag{2.66}$$

This operator can then be projected onto an irrep Γ of the stabilizer group $\mathcal{G}$ of $\mathbf{P}$ using the projection operator defined in Eq. (2.57). A simpler version can be obtained by using the projector defined by [36]

$$\Pi^\Gamma = \frac{d_\Gamma}{G} \sum_{g\in\mathcal{G}} \left(\chi^\Gamma(g)\right)^* g\,, \tag{2.67}$$

where $\chi(g)^\Gamma$ denotes the character of the element g in the irrep Γ. The projected operator then reads as

$$\begin{aligned} O^\Gamma_{\pi\pi}(\mathbf{P}, \mathbf{q}; t) &= \Pi^\Gamma O_{\pi\pi}(\mathbf{P}, \mathbf{q}; t) \\ &= \frac{d_\Gamma}{G} \sum_{g\in\mathcal{G}} \left(\chi^\Gamma(g)\right)^* \sum_{\mathbf{x}_1,\mathbf{x}_2} \mathrm{e}^{\mathrm{i}\mathbf{P}\mathbf{x}_1 + \mathrm{i}\mathbf{q}(\mathbf{x}_2-\mathbf{x}_1)} g(\pi^+(\mathbf{x}_1, t)\pi^+(\mathbf{x}_2, t))\,. \end{aligned} \tag{2.68}$$

The action of the group element on the two pion fields is given by

$$\begin{aligned} g(\pi^+(\mathbf{x}_1, t)\pi^+(\mathbf{x}_2, t)) &= (-1)^{P(g)}\pi^+(g^{-1}\mathbf{x}_1, t)\,(-1)^{P(g)}\pi^+(g^{-1}\mathbf{x}_2, t) \\ &= \pi^+(g^{-1}\mathbf{x}_1, t)\pi^+(g^{-1}\mathbf{x}_2, t)\,, \end{aligned} \tag{2.69}$$

where the factors of $(-1)^{P(g)}$, with $P(g) = -1$ ($P(g) = 1$) if the element g corresponds to an improper (proper) rotation, arise as pions are pseudoscalars. Note that in case of an odd[19] number of pions this factor is not canceled. Moreover, the sums over sites $\mathbf{x}_i$ can be exchanged by sums over $\mathbf{y}_i = g^{-1}\mathbf{x}_i$ as

[19] This can be nicely illustrated by the construction of single pion operators with momentum $\mathbf{k}$ in a definite irrep of the corresponding stabilizer group. Repeating the steps presented above this interpolator can be written as:

$$\pi^{+\Gamma}_{\mathbf{k}}(t) = \frac{d_\Gamma}{G} \sum_{g\in\mathcal{G}} \left(\chi^\Gamma(g)\right)^* (-1)^{P(g)} \pi^+_{\mathbf{k}}(t)\,.$$

Thus, only one dimensional irreps that are odd under improper rotations contribute. For O_h this is the A_1^- irrep, while for C_{4v} only the A_2 irrep yields a non-vanishing result. This is in agreement with Tab. 2.2 as the pions are $\ell^P = 0^-$ states.

these points represent the same lattice. Finally using that $\mathbf{k}(g\mathbf{y}_i) = (g^{-1}\mathbf{k})\mathbf{y}_i$ as well as $g^{-1}\mathbf{P} = \mathbf{P}$ one arrives at

$$O^{\Gamma}_{\pi\pi}(\mathbf{P},\mathbf{q};t) = \frac{d_\Gamma}{G}\sum_{g\in\mathcal{G}}\left(\chi^{\Gamma}(g)\right)^*\sum_{\mathbf{x}_1,\mathbf{x}_2} \mathrm{e}^{\mathrm{i}\mathbf{P}\mathbf{x}_1+\mathrm{i}(g^{-1}\mathbf{q})(\mathbf{x}_2-\mathbf{x}_1)}\pi^+(\mathbf{x}_1,t)\pi^+(\mathbf{x}_2,t)\,. \tag{2.70}$$

For (at least) one particle at rest, i.e. $\mathbf{q} = \mathbf{0}$, as a consequence of $\sum_g \chi^{\Gamma}(g) = 0$ for non-trivial Γ, the result simplifies to:

$$O^{A_1^{(+)}}_{\pi\pi}(\mathbf{P},\mathbf{0};t) = \sum_{\mathbf{x}_1,\mathbf{x}_2}\mathrm{e}^{\mathrm{i}\mathbf{P}\mathbf{x}_1}\pi^+(\mathbf{x}_1,t)\pi^+(\mathbf{x}_2,t)\,,\qquad O^{\Gamma}_{\pi\pi}(\mathbf{P},\mathbf{0};t) = 0\,,\quad \Gamma\neq A_1^{(+)}\,. \tag{2.71}$$

In order to extract the energy levels corresponding to states in a given irrep Γ the following correlator[20] is considered

$$C^{\Gamma}_{\pi\pi}(\mathbf{P},\mathbf{q};t) = \langle 0|O^{\Gamma}_{\pi\pi}(\mathbf{P},\mathbf{q};t)(O^{\Gamma}_{\pi\pi}(\mathbf{P},\mathbf{q};0))^\dagger|0\rangle\,. \tag{2.72}$$

Indeed, inserting a full set of states and using translation invariance

$$C^{\Gamma}_{\pi\pi}(\mathbf{P},\mathbf{q};t) = \sum_n \frac{|\langle 0|O^{\Gamma}_{\pi\pi}(\mathbf{P},\mathbf{q};0)|n;\mathbf{P};\Gamma\rangle|^2}{2E^{\Gamma}_n(\mathbf{P})}\,\mathrm{e}^{-E^{\Gamma}_n(\mathbf{P})t}\,, \tag{2.73}$$

where $|n;\mathbf{P};\Gamma\rangle$ denote states with total momentum $\mathbf{P}$, transforming in the irrep Γ that have the quantum numbers of two positively charged pions. For convenience, also a superscript Γ is attached to the energy, emphasizing that the corresponding spectrum describes only states transforming within this representation. The ground state energy could be determined by a fit to the effective mass as defined in Sec. 2.3.1. On the other hand, using Lüscher's method also exited states should be extracted. This can be achieved by solving a GEVP as described previously in Sec. 2.3.1. Using the quantization condition in the corresponding irrep as formulated in Eq. (2.61) the phase shifts $\delta_\ell(s)$ and thus the infinite-volume scattering amplitudes $T_\ell(s)$ can be determined by a fit to the energy spectrum.

2.3.5 Two-Particle Decays from LQCD

In the context of QCD, decays fall into two categories. The first one describes QCD resonances where the decay is mediated via strong interactions, such as $\rho \to \pi\pi$. The second class includes decays, where the decay products, as well as the initial state are stable particles in pure QCD. Electroweak processes fall into this category, with the probably most prominent decays of a kaons $K \to \pi\pi$. In this case the decay can be considered in first order perturbation theory, as the electroweak coupling is small as compared to the strong interactions. This also applies to processes that proceed via symmetry violation, such as $\omega \to \pi\pi$, where the amplitude is proportional to the isospin-breaking term $m_d - m_u$.

A formalism introduced by Lellouch and Lüscher [45], see also [35, 41, 46], based on the quantization condition, allows the study of two-particle decays that fall into the second category described above. As an example, the following paragraph will introduce the formalism in the context of the $K^+ \to \pi^+\pi^0$

[20] Note that if the correlator would be constructed with interpolators in different irreps, the result would vanish due to the orthogonaliy theorem.

decay in the isospin symmetric case. Restricting to S-wave interactions, it can be shown that the infinite-volume decay amplitude can be written as

$$T(K^+ \to \pi^+\pi^0) = \langle \pi^+(\mathbf{p}_1)\pi^0(\mathbf{p}_2); \text{out}|\mathcal{H}_w(0)|K^+(\mathbf{P}); \text{in}\rangle = A e^{\mathrm{i}\delta_0^{I=2}(s)}, \tag{2.74}$$

where $\mathcal{H}_w$ is a Hamiltonian (density) describing the weak interactions and $\delta_0^{I=2}(s)$ is the S-wave phase shift of isospin[21] $I = 2$. A finite-volume version of the decay amplitude can be calculated from the Euclidean correlator

$$\frac{\langle 0|\pi^+_{\mathbf{p}_1}(t)\pi^0_{\mathbf{p}_2}(t)H_w(K^+_{\mathbf{P}}(t'))^\dagger|0\rangle}{\langle 0|\pi^+_{\mathbf{p}_1}(t)\pi^0_{\mathbf{p}_2}(t)(\pi^+_{\mathbf{p}_1}(t'))^\dagger(\pi^0_{\mathbf{p}_2}(t'))^\dagger|0\rangle\langle 0|K^+_{\mathbf{P}}(t)(K^+_{\mathbf{P}}(t'))^\dagger|0\rangle} \overset{t\to\infty}{\underset{t'\to-\infty}{\longrightarrow}} \langle n;\mathbf{P}|H_w|K^+;\mathbf{P}\rangle\,, \tag{2.75}$$

where $|K^+;\mathbf{P}\rangle$ denotes a one-kaon states with momentum $\mathbf{P}$ and $|n;\mathbf{P}\rangle$ corresponds to a state with quantum numbers of $\pi^+\pi^0$. In the expression above, it is implicitly assumed that the volume is tuned so that the energy of the state n coincides with the one-kaon state if the weak interactions are turned off. As the energy of the kaon in a finite volume only receives exponentially small corrections, that will be dropped throughout, the condition reads as $E_n^{(0)} = E_K$, $E_K^2 = M_K^2 + \mathbf{P}^2$. Now turning on the electroweak interaction, which can be treated perturbatively, most of the energy levels will remain unchanged to first order as H_w only couples states of different strangeness. On the other hand, the degeneracy of the states $|n;\mathbf{P}\rangle$ and $|K^+;\mathbf{P}\rangle$ is lifted. To first order in g_w, where $H_w = O(g_w)$

$$E_n = E_n^{(0)} \pm \langle n;\mathbf{P}|H_w|K^+;\mathbf{P}\rangle + O(g_w^2)\,. \tag{2.76}$$

In the infinite volume, the amplitude $T(\pi^+\pi^0 \to \pi^+\pi^0)$ receives a contribution of order $O(g_w)$ from $\pi^+\pi^0 \to K^+ \to \pi^+\pi^0$. Denoting the momentum of the pion pair by $P^\mu = (E_n, \mathbf{P})$ and using Eqs. (2.74) and (2.76), this contribution is given by

$$\Delta T = \frac{1}{P^2 - M_K^2}|A|^2 e^{2\mathrm{i}\delta_0^{I=2}(s)} = \pm\frac{|A|^2}{2E_n^{(0)}\langle n;\mathbf{P}|H_w|K^+;\mathbf{P}\rangle} e^{2\mathrm{i}\delta_0^{I=2}(s)} + O(g_w^2)\,. \tag{2.77}$$

The phase shift $\tilde{\delta}_0^{I=2}$ in the presence of the weak interaction can be calculated in first order perturbation theory from the well known analytic form (Eq. (2.53) without the symmetry factor of 2) of the S-wave two-pion scattering amplitude $T = T^{(0)} + \Delta T$:

$$\tilde{\delta}_0^{I=2}(s) = \delta_0^{I=2}(s) \pm \frac{q^*}{16\pi\sqrt{s}E_n^{(0)}}\frac{|A|^2}{\langle n;\mathbf{P}|H_w|K^+;\mathbf{P}\rangle} + O(g_w^2)\,. \tag{2.78}$$

Since the energy level E_n corresponds to a solution of the quantization condition (in the presence of weak interaction), the phase shift can be replaced by

$$\tilde{\delta}_0^{I=2}(s_n) = k\pi - \phi^{\mathbf{d}}(s_n), \quad k \in \mathbb{Z}, \quad \cot\phi^{\mathbf{d}}(s) = -\frac{1}{\pi^{3/2}\gamma\eta}Z_{00}^{\mathbf{d}}(1;s), \tag{2.79}$$

[21] Two pion states with $I = 1$ do not exists for pure S-wave interaction due to Bose symmetry. The isospin $I = 0$ channel is excluded by charge conservation.

for $s_n = E_n^2 - \mathbf{P}^2$. Further, one may expand the functions $\phi^{\mathbf{d}}(s_n)$ and $\delta(s_n)$ in a Taylor series around $q_n^* = q_n^{*(0)}$:

$$\begin{aligned}\phi^{\mathbf{d}}(s_n) &= \phi^{\mathbf{d}}(s_n^{(0)}) + (\phi^{\mathbf{d}})'(s_n^{(0)})\Delta q_n^* + O(g_w^2)\\ \delta_0^{I=2}(s_n) &= \delta_0^{I=2}(s_n^{(0)}) + (\delta_0^{I=2})'(s_n^{(0)})\Delta q_n^* + O(g_w^2),\end{aligned} \tag{2.80}$$

where $s_n^{(0)} = E_n^{(0)2} - \mathbf{P}^2 = M_K^2$ and

$$\Delta q_n^* = q_n^* - q_n^{*(0)} = \pm\frac{1}{4}\frac{E_n^{(0)}}{q_n^{*(0)}}\,\langle n;\mathbf{P}|H_w|K^+;\mathbf{P}\rangle + O(g_w^2), \tag{2.81}$$

as obtained form Eq. (2.76). Now using that $E_n^{(0)}$ is a solution to $\delta_0^{I=2}(s_n^{(0)}) = k'\pi - \phi^{\mathbf{d}}(s_n^{(0)})$, the quantization condition in absence of weak interaction, Eq. (2.74) can be rearranged in order to find:

$$|A|^2 = 4\pi M_K \left(\frac{E_n^{(0)}}{q_n^{*(0)}}\right)^2 \left((\delta_0^{I=2})'(M_K^2) + (\phi^{\mathbf{d}})'(M_K^2)\right)\,\langle n;\mathbf{P}|H_w|K^+;\mathbf{P}\rangle^2\,. \tag{2.82}$$

This equation establishes a relation between the absolute value of the infinite-volume decay matrix element A and the finite-volume transition matrix element $\langle n;\mathbf{P}|H_w|K^+;\mathbf{P}\rangle$ that can be extracted from LQCD by considering a correlator as in Eq. (2.75). These two quantities are proportional to each other, the proportionality constant is called the Lellouch-Lüscher (LL) factor. The phase of the decay amplitude coincides with the phase shift $\delta_0^{I=2}(s)$, see Eq. (2.74). It is worth mentioning that the LL factor does not depend on the kaon interactions but is solely described by the rescattering of the final pion states, which can be determined by Lüscher's method as described in the previous section. Based on this framework, a comprehensive lattice study of the $K \to \pi\pi$ decays has been performed by the RBC and UKQCD collaborations [151–153]

2.3.6 Three-Particle Scattering and Decays from Lattice QCD

Having established the principles of hadron spectroscopy in the two-particle sector in the preceding sections, this paragraph should close this chapter by giving an overview of the strategies that allow the study of three-body interactions from three-particle LQCD spectra, which is the main scope of this thesis. The urgency of introducing such a formalism is twofold. First, many QCD resonances have a significant decay rate into three-particles. Moreover, Lüscher's method is invalid above the three-particle threshold in general, but numerical simulations are already probing this regime. Thus the inclusion of three-particle channels represent a major improvement in the study of hadron properties from LQCD.

From the perspective of simulations, despite the fast growing computational complexity, the examination of three- or more-particle energy levels may be regarded as a simple generalization of the strategy outlined before. Namely, although the number of contractions grows factorial like[22], as depicted in Fig. 2.6 for the scattering of three positively charged pions, from a technical point of view the construction of appropriate three-particle operators proceeds as discussed as in Sec. 2.3.4.

Nevertheless, establishing a relation to physical observables is a highly non-trivial task. Use of

[22] For example, for the scattering of N charged pions, the number of possible contractions is $(N!)^2$.

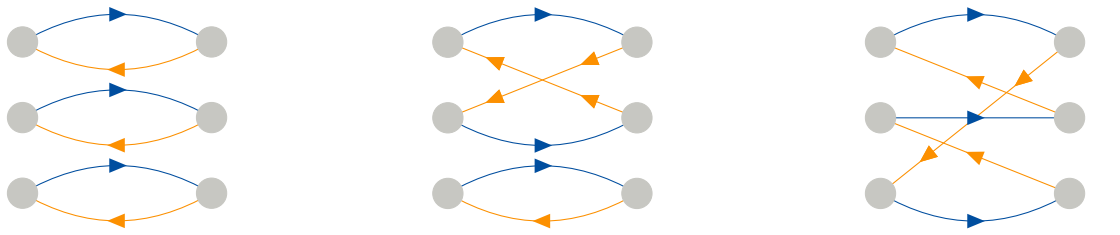

+5 similar contractions +17 similar contractions +11 similar contractions

Figure 2.6: Contractions of the $\pi^+\pi^+\pi^+$ correlator. Pions are indicated by grey solid blobs, blue and yellow fermion lines indicate the u- and d-quark propagator respectively. There are three different topologies of graphs as depicted, each with a multiplicity as noted below the diagrams.

perturbative expansions of energy shifts for the three-particle ground state [4, 6, 143, 144, 154–156] and exited states [157] in powers of $1/L$ is rather limited as these fail in the presence of resonances or shallow bound states. As systems featuring such properties are of great interest, establishing an analog of the Lüscher equation in the three-particle sector is highly desirable.

It should be pointed out that the simplicity of Lüschers framework, relating the finite-volume energy spectrum to the physically observable phase shift directly, relies on the explicitly known analytic form of the two-particle scattering amplitude as formulated in Eq. (2.53). Contrary, the three-particle scattering amplitude obeys integral equations, that usually can be solved only iteratively or numerically. A three-particle quantization condition, that allows for the extraction of physical observables directly is not to be expected in 3+1 dimensions[23].

Nevertheless, triggered by the proof that the finite-volume energy spectra can be solely determined by three-body S-matrix elements [55], the last decade has shown increasing progress in the formulation of a three-particle quantization condition. Nowadays three alternative approaches are available, the Relativistic Field Theory (RFT) [57, 58], Finite Volume Unitarity (FVU) [59] and Non-relativistic Field Theory (NREFT) [60, 61] formulation. Conceptually all these formalisms are similar: Replacing the integrals in the equations of the infinite-volume three-particle scattering amplitude by finite-volume sums, the quantization condition is obtained in the form of a vanishing determinant of this system of equations. Having chosen an appropriate parametrization of the two- and three-body short-range interactions, their corresponding parameters can be determined by using the quantization condition in order to perform a fit to the energy spectrum obtained from LQCD. In return, infinite-volume observables can be calculated solving the three-particle scattering integral equations with the set of extracted parameters.

The RFT approach was subsequently generalized to the inclusion of $2 \leftrightarrow 3$ channels [159], resonant sub-channels [160], the different isospin-channels for the scattering of three pions [161], non-degenerate scalars [162, 163] and the treatment of fermions [164]. However, despite growing interest, the determination of three-particle decay amplitudes from LQCD remained inaccessible until recently only. The following chapters will present the derivation of a relativistic-invariant, three-particle analog of the Lellouch-Lüscher formalism within the NREFT approach.

[23] Note that the authors of [158] derived a quantization condition in 1+1 dimensions containing the three-body scattering amplitude explicitly.

CHAPTER 3

Three Particle Quantization Condition in the Non-Relativistic Field Theory Approach

As already pointed out in the introductory section, effective field theories play an essential role in the analysis of lattice data, which has to be corrected for discretization effects and unphysical large pion masses as well as finite-volume contributions. The scope of this chapter is the introduction of the concepts of non-relativistic effective field theories, that will be used in the derivation of the three-particle analog of the Lellouch-Lüscher equation, in order to study the latter effects.

In order to emphasize the benefits of NREFTs it should be pointed out that the irregular L behavior of the two-particle scattering matrix elements, described by the Lüscher Zeta-function, stem from diagrams that are singular in the physical region, i.e. below the inelastic threshold. These singularities emerge in s-channel two-particle loops. On the other hand, diagrams involving creation and annihilation of particles and antiparticles exhibit an analytic behavior. These will only generate exponentially suppressed corrections as guaranteed by the Poisson summation formula. Clearly, creation and annihilation only play a subordinated role in that context. This situation is exactly recovered in NREFT where only particles correspond to the relevant degrees of freedom. Due to particle number conservation and the absence of antiparticles, NREFTs accomplish a drastic simplification in the calculation of amplitudes. Indeed, in NREFTs, the two-body scattering amplitude is completely described by a tower of s-channel bubbles that reproduce the irregular L behavior in the finite volume, while the regular contributions are included in the LECs implicitly. Thus, in the NREFT treatment of the two-body system a quantization condition can be derived with significant less effort.

3.1 Non-Relativistic Effective Field Theories

Relativistic theories possess a natural scale that separates particles from antiparticles, given by the mass gap, equal to twice the particles mass. If the kinematics under consideration are such that the three-momenta of the particles involved are small as compared to their mass, due to the separation of scales, antiparticles can be disregarded. Thus, a formulation in terms of an EFT, where antiparticles are integrated out explicitly and their effects are absorbed into the LECs, represents an equally good description of the process. As will be shown later, the restriction to the particles three-momenta being non-relativistic can be relaxed, such that the relativistic dispersion law can be reproduced. In that sense, the dynamical aspect that creation and annihilation of antiparticles can be disregarded is more

important. Nevertheless the following section will focus on the non-relativistic kinematics.

A NREFT could be obtained from a relativistic theory by separating particle- and antiparticle degrees of freedom and integrating out the latter explicitly in the path integral formalism. As this might be a rather complicated task, instead one may write down the most general Lagrangian containing all possible operators that respect the symmetries of the underlying model. In the non-relativistic setup, particles are the only degree of freedom. Therefore, in contrast to relativistic theories, fields entering the Lagrangian only contain creation- or annihilation-operators exclusively. The LECs, i.e. the couplings in the Lagrangian, remain undetermined in this process, but can be *matched* to physical observables. In this procedure a set of observables is calculated in the NREFT up to a certain order in some suitable power counting scheme. Afterwards, the LECs entering the expressions for these obervables can be expressed in terms of those. For the non-relativistic kinematical setup, where three-momenta $\mathbf{p}$ are small compared to the particle mass M, the expansion in powers of $|\mathbf{p}|/M = O(\epsilon)$ provides a power counting scheme, that identifies the relevance of operators. Considering the temporal component, the quantity $p^0 - M$ should be counted as $O(\epsilon^2)$.

To lowest order, a NREFT for scalar particles of mass M obeying a $\mathbb{Z}_2$-symmetry that allows interactions with an even number of particles initial- and finial state only reads [70]:

$$\mathcal{L} = \phi^\dagger \left(\mathrm{i}\partial_t - M + \frac{\nabla^2}{2M} \right) \phi + C_0\, \phi^\dagger \phi^\dagger \phi\, \phi + D_0\, \phi^\dagger \phi^\dagger \phi^\dagger \phi\, \phi\, \phi + \dots , \tag{3.1}$$

where

$$\phi(x) = \int \frac{d^3\mathbf{k}}{(2\pi)^3}\, a(\mathbf{k})\, \mathrm{e}^{-\mathrm{i}kx}, \quad k^0 = M + \frac{k^2}{2M}, \tag{3.2}$$

annihilates a particle. The ellipsis contains operators with a higher number of fields as well as operators with derivative couplings. Furthermore, as the field ϕ is not hermitian, all interactions will contain an equal number of creation and annihilation operators. As a consequence particle number is conserved at each vertex.

Unlike the constants C_0 and D_0, the LEC associated with the kinetic term $\nabla^2/(2M)$ is fixed to unity by *reparametrization invariance* [81, 165]. This is a consequence of the Lorentz symmetry of the underlying relativistic theory. Indeed, after matching, S-matrix elements in the NREFT are Lorentz-invariant, up to a given order in the power counting. For the kinetic terms, this guarantees that the relativistic dispersion law is recovered order by order.

As indicated by the ellipsis, the leading order Lagrangian actually contains an infinite tower of vertices with an arbitrary number of fields, seemingly preventing any practical use of NREFT on a first glance. On closer analysis, there exists a hierarchy of the different n-particle sectors, rendering the problem manageable. This specific ordering of interactions is due to particle number conservation at each vertex, in combination with the fact that only particles traveling forwards in time yield a non-vanishing contribution: The non-relativistic propagator

$$D(x-y) = \mathrm{i}\langle 0|T\phi(x)\phi^\dagger(y)|0\rangle = \int \frac{d^4k}{(2\pi)^4}\, \frac{1}{M + \frac{\mathbf{k}^2}{2M} - k^0 - i\varepsilon}\, \mathrm{e}^{-\mathrm{i}k(x-y)}, \tag{3.3}$$

vanishes for $x^0 < y^0$ since there is only a pole in the lower half-plane. Also closed single-particle

loops vanish, as can be seen from the above equation at $x = y$ by performing the k^0 integral explicitly[1] and using the fact that the remaining three-momentum integral vanishes in dimensional regularization. As a consequence the propagator in Eq. (3.3) remains valid up to all orders in perturbation theory, when relativistic corrections of the kinetic term are neglected. Any contribution of vertices to the two-point function demands particles moving backwards in time or looping back to themselves. Only the inclusion of kinetic terms that are of higher order in the power counting will alter the form of the propagator, shifting the pole position to $k^0 = w(\mathbf{k}) = \sqrt{M^2 + \mathbf{k}^2} = M + \mathbf{k}^2/(2M) - \mathbf{k}^4/(8M^3) + \ldots$ By the same arguments, it can be seen that in general, interactions from higher sectors do not contribute to processes which involve a lower number of particles. That is, three-particle scattering at leading order is completely described by the Lagrangian in Eq. (3.1) and any interactions of $n > 3$ particles can be disregarded. Similarly, in order to describe the two-particle sector, all three- or more-particle vertices can be dropped. This property allows for a compact derivation of Lüscher's equation, that will be discussed in the following sections.

3.2 The Two-Particle Sector

3.2.1 Matching in the Two-Particle Sector and Covariant NREFT

In this section the infinite-volume two-particle scattering amplitude for the process $\phi(q_1) + \phi(q_2) \to \phi(p_1) + \phi(p_2)$ is considered. This analysis should be carried out to all orders in the power counting. As discussed above it is sufficient to include two-particle interactions only. The NREFT Lagrangian can be written as

$$\mathcal{L} = \phi^\dagger \left(\mathrm{i}\partial_t - M + \frac{\nabla^2}{2M} + \frac{\nabla^4}{8M^3} + \ldots \right) \phi + \mathcal{L}_2 \,, \tag{3.4}$$

where the terms in brackets reproduce the relativistic energy-momentum relation order by order.

Furthermore, $\mathcal{L}_2 = \mathcal{L}_2^{(0)} + \mathcal{L}_2^{(2)} + \ldots$ is the Lagrangian in the two-particle sector, where the superscript denotes the order in the power counting. For example, $\mathcal{L}_2^{(0)}$ is the two-body term given in Eq. (3.1). In order to determine higher order terms, it should be pointed out that, due to the reduction of Poincare symmetry to conservation of total three-momentum $\mathbf{P} = \mathbf{p}_1 + \mathbf{p}_2 = \mathbf{q}_1 + \mathbf{q}_2$ and rotational invariance in the NREFT setup, the two-particle amplitude can depend on six[2] invariants, which may be chosen as:

$$\mathbf{P}^2, \quad \mathbf{p}^2, \quad \mathbf{q}^2, \quad \mathbf{Pp}, \quad \mathbf{Pq}, \quad \mathbf{pq} \,. \tag{3.5}$$

Here $\mathbf{q} = (\mathbf{q}_1 - \mathbf{q}_2)/2$ and $\mathbf{p} = (\mathbf{p}_1 - \mathbf{p}_2)/2$ denote the relative momentum of the in- and out-going states. Since identical bosons are considered here the three last most operators can only appear in even powers. For example, while for $\phi(p_1) \leftrightarrow \phi(p_2)$ the relative momentum acquires a sign, $\mathbf{p} \to -\mathbf{p}$, the total momentum remains unchanged, $\mathbf{P} \to \mathbf{P}$. Furthermore, hermiticity constraints the operators constructed from the set of invariants Eq. (3.5) to be symmetric with respect to the exchange of $\mathbf{p} \leftrightarrow \mathbf{q}$.

[1] Here the limit $x^0 \to y^0$ with $x^0 > y^0$ should be considered. For $x^0 < y^0$ the integral is vanishing as discussed before.

[2] The 12 degrees of freedom from the four three-momenta $\mathbf{p}_i$ and $\mathbf{q}_j$ are reduced by the three generators of space translation (corresponding to the conservation of total three-momentum $\mathbf{P}$) and another three from the generator of rotations.

Hence, at next-to-leading order (NLO), the two-particle Lagrangian can be written as

$$\mathcal{L}_2^{(2)} = C_1 \left(\phi^\dagger \phi^\dagger \left(\phi \overleftrightarrow{\nabla}^2 \phi \right) + \text{h.c.} \right) + C_2 \left(\phi^\dagger \phi^\dagger \nabla^2 (\phi\, \phi) + \text{h.c.} \right), \tag{3.6}$$

where $\overleftrightarrow{\nabla} = (\overrightarrow{\nabla} - \overleftarrow{\nabla})/2$ is the Galilean invariant derivative, with arrows indicating the derivatives acting on the left or right field. The construction of the higher order Lagrangian proceeds in a similar manner by building polynomials in terms of the operators defined in Eq. (3.5), which are generated by derivatives in position space.

At order $O(\epsilon^4)$ also *off-shell terms* can be written down:

$$O^{(4)}_{\text{off-shell}} = \phi^\dagger \phi^\dagger \left(\phi \overleftrightarrow{\nabla}^4 \phi \right) - \left(\phi^\dagger \overleftrightarrow{\nabla}^2 \phi^\dagger \right) \left(\phi \overleftrightarrow{\nabla}^2 \phi \right) + \text{h.c.} \tag{3.7}$$

The corresponding momentum space expression is given by

$$(\mathbf{p}^2 - \mathbf{q}^2)^2, \tag{3.8}$$

which clearly vanishes if the momenta are taken on-shell, as for $P^0 = E_{\mathbf{p}_1} + E_{\mathbf{p}_2} = E_{\mathbf{q}_1} + E_{\mathbf{q}_1}$, where $E_{\mathbf{k}} = M + \mathbf{k}^2/(2M)$:

$$\mathbf{p}^2 = \mathbf{q}^2 = (q^*)^2 = M \left(P^0 - 2M - \frac{\mathbf{P}^2}{4M} \right). \tag{3.9}$$

Therefore, at tree-level off-shell operators do not contribute. In fact this statement is true to all orders, as can be seen by evaluating the following loop integral

$$I = \int \frac{d^D k}{(2\pi)^D \mathrm{i}} \frac{(\mathbf{k}^2 - \mathbf{q}^2)^2}{\left(E_{\frac{\mathbf{P}}{2}+\mathbf{k}} - \frac{P^0}{2} - k^0 - \mathrm{i}\varepsilon \right) \left(E_{\frac{\mathbf{P}}{2}-\mathbf{k}} - \frac{P^0}{2} + k^0 - \mathrm{i}\varepsilon \right)}, \tag{3.10}$$

that corresponds to a two-particle loop with one insertion of the off-shell vertex. Above dimensional regularization is used and D denotes the number of space-time dimensions. Performing the k^0 integration explicitly

$$I = m \int \frac{d^d k}{(2\pi)^d} \frac{(\mathbf{k}^2 - \mathbf{q}^2)^2}{\mathbf{k}^2 - q^{*2}}, \tag{3.11}$$

where $d = D - 1$ and $(q^*)^2$ is given as in Eq. (3.9). Clearly, if the external momentum is on-shell, $\mathbf{q}^2 = (q^*)^2$, the denominator is canceled and the integral vanishes in dimensional regularization. As the result is scheme-independent, indeed off-shell terms do not contribute even at loop-level.

The unknown LECs, appearing as coupling constants in the Lagrangian $\mathcal{L}_2$, must be expressed in terms of physical obervables in order to obtain a meaningful theory. This could be achieved by matching the amplitude obtained in the NREFT to the relativistic one of the underlying model. The

matching condition for the (on-shell) two-body scattering amplitudes reads as

$$T_{\mathrm{NR}}(\mathbf{p}_1,\mathbf{p}_2;\mathbf{q}_1,\mathbf{q}_2) = \prod_{i=1}^{2} \left(2w(\mathbf{p}_i)2w(\mathbf{q}_i)\right)^{-1/2} T_{\mathrm{R}}(\mathbf{p}_1,\mathbf{p}_2;\mathbf{q}_1,\mathbf{q}_2)\,, \tag{3.12}$$

where T_{NR} and T_{R} denote the non-relativistic and relativistic amplitude respectively. The factors containing the relativistic energy of the particles arise due to the different normalizations of one-particle states:

$$\begin{aligned} \langle \mathbf{p}|\mathbf{q}\rangle &= (2\pi)^3\delta^3(\mathbf{p}-\mathbf{q}), && \text{non-relativisitc}\,, \\ \langle \mathbf{p}|\mathbf{q}\rangle &= (2\pi)^3\, 2w(\mathbf{p})\,\delta^3(\mathbf{p}-\mathbf{q}), && \text{relativisitc}\,. \end{aligned} \tag{3.13}$$

The matching proceeds by adjusting the LECs, appearing in the explicit expression of the non-relativistic amplitude, such that Eq. (3.12) is obeyed up to a given order, expanding both left- and right-hand side in a series of the three-momenta. Although this procedure allows to take into account relativistic effects systematically, at higher orders the matching in an arbitrary moving frame is rather inconvenient as the matching condition is explicitly frame dependent.

In the two-particle sector, explicit Lorentz-covariance can be restored within a slightly modified non-relativistic framework [148, 166, 167]. In order to achieve this, first of all, relativistic insertions should be summed up to all orders. Moreover, to account for the different normalizations of the particle states, a rescaling of the non-relativistic fields is performed: $\phi(x) \to \sqrt{2w(x)}\phi(x)$, where $w(x) = \sqrt{M^2-\nabla^2}$. The *equivalence theorem* [168–171] guarantees that the S-matrix elements obtained from the redefined field theory coincide with the original ones. Due to the modification above, in this *covariant NREFT* approach, the matching condition takes a Lorentz-invariant form, $T_{\mathrm{NR}}(\mathbf{p}_1,\mathbf{p}_2;\mathbf{q}_1,\mathbf{q}_2) = T_{\mathrm{R}}(\mathbf{p}_1,\mathbf{p}_2;\mathbf{q}_1,\mathbf{q}_2)$.

After summing up relativistic insertions to all orders, the Lagrangian describing the two-particle sector is given by

$$\mathcal{L} = \phi^\dagger 2w(\mathrm{i}\partial_t - w)\phi + \mathcal{L}_2\,, \tag{3.14}$$

where $\mathcal{L}_2 = \mathcal{L}_2^{(0)} + \mathcal{L}_2^{(2)} + \ldots$ contains all Lorentz-invariant four-particle operators of different orders $O(\epsilon^i)$ in the power counting scheme. Up to NLO

$$\mathcal{L}_2 = C_0\phi^\dagger\phi^\dagger\phi\,\phi + C_2\left((w_\mu\phi)^\dagger(w^\mu\phi)^\dagger\phi\,\phi - M^2\phi^\dagger\phi^\dagger\phi\,\phi + \text{h.c.}\right)\,, \tag{3.15}$$

where $w^\mu = (w, \mathrm{i}\nabla)$ and $w = \sqrt{M^2-\nabla^2}$.

As a consequence of the resummation of relativistic corrections, the hard scale M is present in the propagator. In order to avoid the breaking of the counting rules introduced in the preceding section, calculations of loop diagrams require choosing an additional renormalization prescription. Within the particular prescreption chosen here, referred to as the *threshold expansion* [172], the integrand of a generic loop integral is expanded in a series of inverse powers of the hard scale M in a first step. These terms are integrated individually in dimensional regularization and the result is summed up to all orders afterwards.

For the two-body loop integral[3] in a reference frame with CM momentum P^μ

$$\begin{aligned} I(P) &= \int \frac{d^d k_1}{(2\pi)^d 2w(\mathbf{k}_1)} \frac{d^d k_2}{(2\pi)^d 2w(\mathbf{k}_2)} \frac{(2\pi)^d \delta^d(\mathbf{P}-\mathbf{k}_1-\mathbf{k}_2)}{w(\mathbf{k}_1)+w(\mathbf{k}_2)-P^0-\mathrm{i}\varepsilon} \\ &= \int \frac{d^d k}{(2\pi)^d} \frac{1}{4w(\mathbf{k})w(\mathbf{P}-\mathbf{k})} \frac{1}{w(\mathbf{k})+w(\mathbf{P}-\mathbf{k})-P^0-\mathrm{i}\varepsilon}, \end{aligned} \tag{3.16}$$

this procedure can be carried out practically using the identity[4]

$$\begin{aligned} &\frac{1}{4w_1 w_2}\left\{\frac{1}{w_1+w_2-P^0}-\frac{1}{w_1+w_2+P^0}+\frac{1}{w_1-w_2+P^0}-\frac{1}{w_1-w_2-P^0}\right\} \\ &\qquad = \frac{1}{2P^0}\frac{1}{\mathbf{k}^2-(\mathbf{kP}/P^0)^2-(q^*)^2}, \end{aligned} \tag{3.17}$$

where $w_1 = w(\mathbf{P}/2+\mathbf{k})$ and $w_2 = w(\mathbf{P}/2-\mathbf{k})$, while $(q^*)^2 = s/4 - M^2$ and $s = P^2 = (P^0)^2 - \mathbf{P}^2$. Expanding the last three terms on the left hand side of Eq. (3.17) in inverse powers of M only gives a polynomial in momenta. Therefore, after shifting the integration variable, $\mathbf{k} \to \mathbf{k} + \mathbf{P}/2$, adding and subtracting these terms to Eq. (3.16), the threshold expansion allows to rewrite the loop integral in a form without explicit dependence on the hard scale M:

$$I(P) = \frac{1}{2P^0}\int \frac{d^d k}{(2\pi)^d} \frac{1}{\mathbf{k}^2-(\mathbf{kP}/P^0)^2-(q^*)^2}. \tag{3.18}$$

Introducing parallel and perpendicular components of the integration momentum with respect to $\mathbf{P}$:

$$\mathbf{k} = \frac{\mathbf{P}}{|\mathbf{P}|}k_\parallel + \mathbf{k}_\perp, \quad k_\parallel = \frac{\mathbf{kP}}{|\mathbf{P}|}, \tag{3.19}$$

the remaining integral can be evaluated and yields:

$$I(P) = \frac{\mathrm{i}q^*}{8\pi\sqrt{s}}. \tag{3.20}$$

Indeed the result is of order $O(\epsilon)$ in agreement with the naive counting rules and coincides with the imaginary part of its relativistic counterpart. Furthermore, it can be seen that applying the threshold expansion, the loop function $I(P) \equiv I(P^2)$ is given by a Lorentz-invariant expression. Moreover, it should be pointed out that only the absorptive part of the integral survives, the replacement

$$\frac{1}{w_1+w_2-P^0-\mathrm{i}\varepsilon} \to \mathrm{i}\pi\delta\left(w_1+w_2-P^0\right) \tag{3.21}$$

is thus justified.

As discussed in the last paragraph of the preceding section, due to the properties of NREFTs all loop

[3] The k_i^0 integrations have already been performed here.

[4] For notational convenience the $\mathrm{i}\varepsilon$ prescription may be used implicitly.

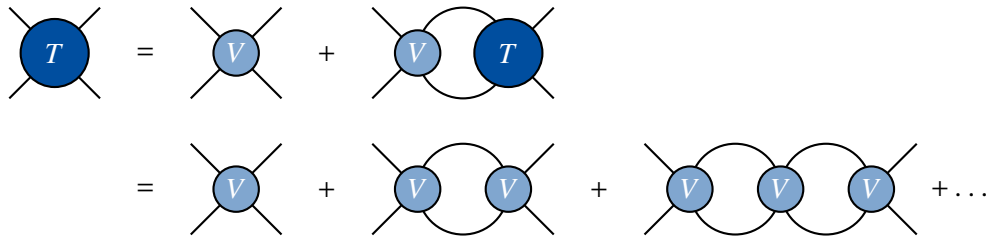

Figure 3.1: Diagrammatic representation of the Lippmann-Schwinger equation for the amplitude T in the non-relativistic EFT. The second line represents the Born series of the amplitude, summed to all orders. The two-particle scattering amplitude is merely given by the bubble sum over elementary loops $I(P)$ with an interaction given by the potential V at each vertex.

diagrams in the two-particle sector can be expressed in terms of the elementary bubble integral $I(P)$ given in Eq. (3.16). This leads to drastic simplifications in the calculation of the two-body scattering amplitude $T_{\rm NR} \equiv T$, which obeys the Lippmann-Schwinger equation of the form:

$$\begin{aligned} T(\mathbf{p}_1,\mathbf{p}_2;\mathbf{q}_1,\mathbf{q}_2) = &- V(\mathbf{p}_1,\mathbf{p}_2;\mathbf{q}_1,\mathbf{q}_2) - \frac{1}{2}\int \frac{d^d k_1}{(2\pi)^d 2w(\mathbf{k}_1)}\frac{d^d k_2}{(2\pi)^d 2w(\mathbf{k}_2)} \\ &\times V(\mathbf{p}_1,\mathbf{p}_2;\mathbf{k}_1,\mathbf{k}_2)\,\frac{(2\pi)^d\delta^d(\mathbf{p}_1+\mathbf{p}_2-\mathbf{k}_1-\mathbf{k}_2)}{w(\mathbf{k}_1)+w(\mathbf{k}_2)-P^0-\mathrm{i}\varepsilon}\,T(\mathbf{k}_1,\mathbf{k}_2;\mathbf{q}_1,\mathbf{q}_2)\,, \end{aligned} \tag{3.22}$$

where $P^0 = w(\mathbf{q}_1) + w(\mathbf{q}_2)$. Diagrammatically this can be represented as in Fig. 3.1. The potential V is given by the matrix elements of the interaction Hamiltonian

$$(2\pi)^d\delta^d(\mathbf{p}_1+\mathbf{p}_2-\mathbf{q}_1-\mathbf{q}_2)V(\mathbf{p}_1,\mathbf{p}_2;\mathbf{q}_1,\mathbf{q}_2) = \langle \mathbf{p}_1,\mathbf{p}_2|H_I|\mathbf{q}_1,\mathbf{q}_2\rangle \tag{3.23}$$

and is a Lorentz-invariant polynomial. For instance, using Eq. (3.15), up to NLO the potential is given by:

$$-V(\mathbf{p}_1,\mathbf{p}_2;\mathbf{q}_1,\mathbf{q}_2) = 4C_0 + 4C_2\left((p_1\cdot p_2)+(q_1\cdot q_2)-2M^2\right), \tag{3.24}$$

with on-shell four-momenta p_i and q_j.

Defining the CM and relative four-momenta $P = p_1 + p_2 = q_1 + q_2$, $p = (p_1 - p_2)/2$ and $p = (q_1 - q_2)/2$, the partial wave expansion of the potential V can be performed in the rest frame:

$$V(\mathbf{p}_1,\mathbf{p}_2;\mathbf{q}_1,\mathbf{q}_2) = 4\pi\sum_{\ell m}\mathcal{Y}_{\ell m}(\mathbf{p}^*)v_\ell(|\mathbf{p}^*|,|\mathbf{q}^*|)\mathcal{Y}^*_{\ell m}(\mathbf{q}^*), \tag{3.25}$$

where

$$\begin{aligned} \mathbf{p}^* &= \mathbf{p} + \mathbf{P}\left((\gamma-1)\frac{\mathbf{pP}}{\mathbf{P}^2} - \gamma v\frac{p^0}{|\mathbf{P}|}\right), \\ \mathbf{q}^* &= \mathbf{q} + \mathbf{P}\left((\gamma-1)\frac{\mathbf{qP}}{\mathbf{P}^2} - \gamma v\frac{q^0}{|\mathbf{P}|}\right), \end{aligned} \tag{3.26}$$

with $v = |\mathbf{P}|/P^0$ and $\gamma = (1-v^2)^{-1/2}$, denote the relative three-momenta boosted into the rest frame respectively and $\mathcal{Y}_{\ell m}(\mathbf{p}) = |\mathbf{p}|^\ell Y_{\ell m}(\hat{\mathbf{p}})$ is given in terms of the spherical harmonics $Y_{\ell m}$. Applying a similar expansion to the scattering amplitude, the Lippmann-Schwinger equation in the partial wave ℓ is given by:

$$\begin{aligned} t_\ell(|\mathbf{p}^*|,|\mathbf{q}^*|) = &- v_\ell(|\mathbf{p}^*|,|\mathbf{q}^*|) - \frac{1}{2}\int \frac{d^d k_1}{(2\pi)^d 2w(\mathbf{k}_1)} \frac{d^d k_2}{(2\pi)^d 2w(\mathbf{k}_2)} 4\pi \mathcal{Y}_{\ell m}(\mathbf{k}^*)\mathcal{Y}^*_{\ell m}(\mathbf{k}^*) \\ &\times v_\ell(|\mathbf{p}^*|,|\mathbf{k}^*|) \frac{(2\pi)^d \delta^d(\mathbf{P}_1-\mathbf{k}_1-\mathbf{k}_2)}{w(\mathbf{k}_1)+w(\mathbf{k}_2)-P^0-\mathrm{i}\varepsilon} t_\ell(|\mathbf{k}^*|,|\mathbf{q}^*|), \end{aligned} \tag{3.27}$$

where $\mathbf{k}^*$ is the relative three-momentum $\mathbf{k} = (\mathbf{k}_1 - \mathbf{k}_2)/2$ boosted into the rest frame. As discussed above, only the absorptive part of the integrand contributes when using dimensional regularization in combination with the threshold expansion. One may replace

$$\frac{\delta^d(\mathbf{p}_1+\mathbf{p}_2-\mathbf{k}_1-\mathbf{k}_2)}{w(\mathbf{k}_1)+w(\mathbf{k}_2)-P^0-\mathrm{i}\varepsilon} \to \mathrm{i}\pi\delta^D(P-k_1-k_2) = \mathrm{i}\pi\delta^D(P^*-k_1^*-k_2^*)\,. \tag{3.28}$$

Moreover, since the integral measures in the above equation are also Lorentz-invariant, the integrals might be evaluated in the CM frame. Using the properties of the delta-distribution and spherical harmonics the Lippmann-Schwinger equation reduces to an algebraic relation for the partial-wave scattering amplitudes:

$$t_\ell(|\mathbf{p}^*|,|\mathbf{q}^*|) = -v_\ell(|\mathbf{p}^*|,|\mathbf{q}^*|) - \mathrm{i}\,\frac{(q^*)^{2\ell+1}}{16\pi\sqrt{s}}\, v_\ell(|\mathbf{p}^*|,q^*)\, t_\ell(q^*,|\mathbf{q}^*|), \tag{3.29}$$

where $(q^*)^2 = s/4 - M^2$ amd $s = P^{*2} = P^2$. Thus, on the energy shell where $|\mathbf{q}^*| = |\mathbf{p}^*| = q^*$, the non-relativistic two-body scattering amplitude $t_\ell(s) = t_\ell(q^*,q^*)$ is given by:

$$t_\ell(s) = \frac{16\pi\sqrt{s}(q^*)^{-2\ell}}{-16\pi\sqrt{s}(q^*)^{-2\ell} v_\ell^{-1}(s) - \mathrm{i}q^*}\,. \tag{3.30}$$

This amplitude should be matched to its relativistic counterpart, which allows to fix the values of the LECs C_i, appearing in the potential $v_\ell(s) = v_\ell(q^*,q^*)$. As the relativistic amplitude obeys the unitarity condition[5] Eq. (2.53), demanding that it should be equal to the NREFT amplitude $t_\ell(s)$ yields the condition

$$v_\ell(s) = -\frac{16\pi\sqrt{s}}{(q^*)^{2\ell+1}} \tan\delta_\ell(s)\,. \tag{3.31}$$

Therefore the LECs are completely determined by the phase shifts δ_ℓ of the underlying model. In the vicinity of the threshold $s = 4M^2$, where the NREFT is applicable, it is advantageous to make use of the effective range expansion Eq. (2.54). Expanding the right hand side of Eq. (3.31) around threshold will lead to a polynomial in $s - 4M^2$. As $v_\ell(s)$ is a polynomial in the same argument, the matching of the LECs can be performed conveniently by comparing the expansion coefficients. For

[5] Note the different normalization in the partial wave expansions, due to $\mathcal{Y}_{\ell m}(\mathbf{p}) = |\mathbf{p}|^\ell Y_{\ell m}(\hat{\mathbf{p}})$.

example, up to NLO only $\ell = 0$ contributes:

$$\begin{aligned} v_0(s) &= -4C_0 - 4C_2\,(s - 4M^2) + \dots\,, \\ -\frac{16\pi\sqrt{s}}{q^*}\tan\delta_0(s) &= -32\pi a_0 M - 4\pi a_0^2 M\left(r_0 + \frac{1}{a_0 M^2}\right)(s - 4M^2) + \dots\,. \end{aligned} \tag{3.32}$$

One can read off:

$$C_0 = 8\pi a_0 M\,, \quad C_2 = \pi a_0^2 M\left(r_0 + \frac{1}{a_0 M^2}\right). \tag{3.33}$$

The advantages of the covariant formulation of the NREFT approach become clear now. Not only does it relax the condition of the scattering particles moving non-relativistically. It further provides an explicitly Lorentz-invariant matching condition that allows to express the LECs in terms of the parameters of the underlying model in a very convenient way. In order to stress this point, one may define the relativistic K-matrix

$$K(\mathbf{p}_1, \mathbf{p}_2; \mathbf{q}_1, \mathbf{q}_2) = 4\pi \sum_{\ell m} \mathcal{Y}_{\ell m}(\mathbf{p}) k_\ell(s) \mathcal{Y}^*_{\ell m}(\mathbf{q})\,, \quad k_\ell(s) = -\frac{16\pi\sqrt{s}}{(q^*)^{2\ell+1}}\tan\delta_\ell(s)\,. \tag{3.34}$$

The matching condition Eq. (3.31) implies that

$$K(\mathbf{p}_1, \mathbf{p}_2; \mathbf{q}_1, \mathbf{q}_2) = V(\mathbf{p}_1, \mathbf{p}_2; \mathbf{q}_1, \mathbf{q}_2)\,. \tag{3.35}$$

Repeating a similar derivation in the original NREFT formalism on the other hand gives

$$K(\mathbf{p}_1, \mathbf{p}_2; \mathbf{q}_1, \mathbf{q}_2) = \prod_{i=1}^{2} \left(2w(\mathbf{p}_i) 2w(\mathbf{q}_i)\right)^{1/2} V_{\mathrm{NR}}(\mathbf{p}_1, \mathbf{p}_2; \mathbf{q}_1, \mathbf{q}_2)\,. \tag{3.36}$$

Again, the appearance of factors containing the relativistic energy is related to the different normalizations of relativistic and non-relativistic particle states. In Eq. (3.35), both K and the potential V in the covariant NREFT are Lorentz-invariant polynomials in the variables s and $(p \cdot q)$. This allows to relate the LECs, appearing in V, in a one-to-one correspondence to the parameters of the underlying model, present in the expansion of K. This is not the case in Eq. (3.36), as V_{NR} is not a Lorentz-invariant quantity, for which the factors $\left(2w(\mathbf{p}_i)2w(\mathbf{q}_i)\right)^{-1/2}$ account for. Instead it is a polynomial in the variables build from the invariants defined in Eq. (3.5), such that hermiticity and Bose-symmetry is obeyed in case of three identical bosons. This leads to an inflation of couplings. Hence the original approach leads to the inclusion of redundant parameters, obeying certain constraints.

Now one should keep in mind that the aim is to extract the parameters of QCD, governing the finite-volume spectra obtained from lattice calculations, using a quantization condition derived in a NREFT framework. Without performing the matching Eq. (3.36), in the original NREFT formalism the quantization condition contains superfluous parameters, deteriorating the quality of the fit to the energy spectrum. As the number of redundancies will grow fast when going to higher orders and the matching becomes tedious at the same time, using the modified covariant approach represents a great advantage. As described above, here the number of fit parameters, the LECs in V, are in a one-to-one

correspondence with the parameters of the underlying model, the coefficients in the K-matrix that describes the QCD process under consideration. Finally, a quantization condition that is valid in arbitrary moving frames at the same time, which is of practical importance for lattice calculations, can not be established in a non-covariant framework. Therefore in the next section, such a quantization condition will be derived in the modified covariant NREFT formalism.

3.2.2 Derivation of Lüscher's Equation in the NREFT Formalism

The general idea of applying the NREFT approach to the analysis of LQCD data is to derive quantization conditions that determine the finite-volume energy spectra. Here the unknown LECs appear as parameters that can be fixed by a fit to the spectra, measured in lattice calculations. In return, using the values of the LECs found in this manner, allows for the calculation of infinite-volume quantities from the NREFT Lagrangian. This procedure enables the extraction of infinite-volume QCD observables from LQCD data. As discussed in the previous paragraph, the covariant NREFT approach provides a convenient matching condition between the LECs and the physical observables of the underlying model that appear in the ERE. Moreover the effective range parameters fully determine the two-body scattering amplitude. Therefore, in the two-particle sector, the calculation of infinite-volume observables from the NREFT Lagrangian can be skipped.

However, the lattice must obey certain conditions such that an EFT treatment can be utilized. In the following a Euclidean lattice with extend L in all spatial directions and large temporal elongation T is considered. Assuming periodic boundary conditions, the momenta are quantized according to Eq. (2.47). Furthermore, the lattice spacing a and the box length L should be chosen such that $1/L \ll \Lambda \ll 1/a$, where Λ is the hard scale of the process under consideration. This condition allows to study finite-volume effects, that are of characteristic scale $1/L$, independently from other lattice artifacts: Since $1/L \ll 1/a$ one can effectively work in the continuum limit $a \to 0$. Moreover, as $1/L \ll \Lambda$, the EFTs in the finite and infinite volume coincide; the LECs encoding the UV dynamics at the scale Λ or higher are not effected by the IR effects of order $1/L$. Such a lattice setup is crucial in order to apply the EFT approach to the study of finite-volume effects.

The derivation of the quantization condition presented here closely follows Refs. [50, 70]. Formally a scattering amplitude does not exists in a finite volume, since asymptotic states can not be defined. However, the LQCD correlation functions used to determine the finite-volume energy spectra, see e.g. Eq. (2.72), can be calculated in an EFT framework. Considering identical particles, one may define the following two-particle interpolator[6]:

$$O(\mathbf{P},\mathbf{q};t) = \int_{-L/2}^{L/2} d^3\mathbf{x}_1 d^3\mathbf{x}_2 \, \mathrm{e}^{-\mathrm{i}(\mathbf{P}-\mathbf{q})\mathbf{x}_1 - \mathrm{i}\mathbf{q}\mathbf{x}_2} \, \phi(t,\mathbf{x}_1)\phi(t,\mathbf{x}_2)\,. \tag{3.37}$$

In NREFT, the correlator[7] to extract energy levels can be evaluated diagrammatically as represented

[6] In the EFT analysis of LQCD data the continuum limit is applied, such that spatial integrals appear in the definition of the interpolating fields.

[7] The calculation here is performed in Minkowski space. One may use a Wick rotation in order to relate the result to the LQCD correlator.

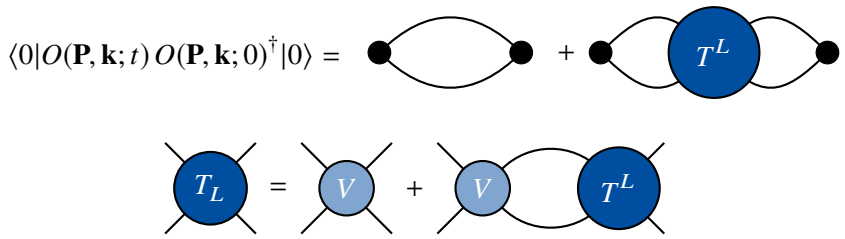

Figure 3.2: Correlation function in the NREFT. Black dots denote two-particle interpolators, while the lines correspond to a particle propagator. The amplitude T_L obeys the Lippmann-Schwinger equation with potential V as displayed in the second line. The two-particle loop should be understood to be evaluated as a finite-volume sum.

in Fig. 3.2:

$$\langle 0|O(\mathbf{P},\mathbf{q};t)O(\mathbf{P},\mathbf{q};0)^\dagger|0\rangle = \int \frac{dP^0}{2\pi \mathrm{i}}\, \mathrm{e}^{-\mathrm{i}P^0 t}\left\{ \frac{L^6(1+\delta_{\mathbf{q},\mathbf{P}-\mathbf{q}})}{4w(\mathbf{q})w(\mathbf{P}-\mathbf{q})(w(\mathbf{q})+w(\mathbf{P}-\mathbf{q})-P^0-\mathrm{i}\varepsilon)} + \frac{L^3 T^L(\mathbf{q},\mathbf{P}-\mathbf{q};\mathbf{q},\mathbf{P}-\mathbf{q})}{(4w(\mathbf{q})w(\mathbf{P}-\mathbf{q})(w(\mathbf{q})+w(\mathbf{P}-\mathbf{q})-P^0-\mathrm{i}\varepsilon))^2} \right\}. \tag{3.38}$$

Here the amplitude T^L obeys a similar Lippmann-Schwinger equation as its infinite-volume counterpart T. The only difference comes from the two-body loop function, where the infinite volume integration should be replaced by a sum over the qunatized finite-volume momenta. Thus T^L will be referred to as the finite-volume scattering amplitude.

Following the preceding discussion, the potential V is an infinite-volume quantity since it is fully determined by the LECs of the EFT that coincide[8] in the infinite and finite volume. Thus the partial wave expansion in Eq. (3.25) still holds. On the other hand, as rotational symmetry is explicitly broken in the finite volume, the expansion of the scattering amplitude takes the form

$$T^L(\mathbf{p}_1,\mathbf{p}_2;\mathbf{q}_1,\mathbf{q}_2) = 4\pi \sum_{\ell m} \mathcal{Y}_{\ell m}(\mathbf{p}^*) t_{\ell m,\ell' m'}(|\mathbf{p}^*|,|\mathbf{q}^*|;\mathbf{P}) \mathcal{Y}^*_{\ell m}(\mathbf{q}^*)\,. \tag{3.39}$$

In the finite volume, using the Feynman rules, on the energy shell the Lippmann-Schwinger equation for the finite-volume scattering amplitudes reads as

$$t_{\ell m,\ell' m'}(s;\mathbf{P}) = -\delta_{\ell\ell'}\delta_{mm'} v_\ell(s) - \frac{1}{2} 4\pi \sum_{\ell'',m''} v_\ell(s) \chi_{\ell m,\ell'' m''}(s;\mathbf{P}) t_{\ell'' m'',\ell' m'}(s;\mathbf{P}), \tag{3.40}$$

where

$$\chi_{\ell m,\ell' m'}(s;\mathbf{P}) = \frac{1}{L^3} \sum_{\mathbf{k}_1 = 2\pi/L\mathbf{n}} \frac{\mathcal{Y}^*_{\ell m}(\mathbf{k}^*)\mathcal{Y}_{\ell' m'}(\mathbf{k}^*)}{4w(\mathbf{k}_1)w(\mathbf{P}-\mathbf{k}_1)(w(\mathbf{k}_1)+w(\mathbf{P}-\mathbf{k}_1)-P^0)}, \tag{3.41}$$

[8] The LECs coincide up to exponentially small corrections of order $O(\mathrm{e}^{-\Lambda L})$ which will be dropped due to the assumption $1/L \ll \Lambda$.

is the finite-volume version of the bubble integral (including the spherical functions from the partial wave projections). Above, $\mathbf{k}^*$ denotes the relative three-momentum boosted into the CMS. Making use of the identity Eq. (3.17) it can be seen that, up to exponentially suppressed terms

$$\mathcal{X}_{\ell m,\ell' m'}(s;\mathbf{P}) = \frac{1}{2P^0}\frac{1}{L^3}\sum_{\mathbf{k}=\mathbf{k}_1-\mathbf{P}/2}\frac{\mathcal{Y}^*_{\ell m}(\mathbf{k}^*)\mathcal{Y}_{\ell' m'}(\mathbf{k}^*)}{\mathbf{k}^2-(\mathbf{k}\mathbf{P}/P^0)^2-(q^*)^2}\,. \tag{3.42}$$

The validity of the equation above can be confirmed by noting that the last three terms on the left hand side of Eq. (3.17) are analytic in the physical region. Therefore, by Poissons summation formula, the sum over $\mathbf{k}_1$ of thee three individual terms is equal to the corresponding integral up to exponential corrections in the volume L. Applying the threshold expansion, in dimensional regularization these integrals vanish. To further simplify the expression one may define parallel and perpendicular components of the momentum with respect to $\mathbf{P}$:

$$\mathbf{k}^* = (k^*_\parallel, \mathbf{k}^*_\perp), \quad k^*_\parallel = (\gamma^*)^{-1}k_\parallel, \quad \mathbf{k}^*_\perp = \mathbf{k}_\perp, \quad \gamma^* = (1-(v^*)^2)^{-1/2}, \quad v^* = \frac{|\mathbf{P}|}{E^*}, \tag{3.43}$$

where $E^* = 2w(\mathbf{k}^*)$. On-shell $E^* = P^0$, such that $\mathbf{k}^* = (\gamma^{-1}k_\parallel, \mathbf{k}_\perp) \equiv \mathbf{r}$ with $\gamma = (1-(|\mathbf{P}|/P^0)^2)^{-1/2} = P^0/\sqrt{s}$. Thus

$$\mathcal{X}_{\ell m,\ell' m'}(s;\mathbf{P}) = \frac{1}{2P^0}\frac{1}{L^3}\sum_{\mathbf{r}\in P_\mathbf{d}}\frac{\mathcal{Y}^*_{\ell m}(\mathbf{r})\mathcal{Y}_{\ell' m'}(\mathbf{r})}{\mathbf{r}^2-(q^*)^2}\,, \tag{3.44}$$

where $P_\mathbf{d} = \left\{\mathbf{r}\in\mathbb{R}^3 \middle| r_\parallel = \gamma^{-1}(n_\parallel - |\mathbf{d}|/2),\ \mathbf{r}_\perp = \mathbf{n}_\perp,\ \mathbf{n}\in\mathbb{Z}^3\right\}$ with $\mathbf{d} = L/(2\pi)\mathbf{P}$. Using the well known multiplication rules for spherical harmonics

$$\mathcal{Y}^*_{\ell m}(\mathbf{r})\mathcal{Y}_{\ell' m'}(\mathbf{r}) = \frac{1}{\sqrt{4\pi}}\sum_{j=|\ell-\ell'|}^{\ell+\ell'}\sum_{s=-j}^{j}\mathrm{i}^{j-\ell-\ell'}|\mathbf{r}|^{\ell+\ell'-j}C_{\ell m,js,\ell'' m''}\mathcal{Y}^*_{js}(\mathbf{r}), \tag{3.45}$$

where $C_{\ell m,js,\ell'' m''}$ is expressed in terms of the Wigner $3j$-symbol, see Eq. (2.50). Now noting that $|\mathbf{r}|^{\ell+\ell'-j} - (q^*)^{\ell+\ell'-j} = (|\mathbf{r}|^2-(q^*)^2)\times$(polyomial in $|\mathbf{r}|^2$) in Eq. (3.45), canceling the denominator in Eq. (3.44), one may replace $|\mathbf{r}|^{\ell+\ell'-j}\to(q^*)^{\ell+\ell'-j}$, as the difference is only exponentially small in the volume L. After some rearrangement one arrives at the expression

$$\begin{aligned}
\mathcal{X}_{\ell m,\ell' m'}(s;\mathbf{P}) &= \frac{(q^*)^{\ell+\ell'+1}}{32\pi^2\sqrt{s}}\mathrm{i}^{\ell-\ell'}\mathcal{M}_{\ell m,\ell' m'}(s;\mathbf{P}),\\
\mathcal{M}_{\ell m,\ell' m'}(s,\mathbf{P};L) &= \frac{(-1)^\ell}{\pi^{3/2}\gamma}\sum_{j=|\ell-\ell'|}^{\ell+\ell'}\sum_{s=-j}^{j}\frac{\mathrm{i}^j}{\eta^{j+1}}C_{\ell m,js,\ell' m'}Z^\mathbf{d}_{js}(1;s),\\
C_{\ell m,js,\ell' m'} &= (-1)^{m'}i^{\ell-j+\ell'}\sqrt{(2\ell+1)(2j+1)(2\ell'+1)}\begin{pmatrix}\ell & j & \ell'\\ m & s & -m'\end{pmatrix}\begin{pmatrix}\ell & j & \ell'\\ 0 & 0 & 0\end{pmatrix},
\end{aligned} \tag{3.46}$$

where $\eta = q^* L/(2\pi)$ and

$$Z^{\mathbf{d}}_{\ell m}(1;s) = \sum_{\mathbf{r}\in P_{\mathbf{d}}} \frac{\mathcal{Y}_{\ell m}(\mathbf{r})}{r^2-\eta^2}, \quad P_{\mathbf{d}} = \left\{ \mathbf{r}\in\mathbb{R}^3 \middle| r_\parallel = \gamma^{-1}(n_\parallel - |\mathbf{d}|/2),\, \mathbf{r}_\perp = \mathbf{n}_\perp,\, \mathbf{n}\in\mathbb{Z}^3 \right\} \tag{3.47}$$

is the Lüscher Zeta-function.

The energy levels in the finite volume correspond to poles in the amplitudes $t_{\ell m,\ell' m'}(s;\mathbf{P})$ given as in Eq. (3.40). Expressing the potential in terms of the infinite-volume phase shift, see Eq. (3.31), these poles correspond to solutions of the equation

$$\begin{aligned} &\det A = 0\,, \\ &A_{\ell m,\ell' m'} = \delta_{\ell\ell'}\delta_{mm'}\cot\delta_\ell(s) - \mathcal{M}_{\ell m,\ell' m'}(s,\mathbf{P};L)\,. \end{aligned} \tag{3.48}$$

In summary, the modified NREFT framework enables a derivation of the two-body quantization condition that is valid in arbitrary moving frames in a very transparent way, keeping the bookkeeping of the Feynman diagrams trivial. Only the bubble diagram leading to the same non-regular L behavior as the relativistic s-channel loop is kept explicitly, while contributions of diagrams in the relativistic theory exhibiting an exponential L dependence are included in the values of the LECs from the beginning. These exponentially small corrections to the infinite-volume quantities are usually dropped throughout. Due to these convenient properties, the formulation in terms of a covariant NREFT seems to be suitable also for the analysis of more complicated processes. For example, further applications in the two-particle sector can be found in [50], deriving the Lellouch-Lüscher equation as well as providing a formalism that allows to extract matrix element of resonances coupling to an external field. The analysis of three-body LQCD data in a NREFT approach is the main scope of this thesis and will be discussed in the following sections. As it will turn out, further adjustments are required in order to derive a Lorentz-invariant three-particle quantization condition.

3.3 The Three-Particle Sector

3.3.1 Introduction of Dimer Fields

Having discussed the description of two-body dynamics within the NREFT formalism, the following section will turn towards the three-particle sector, aiming to derive a quantization condition.

Extracting the three-particle finite-volume energy levels in general requires a non-perturbative treatment of the three-body scattering amplitude. This especially applies to (the most interesting) processes where shallow bound states or resonances are present, such that a perturbative expansion, e.g. in the scattering length, fails. In that case a full resummation of the two-body sub-processes entering the expression for the three-body amplitude is needed. Such a treatment was already performed in the previous section, but a further simplification can be achieved by introducing auxiliary *dimer fields* [98, 173].

To keep the discussion simple, only the leading order should be considered first, where the Lagrangian for the three-body sector reads

$$\mathcal{L} = \phi^\dagger 2w(\mathrm{i}\partial_t - w)\phi + C_0\,\phi^\dagger\phi^\dagger\phi\,\phi + D_0\,\phi^\dagger\phi^\dagger\phi^\dagger\phi\,\phi\,\phi\,. \tag{3.49}$$

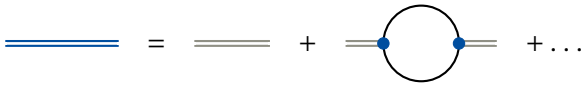

Figure 3.3: Graphical representation of the Dyson equation for the full dimer propagator (blue double line). The grey double line denotes the free dimer propagator σ while the blue dots represent the particle-dimer conversion vertex.

Instead, one might write down the following particle-dimer Lagrangian:

$$\mathcal{L}_d = \phi^\dagger 2w(\mathrm{i}\partial_t - w)\phi + \sigma T^\dagger T + \frac{f_0}{2}(T^\dagger\phi\phi + \text{h.c.}) + h_0 T^\dagger T\phi^\dagger\phi\,, \tag{3.50}$$

where $T(x)$ denotes the dimer field and $\sigma = \sigma^{-1} = \pm 1$ for reasons seen below. The dimer field can be integrated out int the path integral formalism:

$$\begin{aligned}\int \mathcal{D}T\mathcal{D}T^\dagger\ \exp\left\{\mathrm{i}\int d^4x\,\left(T^\dagger(\sigma + h_0\phi^\dagger\phi)T + \frac{f_0}{2}T^\dagger\phi\phi + \frac{f_0}{2}\phi^\dagger\phi^\dagger T\right)\right\}\\ = \exp\left\{-\mathrm{i}\int d^4x\, f_0^2\frac{\phi^\dagger\phi^\dagger\phi\phi}{4(\sigma + h_0\phi^\dagger\phi)}\right\}.\end{aligned} \tag{3.51}$$

The resulting expression can be expanded in powers of fields. Due to the separation of the different particle sectors, it is sufficient to drop terms of eight and more fields

$$-f_0^2\,\frac{\phi^\dagger\phi^\dagger\phi\phi}{4(\sigma + h_0\phi^\dagger\phi)} = -\sigma\frac{f_0^2}{4}\,\phi^\dagger\phi^\dagger\phi\,\phi + \frac{h_0 f_0^2}{4}\,\phi^\dagger\phi^\dagger\phi^\dagger\phi\,\phi\,\phi + \ldots \tag{3.52}$$

Indeed, if the conditions

$$C_0 = -\sigma\frac{f_0^2}{4}\,, \quad D_0 = \frac{h_0 f_0^2}{4}\,, \tag{3.53}$$

are fulfilled, the two theories are equivalent at tree level, i.e. the generating functional coincides

$$\begin{aligned}Z(j, j^\dagger) &= \int \mathcal{D}\phi\mathcal{D}\phi^\dagger\ \exp\left\{\mathrm{i}\int d^4x\,\left(\mathcal{L} + j^\dagger\phi + \phi^\dagger j\right)\right\}\\ &= \int \mathcal{D}\phi\mathcal{D}\phi^\dagger\mathcal{D}T\mathcal{D}T^\dagger\ \exp\left\{\mathrm{i}\int d^4x\,\left(\mathcal{L}_d + j^\dagger\phi + \phi^\dagger j\right)\right\},\end{aligned} \tag{3.54}$$

such that the correlation functions, obtained by functional differentiation with respect to j and $j^\dagger$, are the same. Due to the matching of f_0 to C_0 the role of $\sigma = \sigma^{-1} = \pm 1$ becomes clear. While f_0^2 is always positive, C_0 which can be further matched to the S-wave scattering length, that can have a positive or negative sign.

The introduction of the dimer field represents a major simplification in the bookkeeping of diagrams in the three-particle sector, as it essentially incorporates the whole two-body dynamics. The fully

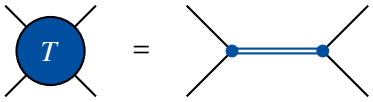

Figure 3.4: Two-particle scattering amplitude in terms of the full dimer propagator (blue double line). The blue dots represent the particle-dimer conversion vertex.

resummed dimer propagator is given by

$$\mathrm{i}\langle 0|\mathcal{T}(T(x)T^\dagger(y))|0\rangle = \int \frac{d^4P}{(2\pi)^4}\,\mathrm{e}^{-\mathrm{i}P(x-y)}\,D(P)\,, \tag{3.55}$$

where $D(P)$ obeys the Dyson equation, see Fig. 3.3:

$$D(P) = -\sigma - \sigma\frac{f_0^2}{2}I(P)D(P)\,. \tag{3.56}$$

Here $I(P)$ is the two-particle bubble integral, given in Eq. (3.16). Using the previous results for this loop one finds that indeed $D(P) \equiv D(P^2)$ with

$$D(P^2) = \frac{16\pi\sqrt{s}f_0^{-2}}{-16\pi\sqrt{s}\sigma f_0^{-2} - \mathrm{i}q^*}\,. \tag{3.57}$$

Finally, in order to obtain the two-particle scattering amplitude it suffices to attach the vertices converting the dimer back into two-particle pairs, as depicted in Fig. 3.4. The resulting expression at the leading order is given by:

$$T(\mathbf{p}_1,\mathbf{p}_2;\mathbf{q}_1,\mathbf{q}_2) = \tau(P^2) = f_0\,D(P^2)\,f_0 = \frac{16\pi\sqrt{s}}{-16\pi\sqrt{s}\sigma f_0^{-2} - \mathrm{i}q^*}\,, \tag{3.58}$$

which coincides with Eq. (3.30) for $\ell = 0$, taking into account the matching condition Eq. (3.53).

3.3.2 Inclusion of Higher Partial Waves

Since effects due to partial wave mixing in a finite volume can be significant, the inclusion of higher partial waves is crucial in order to analyze LQCD data. In the NREFT framework these enter as higher order operators. Keeping the discussion restricted to identical particles, P-wave contributions are absent and the first contribution from the D-wave enters at next-to-next-to leading order (N2LO), $O(p^4)$. At the same order, another S-wave operator can be constructed in addition to those given in Eq. (3.15). In the usual two-particle picture these can be written as

$$\begin{aligned}\mathcal{L}_2^{(4),\mathrm{D}} &= \frac{5}{2}C_4'\Big(3(w_\mu\phi)^\dagger(w_\nu\phi)^\dagger(w^\mu\phi)(w^\nu\phi) - (w_\mu\phi)^\dagger(w^\mu\phi)^\dagger(w_\nu\phi)(w^\nu\phi)\\ &\qquad - \frac{M^2}{2}\Big((w_\mu\phi)^\dagger(w^\mu\phi)^\dagger\phi\phi + \mathrm{h.c.}\Big) - M^4\phi^\dagger\phi^\dagger\phi\phi\Big)\,,\\ \mathcal{L}_2^{(4),\mathrm{S}} &= C_4\left((w_\mu\phi)^\dagger(w^\mu\phi)^\dagger - M^2\phi^\dagger\phi^\dagger\right)\left((w_\nu\phi)(w^\nu\phi) - M^2\phi\phi\right)\,,\end{aligned} \tag{3.59}$$

respectively. By construction, the potential up to N2LO is given by

$$-V(\mathbf{p}_1,\mathbf{p}_2;\mathbf{q}_1,\mathbf{q}_2) = 4C_0 + 16C_2\,(q^*)^2 + 16C_4\,(q^*)^4 + 4C_4'\,(q^*)^4\,5P_2(\cos\theta)\,, \tag{3.60}$$

where q^* is the magnitude of the relative momentum and θ is the scattering angle in the CMS. Note that the coefficients in $\mathcal{L}_2^{(4),\mathrm{D}}$, especially the factor of three in the first term, are chosen such that $P_2(\cos\theta) = (3\cos^2\theta - 1)/2$ is obtained. Expanding in spherical harmonics according to Eq. (3.25) it can be read off that:

$$v_0(s) = -4C_0 - 16C_2\,(q^*)^2 - 16C_4\,(q^*)^4\,, \quad v_2(s) = -4C_4'\,. \tag{3.61}$$

The inclusion of higher partial wave interactions can also be applied in the particle-dimer picture in a simple manner. Neglecting three-body interactions first, one might couple a set of $2\ell+1$ spin-ℓ dimer fields $T_{\ell m}$, where $m = -\ell,\ldots,\ell$, to two-particle operators $O_{\ell m}$ in the same representation:

$$\mathcal{L}_d = \phi^\dagger 2w(\mathrm{i}\partial_t - w)\phi + \sum_{\ell m}\sigma_\ell T_{\ell m}^\dagger T_{\ell m} + \sum_{\ell m}(T_{\ell m}^\dagger O_{\ell m} + \text{h.c.})\,. \tag{3.62}$$

Integrating out the auxiliary dimer fields in the path integral formalism, the resulting two-body interaction Lagrangian reads as:

$$\mathcal{L}_I = -\sum_{\ell m}\sigma_\ell O_{\ell m}^\dagger O_{\ell m}\,. \tag{3.63}$$

By virtue of the potentials partial wave expansion Eq. (3.25) the two-particle operators should obey:

$$\langle 0|O_{\ell m}|\mathbf{q}_1,\mathbf{q}_2\rangle = \sqrt{4\pi}\,f_\ell(s)\,\mathcal{Y}_{\ell m}^*(\mathbf{q}^*)\,, \tag{3.64}$$

where $\mathbf{q}^*$ is the relative momentum in the center of mass frame and $f_\ell(s) = f_\ell^{(0)} + f_\ell^{(2)}(s/4 - M^2) + \ldots$ are polynomials in $(q^*)^2 = s/4 - M^2$, such that

$$v_\ell(s) = \sigma_\ell f_\ell(s)^2\,. \tag{3.65}$$

The actual expressions for these operator in position space

$$O_{\ell m} = \sqrt{4\pi}\,\phi\,f_\ell\left(-\overleftrightarrow{\nabla}^{*2}\right)\mathcal{Y}_{\ell m}^*\left(\mathrm{i}\overleftrightarrow{\nabla}^*\right)\phi\,, \quad \overleftrightarrow{\nabla}^* = \frac{1}{2}\left(\overrightarrow{\nabla}^* - \overleftarrow{\nabla}^*\right) \tag{3.66}$$

are rather complicated and highly non-local as they depend on the Lorentz transformation $\Lambda_\nu^\mu(P)$ into the CMS, where the total momentum P^μ should be expressed in terms of the differential operators $w^\mu = (w, \mathrm{i}\nabla)$ itself:

$$\left(\mathrm{i}\overrightarrow{\nabla}^*\right)^i = \Lambda_\mu^i(P)\,\overrightarrow{w}^\mu\,, \quad \Lambda_0^i(P) = -\gamma\frac{P^i}{P^0}\,, \quad \Lambda_j^i(P) = \delta^{ij} + (\gamma-1)\frac{P^jP^i}{\mathbf{P}^2}\,,$$
$$\gamma = \left(1 - \left(\frac{\mathbf{P}}{P^0}\right)^2\right)^{-1/2}\,, \quad P^\mu = \overrightarrow{w}^\mu + \overleftarrow{w}^\mu\,. \tag{3.67}$$

Again, in the expressions above, arrows denote the direction the derivatives are acting on.

Despite these rather inconvenient representations of operators, the calculation of the two-body scattering amplitude turns out to be simple. Considering the second diagram in Fig. 3.3 contributing to the full dimer propagator $\mathrm{i}\langle 0|\mathcal{T}(T_{\ell m}(x)T^{\dagger}_{\ell' m'}(y))|0\rangle$ one obtains the following loop integral:

$$I_{\ell m,\ell' m'}(P) = \int \frac{d^d k_1}{(2\pi)^d 2w(\mathbf{k}_1)} \frac{d^d k_2}{(2\pi)^d 2w(\mathbf{k}_2)} \frac{4\pi\, f_\ell(\mathbf{k}^{*2}) \mathcal{Y}^*_{\ell m}(\mathbf{k}^*) \mathcal{Y}_{\ell' m'}(\mathbf{k}^*) f_{\ell'}(\mathbf{k}^{*2})}{w(\mathbf{k}_1) + w(\mathbf{k}_2) - P^0 - \mathrm{i}\varepsilon} \times \\ \times (2\pi)^d \delta^d(\mathbf{P} - \mathbf{k}_1 - \mathbf{k}_2)\,. \tag{3.68}$$

Noting that the numerator is a low energy polynomial and using the properties of dimensional regularization, together with the threshold expansion, only the absorptive part of the denominator contributes. Furthermore, as the measure is Lorentz-invariant, the integral can be solved in the CMS. Due to the orthogonality of the spherical harmonics, the integral reduces to

$$I_{\ell m,\ell' m'}(P) = \delta_{\ell\ell'}\delta_{mm'} f_\ell^2((q^*)^2)(q^*)^{2\ell} I(P^2), \tag{3.69}$$

with $I(P^2)$ the generic bubble integral, given in Eq. (3.20). Therefore the full dimer propagator is given by:

$$\mathrm{i}\langle 0|\mathcal{T}(T_{\ell m}(x)T^{\dagger}_{\ell' m'}(y))|0\rangle = \delta_{\ell\ell'}\delta_{mm'} \int \frac{d^4 P}{(2\pi)^4} \mathrm{e}^{-\mathrm{i}P(x-y)} D_\ell(P), \tag{3.70}$$

where

$$D_\ell(P) = -\sigma_\ell - \sigma_\ell f_\ell^2((q^*)^2)(q^*)^{2\ell} \frac{1}{2} I(P^2) D_\ell(P)\,. \tag{3.71}$$

Finally, attaching the vertices that convert the dimer into two-particle pairs, one arrives at the expression for the on shell two-body scattering amplitude

$$T(\mathbf{p}_1, \mathbf{p}_2; \mathbf{q}_1, \mathbf{q}_2) = 4\pi \sum_{\ell m} \mathcal{Y}_{\ell m}(\mathbf{p}^*)\, \tau_\ell(s)\, \mathcal{Y}^*_{\ell m}(\mathbf{q}^*), \tag{3.72}$$

where

$$\tau_\ell(s) = f_\ell(s)\, D_\ell(P)\, f_\ell(s) = \frac{16\pi\sqrt{s}(q^*)^{-2\ell}}{-16\pi\sqrt{s}\sigma_\ell f_\ell^{-2}(s)(q^*)^{-2\ell} - \mathrm{i}q^*}\,. \tag{3.73}$$

A comparison with Eq. (2.53) yields the matching condition[9]

$$-16\pi\sqrt{s}\sigma_\ell f_\ell^{-2}(s) = (q^*)^{2\ell+1} \cot\delta_\ell(s)\,. \tag{3.74}$$

Both sides being Lorentz-invariant quantities that can be expanded in a series around threshold again guarantees a one-to-one correspondence between the number of effective couplings $f_\ell^{(i)}$ and parameters appearing in the ERE of the underlying model. In practice one may just replace the

[9] Here, again, the different normalizations in the partial wave expansion, due to the use of $\mathcal{Y}_{\ell m}(\mathbf{p}) = |\mathbf{p}|^\ell Y_{\ell m}(\hat{\mathbf{p}})$, should be taken into account.

expression $-16\pi\sqrt{s}\sigma_\ell f_\ell^{-2}(s)$ appearing in the dimer propagator in favor of the ERE:

$$\tau_\ell(s) = \frac{16\pi\sqrt{s}}{-\frac{1}{a_\ell} + \frac{1}{2}r_\ell(q^*)^2 + \cdots - \mathrm{i}(q^*)^{2\ell+1}}\,. \tag{3.75}$$

In a finite volume, due to the lack of rotational invariance, the full dimer propagator is non-diagonal in angular momentum:

$$\mathrm{i}\langle 0|\mathcal{T}(T_{\ell m}(x)T^\dagger_{\ell' m'}(y))|0\rangle = \int \frac{dP^0}{2\pi}\,\frac{1}{L^3}\sum_{\mathbf{P}} \mathrm{e}^{-\mathrm{i}P(x-y)}\, D^L_{\ell m,\ell' m'}(P)\,, \tag{3.76}$$

where

$$D^L_{\ell m,\ell' m'}(P) = -\delta_{\ell\ell'}\delta_{mm'}\sigma_\ell - \sigma_\ell\frac{1}{2}\sum_{\ell'' m''} I^L_{\ell m,\ell'' m''}(P) D^L_{\ell'' m'',\ell' m'}(P)\,. \tag{3.77}$$

Here, $I^L_{\ell m,\ell'' m''}(P)$ denotes the finite-volume version of the loop integral in Eq. (3.68) and is given by

$$I^L_{\ell m,\ell' m'}(P) = \frac{1}{L^3}\sum_{\mathbf{k}_1=2\pi/L\mathbf{n}} \frac{4\pi f_\ell(\mathbf{k}^{*2})\mathcal{Y}^*_{\ell m}(\mathbf{k}^*)\mathcal{Y}_{\ell m}(\mathbf{k}^*) f_{\ell'}(\mathbf{k}^{*2})}{4w(\mathbf{k}_1)w(\mathbf{P}-\mathbf{k}_1)(w(\mathbf{k}_1)+w(\mathbf{P}-\mathbf{k}_1)-P^0)}\,. \tag{3.78}$$

The similarity to Eq. (3.41) is obvious. The expressions only differ by the factor of $4\pi f_\ell(\mathbf{k}^{*2})f_{\ell'}(\mathbf{k}^{*2})$. Following the discussion below Eq. (3.41), the loop sum can be calculated completely analogous. Especially, using the properties of dimensional regularization, the replacement $\mathbf{k}^{*2} \to (q^*)^2 = s/4 - M^2$ only amounts to exponentially corrections. Thus

$$I^L_{\ell m,\ell' m'}(P) = 4\pi\, f_\ell(s)\,\chi_{\ell m,\ell' m'}(s;\mathbf{P})\, f_{\ell'}(s)\,. \tag{3.79}$$

Since poles in the dimer propagator correspond to two-particle energy levels due to the trivial relation to the two-body scattering amplitude, the quantization condition can be read off from Eq. (3.77). After some simple rearrangements and using the matching condition Eq. (3.74) one arrives at the Lüscher equation Eq. (3.48).

3.3.3 The Three-Body Force in the Particle-Dimer Picture

Having concluded the two-particle sector in the particle-dimer picture it is now time to include the three-body short range interaction. Keeping in mind that the auxiliary dimer field does not represent a physical particle in general, it seems advantageous to start the discussion in the pure particle picture. For the scattering of three on-shell identical scalars $\phi(q_1)+\phi(q_2)+\phi(q_2) \to \phi(p_1)+\phi(p_2)+\phi(p_3)$ the following Lorentz-invariants can be defined [174]:

$$\begin{aligned} s &= (p_1+p_2+p_3)^2 = (q_1+q_2+q_3)^2\,,\\ s_{ij} &= (p_i+p_j)^2\,, \quad s'_{ij} = (q_i+q_j)^2\,, \quad i,j=1,2,3\,,\ i\neq j\\ t_{ij} &= (p_i-q_j)^2\,, \quad i,j=1,2,3\,. \end{aligned} \tag{3.80}$$

In order to apply a consistent power counting, it is convenient to define the following quantities:

$$\Delta = s - 9M^2\,, \quad \Delta_p^i = s_{jk} - 4M^2\,, \quad \Delta_q^i = s'_{jk} - 4M^2\,, \tag{3.81}$$

where (i, j, k) are cyclic permutations of $(1, 2, 3)$. Owing to the imposed counting rule of $|\mathbf{k}| = O(\epsilon)$ for a generic momentum $\mathbf{k}$, the quantities above as well as t_{ij} are of order $O(\epsilon^2)$.

This set of operators is still overcomplete. Due to Poincare invariance, three-body scattering should be described in total by eight[10] independent variables. Indeed the sixteen quantities above are subject to eight constraints [174]:

$$\sum_{i=1}^{3} \Delta_p^i = \sum_{i=1}^{3} \Delta_q^i = \Delta\,, \quad \sum_{j=1}^{3} t_{ij} = \Delta_p^i - \Delta\,, \quad \sum_{j=1}^{3} t_{ji} = \Delta_q^i - \Delta\,, \quad i = 1, 2, 3\,. \tag{3.82}$$

Due to the short ranged nature of hadronic interactions, the (tree-level) three-body force K_3 can be expanded in a series with respect to the variables $\Delta, \Delta_p^i, \Delta_q^i$ and t_{ij}.

Considering identical particles leads to further constraints due to Bose symmetry: The three-particle amplitude, and therefore also the corresponding three-body short range interaction, must be invariant under the exchange of any two incoming or outgoing particles. Furthermore, time-reversal allows for the interchange of incoming and outgoing states. The operators defined above transform according to:

$$\begin{aligned} p_i \leftrightarrow p_j \;:&\quad \Delta_p^i \leftrightarrow \Delta_p^j\,, \quad t_{ik} \leftrightarrow t_{jk}\,, \\ q_i \leftrightarrow q_j \;:&\quad \Delta_q^i \leftrightarrow \Delta_q^j\,, \quad t_{ki} \leftrightarrow t_{kj}\,, \\ p_i \leftrightarrow q_i \;:&\quad \Delta_q^i \leftrightarrow \Delta_q^i\,, \quad t_{ij} \leftrightarrow t_{ji}\,, \end{aligned} \tag{3.83}$$

where the last line should be understood for all $i, j = 1, 2, 3$ at the same time. At $O(\epsilon^2)$ there exists only one[11] independent invariant operator Δ. Therefore up to NLO:

$$K_3(\Delta) = z_0 + z_2\Delta + O(\epsilon^4)\,. \tag{3.84}$$

Due to unitarity, the coefficients are real.

Now turning to the particle-dimer picture, the dynamics are effectively those of a two-body system. Letting p, q and P, Q denote the momenta of the incoming and outgoing particles and dimers respectively, the following Lorentz-invariants can be defined:

$$s = K^2 = (p + P)^2 = (q + Q)^2\,, \quad t = (p - q)^2 = (P - Q)^2\,. \tag{3.85}$$

Here $K^\mu = (p + P)^\mu$ denotes the total four-momentum. Furthermore, since the auxiliary dimer does

[10] The counting is as follows: The six on-shell momenta are constraint by total four-momentum conservation due to translation invariance. Lorentz-invariance further reduces the number of degrees of freedom, e.g. one can always perform a boost into the center of mass frame, where the total three-momentum is vanishing. Finally, rotational invariance can be used. For a general $n \to m$ scattering process, the number N of degrees of freedom is given by:

$$N = 3 \times (n + m) - 10\,,$$

due to the 10 generators of Poincare symmetry.

[11] Applying the transformations Eq. (3.83), three operators are invariant: $O_1 = \Delta$, $O_2 = \sum_i (\Delta_p^i + \Delta_q^i)$ and $O_3 = \sum_{ij} t_{ij}$. This set can be reduced using the kinematical constraints Eq. (3.82).

not correspond to a physical particle in general and thus should not be considered on-shell (in contrast to the particles), the following variables are included:

$$\sigma_p^2 = P^2\,, \quad \sigma_q^2 = Q^2\,. \tag{3.86}$$

Counting rules can be imposed on the variables[12]:

$$\begin{aligned} \Delta &= s - 9M^2 = O(\epsilon^2), \qquad t = O(\epsilon^2), \\ \Delta_p &= \sigma_p^2 - 4M^2 = O(\epsilon^2), \quad \Delta_q = \sigma_q^2 - 4M^2 = O(\epsilon^2)\,. \end{aligned} \tag{3.87}$$

In the CMS, $\underline{K}^\mu = (\sqrt{s}, \mathbf{0})$, the particle-dimer short-range interactions $V_{\text{pd}}^{\ell m, \ell' m'}(t, s, \sigma_p^2, \sigma_q^2)$ obtained from $\langle \underline{\mathbf{p}}, (\ell m)|H_I|\underline{\mathbf{q}}, (\ell' m')\rangle$ can be expanded into partial waves:

$$V_{\text{pd}}^{\ell m, \ell' m'}(t, s, \sigma_p^2, \sigma_q^2) = -4\pi \sum_{JM} \sum_{LL'} \mathcal{Y}_{JM}^{L\ell}(\underline{\mathbf{p}}, m)\, H_{JLL'}^{\ell\ell'}(\Delta, \Delta_p, \Delta_q)\, (\mathcal{Y}_{JM}^{L'\ell'}(\underline{\mathbf{q}}, m'))^*\,, \tag{3.88}$$

where (ℓm) and $(\ell' m')$ denotes the angular momentum of the dimers. The functions[13] $\mathcal{Y}_{JM}^{L\ell}(\mathbf{k}, m)$ are given by

$$\mathcal{Y}_{JM}^{L\ell}(\mathbf{k}, m) = \langle L(M-m), \ell m|JM\rangle\, \mathcal{Y}_{L(M-m)}(\mathbf{k}) \tag{3.89}$$

and $\underline{\mathbf{p}}$ and $\underline{\mathbf{q}}$ denote the particle momenta in the particle-dimer CMS. By momentum conservation:

$$\underline{\mathbf{p}}^2 = \frac{\lambda(s, \sigma_p^2, M^2)}{4s}\,, \quad \underline{\mathbf{q}}^2 = \frac{\lambda(s, \sigma_q^2, M^2)}{4s}\,, \tag{3.90}$$

where $\lambda(a, b, c) = a^2 + b^2 + c^2 - 2(ab + bc + ca)$ is the Källén-function. Finally $H_{JLL'}^{\ell\ell'}(\Delta, \Delta_p, \Delta_q)$ is a polynomial in its arguments. The appearance of different angular momenta can be understood qualitatively. While J, M describes the total angular momentum L' and L can be interpreted as the orbital momentum between the incoming and outgoing particles-dimer pairs respectively.

It is now a straightforward task to write down a Lagrangian that leads to such a potential:

$$\mathcal{L}_I = 4\pi \sum_{\ell m} \sum_{\ell' m'} \sum_{JM} \sum_{LL'} T_{\ell m}^\dagger \left(\mathcal{Y}_{JM}^{L\ell}(\mathrm{i}\nabla, m)\phi^\dagger\right)\, H_{JLL'}^{\ell\ell'}(\Delta, \overleftarrow{\Delta}_T, \overrightarrow{\Delta}_T)\, \left((\mathcal{Y}_{JM}^{L'\ell'}(\mathrm{i}\nabla, m'))^*\phi\right) T_{\ell' m'}\,. \tag{3.91}$$

In the above expression, the differential operator Δ acts on the particle-dimer pairs and can be replaced by $s - 9M^2$ in momentum space. On the other hand $\overleftarrow{\Delta}_T$ and $\overrightarrow{\Delta}_T$ only act on the dimers to the left and right respectively, leading to the expressions Δ_p and Δ_q in momentum space.

[12] The use of similar symbols is deliberate. This, as well as the counting rules will become clear later.

[13] The appearance of these functions emerges when expressing the matrix element in the total spin. First, inserting a full set of states, the incoming and outgoing states can be rewritten as

$$|\mathbf{k}, (\ell m)\rangle = \sum_{LM} \langle L, M|\mathbf{k}\rangle\, |LM, \ell m\rangle = \sum_{LM} \mathcal{Y}_{LM}^*(\mathbf{k})\, |LM, \ell m\rangle\,.$$

Then, inserting another full set of states $\sum_{JN} = |JN\rangle\langle JN|$ for the total spin, these functions appear.

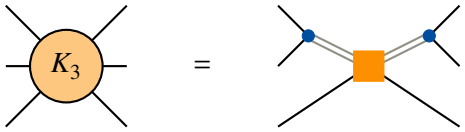

Figure 3.5: Graphical representation of the relation between the three-body force and the particle-dimer short-range interaction. Gray double lines denote the dimer propagator at tree level, while the blue dots correspond to the particle-dimer conversion vertices. The orange rectangle represents the particle-dimer potential.

In the case of a shallow two-particle bound state, the dimer corresponds to a physical particle. Thus, a matching to the effective range parameters of the particle-dimer scattering can be performed. However, a key observation is that the couplings appearing in $H^{\ell\ell'}_{JLL'}(\Delta, \overleftarrow{\Delta}_T, \overrightarrow{\Delta}_T)$ are not independent if a physical dimer, i.e. bound state, does not exist. While the description of the three-body sector in terms of the particle-dimer picture should in principle lead to an equivalent theory, as can be seen in the path integral formalism, solely writing down the most general particle-dimer interactions does not guarantee that the theories coincide. Instead a matching should be performed. Similarly to the two-body sector, cf. the step from Eq. (3.57) to Eq. (3.58) or form Eq. (3.71) to Eqs. (3.72) and (3.73), the tree-level three-body force can be easily obtained from the (tree-level) particle-dimer interaction by attaching the vertices converting dimers back into particles[14]. Diagrammatically this is shown in Fig. 3.5.

An instructive example can be given at NLO. Here only the S-wave dimer is present. Inspection of the particle-dimer potential Eq. (3.88), owing to the fact that $\mathcal{Y}^{L\ell}_{JM}(\mathbf{k}, m) = O(\epsilon^L)$, only[15] $J, L, L' = 0, 1$ contribute at this order. Thus, up to NLO, dropping the $\ell = m = 0 = \ell' = m'$ superscripts, the particle-dimer potential is given by:

$$\begin{aligned} V_{\text{pd}}(t, s, \sigma_p^2, \sigma_q^2) &= -H_0(\Delta, \Delta_p, \Delta_q) - 3\,\underline{\mathbf{p}}\,\underline{\mathbf{q}}\,H_2(\Delta, \Delta_p, \Delta_q) + O(\epsilon^4)\,, \\ H_0(\Delta, \Delta_p, \Delta_q) &= h_0^{(0)} + h_0^{(1)}\,\Delta + h_0^{(2)}\,(\Delta_p + \Delta_q)\,, \quad H_2(\Delta, \Delta_p, \Delta_q) = h_2^{(0)}\,. \end{aligned} \tag{3.92}$$

The symmetric combination of Δ_p and Δ_q appears due to time-reversal invariance. Moreover

$$\underline{\mathbf{p}}\,\underline{\mathbf{q}} = \frac{1}{2}t - M^2 + \frac{(s + M^2 - \sigma_p^2)(s + M^2 - \sigma_q^2)}{4s} = \frac{1}{2}t + \frac{2}{9}\Delta - \frac{1}{6}(\Delta_p + \Delta_q) + O(\epsilon^4)\,. \tag{3.93}$$

Now attaching the conversion vertices, this potential has to be multiplied by $f_0(\sigma^2) = f_0^{(0)} + f_0^{(2)}(\sigma^2/4 - M^2)$ with $\sigma^2 = \sigma_q^2, \sigma_p^2$ for the incoming and outgoing dimer respectively. As any two of the particles can combine into a dimer, those quantities have to be equipped with indices. Denoting the spectator particle with the index i, one may define:

$$\Delta_p^i = \sigma_{p_i}^2 - 4M^2\,, \quad \Delta_q^i = \sigma_{q_i}^2 - 4M^2\,, \quad t_{ij} = (p_i - q_j)\,, \tag{3.94}$$

where $\sigma_{p_i}^2 = P_i^2 = (p_j + p_k)^2$ for (i, j, k) cyclic permutations of $(1, 2, 3)$ and similarly for $\sigma_{q_j}^2$. These variables now coincide with those in the three-body system defined in Eq. (3.80) and obey similar

[14] This is equivalent to integrating out the dimer fields at tree level.

[15] As $\ell = \ell' = 0$ the Clebsch-Gordan coefficient implies $L = L' = J$. This further excludes the appearance of $L = 2$.

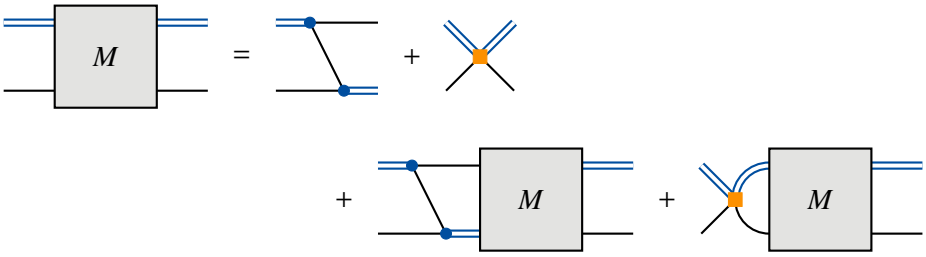

Figure 3.6: Graphical representation of the Faddeev equation for the particle-dimer scattering amplitude. Blue double lines denote a fully resummed dimer propagator, while the particle is depicted as a single black line. Orange boxes and blue dots represent particle-dimer interaction and dimer-conversion vertices respectively.

constraints as in Eq. (3.82). Finally, in order to obtain the full amplitude one has to sum over $i, j = 1, 2, 3$. The matching condition reads:

$$K_3(\Delta) = z_0 + z_2\Delta = \sum_{ij} f_0(\sigma_{p_i}^2)\, V_{\text{pd}}(t_{ij}, s, \sigma_{p_i}^2, \sigma_{q_j}^2) f_0(\sigma_{q_j}^2)\,. \tag{3.95}$$

Indeed using the constraints Eq. (3.82), this equation is fulfilled. Therefore, without loss of generality, one may set $h_0^{(2)} = h_2^{(0)} = 0$ from the beginning.

On the contrary, if a physical S-wave dimer exists, the variables σ_p^2 and σ_q^2 are not independent anymore. Instead they correspond to the mass squared of the corresponding bound state. Thus, the relations Eq. (3.82) are not valid anymore. In the particle-dimer potential Eq. (3.92) the coefficients in H_0 should be matched to the S-wave scattering length and effective range parameter, while $h_2^{(0)}$ can be related to the P-wave scattering length.

It should be pointed out once again, that, similar to the two-particle sector, an actual matching of the three-body couplings to the underlying model will not be performed. Instead a three-particle quantization condition will be derived, that allows to fix the values of the three-body LECs by a fit to the energy spectrum obtained from LQCD. Having determined these parameters, the Lagrangian can then be used in order to calculate infinite-volume observables. Most commonly these quantities, such as resonance masses and decay width, are directly derived from the three-particle scattering amplitude.

The following section will focus on the description of three-particle scattering in the infinite volume. This is a rich field of research itself and besides the NREFT framework that is discussed here two other main formalisms have been developed that have been applied to physical systems extensively: the RFT approach [58, 159, 160, 175, 176] and unitarity approaches [177, 178] as well as [179–181]

3.3.4 Faddeev Equations for the Particle-Dimer Scattering Amplitude

The dynamics of a three-body system are governed by the so called *Faddeev equations* [182]. In the particle-dimer picture the three-particle scattering amplitude can be straightforwardly related to the particle-dimer amplitude. Diagrammatically the scattering of a particle and a dimer can be represented as in Fig. 3.6, which should be understood to be solved self-consistently. Since the particle-dimer amplitude will be related to the scattering of three particles in the end, the dimer fields should be considered off-shell in general. The following calculation will be performed in the three-particle rest frame only. The generalization to moving frames represents a major subject of this thesis and will be addressed in Chapters 5 and 6. Assigning on-shell momenta q^μ and p^μ to the incoming and outgoing

particles respectively and denoting the total four momentum by $K^\mu = (E, \mathbf{0})$, the particle-dimer scattering amplitude obeys the following integral equation:

$$M_{\ell m,\ell' m'}(p,q;E) = Z_{\ell m,\ell' m'}(p,q;E) + \sum_{\ell'' m''} \int \frac{dk^0}{2\pi \mathrm{i}} \int^{\Lambda} \frac{d^3\mathbf{k}}{(2\pi)^3} Z_{\ell m,\ell'' m''}(p,k;E) D_{\ell''}((K-k)^2) \times \frac{1}{2w(\mathbf{k})(w(\mathbf{k}) - k^0 - \mathrm{i}\varepsilon)} M_{\ell'' m'',\ell' m'}(k,q;E), \quad (3.96)$$

where $\ell' m'$ and ℓm denote the spin of the incoming and outgoing dimers. Moreover, Λ is a cutoff on the three-momentum of the spectator particle in the loop that renders the equation UV finite. Above, the integral kernel Z corresponds to the sum of the first two diagrams, which can be read off from the particle-dimer Lagrangian. The expression is rather clumsy and will be given below.

In order to perform the k^0 integral, it is sufficient to consider the pole structure of the integrand. The kernel Z contributes a pole at $w(\mathbf{p}+\mathbf{k}) + w(\mathbf{p}) - E + k^0 - \mathrm{i}\varepsilon = 0$, stemming from the particle propagating in the exchange diagram, which is located in the upper half plane. Going back to the derivation of the dimer propagator $D_\ell(P^2)$, restoring the the factor of $\mathrm{i}\varepsilon$ in the two-body loop diagram Eq. (3.16) in the result Eq. (3.20), i.e. $P^0 \to P^0 + \mathrm{i}\varepsilon$, it can be seen that also the poles in $D_\ell((K-k)^2)$ are located in the upper half plane. Therefore the k^0 contour can be chosen, such that only the pole at $k^0 = w(k) - \mathrm{i}\varepsilon$ contributes. Thus the integral equation above reduces to a three-dimensional one, where all particles are on-shell, i.e. $k^0 = w(\mathbf{k})$:

$$M_{\ell m,\ell' m'}(p,q;E) = Z_{\ell m,\ell' m'}(p,q;E) + \sum_{\ell'' m''} \int^{\Lambda} \frac{d^3\mathbf{k}}{(2\pi)^3 2w(\mathbf{k})} Z_{\ell m,\ell'' m''}(p,k;E) D_{\ell''}((K-k)^2)\, M_{\ell'' m'',\ell' m'}(k,q;E)\,. \quad (3.97)$$

This equation is referred to as the Faddeev equation for the particle-dimer scattering amplitude. Furthermore, the kernel is given by

$$Z_{\ell m,\ell' m'}(p,q;E) = \frac{4\pi\, \mathcal{Y}^*_{\ell m}(\mathbf{k}^*_p) f_\ell(s_p)\, f_{\ell'}(s_q) \mathcal{Y}_{\ell' m'}(\mathbf{k}^*_q)}{2w(\mathbf{p}+\mathbf{q})(w(\mathbf{p}) + w(\mathbf{q}) + w(\mathbf{p}+\mathbf{q}) - E - \mathrm{i}\varepsilon)} + 4\pi \sum_{JM} \sum_{LL'} \mathcal{Y}^{L\ell}_{JM}(\mathbf{p},m)\, H^{\ell\ell'}_{JLL'}(\Delta,\Delta_p,\Delta_q)\, (\mathcal{Y}^{L'\ell'}_{JM}(\mathbf{q},m'))^*\,. \quad (3.98)$$

Here

$$s_p = (k+q)^2, \qquad s_q = (k+p)^2, \qquad k^\mu_p = \frac{1}{2}(q-k)^\mu, \quad k^\mu_q = \frac{1}{2}(p-k)^\mu, \quad (3.99)$$

with $k^\mu = (w(\mathbf{p}+\mathbf{q}), -\mathbf{p}-\mathbf{q})$. Variables with an asterix superscript are defined in the respective two-body center of mass frame.

One may express the quantities in the numerator of the first term in Eq. (3.98) also in terms of the

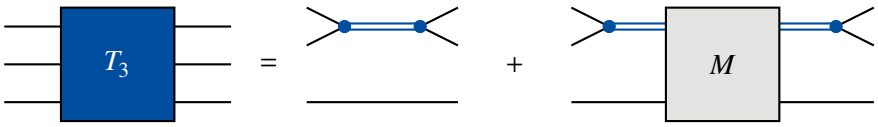

Figure 3.7: Three-particle scattering in terms of the particle-dimer amplitude.

off-shell dimer momenta. In order to do so note that the difference of s_p^2 and $\sigma_p^2 = (K-p)^2$ is given by

$$\begin{aligned}\sigma_p^2 - s_p^2 &= (E - w(\mathbf{p}))^2 - (w(\mathbf{p}+\mathbf{q}) + w(\mathbf{q}))^2 \\ &= (E - w(\mathbf{p}) - w(\mathbf{q}) - w(\mathbf{p}+\mathbf{q}))\,(E - w(\mathbf{p}) + w(\mathbf{q}) + w(\mathbf{p}+\mathbf{q}))\,,\end{aligned} \tag{3.100}$$

exactly canceling the denominator. Thus one may replace $f_\ell(s_p) \to f_\ell(\sigma_p^2)$ by modifying the regular second part on the right hand side of Eq. (3.98). The same argument holds for the replacement $f_\ell(s_q) \to f_\ell(\sigma_q^2)$. Furthermore, defining $\tilde{p}^\mu = (p - (K-p-q))^\mu/2$ and $\tilde{q}^\mu = (q - (K-p-q))^\mu/2$, it can be seen that

$$\tilde{p}^0 - k_p^0 = w(\mathbf{p}) + w(\mathbf{q}) + w(\mathbf{p}+\mathbf{q}) - E\,, \quad \tilde{\mathbf{p}} - \mathbf{k}_p = \mathbf{0}\,, \tag{3.101}$$

and similarly for $\tilde{q}^\mu - k_q^\mu$, such that the spherical functions can be expressed in terms of $\tilde{\mathbf{p}}^*$ and $\tilde{\mathbf{q}}^*$.

The on-shell three-particle scattering amplitude is finally obtained by equipping the particle-dimer amplitude with the external vertices, see Fig. 3.7. Furthermore, a disconnected piece should be included, where only a two-particle subsystem is interacting. As each particle can be the spectator, in the total amplitude a sum over all different combinations of spectators should be performed:

$$\begin{aligned}
&T_3(\mathbf{p}_1,\mathbf{p}_2,\mathbf{p}_3;\mathbf{q}_1,\mathbf{q}_2,\mathbf{q}_3) = T_3^{\text{disc}} + T_3^{\text{conn}}\,,\\
&T_3^{\text{disc}} = \sum_{\alpha,\alpha'=1}^{3} \sum_{\ell m} (2\pi)^3 2w(\mathbf{p}_\alpha)\delta^3(\mathbf{p}_\alpha - \mathbf{q}_{\alpha'})\, 4\pi\, \mathcal{Y}_{\ell m}(\mathbf{p}^*_{\beta\gamma})\, \tau_\ell((K-p_\alpha)^2)\, \mathcal{Y}^*_{\ell' m'}(\mathbf{q}^*_{\beta'\gamma'})\,,\\
&T_3^{\text{conn}} = \sum_{\alpha,\alpha'=1}^{3} \sum_{\ell m} \sum_{\ell' m'} 4\pi\, \mathcal{Y}_{\ell m}(\mathbf{p}^*_{\beta\gamma})\, \tau_\ell((K-p_\alpha)^2)\, f_\ell^{-1}((K-p_\alpha)^2)\, M_{\ell m,\ell' m'}(p_\alpha, q_{\alpha'})\\
&\qquad\qquad \times f_\ell^{-1}((K-q_{\alpha'})^2)\tau_{\ell'}((K-q_{\alpha'})^2)\mathcal{Y}^*_{\ell' m'}(\mathbf{q}^*_{\beta'\gamma'})\,.
\end{aligned} \tag{3.102}$$

Here, (α,β,γ) and (α',β',γ') are permutations of $(1,2,3)$. Furthermore $p^\mu_{\beta\gamma} = (p_\beta - p_\gamma)^\mu/2$ is the relative momentum of the two-body subsystem of the particles β and γ. Moreover, $K = p_1+p_2+p_3 = q_1+q_2+q_3$ is implicit.

An important remark is in order. In contrast to the two-particle sector, where dimensional regularization was used in the calculation of the elementary bubble diagram, the particle-dimer amplitude is evaluated using cutoff regularization. The reason is that due to the non-perturbative treatment and the complex diagrammatic structure, the amplitude should be obtained by solving the integral equation Eq. (3.97) self-consistently. Usually a solution must be obtained numerically, which can be done conveniently in cutoff regularization. Since physical quantities like the particle-dimer scattering amplitude are cutoff-independent, the introduction of a UV cutoff necessarily leads to a cutoff-dependence of the couplings $h_0^{(0)}, h_0^{(1)}, h_0^{(2)}, h_2^{(0)}, \ldots$, compensating the explicit dependence on

Λ.

Another important observation is that the dimer propagator entering the Faddeev equation is evaluated at momenta that typically exceed the range of applicability of the NREFT framework in the two-body sector. Removing the cutoff on the spectator momentum, $\Lambda \to \infty$, the CM energy square of the dimer $(K-k)^2$ can take arbitrary negative values and thus requires knowledge of the whole subthreshold behavior of the two-body scattering amplitude. Clearly the NREFT is not expected to give any meaningful description of that region. However, due to the decoupling of low- and high-energy regimes, three-body observables should not depend on the details of the interactions in this region. Integrating out the high-energy degrees of freedom consistently, the details of the two-body scattering amplitude in the far subthreshold region should not be resolved by the particle-dimer scattering amplitude as the high-energy behavior of the three-body short-range interaction should compensate any dependence.

However, the exact form of the two-particle amplitude is not known and has to be parametrized by an ERE in the NREFT formalism. While in the region of applicability of the NREFT this is expected to yield a good approximation of the exact amplitude, severe discrepancies can arise outside the vicinity of threshold. This can lead to practical problems if the NREFT amplitude is subject to *spurious poles*. Considering the S-wave ERE up to NLO, the NREFT two-particle scattering amplitudes has subthreshold poles $\kappa = \mathrm{i}q^*$ at

$$\kappa_{1,2} = \frac{1 \mp \sqrt{1 - 2r_0/a_0}}{r_0} \,. \tag{3.103}$$

If[16] $r_0 > 0$ and $a_0 \gg r_0$, the pole κ_1 corresponds to a existing (shallow) bound state, while κ_2 is an unphysical spurious pole with negative residue that lies far below threshold. Nevertheless, using this form of ERE in the Faddeev equation, this spurious pole will lead to a violation of unitarity in the particle-dimer amplitude. Following the discussion in the previous paragraph, the pole was only artificially introduced using the ERE and it should be possible to cancel its influence by adjusting the renormalization prescription of the three-body short range interactions. Such a formalism was developed in [183] in the infinite volume and in [5] for the finite volume.

3.3.5 The Three-Particle Quantization Condition

In a finite volume, following the discussion in Sec. 3.2.2, an analog of the particle-dimer scattering amplitude can be defined, obeying the Faddeev equations as depicted in Fig. 3.6 with loop integrals replaced by finite-volume sums. Taking into account that the finite-volume dimer propagator, Eq. (3.77), is non-diagonal in angular momentum space, the finite-volume particle-dimer amplitude in the rest frame $K^\mu = (E, \mathbf{0})$ is given by the solution of the equations

$$\begin{aligned} M^L_{\ell m,\ell' m'}(p,q;E) = {} & Z_{\ell m,\ell' m'}(p,q;E) \\ & + \sum_{jn,j'n'} \frac{1}{L^3} \sum_{\mathbf{k}}^{\Lambda} \frac{1}{2w(\mathbf{k})} Z_{\ell m,jn}(p,k;E) D^L_{jn,j'n'}(K-k)\, M^L_{j'n',\ell' m'}(k,q;E) \,, \end{aligned} \tag{3.104}$$

[16] This setup is relevant in the two-nucleon problem. Here, κ_1 corresponds to the binding momentum of the deuteron.

where $k^0 = w(\mathbf{k})$ is on-shell and the three-momentum sum is equipped with an UV cutoff Λ.

The finite-volume three-particle scattering amplitude is again obtained from the particle-dimer amplitude as in the infinite volume. Since the expression will be rather voluminous, only an abbreviated from will be given in order to describe the pole structure qualitatively. Such an analysis should be carried out, since the particle-dimer scattering amplitude explicitly involves poles from both, the kernel Z at the non-interacting levels $E = w(\mathbf{p}) + w(\mathbf{q}) + w(\mathbf{p}+\mathbf{q})$ as well as the dimer propagator D^L, corresponding to the two-particle energy levels. Thus, in that perspective it is not clear from the beginning that the three-particle amplitude only contains three-particle energy levels. One may define

$$\tilde{T}_3^L(E) = D^L(E) + D^L(E)\, M^L(E)\, D^L(E)\,, \tag{3.105}$$

where D^L and M^L are operators in the space of spectator momentum and dimer angular momentum for a given total momentum $K^\mu = (E, \mathbf{0})$:

$$\begin{aligned} \langle \mathbf{p}, (\ell m)|D^L(E)|\mathbf{q}, (\ell' m')\rangle &= 2w(\mathbf{p})L^3\delta_{\mathbf{p},\mathbf{q}}\, D^L_{\ell m,\ell' m'}(K-p)\,, \\ \langle \mathbf{p}, (\ell m)|M^L(E)|\mathbf{q}, (\ell' m')\rangle &= M^L_{\ell m,\ell' m'}(p,q;E)\,. \end{aligned} \tag{3.106}$$

Similarly the Faddeev equation for the particle-dimer amplitude can be written in operator form:

$$M^L(E) = Z(E) + Z(E)\, D^L(E)\, M^L(E)\,, \tag{3.107}$$

where $\langle \mathbf{p}, (\ell m)|Z(E)|\mathbf{q}, (\ell' m')\rangle = Z_{\ell m,\ell' m'}(p,q;E)$. The quantity $\tilde{T}_3^L$ defined in this way corresponds to the finite-volume three-particle scattering amplitude with the vertices converting dimers into particles amputated. The absence of poles from the kernel and the dimer propagator in $\tilde{T}_3^L$ was observed in [55, 56, 59, 146] and can be traced back to cancellations in the definition of this amplitude, as shown below.

Considering the poles in $Z_{\ell m,\ell' m'}(p,q;E)$ at the non-interacting levels first, it can be seen from the solution to the Dyson-Schwinger equation for the dimer propagator Eq. (3.77) that $D^L_{\ell m,\ell' m'}(K-p)$ exactly vanishes at these energies, since the finite-volume loop $I^L_{\ell m,\ell' m'}(K-p)$ diverges. Therefore $\tilde{T}_3^L(E)$, where $M^L(E)$ is multiplied by the dimer propagator from the left and right, also vanishes at these energies.

For the second class of poles from $D^L(E)$ at the two-particle energy levels in the finite volume one may write the solution to Eq. (3.107) in the form

$$M^L(E) = \Big(D^L(E)\Big)^{-1}\left[\Big(D^L(E)\Big)^{-1} - Z(E)\right]^{-1} Z(E)\,. \tag{3.108}$$

It can be seen that, with the inclusion of the disconnected piece, these poles get canceled in $\tilde{T}_3^L$.

Following the preceding discussion, a three-particle quantization condition can be derived from the finite-volume Faddeev equation of the particle-dimer amplitude directly. This is a system of equations in the space of on-shell spectator momenta p^μ and q^μ, as well as angular momenta ℓ, m and ℓ', m'. The finite-volume energy levels correspond to poles in the particle-dimer amplitude, these emerge at energies E where the system of equations Eq. (3.104) is singular. Ignoring the singularities stemming

from the kernel, these energies are determined by[17]

$$\det B = 0\,,$$
$$B_{\ell m,\ell' m'}(p,q;E) = 2w(\mathbf{p})L^3\delta_{\mathbf{p},\mathbf{q}}\left(D^L_{\ell m,\ell' m'}(K-p)\right)^{-1} - Z_{\ell m,\ell' m'}(p,q;E)\,. \tag{3.109}$$

Here, in contrast to the two-particle quantization condition, the determinant is not only taken over angular momentum, but also the space of on-shell spectator momenta. Due to the cutoff, these are restricted by $|\mathbf{p}|, |\mathbf{q}| \leq \Lambda$.

The three-particle quantization condition is the key element that allows to relate LQCD data to three-body infinite-volume QCD observables. The procedure of extracting these physical parameters is as follows: In a first step, based on power counting arguments, the expansion of the NREFT Lagrangian that is tailored to describe the process under consideration must be truncated. This yields a cutoff on the spin of the dimer fields and the number of LECs. Now the two-particle quantization condition can be used in order to determine the values of the two-body couplings by performing a fit to the corresponding energy spectrum, obtained in a LQCD calculation. Since these LECs can be directly related to the effective range parameters and thus correspond to physical quantities, no further step is required here. Having fixed a cutoff Λ, the quantization condition Eq. (3.109) can be used to fix the values of the remaining three-body LECs by a fit to the three-particle energy spectrum in the rest frame. Establishing a relation to physical observables directly for these parameters was not yet successful. However, the NREFT is complete now in the sense that all couplings are known. Once again it should be pointed out that for a sufficient lattice setup, the LECs are guaranteed to exhibit exponentially small finite-volume corrections. Therefore, in a final step the Lagrangian can be used in order to calculate infinite-volume observables from the three-body scattering amplitude. This requires solving the Faddeev equations (3.97), where, due to the cutoff-dependence of the three-particle LECs, the same cutoff Λ as chosen in the quantization condition has to be used.

3.3.6 Towards Relativistic Invariance and a Description of Three-Particle Decays

One major challenge is to establish a relativistically invariant three-particle quantization condition, that allows for the application in different moving frames defined by the total three-momentum $\mathbf{K}$ of the three-body system. Unfortunately, the infinite-volume Faddeev equations and similarly the

[17] The same quantization condition may also be derived from the amplitude $\tilde{T}_3^L$. Plugging Eq. (3.107) into Eq. (3.105) and regrouping terms, a Faddeev equation for $\tilde{T}_3^L$ can be derived:

$$\tilde{T}_3^L(E) = D^L(E) + D^L(E)\,Z(E)\,\tilde{T}_3^L(E)\,.$$

The solution to this equation formally is given by:

$$\tilde{T}_3^L(E) = \left[\left(D^L(E)\right)^{-1} - Z(E)\right]^{-1}\,.$$

The three-particle energy levels correspond to poles of $\tilde{T}_3^L(E)$, i.e. to energies where $\left(D^L(E)\right)^{-1} - Z(E)$ is not invertable:

$$\det\left(\left(D^L(E)\right)^{-1} - Z(E)\right) = 0\,.$$

three-particle quantization condition given in the form above turn out to be frame-dependent. Although a precise scrutiny of the covariance of all quantities entering the kernel is needed, which will only be discussed in one of the following chapters, the failure of invariance can be primarily attributed to the three-particle propagator

$$\frac{1}{2w(\mathbf{K}-\mathbf{p}-\mathbf{q})(w(\mathbf{p})+w(\mathbf{q})+w(\mathbf{K}-\mathbf{p}-\mathbf{q})-K^0-\mathrm{i}\varepsilon)}\,, \tag{3.110}$$

entering the expression of the kernel via the exchange diagram. Due to the explicit non-covariance, the particle-dimer scattering amplitude will be frame dependent, also rendering the use of the quantization condition in different frames at the same time impossible. Fortunately, it can be shown that modifying the NREFT approach slightly, relativistic covariance can be restored also in the three-particle sector. In this approach, inspired by heavy quark EFT and heavy baryon ChPT, the NREFT is quantized in an arbitrary frame with four-velocity v^μ, $v^2 = 1$. That is, the momentum $p^\mu_\perp = p^\mu - v^\mu(v\cdot p)$, "perpendicular" to v^μ, is considered to be small. The revision of the NREFT framework under this adjustment and a derivation of a Lorentz-invariant three-particle quantization condition represents one of the central topics of the subsequent parts of this thesis.

Another substantial part concerns the derivation of a three-particle analog of the Lellouch-Lüscher formula in the NREFT framework. Conceptually the basic idea is quite simple. The Lagrangian is extended in order to describe the initial decay process, while the two- and three-body interactions cause the rescattering of the decay products. While the latter couplings can be fixed form LQCD data by a fit to the corresponding energy spectra, the LECs multiplying the operators that describe the initial decay remain undetermined. Nevertheless, as the initial decay process is considered to be perturbative, to fist order these coefficients enter the infinite- and finite-volume decay elements both linearly only. Therefore the dependence on these LECs can be eliminated completely in the end, yielding a linear relation between the infinite-volume decay amplitude in terms of finite-volume decay matrix elements.

It is important to note that, in contrast to the two-particle decays where the magnitudes of momenta of the decay products are fixed, the decay Lagrangian in the three-particle sector consists out of an infinite tower of operators. Eliminating the dependence on more than one of the corresponding LECs one has to extract finite-volume decay amplitudes in different moving frames. Thus a general three-particle analog of the Lellouch-Lüscher formalism turns out to rely on a Lorentz-invariant formulation. However the lack of Lorentz invariance is not an issue at the leading order, where derivative couplings are absent and the decay process is completely described by a single operator.

The remaining chapters of this thesis are excerpts of publications, organized as follows: In Chapter 4 an analog of the Lellouch-Lüscher formalism is derived in the three-particle sector at the leading order for three identical spinless particles in the rest frame. As discussed above, for a general treatment of three-body decays in the NREFT approach a relativistic-invariant formalism is inevitable which will be derived in Chapter 5. The three-particle quantization condition is rederived in a Lorentz-invariant form and examined numerically. Finally in Chapter 6 the three-particle Lellouch-Lüscher formalism is generalized to arbitrary moving frames, allowing the determination of three-particle decay amplitudes from LQCD data at higher orders.

CHAPTER 4

On the Three-Particle Analog of the Lellouch-Lüscher Formula

The content of this chapter following this prologue is based on the publication

- F. Müller and A. Rusetsky, *On the three-particle analog of the Lellouch-Lüscher formula*, JHEP **03** (2021) 152, arXiv: 2012.13957 [hep-lat]

Using non-relativistic effective field theory, in this chapter a three-particle analog of the Lellouch-Lüscher formula in the three-body center of mass frame is derived at the leading order in the NREFT power counting. This formula relates the three-particle decay matrix elements in a finite volume to their infinite-volume counterparts and, hence, can be used to study three-particle decays on the lattice. Such a method was not available before. The generalization of the approach to higher orders is briefly discussed.

For typical hadronic three-body decay processes, the momenta of the decay products are not small as compared to their mass. An application of the original NREFT setup, where relativistic corrections are treated perturbatively, thus proves inappropriate. Although not being wrong in principle, achieving relativistic invariance in the two-particle sector order by order is cumbersome and rather intransparent. Instead the use of the covariant form of NREFT, actually introduced in [166, 167] in the context of the decay $K \to 3\pi$, reproduces the singularity structure in the two-body subsystem directly. In the context of finite-volume three-body dynamics the modified NREFT framework was not applied before. Thus, in a first step, the author of this thesis rederived the three-particle quantization condition for three identical bosons in the covariant NREFT at the leading order in the particle-dimer picture.

In order to keep the derivation of the three-particle analogue of the Lellouch-Lüscher formula as simple as possible, although not describing a physical process, the decay of a spinless particle into three identical likewise spinless particles was considered. Accordingly the three-particle Lagrangian was augmented with an operator that describes the initial decay process. As the decay is considered to be perturbative, the resulting infinite- and finite-volume decay matrix elements should be proportional to the coupling that describes the initial decay to the first order. Therefore it should be possible to derive a linear relation between the infinite-volume decay amplitude in terms of the finite-volume decay matrix element, where the proportionality factor, referred to as Lellouch-Lüscher factor, only depends on the LECs that describes the rescattering of the final-state particles. Furthermore, it should

contain the non-regular volume dependence that arises due to the dynamics of the final-state particles in a finite volume.

For the actual derivation of the LL factor the author of this thesis closely followed Ref. [50], where a derivation of the LL factor in the two-particle sector was derived within the covariant NREFT formulation. Using the Feynman rules of the effective theory, the author derived an expression for the infinite-volume decay amplitude in terms of the particle-dimer scattering amplitude first. The calculation of the corresponding decay matrix element in a finite volume then proceeded by considering the correlation function of a three-body annihilation operator with a source operator describing the initial decay. Within the NREFT treatment the author calculated this correlator to first order perturbation theory in the decay coupling, while the final state interactions were summed up to all orders. Furthermore, if the overlap of the three-body annihilation operator with a three-particle state at the energy of the initial particle is known, the finite-volume decay matrix element can be determined. An expression for this overlap can be obtained by calculating the finite-volume six-point correlation function from the three-body operator in the NREFT. Comparing the expressions for the infinite- and finite-volume decay matrix elements the author was finally able to derive the three-particle LL factor.

Although the leading order result of this chapter will probably be sufficient for actual applications, considering the present status of lattice calculations in the three-body sector, a complete description of three-body decays requires the inclusion of higher derivative couplings. This is in contrast to the two-body sector, where the absolute values of the momenta of the final particles are fixed by kinematics. Nevertheless this chapter introduces the fundamental techniques that will be similarly applied in the derivation of the LL equation at higher orders.

4.1 Introduction

Back in 2000, Lellouch and Lüscher [45] derived a formula, which related the matrix element of the weak $K \to 2\pi$ decay in a finite volume to its infinite-volume counterpart. These two quantities turn out to be proportional with a factor (Lellouch-Lüscher (LL) factor), depending on the size L of a cubic box and on the elastic two-body pion-pion scattering phase shift. The result of Ref. [45] paved the way to the systematic studies of various two-body decays on the lattice. Later, different generalizations of the method emerged, e.g., for moving frames [35, 46], or for the case of coupled two-body channels [41]. A simple and transparent derivation of the LL formula with the use of the non-relativistic effective Lagrangians has been given in [50]. For the application of the formalism, we refer here, e.g., to a comprehensive study of the $K \to \pi\pi$ decays, which has been carried out recently by the RBC and UKQCD Collaborations [152]. From the related work, we mention the study of the matrix elements of currents, corresponding to the $1 \to 2$ transition [47, 184], and of the timelike pion form factor [185], which all feature the similar factor in a finite volume. Generally, in the LL type formulae, this L-dependent factor emerges from the multiple rescattering of two particles in the final state (pions), and the phase shift, which also enters the expression, should be measured on the same lattice, simultaneously with the measurement of the decay matrix element. It can be done by using the Lüscher formula that relates the phase shift to the volume-dependent spectrum in the two-particle sector.

To summarize, the two-body problem is completely understood from the conceptual point of view – both the scattering, as well as two-body decays. On the contrary, the three-body formalism

is still in development. Recently, three physically equivalent forms of the quantization condition have been proposed [55, 58–61], which relate the three-body spectrum in a finite volume with the infinite-volume parameters in the three-body sector. However, in contrast to the two-body case, where the Lüscher equation enables one to extract the two-body phase shift from the measured spectrum in one step, the procedure in the three-particle sector is more complicated. To start with, the three-body quantization condition becomes tractable only if the three-body interactions are expressed in terms of few parameters. In the approach of Refs. [60, 61], such a parameterization naturally emerges, when the three-body interactions are evaluated from the effective Lagrangian at tree level that allows one to impose a consistent power counting. Similarly, the three-body kernels in the approaches of Refs. [55, 58] and Ref. [59] can be expanded in the external momenta (up to a given order) in the vicinity of the threshold. Thus, the fit of the quantization condition to the three-particle spectrum, which is measured on the lattice, enables one to extract few parameters (the effective three-particle couplings, or the coefficients in the expansion of the three-particle kernel). These can be substituted into the infinite-volume equations to calculate observables in the three-particle sector. Consequently, extracting the three-particle observables from data necessarily involves an intermediate step, and cannot be done directly, as in case of two particles.

It should be mentioned that the above theoretical developments have largely boosted the study of three (and more particles) on the lattice, be this in QCD or other field-theoretical models [28, 29, 65, 157, 186–190]. In view of these activities, the need for the three-particle analog of the LL formula, which should be used for the extraction of the matrix elements, becomes obvious. Such a formula, however, was not available in the literature so far. Moreover, bearing in mind the above discussion, it is not even clear, whether the relation between the finite- and infinite-volume matrix elements, which one is after, should contain a single overall factor (a counterpart of the LL factor), or should be more complicated. On the other hand, recent years have seen a growing interest to the study of three-particle decays. The most obvious candidates for this study in the beginning are provided by the three-pion decays of low-mass light-flavored mesons $K \to 3\pi$, $\eta \to 3\pi$ and $\omega \to 3\pi$. The decays of the heavier pseudovector mesons $a_1(1260) \to \rho\pi \to 3\pi$ and $a_1(1420) \to f_0(980)\pi \to 3\pi$ are also very interesting[1]. Further, the candidates for exotica, $X(3872)$ and $X(4260)$, decay largely into the three-particle final states as well. Last but not least, the extraction of the parameters of the Roper resonance on the lattice has proven to be very challenging. That might be, in part, related to the lack of proper treatment of the three-particle decay channel in a finite volume. Our paper intends to make the first step towards the creation of a systematic finite-volume framework for the study of three-body decays on the lattice that will contribute to the solution of the above-mentioned problems[2].

Note that the resonances, which are studied in lattice QCD, fall into two categories. To the first category belong the ones, which are stable in pure QCD, like kaons that decay through weak interactions. Further, the η-mesons are not stable in QCD. However, the decay amplitude is proportional to the u- and d-quark mass difference $m_u - m_d$ and thus vanishes in the isospin limit. So, if one wants to know this amplitude only at the first order in $m_u - m_d$ (this completely suffices for practical reasons), one could also formally categorize this decay into the first group and treat the final state interactions in the isospin-symmetric QCD, where the η-mesons are stable. The second, larger group consists

[1] As one will see later, in the lattice study of all these decays, a prior knowledge of the three-pion amplitude is necessary. The total isospin of the decay products in the above processes is different, but neither of them equals the maximal possible isospin $I = 3$, available in the system of three pions. It is important to note that the three-body finite-volume formalism, which enables one to explore the systems with an arbitrary isospin, has become available only very recently [4, 161].

[2] After the present paper was submitted to the archive, Ref. [191], which deals with the same issue, has appeared.

of the genuine QCD resonances. In this paper, like in the original paper by Lellouch and Lüscher, we concentrate our effort on the first group. The treatment of the QCD resonances is a more subtle issue that includes, in particular, analytic continuation into the complex energy plane to the resonance pole. In the case of two-body decays, this procedure is discussed, in particular, in Refs. [50, 51, 192–194]. We postpone the discussion of a similar procedure in the three-particle sector to our future investigations.

The layout of the paper is as follows: In Sect. 4.2, we display the lowest-order non-relativistic effective Lagrangian and write down the quantization condition in a finite volume. In Sect. 4.3, we derive the LL equation at leading order. The extension of the approach to higher orders is discussed in Sect. 4.4. Section 4.5 contains our conclusions.

4.2 Non-Relativistic Framework

The non-relativistic EFT framework, which was tailored to study the singularity structure of the amplitudes in three-body decays, was proposed in Ref. [166]. It has been successfully used in the study of the three-body decays of charged and neutral kaons, as well as ω, η and η' mesons [195–199]. A brief review of the essential points of the approach is given in Ref. [167]. The main difference of this approach from the conventional ones consists in the treatment of the relativistic corrections to the internal particle lines. Whereas in the conventional approach, these corrections are treated perturbatively, in the new one they are summed up to all orders, ensuring the correct relativistic dispersion law. As a result, the location of singularities in the decay amplitude stays fixed to all orders and coincides with the singularity structure of the relativistic amplitude. There is a price to pay for this, however: the resummed propagators feature the hard scale – the particle mass – explicitly. This, as known, leads to the breakdown of the naive counting rules. In order to rectify the counting rules, one then has to amend the procedure for the calculation of the Feynman integrals – dimensional regularization plus minimal subtraction does not suffice. The modification of the procedure, which is equivalent to the change of the renormalization prescription, is described in detail in [167], and we refer an interested reader to that article.

To purify the problem from the inessential details as much as possible, we shall consider below a decay of a spinless particle ("kaon") into three likewise spinless particles ("pions"). Isospin and other quantum numbers are discarded. We also assume that there exists some discrete symmetry (like G-parity), which forbids transitions with an odd number of the external pion legs. The non-relativistic fields $K(x)$ and $\phi(x)$ describe kaons and pions, respectively, and M, m denote their masses. The lowest-order Lagrangian, which describes the decay, is given by

$$\begin{aligned} \mathcal{L} &= K^\dagger 2W(i\partial_t - W)K + \phi^\dagger 2w(i\partial_t - w)\phi \\ &+ \frac{C_0}{4}\phi^\dagger\phi^\dagger\phi\phi + \frac{D_0}{36}\phi^\dagger\phi^\dagger\phi^\dagger\phi\phi\phi + \frac{G_0}{6}\left(K^\dagger\phi\phi\phi + \text{h.c.}\right), \end{aligned} \tag{4.1}$$

where $W = \sqrt{M^2 - \nabla^2}$ and $w = \sqrt{m^2 - \nabla^2}$.

In the above Lagrangian, the constant G_0 describes the elementary act of the kaon decay into three pions. It is proportional to the weak coupling constant and enters the amplitudes, by definition, only at the first order. If the weak interactions are switched off, the kaon is stable. Further, the constants C_0 and D_0 describe the strong final state interactions in the system of two and three pions respectively.

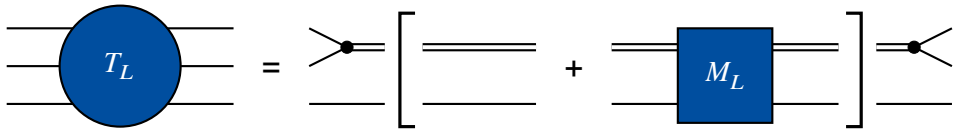

Figure 4.1: Expressing the three-particle scattering amplitude through the particle-dimer scattering amplitude, see Eq. (4.13). The single and double lines are the particle and the dimer propagators, respectively, and the filled circle denotes the two-particle-dimer vertex.

Unlike the constant G_0, these enter the expression of the amplitude at all orders. The matching at the two-pion threshold relates the constant C_0 to the pion-pion scattering length a:

$$C_0 = -32\pi am\,. \tag{4.2}$$

In Eq. (4.1), only the leading-order terms are displayed. The power counting at the Lagrangian level is defined by the (formal) requirement that all three-momenta count at $O(p)$, whereas the kinetic energies of the individual pions, as well as the quantity $M - 3m$ count at $O(p^2)$. The higher-order Lagrangians would contain an even number of spatial derivatives, acting on all fields. Below, we shall concentrate on the derivation of the LL formula at the leading order, using the Lagrangian in Eq. (4.1). The inclusion of the higher-order terms will be considered briefly in Sect. 4.4.

Moreover, in order to write down the equation that determines the three-particle scattering amplitude, we shall switch to the particle-dimer picture. It is well-known that this formulation, which is equivalent to the original one, enables one to drastically simplify the bookkeeping of Feynman diagrams and arrive at the result with a surprising ease [95, 98, 173]. The Lagrangian in the particle-dimer picture in our case is given by:

$$\begin{aligned} \mathcal{L} &= K^\dagger 2W(i\partial_t - W)K + \phi^\dagger 2w(i\partial_t - w)\phi + \sigma d^\dagger d \\ &+ \frac{f_0}{2}\left(d^\dagger\phi\phi + \text{h.c.}\right) + h_0 d^\dagger d\phi^\dagger\phi + g_0\left(K^\dagger d\phi + \text{h.c.}\right)\,. \end{aligned} \tag{4.3}$$

Here, d denotes the dimer field, and $\sigma = \pm 1$, depending on the sign of the constant C_0. Integrating out the field d in the path integral and expanding in the powers of fields, one arrives at the Lagrangian, given in Eq. (4.1), if the following relations are fulfilled:

$$\sigma f_0^2 = -C_0, \qquad 9f_0^2 h_0 = D_0, \qquad 3\sigma f_0 g_0 = -G_0\,. \tag{4.4}$$

We would like to stress here that the validity of the particle-dimer picture does not imply that a two-body bound state really exists. As one sees, the dimer field is introduced in the path integral as a dummy integration variable and, hence, the resulting formulation is mathematically equivalent to the initial one without a dimer field. If a dimer (or a narrow low-lying resonance) indeed exists, this may affect only the convergence of the expansion. In this case, the bulk of the two-particle interaction will be described by the dimer exchange in the s-channel, and the contribution from the higher orders will be small.

The Lagrangian (4.3) will be used for the calculation of the Feynman diagrams in a finite volume – as it is well-known, the sole change is the replacement of the infinite-momentum integrals by the

sums over the discrete three-momenta of particles in a finite cubic box[3]. The propagator of the non-relativistic field $\phi(x)$ in a finite volume is given by:

$$i\langle 0|T\phi(x)\phi^\dagger(y)|0\rangle = \int \frac{dp_0}{2\pi}\,\frac{1}{L^3}\sum_{\mathbf{p}}\frac{e^{-ip_0(x_0-y_0)+i\mathbf{p}(\mathbf{x}-\mathbf{y})}}{2w(\mathbf{p})(w(\mathbf{p})-p_0-i\varepsilon)}\,,\qquad w(\mathbf{p})=\sqrt{m^2+\mathbf{p}^2}\,. \tag{4.5}$$

The dimer propagator is obtained by summing pion loops to all orders:

$$i\langle 0|Td(x)d^\dagger(y)|0\rangle = \int \frac{dP_0}{2\pi}\,\frac{1}{L^3}\sum_{\mathbf{P}} e^{-iP_0(x_0-y_0)+i\mathbf{P}(\mathbf{x}-\mathbf{y})}\,D_L(\mathbf{P};P_0)\,. \tag{4.6}$$

Here D_L obeys the following equation:

$$D_L(\mathbf{P};P_0) = -\frac{1}{\sigma}-\frac{f_0^2}{2\sigma}\,J_L(\mathbf{P};P_0)D_L(\mathbf{P};P_0)\,, \tag{4.7}$$

where J_L denotes a single pion loop:

$$\begin{aligned} J_L(\mathbf{P};P_0) &= \frac{1}{L^3}\sum_{\mathbf{k}}\frac{1}{4w(\mathbf{k})w(\mathbf{P}-\mathbf{k})(w(\mathbf{k})+w(\mathbf{P}-\mathbf{k})-P_0-i\varepsilon)} \\ &= \frac{p^*}{8\pi^{5/2}\sqrt{s}\gamma\eta}Z_{00}^{\mathbf{d}}(1;s)\,, \end{aligned} \tag{4.8}$$

and

$$s=P_0^2-\mathbf{P}^2,\quad \gamma=\frac{P_0}{\sqrt{s}},\quad p^*=\sqrt{\frac{s}{4}-m^2},\quad \eta=\frac{p^*L}{2\pi},\quad \mathbf{d}=\frac{\mathbf{P}L}{2\pi}\,. \tag{4.9}$$

Further, in Eq. (4.8), $Z_{00}^{\mathbf{d}}(1;s)$ is the usual Lüscher zeta function, boosted to the moving frame defined by the vector $\mathbf{d}$. For a general (lm), this function is given by:

$$Z_{lm}^{\mathbf{d}}(1;s)=\sum_{\mathbf{r}\in P_d}\frac{\mathcal{Y}_{lm}(\mathbf{r})}{\mathbf{r}^2-\eta^2}\,,\quad P_d=\left\{\mathbf{r}\in\mathbb{R}^3\middle|r_\parallel=\gamma^{-1}\left(n_\parallel-|\mathbf{d}|/2\right),\ \mathbf{r}_\perp=\mathbf{n}_\perp,\ \mathbf{n}\in\mathbb{Z}^3\right\}, \tag{4.10}$$

where $\mathcal{Y}_{lm}(\mathbf{r})=|\mathbf{r}|^l Y_{lm}(\hat{r})$, and $Y_{lm}(\hat{r})$ denotes the usual spherical function that depends on the unit vector $\hat{r}$. Finally, after using the matching condition, for the dimer propagator one obtains:

$$D_L(\mathbf{P};P_0)=\frac{\sigma\sqrt{s}/(2am)}{-\sqrt{s}/(2am)+p^*\cot\phi^{\mathbf{d}}(s)},\qquad \cot\phi^{\mathbf{d}}(s)=-\frac{Z_{00}^{\mathbf{d}}(1;s)}{\pi^{3/2}\gamma\eta}\,. \tag{4.11}$$

In the non-relativistic limit, $\sqrt{s}/(2m)\to 1$, $\gamma\to 1$, and we arrive at the expression displayed in Refs. [60, 61]. At higher orders, the expression $-1/a$ both in the numerator and the denominator gets

[3] For simplicity, below we display all formulae in the Minkowski space. The final results, obtained with the use of Wick rotation, are identical.

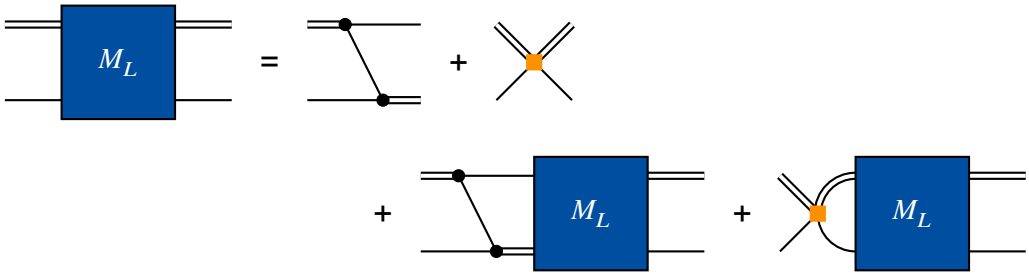

Figure 4.2: The Faddeev equation for the particle-dimer scattering amplitude. The red shaded squares denote the particle-dimer coupling.

replaced by $p^* \cot\delta(p^*) = -1/a + r{p^*}^2/2 + \ldots$. Further, the infinite-volume counterpart of Eq. (4.11) reads:

$$D(\mathbf{P}; P_0) = \frac{\sigma\sqrt{s}/(2am)}{-\sqrt{s}/(2am) - ip^*}\,. \tag{4.12}$$

The finite-volume energy levels in the three-particle system coincide with the location of the poles of the three-particle scattering amplitude. In the particle-dimer picture, this quantity can be directly related to the particle-dimer scattering amplitude [60, 61, 146], see Fig. 4.1. At the lowest order, the relation is given by:

$$\begin{aligned} T_L(\{\mathbf{p}\},\{\mathbf{q}\};P_0) \;=\; & \sum_{\alpha,\beta=1}^{3}\Big[\tau_L(-\mathbf{p}_\alpha;P_0)2w(\mathbf{p}_\alpha)L^3\delta_{\mathbf{p}_\alpha\mathbf{q}_\beta} \\ & +\; \tau_L(-\mathbf{p}_\alpha;P_0)M_L(-\mathbf{p}_\alpha,-\mathbf{q}_\beta;P_0)\tau_L(-\mathbf{q}_\beta;P_0)\Big], \end{aligned} \tag{4.13}$$

where $\{\mathbf{p}\}$ stands for the set of all three particle momenta $\mathbf{p}_\alpha$ with $\alpha = 1,2,3$. In the center-of-mass frame, the dimer momenta are equal to $-\mathbf{p}_\alpha$. The sets $\{\mathbf{q}\}$, $\{\mathbf{k}\}$ are defined similarly. Further,

$$\tau_L(\mathbf{p};P_0) = f_0^2 D_L(\mathbf{p};P_0 - w(\mathbf{p}))\,. \tag{4.14}$$

In the infinite volume, the relation between the quantities $\tau(\mathbf{p};P_0)$ and $D(\mathbf{p};P_0)$ takes a similar form. Further, $M_L(\mathbf{p},\mathbf{q};P_0)$ denotes the particle-dimer scattering amplitude, which obeys the Faddeev equation in a finite volume, see Fig. 4.2:

$$M_L(\mathbf{p},\mathbf{q};P_0) = Z(\mathbf{p},\mathbf{q};P_0) + \frac{1}{L^3}\sum_{\mathbf{k}}^{\Lambda} Z(\mathbf{p},\mathbf{k};P_0)\frac{\tau_L(\mathbf{k};P_0)}{2w(\mathbf{k})}M_L(\mathbf{k},\mathbf{q};P_0), \tag{4.15}$$

where Λ denotes an ultraviolet cutoff and

$$Z(\mathbf{p},\mathbf{q};P_0) = \left[\frac{1}{2w(\mathbf{p}+\mathbf{q})(w(\mathbf{p}+\mathbf{q})+w(\mathbf{p})+w(\mathbf{q})-P_0-i\varepsilon)} + \frac{h_0}{f_0^2}\right]. \tag{4.16}$$

In the infinite volume, the Faddeev equation becomes the integral equation with the same kernel Z and cutoff Λ:

$$M(\mathbf{p},\mathbf{q};P_0) = Z(\mathbf{p},\mathbf{q};P_0) + \int^{\Lambda} \frac{d^3\mathbf{k}}{(2\pi)^3}\, Z(\mathbf{p},\mathbf{k};P_0)\frac{\tau(\mathbf{k};P_0)}{2w(\mathbf{k})}M(\mathbf{k},\mathbf{q};P_0)\,. \tag{4.17}$$

The quantization condition in a finite volume takes the form:

$$\det(A) = 0\,, \qquad A_{\mathbf{pq}} = 2w(\mathbf{p})\tau_L^{-1}(\mathbf{p};P_0)L^3\delta_{\mathbf{pq}} - Z(\mathbf{p},\mathbf{q};P_0)\,. \tag{4.18}$$

The discrete solutions $P_0 = E_n$ of the quantization condition determine the finite-volume spectrum of the three-particle system. Further, in the vicinity of a pole $P_0 = E_n$, the residue of the particle-dimer amplitude factorizes:

$$M_L(\mathbf{p},\mathbf{q};P_0)\Big|_{P_0\to E_n} = \frac{\psi_L^{(n)}(\mathbf{p})\psi_L^{(n)}(\mathbf{q})}{E_n - P_0} + \text{regular}\,. \tag{4.19}$$

The particle-dimer wave function obeys a homogeneous equation:

$$\psi_L^{(n)}(\mathbf{p}) = \frac{1}{L^3}\sum_{\mathbf{k}}^{\Lambda} Z(\mathbf{p},\mathbf{k};E_n)\frac{\tau_L(\mathbf{k};E_n)}{2w(\mathbf{k})}\psi_L^{(n)}(\mathbf{k})\,. \tag{4.20}$$

The normalization condition for the finite-volume wave function $\psi_L^{(n)}(\mathbf{p})$ can be derived in a standard manner by using Eqs. (4.17), (4.19) and (4.20). Since both Z and τ_L are energy-dependent, $\psi_L(\mathbf{p})$ is not merely normalized to unity. Instead, the normalization condition takes the form:

$$\begin{aligned}&\frac{1}{L^6}\sum_{\mathbf{p},\mathbf{k}}^{\Lambda}\psi^{(n)}(\mathbf{p})\frac{\tau_L(\mathbf{p};E_n)}{2w(\mathbf{p})}\frac{dZ(\mathbf{p},\mathbf{k};E_n)}{dE_n}\frac{\tau_L(\mathbf{k};E_n)}{2w(\mathbf{k})}\psi_L^{(n)}(\mathbf{k})\\ &+\frac{1}{L^3}\sum_{\mathbf{p}}^{\Lambda}\psi^{(n)}(\mathbf{p})\frac{1}{2w(\mathbf{p})}\frac{d\tau_L(\mathbf{p};E_n)}{dE_n}\psi_L^{(n)}(\mathbf{p}) = 1\,.\end{aligned} \tag{4.21}$$

The three-particle scattering amplitude factorizes as well:

$$T_L(\{\mathbf{p}\},\{\mathbf{q}\};P_0)\Big|_{P_0\to E_n} = \frac{\Psi_L^{(n)}(\{\mathbf{p}\})\Psi_L^{(n)}(\{\mathbf{q}\})}{E_n - P_0} + \text{regular}\,, \tag{4.22}$$

where

$$\Psi_L^{(n)}(\{\mathbf{p}\}) = \sum_{\alpha=1}^{3}\tau_L(-\mathbf{p}_\alpha;E_n)\psi_L^{(n)}(-\mathbf{p}_\alpha)\,. \tag{4.23}$$

Up to the change to the relativistic normalization and the use of the relativistic kinematics in the dimer propagator, these equations are equivalent to the ones displayed in Refs. [60, 61, 146]. The numerical solution of similar equations in a finite volume has been considered also, e.g., in Refs. [101–104].

4.3 Derivation of the Three-Particle Analog of the LL Formula at the Leading Order

The derivation of the counterpart of the LL formula in the three-particle sector proceeds along the path already used in the two-particle case [50]. The main idea can be formulated in few words. The non-relativistic effective Lagrangians, used to describe physics in the infinite and in a finite volume, are the same. At the leading order, the only unknown, which can be extracted from the measured $K \to 3\pi$ decay matrix element on the lattice, is the coupling G_0 (other couplings, C_0 and D_0, can be independently determined by measuring the two- and three-body energy levels). Hence, the only thing that one has to do is to calculate the decay matrix elements in the effective theory twice: in a finite and in the infinite volume. Since at the leading order this matrix element is merely proportional to G_0, in the ratio of the results of the two calculations, which is the three-particle analog of the LL factor we are looking for, this constant drops out. Thus, the final answer is expressed solely in terms of known constants C_0 and D_0.

The crucial point in this derivation is to concentrate on G_0 which, by definition, is the same in a finite and in the infinite volume, up to the exponentially suppressed corrections. In these corrections, the hard scale of the effective theory appears in the argument of the exponent (in our case, this hard scale is given by the pion mass m). On the contrary, the measured matrix element contains a non-trivial, power-law L-dependence, which emerges via the final state interactions. Hence, no regular $L \to \infty$ limit exists for this matrix element.

After this introductory remark, we proceed with the calculation of the decay matrix element. Following Ref. [50], first, one has to calculate the wave function renormalization constant for the composite operator $O(x_0; \{\mathbf{k}\})$, which creates three pions with momenta $\mathbf{k}_1, \mathbf{k}_2, \mathbf{k}_3$, acting on the vacuum bra-vector $\langle 0|$:

$$O(x_0; \{\mathbf{k}\}) = \int d^3\mathbf{x}_1 d^3\mathbf{x}_2 d^3\mathbf{x}_3 \; e^{-i\mathbf{k}_1\mathbf{x}_1 - i\mathbf{k}_2\mathbf{x}_2 - i\mathbf{k}_3\mathbf{x}_3} \phi(x_0, \mathbf{x}_1)\phi(x_0, \mathbf{x}_2)\phi(x_0, \mathbf{x}_3)\,. \tag{4.24}$$

Assume now that $x_0 > y_0$. Inserting a complete set of the intermediate states, for the two-body correlator one gets:

$$\langle 0|O(x_0; \{\mathbf{k}\})O^\dagger(y_0; \{\mathbf{k}\})|0\rangle = \sum_n |\langle 0|O(0; \{\mathbf{k}\})|n\rangle|^2 \, e^{-iE_n(x_0 - y_0)}\,. \tag{4.25}$$

On the other hand, one can evaluate this correlator in the perturbation theory. Summing up all diagrams, one obtains:

$$\begin{aligned}\langle 0|O(x_0; \{\mathbf{k}\})O^\dagger(y_0; \{\mathbf{k}\})|0\rangle = \int \frac{dP_0}{2\pi i} \, e^{-iP_0(x_0 - y_0)} \\ \times \left\{ \frac{L^9 \left(1 + \delta_{\mathbf{k}_1\mathbf{k}_2} + \delta_{\mathbf{k}_1\mathbf{k}_3} + \delta_{\mathbf{k}_2\mathbf{k}_3} + 2\delta_{\mathbf{k}_1\mathbf{k}_2}\delta_{\mathbf{k}_2\mathbf{k}_3}\right)}{8w(\mathbf{k}_1)w(\mathbf{k}_2)w(\mathbf{k}_3)(w(\mathbf{k}_1) + w(\mathbf{k}_2) + w(\mathbf{k}_3) - P_0 - i\varepsilon)} \right. \\ \left. + \frac{L^3 T_L(\{\mathbf{k}\}, \{\mathbf{k}\}; P_0)}{\left(8w(\mathbf{k}_1)w(\mathbf{k}_2)w(\mathbf{k}_3)(w(\mathbf{k}_1) + w(\mathbf{k}_2) + w(\mathbf{k}_3) - P_0 - i\varepsilon)\right)^2} \right\}.\end{aligned} \tag{4.26}$$

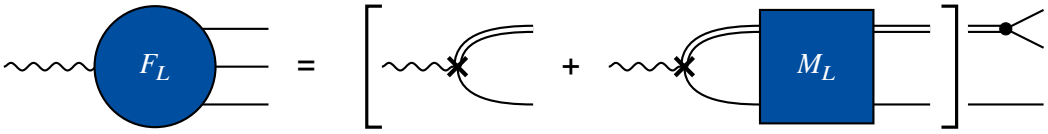

Figure 4.3: The amplitude of the $K \to 3\pi$ decay in the particle-dimer picture. The notations are the same as in Figs. 4.1 and 4.2. The cross denotes the vertex, which correspond to the decay of a kaon into a particle-dimer pair. This vertex comes with the coupling g_0.

Using Eq. (4.22) and performing contour integration by means of the Cauchy theorem, one gets:

$$\langle 0|O(x_0;\{\mathbf{k}\})O^\dagger(y_0;\{\mathbf{k}\})|0\rangle = \sum_n \frac{e^{-iE_n(x_0-y_0)}L^3\left(\Psi_L^{(n)}(\{\mathbf{k}\})\right)^2}{\left(8w(\mathbf{k}_1)w(\mathbf{k}_2)w(\mathbf{k}_3)(w(\mathbf{k}_1)+w(\mathbf{k}_2)+w(\mathbf{k}_3)-E_n)\right)^2}\,. \tag{4.27}$$

From this, we finally obtain:

$$|\langle 0|O(0;\{\mathbf{k}\})|n\rangle| = L^{3/2}\frac{\left|\Psi_L^{(n)}(\{\mathbf{k}\})\right|}{\left|8w(\mathbf{k}_1)w(\mathbf{k}_2)w(\mathbf{k}_3)(w(\mathbf{k}_1)+w(\mathbf{k}_2)+w(\mathbf{k}_3)-E_n)\right|}\,. \tag{4.28}$$

In the above derivation, it was assumed that the free-particle singularities, emerging from the energy denominators in Eq. (4.26), cancel in the full expression for the correlator. This statement, which is evident on general grounds, was verified (in threshold kinematics) in Ref. [55]. We refer an interested reader to that paper for more details.

Next, we calculate the decay matrix element. First, note that the kaon interaction term in the particle-dimer Lagrangian (4.3) can be rewritten in a form $J_K^\dagger(x)K(x) + \text{h.c.}$, where

$$J_K^\dagger = g_0 d^\dagger \phi^\dagger\,. \tag{4.29}$$

Consequently, on the one hand, assuming $x_0 > 0$, one gets:

$$\langle 0|O(x_0;\{\mathbf{k}\})J_K^\dagger(0)|0\rangle = \sum_n e^{-iE_n x_0}\langle 0|O(0;\{\mathbf{k}\})|n\rangle\langle n|J_K^\dagger(0)|0\rangle\,. \tag{4.30}$$

On the other hand, using perturbation theory and summing up pertinent diagrams results in:

$$\langle 0|O(x_0;\{\mathbf{k}\})J_K^\dagger(0)|0\rangle = \int\frac{dP_0}{2\pi i}\,\frac{e^{-iP_0x_0}F_L(\{\mathbf{k}\};P_0)}{8w(\mathbf{k}_1)w(\mathbf{k}_2)w(\mathbf{k}_3)(w(\mathbf{k}_1)+w(\mathbf{k}_2)+w(\mathbf{k}_3)-P_0-i\varepsilon)}\,, \tag{4.31}$$

where (see Fig. 4.3):

$$F_L(\{\mathbf{k}\};P_0) = \frac{g_0}{f_0}\sum_{\alpha=1}^{3}\tau_L(-\mathbf{k}_\alpha;P_0)\left[1+\frac{1}{L^3}\sum_{\mathbf{q}}^{\Lambda}M_L(-\mathbf{k}_\alpha,-\mathbf{q};P_0)\frac{1}{2w(\mathbf{q})}\tau_L(-\mathbf{q};P_0)\right]\,. \tag{4.32}$$

Further, using Eq. (4.19) and performing Cauchy integration in Eq. (4.31), one gets:

$$L^{3/2}|\langle n|J_K^\dagger(0)|0\rangle| = \left|\frac{g_0}{f_0}\,\frac{1}{L^3}\sum_{\mathbf{q}}^{\Lambda}\psi_L^{(n)}(-\mathbf{q})\frac{1}{2w(\mathbf{q})}\,\tau_L(-\mathbf{q};E_n)\right|. \tag{4.33}$$

Now, carrying out the calculations in the infinite volume, we get:

$$\begin{aligned}&\langle\pi(\mathbf{k}_1)\pi(\mathbf{k}_2)\pi(\mathbf{k}_3);\text{out}|J_K^\dagger(0)|0\rangle\\ &= \frac{g_0}{f_0}\sum_{\alpha=1}^{3}\tau(-\mathbf{k}_\alpha;P_0)\left[1+\int^{\Lambda}\frac{d^3\mathbf{q}}{(2\pi)^3}\,M(-\mathbf{k}_\alpha,-\mathbf{q};P_0)\frac{1}{2w(\mathbf{q})}\,\tau(-\mathbf{q};P_0)\right],\end{aligned} \tag{4.34}$$

where the particle-dimer scattering amplitude M is the solution of Eq. (4.17).

Finally, comparing Eqs. (4.33) and (4.34), one gets:

$$\langle\pi(\mathbf{k}_1)\pi(\mathbf{k}_2)\pi(\mathbf{k}_3);\text{out}|J_K^\dagger(0)|0\rangle = \Phi_3(\{\mathbf{k}\})\cdot L^{3/2}\langle n|J_K^\dagger(0)|0\rangle\,, \tag{4.35}$$

where the leading-order three-particle LL factor is given by:

$$\Phi_3(\{\mathbf{k}\}) = \pm\frac{\displaystyle\sum_{\alpha=1}^{3}\tau(-\mathbf{k}_\alpha;P_0)\left[1+\int^{\Lambda}\frac{d^3\mathbf{q}}{(2\pi)^3}\,M(-\mathbf{k}_\alpha,-\mathbf{q};P_0)\frac{1}{2w(\mathbf{q})}\,\tau(-\mathbf{q};P_0)\right]}{\displaystyle\frac{1}{L^3}\sum_{\mathbf{q}}^{\Lambda}\psi_L^{(n)}(-\mathbf{q})\frac{1}{2w(\mathbf{q})}\,\tau_L(-\mathbf{q};E_n)}\,. \tag{4.36}$$

The above equation implies that in the lattice measurement the box size L was adjusted so that $P_0 = E_n = M$ is exactly fulfilled in the rest frame of the kaon. Note also that the numerator in Eq. (4.36) is a complex quantity and the Eq. (4.35) predicts both the real and imaginary parts of the infinite-volume matrix element, up to an overall sign. The phase of the infinite-volume decay amplitude is determined by what can be termed the Watson theorem in the three-body case.

The equations (4.35) and (4.36) describe our final result. As seen, all quantities in Eq. (4.36) can be expressed through the couplings C_0 and D_0 which, in their turn, can be extracted from the independent measurement of the two- and three-particle spectra. The analogy with the two-body LL formula is now complete.

4.4 Higher Orders

For a two-particle system, the LL formula contains a single factor to all orders. This is not the case for three particles anymore. The situation is completely similar to the three-particle quantization condition. In this section, we would like to briefly discuss the generalization of the approach, described above, in the case when the higher-order (derivative) couplings are included in the effective Lagrangian.

We start our discussion from the two-body decays. Suppose, the particle with a mass M decays in the CM frame into two identical particles with the mass m. In the infinite volume, the physical back-to-back momenta are then fixed by energy conservation $M = 2\sqrt{m^2+k^2}$. On the lattice, let us fix the momenta, say, along the third axis, assuming $\mathbf{k}_1 = (0,0,n)$ and $\mathbf{k}_2 = (0,0,-n)$ in the units of

$2\pi/L$. Here, n is an integer number (the choice of the direction does not matter, due to the rotational invariance). For a fixed n, one may adjust L so that the energy of the two-particle state equals to the mass of the decaying particle. One then measures the finite-volume decay matrix element exactly at this value of L, applies the LL formula and finally extracts the infinite-volume matrix element one is looking for. What remains veiled in this discussion is that one could choose different values of n and L, so that the total energy stays the same. In practice, this corresponds to considering the different (ground and excited) states. The matrix elements, measured in these states, are different, and so are the pertinent LL factors. The crucial point is that these two quantities are always correlated, so that one always extracts the same physical infinite-volume amplitude out of the different measurements. The mathematical reason for this correlation is that there exists only one independent two-body decay coupling at all orders, and the finite-volume decay amplitudes in different states should be expressed in terms of this single coupling.

It becomes now crystal clear, what changes in case of three-particle decays. The distribution of energies between three decay products is not fixed by the energy conservation anymore. This results in a non-trivial momentum dependence of the decay amplitude, which is conveniently described by a tower of the effective couplings $G_0, G_1, G_2, \ldots$ in the Lagrangian, multiplying the operators containing more and more spatial derivatives. Truncating the expansion at a given order, one gets N independent couplings, which should be fixed by the measurement of N linearly independent finite-volume amplitudes. Consequently, in general, the LL factor is not a single function. It is rather a $N \times N$ matrix, depending of the pion interaction parameters in the two-body ($C_0, \ldots$) and three-body ($D_0, \ldots$) sectors. Using this matrix enables one to map the results of the measurements of the matrix elements in different states onto the couplings $G_0, G_1, G_2, \ldots$ (note that the states n implicitly depend on the momenta $\mathbf{k}_1, \mathbf{k}_2, \mathbf{k}_3$, which enter the source/sink operator). At the next step, using the infinite-volume scattering equations, it is possible to calculate pion rescattering in the final state and express the physical decay matrix element in arbitrary kinematics. The above discussion also shows that the extraction of the effective couplings represents a convenient strategy in the analysis of the lattice data.

The second question, which emerges during the generalization of the approach to higher orders, is predominantly of a technical nature. Namely, in the present formulation, the final-state rescattering corrections in the three-particle states at higher orders are not given in an explicitly Lorentz-invariant form. Albeit there is nothing wrong with this in principle, an explicitly Lorentz-invariant setting in the three-particle sector would provide a far nicer and more compact framework at higher orders, containing less effective couplings from the beginning (nothing will change at the leading order we are working in). Note that such a technical modification has already been considered within an alternative formulation of the three-body quantization condition. The modification, which boils down to the replacement of the energy denominators by the explicitly Lorentz-invariant expressions that coincide with the former on the energy shell, has been discussed in detail in Refs. [159, 174, 200, 201]. It remains to be seen, how (and whether) the similar idea can be implemented within our approach.

4.5 Conclusions

i) In the present paper, using the non-relativistic effective Lagrangian approach, we have derived the leading-order counterpart of the LL formula for three-particle decays. As in the two-particle case, the LL factor depends on the parameters of the pion interactions only (both in the two- and

three-particle sectors), which can be measured independently from the decay matrix element in the same lattice setup.

ii) At higher orders, the LL factor becomes a $N \times N$ matrix, where N denotes the number of independent couplings that describe the elementary act of the three-particle decay at this order. These couplings provide a convenient parameterization of the decay amplitude for the extraction on the lattice. The infinite-volume amplitudes (in an arbitrary continuum kinematics) can be calculated *a posteriori,* solving the scattering equations in the infinite volume.

iii) Some technical issues remain to be solved in higher orders. For example, an explicitly Lorentz-invariant framework would be more convenient (albeit not obligatory) to carry out the extraction, because the invariance puts stringent constraints on the possible form of the amplitude, reducing the number of the effective couplings needed at a given order. At the leading order, where the pertinent operator in the Lagrangian does not contain derivatives at all, this issue is not relevant. Other technical modifications concern the decays of particles with spin, partial wave mixing, moving frames, etc. The work in this direction is already in progress, and the results will be reported elsewhere.

iv) As noted already, the above-mentioned modifications do not affect our result, obtained at the leading order in the non-relativistic EFT. Taking into account the present state of lattice studies in the three-particle sector, one expects that in the beginning, all these higher-order effects will be of mainly academic interest, and the leading-order formula will completely suffice in the applications.

CHAPTER 5

Relativistic-Invariant Formulation of the NREFT Three-Particle Quantization Condition

The content of this chapter following this prologue, including Appendix A.2 is based on the publication

- F. Müller, J.-Y. Pang, A. Rusetsky and J.-J. Wu, *Relativistic-invariant formulation of the NREFT three-particle quantization condition*, JHEP **02** (2022) 158, arXiv: 2110.09351 [hep-lat]

Deriving a three-particle quantization condition that can be used in order to analyze data from different moving frames collectively remained an unsolved problem in the context of the NREFT treatment. This necessarily raised questions about the Lorentz-covariance of the approach, which is rather obscure in the three-body sector. The benefits of working in a manifestly Lorentz-invariant framework are obvious. A similar issue was discussed in the last chapter, regarding the generalization of the three-particle analogue of the Lellouche-Lüscher equation to higher orders.

This problem is addressed in this chapter. In a modified framework, the NREFT is reformulated in an arbitrary frame, characterized by a timelike unit vector v^μ. Introducing an external frame explicitly breaks Lorentz-invariance. However amplitudes are rendered invariant, if v^μ is expressed in terms of the incoming- and outgoing momenta of the particles, such that these quantities transform in the same way. The method presented here is inspired by formulating scattering for an arbitrary quantization axis [202] where a covariant form of time-order perturbation theory is utilized [203]. In the context of effective field theories, the quantization with respect to an arbitrary moving frame is used in the description of heavy quarks and heavy baryons.

Within the modified framework a three-particle quantization condition is written down in a manifestly relativistic-invariant form by using this generalization of the non-relativistic effective field theory approach. The inclusion of the higher partial waves is explicitly addressed. A partial diagonalization of the quantization condition into the various irreducible representations of the (little groups of the) octahedral group has been carried out both in the center-of-mass frame and in moving frames. Furthermore, producing synthetic data in a toy model, the relativistic invariance is explicitly demonstrated for the three-body bound state spectrum.

The project started by revisiting the pure two-body sector in the infinite volume under the modifications. Using dimensional regularization and the threshold expansion it was possible to show that the two-body scattering amplitude is independent of the quantization axis v^μ. Indeed upon a change in the renormalization prescription, the modified framework is equivalent to the covariant

NREFT approach. Based on these observations the author of this thesis derived a three-particle quantization condition at the leading order, contributing a calculation for the two-body amplitude in a finite volume. This leading order result was later used in order to explore the relativistic invariance of the new approach numerically.

The author of this article subsequently was involved with the numerical studies of the three-particle system that were independently performed by Jin-Yi Pang. A first check of the modified framework was conducted by calculating the bound-state spectrum of the infinite-volume particle-dimer scattering amplitude. In the unitary limit $a \to \infty$, the spectrum of non-relativistic particles consists out of an infinite number of *Efimov states* [173, 176, 204, 205] that exhibit a universal scaling property. This behavior should be reproduced also in the relativistic setup in the vicinity of the threshold, since the particles momenta are small in this region such that non-relativistic kinematics can be assumed. On the other hand, unlike in the non-relativistic case, the Efimov states are not expected to reach arbitrarily deep energies. Indeed, close to threshold, an Efimov spectrum could be observed.

The author of this thesis further implemented a routine to determine the three-body finite-volume energy spectra in different moving frames above and below threshold. The relativistic invariance of the quantization condition was then tested by considering the bound state spectrum in a finite volume in the following procedure: For a given value of the scattering length and cutoff, the leading order three-body coupling was chosen such that there exists a deep bound state of an input binding energy. Another shallow bound state close to threshold was observed. The cutoff here was chosen such that no significant dependence on this parameter was observed. Namely, the cutoff was raised at least until the resulting spectrum did not show any significant changes when further increasing the cutoff. Since bound states correspond to one-particle states, their finite-volume energy levels should obey the relativistic energy-momentum dispersion law up to exponentially suppressed corrections. This was confirmed in various moving frames.

5.1 Introduction

Recent years have witnessed a rapid growth of interest to the three-body problem on the lattice. This interest dates back to 2012, when it was shown, for the first time, that the three-body spectrum in a finite volume is determined solely by the three-body S-matrix elements [55]. In the next years, three different but conceptually equivalent settings emerged that allow to study the three-body problem in a finite volume: the so-called Relativistic Field Theory (RFT) [57, 58], Non-Relativistic Effective Field Theory (NREFT) [60, 61] and Finite Volume Unitarity (FVU) [59, 206] approaches. Besides this, much work has been done, see, e.g., [56, 63, 64, 66, 101–104, 146, 158–163, 174, 200, 201, 207–226]. The finite-volume spectrum has been also studied in perturbation theory. In fact, these investigations go back to the 1950's and have been re-activated recently with the use of the modern technique of the non-relativistic effective Lagrangians [4, 143, 144, 154, 155, 157, 210, 222, 227–229]. Furthermore, in quite a few recent papers, the theoretical approaches mentioned above have been successfully used to analyze data from lattice calculations [28, 29, 65, 66, 157, 186–190, 230–232]. Last but not least, a three-body analog of the Lellouch-Lüscher formula for the finite-volume matrix elements [45] has been recently derived in two different settings [1, 191]. These developments are extensively covered in the latest reviews on the subject, to which the reader is referred for further details [30, 62].

In this paper, we put the issue of the relativistic invariance of the quantization condition under a detailed scrutiny. The reason for this is obvious. Typical momenta of light particles (most notably,

pions), which are studied on the lattice, are not small as compared to their masses. Albeit the four- and more particle channels might be closed, or contribute very little, a purely kinematic effect of the relativistic invariant treatment could be still sizable, especially, if data from the moving frames are considered. For this reason, providing a manifestly relativistic invariant framework for three particles is extremely important[1].

On the other hand, in the derivation of the quantization condition in a field theory one faces a dilemma (this problem concerns all formulations, albeit it is treated differently in different formulations). The amplitudes that enter the quantization condition should be on mass shell – otherwise, these will not be observables and there will be little use of such a quantization condition. Hence, the quantization condition is inherently three-dimensional (i.e., it involves integrations/sums over three-momenta, with the fourth component fixed on mass shell), and further effort is needed to rewrite it in the manifestly invariant form.

It is natural to ask the question why the manifest invariance of the setting is important. The (three-dimensional) Faddeev equation, which is obeyed by the infinite-volume amplitude, contains what can be termed as a short-range three-body force (this quantity enters the finite-volume quantization condition as well, and its name is different in different approaches). In principle, choosing this three-body force properly, it should be always possible to achieve the invariance of the amplitude (because the true amplitude is invariant and obeys the same equation). However, implementing this program in practice represents a very difficult task. Namely, finding an explicit parameterization of the three-body force that renders the solution of the Faddeev equations invariant most probably will prove impossible. Furthermore, making the tree-level kernel of the Faddeev equation relativistic invariant order by order in the effective field theory expansion will not suffice – without further ado – to ensure the invariance of the amplitude at the same order, because the cutoff regularization, which is used in Faddeev equation, breaks counting rules. All this results in a very cumbersome and obscure treatment of the problem that one should better avoid. On the contrary, in case of a manifestly invariant formulation, the three-body force can be readily parameterized in terms of Lorentz-invariant structures only, see, e.g., a nice discussion in Ref. [174]. The couplings appearing in front of these structures are mutually independent and the expansion of the short-range part can be organized in accordance with the well-defined counting rules. Hence, the advantages of having a manifestly invariant formulation are evident.

As mentioned above, additional effort is needed to rewrite the three-dimensional Faddeev equations (infinite volume) and the quantization condition (finite volume) in the manifestly invariant form. As we shall see later, the problem arises because the three-particle propagator, which originally appears in these equations, is non-invariant. As a cure to the problem, within the RFT approach, it was proposed to modify the three-body propagator, bringing it to a manifestly invariant form (the pertinent formulae are given, e.g., in Ref. [65], see also Ref. [177]) [2]. We shall briefly consider this prescription below, in Sect. 5.3. It can be however shown that the modified propagator breaks unitarity at low energies (in the infinite volume) and leads to the spurious energy levels below three-particle threshold (in a finite volume), if the cutoff on the spectator momentum exceeds some critical value of order of the particle mass itself. As a result, if one uses the modified propagator, one cannot choose an arbitrarily high cutoff. This is a limitation of the RFT method.

[1] This statement, obviously, refers to the three-particle system in the infinite volume. In a finite volume, the relativistic invariance is anyway broken by the presence of a box.

[2] Note that the same technique could be used, without any modification, in the NREFT approach as well.

The aim of the present paper is to close the above gap. Our method is based on the "covariant" version of the NREFT, considered in Refs. [166, 167, 195–197]. We modify that framework, choosing the quantization axis along arbitrary timelike unit vector v^μ and demonstrate an explicit relativistic invariance of the obtained Faddeev equations with respect to the Lorentz boosts (the original framework corresponded to the choice $v^\mu = v_0^\mu = (1, \mathbf{0})$). The explicit relativistic invariance of the framework emerges if the vector v^μ is fixed in terms of the initial and final momenta in the three-particle system (an obvious choice is to take v^μ proportional to the total four-momentum). It is further shown that there is no restriction on the cutoff within our approach, no breaking of unitarity and no spurious poles for high values of the cutoff.

Last but not least, we carry out a full group-theoretical analysis of the quantization condition both in the center-of-mass (CM) frame and in moving frames. Namely, the quantization condition is diagonalized into the various irreducible representations (irreps) of the pertinent point groups. The theoretical constructions are verified numerically, solving the quantization condition for a toy model.

To simplify the argument as much as possible, we consider the case of three identical bosons with a mass m and assume that all Green functions with odd number of external legs identically vanish. These simplifications are of purely technical nature and can be straightforwardly relaxed. The layout of the paper is the following. In Sect. 5.2 we consider the two-body sector of the theory and the introduction of auxiliary dimer fields. The three-body sector is considered in Sect. 5.3, where it is shown that the obtained Faddeev equation for the particle-dimer scattering is explicitly relativistic invariant. In this section, we also derive the relativistic invariant quantization condition and carry out a partial diagonalization of this condition into different irreps. In Sect. 5.4 we investigate the synthetic three-particle spectrum, obtained in a toy model with the use of the novel quantization condition. Sect. 5.5 contains our conclusions.

5.2 Two-Body Sector

5.2.1 Threshold Expansion

The non-relativistic approach treats time and space directions differently that leads to an inherent non-covariance. A trick which allows one to rewrite all expressions in an explicitly covariant manner is to introduce an arbitrary unit timelike vector v^μ and to consider the time evolution along the axis defined by this vector. The choice of the "rest frame" $v^\mu = v_0^\mu = (1, \mathbf{0})$ corresponds to the "standard" NREFT. According to the Lorentz invariance, all choices of v^μ are physically equivalent and describe the time evolution as seen by different moving observers. Note also that a similar trick (albeit in a slightly different physical context) is also used in the Heavy Quark Effective Theory and the Heavy Baryon Chiral Perturbation Theory.

Of course, indroducing the vector v^μ alone does not solve the problem of the non-covariance – it just allows to recast it fancier. The presence of an *external* vector v^μ signals non-covariance. The situation however changes, if it is possible to express v^μ through the momenta that characterize a given process. Then, if the latter are boosted, v^μ is boosted as well, rendering the amplitudes explicitly Lorentz-covariant. This provides exactly the solution we are looking for. In the discussion below, we keep v^μ arbitrary in the beginning, and fix it in terms of the physical momenta at a later stage.

We start with the construction of the non-relativistic Lagrangians. In the "rest frame," these are written down, e.g., in Refs. [166, 167] on the basis of the following considerations:

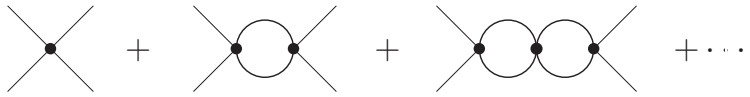

Figure 5.1: Two-body amplitude in the non-relativistic theory. The filled dots denote the full four-particle vertex that can be read off from the interaction Lagrangian. This vertex is a low-energy polynomial.

- The nonrelativistic theories do not include the creation and annihilation of particles and antiparticles explicitly (the latter can be barred from the theory altogether, if one considers the processes with only particles in the initial/final states). The effects of creation and annihilation are not neglected but consistently included in the effective couplings. Hence, the non-relativistic Lagrangian is linear in the time derivative, and the propagators feature only particle or only antiparticle pole.

- No approximation is made in the energy of the free particle $w(\mathbf{k}) = \sqrt{m^2 + \mathbf{k}^2}$. This ensures that the low-energy singularities of the Feynman diagrams are located exactly at the right place at all orders of the non-relativistic expansion.

- The normalization of the non-relativistic field is chosen so that the normalization of the one-particle states in the relativistic and non-relativistic theories is the same.

Below, the Lagrangians derived in Refs. [166, 167] are rewritten in an arbitrary frame defined by the vector v^μ. The kinetic part then takes the form

$$\mathcal{L}_{\text{kin}} = \phi^\dagger 2w_v(i(v\partial) - w_v)\phi\,. \tag{5.1}$$

Here, $\phi(x)$ is the non-relativistic field, describing the particle and w_v denotes the differential operator

$$w_v = \sqrt{m^2 + \partial^2 - (v\partial)^2}\,. \tag{5.2}$$

The free non-relativistic propagator is given by

$$\begin{aligned} i\langle 0|T[\phi(x)\phi^\dagger(y)]|0\rangle &= \int \frac{d^4k}{(2\pi)^4}\, e^{-ik(x-y)} D(k)\,, \\ D(k) &= \frac{1}{2w_v(k)(w_v(k) - vk - i\varepsilon)}\,, \end{aligned} \tag{5.3}$$

where $w_v(k) = \sqrt{m^2 - k^2 + (vk)^2}$. In case of $v^\mu = v_0^\mu$, the above formulae coincide with the ones from Refs. [166, 167].

Next, let us consider the interactions in the two-particle sector. The full Lagrangian consists of an infinite tower of terms with zero, two,. . . derivatives in the interaction part

$$\mathcal{L} = \mathcal{L}_{\text{kin}} + \mathcal{L}_0 + \mathcal{L}_2 + \cdots\,. \tag{5.4}$$

The lowest-order term is given by

$$\mathcal{L}_0 = C_0 \phi^\dagger \phi^\dagger \phi \phi \,. \tag{5.5}$$

The coupling C_0 can be easily related to the two-body S-wave scattering lengths a_0 through the matching condition.

As usual, calculating the two-particle scattering amplitude for the process $p_1 + p_2 \to q_1 + q_2$ with this Lagrangian amounts to summing up all bubble diagrams, see Fig. 5.1. In the S-wave amplitude, this gives:

$$T_0 = (4C_0) + (4C_0)^2 \frac{1}{2} I + (4C_0)^3 \frac{1}{4} I^2 + \cdots = \frac{1}{(4C_0)^{-1} - \frac{1}{2} I} \,. \tag{5.6}$$

Here, I denotes a loop integral

$$I = \int \frac{d^D k}{(2\pi)^D i} \frac{1}{2w_v(k)(w_v(k) - vk - i\varepsilon)} \frac{1}{2w_v(P-k)(w_v(P-k) - v(P-k) - i\varepsilon)} \,, \tag{5.7}$$

and $P = p_1 + p_2 = q_1 + q_2$ is the total CM momentum of a particle pair.

Before the evaluation of the above integral the following remarks are in order. First of all, the integrals are ultraviolet-divergent and should be regularized. We use dimensional regularization throughout this paper. This is however not sufficient for ensuring the preservation of counting rules in the loops. To this end, the so-called *threshold expansion* (see, e.g., [172]) should be applied to the loops. One namely first uses the identity

$$\begin{aligned} \frac{1}{2w_v(k)(w_v(k) - vk - i\varepsilon)} &= \frac{w_v(k) + vk}{2w_v(k)(m^2 - k^2 - i\varepsilon)} \\ &= \frac{1}{m^2 - k^2 - i\varepsilon} - \frac{1}{2w_v(k)(w_v(k) + vk - i\varepsilon)} \,, \end{aligned} \tag{5.8}$$

and a similar identity for the second propagator. Substituting these expression in Eq. (5.7), one gets four terms. Furthermore, the threshold expansion is applied in the vicinity of the *particle* poles, $vk = w_v(k)$ and $v(P-k) = w_v(P-k)$, respectively. Moreover, it is assumed that the "three-momenta" with respect to the quantization axis v^μ, defined as $k_\perp^\mu = k^\mu - v^\mu vk$ and $(P-k)_\perp^\mu = (P-k)^\mu - v^\mu v(P-k)$ are small as compared to the particle mass m.[3] This means that the second term in the above expression

[3] In the standard formulation of the threshold expansion (in the "rest frame"), it is assumed that the components of the three-momentum are small, $\mathbf{k}^2 \ll m^2$. More precisely, one introduces a generic small parameter ϵ and counts $\mathbf{k} = O(\epsilon)$, $k^0 = O(1)$. Now, assumming (formally) that $\mathbf{v} = O(\epsilon)$, one immediately sees that the components of the vector $k_\perp^\mu = k^\mu - v^\mu vk$ are of order ϵ as well. This counting holds, even if k^μ is an integration momentum. In this case, it is understood merely as a prescription that generates threshold expansion in the Feynman integrals. It should be further stressed that ϵ is just a parameter that is used in bookkeeping of various contributions. In actual calculations, this parameter may turn out not to be too small. A nice example is provided by the three-particle decays of kaons and η-mesons, where the decay products move with the momenta that are not so small as compared to their masses. Despite this fact, the approach works very well [166, 167]. Note also that the results of the present paper (a derivation of the relativistically invariant quantization condition, see below) are exact (to all orders in ϵ) and do not use a particular numerical value of ϵ. They simply rely on the fact that one can expand the integrand in powers of ϵ, carry out the integration in dimensional regularization and resum the final result again.

can be expanded as

$$-\frac{1}{2w_v(k)(w_v(k)+vk-i\varepsilon)} = -\frac{1}{4w_v^2(k)} - \frac{w_v(k)-vk}{8w_v^3(k)} + \cdots$$
$$= -\frac{1}{4m^2} + \frac{k_\perp^2}{4m^4} + \cdots - \frac{m-vk}{8m^3} + \cdots , \tag{5.9}$$

where the relation $w_v^2(k) = m^2 - k_\perp^2$ has been used. A similar expansion can be written down for the second propagator. It is now immediately seen that only one term contributes to I after the threshold expansion since, in the other terms, the integrand becomes a low-energy polynomial that leads to a vanishing integral in dimensional regularization. Hence, after performing the threshold expansion, we get:

$$I = I(s) = \int \frac{d^D k}{(2\pi)^D i} \frac{1}{(m^2-k^2)(m^2-(P-k)^2)} = \text{const} + \frac{\sigma}{16\pi^2} \ln\left(\frac{\sigma-1}{\sigma+1}\right), \tag{5.10}$$

where

$$s = P^2, \qquad \sigma = \left(1 - \frac{4m^2}{s+i\varepsilon}\right)^{1/2} . \tag{5.11}$$

The renormalization prescription is chosen so that $I(s)$ vanishes at the two-particle threshold $s = 4m^2$.

The expression of the loop function, given in Eq. (5.10), is explicitly Lorentz-invariant (depends on the variable s only). It also differs from the expression used in Refs. [166, 167, 195–197]. Namely, the imaginary parts of these two expressions coincide above elastic threshold that ensures two-body unitarity. Moreover, their difference is a low-energy polynomial with real coefficients and, hence, the choice of the loop function in a form given by Eq. (5.10) is as legitimate as the choice made earlier in Refs. [166, 167, 195–197] – these two correspond to a different renormalization prescription in the effective theory. Below, we shall stick to the definition given in Eq. (5.10). It has the advantage that the loop function is real and non-singular below threshold, whereas the original definition leads to a spurious singularity at $s = 0$ and to an imaginary part below this value (we remind the reader that the point $s = 0$ lays already outside the region of the applicability of the NREFT, so the question about the consistency of the approach does not arise here).

Note also that the original derivation given in the above papers was much shorter – there, one first integrated over the variable k^0 and then manipulated the integrand, depending on the three-momenta only. In case of arbitrary v^μ, the dependence of the integrand on k^0 is more complicated. In principle, in the infinite volume, one could first perform a Lorentz boost that brings the vector v^μ to v_0^μ and then repeat the steps outlined in these papers. The result will of course be the same. We however stick to this derivation that can be applied in a finite volume without much ado.

In the following, it will be useful to rewrite the loop function as

$$I(s) = J(s) + \frac{i\sigma}{16\pi} . \tag{5.12}$$

Here, as mentioned before, the function $J(s)$ is a low-energy polynomial with real coefficients.

5.2.2 Terms with Higher Derivatives

The terms with higher derivatives, present in the Lagrangian, are of two types. The terms of the first type correspond to the effective-range expansion in a given partial wave (S-wave, in our case), and the terms of a second type describe higher partial waves.

Let us start with the former. The Lagrangian

$$\mathcal{L}_2 = C_2\Big\{\big((w_\mu\phi)^\dagger(w^\mu\phi)^\dagger\phi\phi - m^2\phi^\dagger\phi^\dagger\phi\phi\big) + \text{h.c.}\Big\} \tag{5.13}$$

encodes the term related to the S-wave effective range r_0. Here,

$$w^\mu = v^\mu w_v + i\partial_\perp^\mu\,, \qquad \partial_\perp^\mu = \partial^\mu - v^\mu v\partial\,. \tag{5.14}$$

Furthermore, the tree amplitude in a theory consists of the contributions from $\mathcal{L}_0$, $\mathcal{L}_2, \ldots$, see Eqs. (5.4), (5.2.1) and (5.13):

$$T_{\text{tree}} = T_{\text{tree}}^{(0)} + T_{\text{tree}}^{(2)} + \cdots\,. \tag{5.15}$$

As we already know, at lowest order,

$$T_{\text{tree}}^{(0)} = 4C_0\,. \tag{5.16}$$

Using now Eq. (5.13), it is straightforward to derive that, on mass shell,

$$T_{\text{tree}}^{(2)} = 4C_2\big(s - 4m^2\big)\,, \tag{5.17}$$

where $s = (\tilde{p}_1 + \tilde{p}_2)^2 = (\tilde{q}_1 + \tilde{q}_2)^2$, and $\tilde{p}_i^\mu = v^\mu w_v(p_i) + p_{i\perp}^\mu$ (similarly for $\tilde{q}_i^\mu$ and any other vector). On the mass shell, where $w_v(p_i) = vp_i$, $w_v(q_i) = vq_i$ and, consequently, $\tilde{p}_i = p_i$, $\tilde{q}_i = q_i$, it also follows that $s = (p_1 + p_2)^2 = (q_1 + q_2)^2$.

It is now crystal clear, how things proceed at higher orders. The tree-level amplitude in the S-wave represents a Taylor series in $s - 4m^2$:

$$T_{\text{tree}}^{\text{S-wave}} = 4C_0 + 4C_2(s - 4m^2) + 4C_4(s - 4m^2)^2 + \cdots\,, \tag{5.18}$$

All this is fine at tree level, on the mass shell. In the bubble sum, however, the intermediate particles are off the mass shell. Consider, for example the process $p_1 + p_2 \to k_1 + k_2$, where $p_i^2 = m^2$ and $k_i^2 \neq m^2$. Then, $s_p = (\tilde{p}_1 + \tilde{p}_2)^2$ is not equal to $s_k = (\tilde{k}_1 + \tilde{k}_2)^2$, even if the relation $p_1 + p_2 = k_1 + k_2$ always holds. Furthermore, the difference between s_p and s_k is proportional to $w_v(p_1) + w_v(p_2) - w_v(k_1) - w_v(k_2)$. Carrying out now the contour integration, one can straightforwardly ensure that such a term in the numerator cancels exactly with the denominator. One is left with a low-energy polynomial, and the integral over this polynomial vanishes in dimensional regularization. Therefore, replacing s_k by $s_p = s$ everywhere in the numerator is justified. One may finally conclude that one could consistently pull out the numerator from the integral and evaluate it on shell. This results in the following S-wave amplitude:

$$T_0(s) = \frac{1}{(T_{\text{tree}}^{\text{S-wave}})^{-1} - \frac{1}{2}\,I(s)}\,. \tag{5.19}$$

Just above threshold, $s > 4m^2$, one may rewrite this expression as

$$T_0(s) = \frac{16\pi\sqrt{s}}{16\pi\sqrt{s}((T_{\rm tree}^{\rm S-wave})^{-1} - \frac{1}{2}\,J(s)) - ip(s)}\,, \qquad p(s) = \sqrt{\frac{s}{4} - m^2}\,. \tag{5.20}$$

Thus, just above threshold, the tree amplitude can be related to the S-wave scattering phase shift

$$16\pi\sqrt{s}((T_{\rm tree}^{\rm S-wave})^{-1} - \frac{1}{2}\,J(s)) = p(s)\cot\delta_0(s)\,. \tag{5.21}$$

Expanding both sides in powers of $(s - 4m^2)$, one may carry out the matching of the constants $C_0, C_2, \ldots$ and the effective-range parameters in the S-wave $a_0, r_0, \ldots$. The lowest-order relation $C_0 = -8\pi m a_0$ is the same as in Refs. [166, 167] – the modifications emerge, starting from the second order only.

Considering higher partial waves is a bit more subtle because the pertinent amplitudes depend on the directions of momenta as well. In the simple model considered, there is no P-wave. The lowest-order contribution of the D-wave is captured by the Lagrangian

$$\begin{aligned}
\mathcal{L}_4 &= \mathcal{L}_4^{\rm S} + \mathcal{L}_4^{\rm D}\,,\\
\mathcal{L}_4^{\rm S} &= 4C_4\Big(\big((w_\mu\phi)^\dagger(w^\mu\phi)^\dagger - m^2\phi^\dagger\phi^\dagger\big)\big((w_\nu\phi)(w^\nu\phi) - m^2\phi\phi\big)\Big)\,,\\
\mathcal{L}_4^{\rm D} &= \frac{5}{2}\,D_4\Big(3(w_\mu\phi)^\dagger(w_\nu\phi)^\dagger(w^\mu\phi)(w^\nu\phi) - (w_\mu\phi)^\dagger(w^\mu\phi)^\dagger(w_\nu\phi)(w^\nu\phi)\\
&\quad - \frac{m^2}{2}\,\big((w_\mu\phi)^\dagger(w^\mu\phi)^\dagger\phi\phi + \text{h.c.}\big) - m^4\phi^\dagger\phi^\dagger\phi\phi\Big)\,.
\end{aligned} \tag{5.22}$$

The contribution from $\mathcal{L}_4^{\rm S}$ in the S-wave amplitude is already shown in Eq. (5.18). The contribution of the second term contributes to the on-shell tree amplitude in the D-wave:

$$\begin{aligned}
T_{\rm tree}^{\rm D-wave} &= \frac{5}{2}\,D_4\Big(6\big((\tilde p_1\tilde q_1)(\tilde p_2\tilde q_2) + (\tilde p_1\tilde q_2)(\tilde p_2\tilde q_1)\big) - 4(\tilde p_1\tilde p_2)(\tilde q_1\tilde q_2)\\
&\quad - 2m^2\big((\tilde p_1\tilde p_2) + (\tilde q_1\tilde q_2)\big) - 4m^4\Big) + \cdots\\
&= 4D_4p^4(s)(2\cdot 2+1)P_2(\cos\theta) + \cdots\,,
\end{aligned} \tag{5.23}$$

where $P_\ell(\cos\theta)$ stand for the Legendre polynomials, and

$$\cos\theta = \frac{t-u}{s-4m^2}\,. \tag{5.24}$$

Here s, t, u denote usual Mandelstam variables. Note that we have already used Lorentz invariance – the above expression does not depend on the vector v^μ.

Next, let us consider summing up all bubble diagrams in the D-wave amplitude. The second

iteration, for example, can be written as

$$\begin{aligned} \text{second iteration} &= \int \frac{d^D k_1}{(2\pi)^D i} \frac{d^D k_2}{(2\pi)^D i} (2\pi)^D \delta^D(p_1 + p_2 - k_1 - k_2) \\ &\times T_{\text{tree}}^{\text{D-wave}}(\tilde{p}_1, \tilde{p}_2; \tilde{k}_1, \tilde{k}_2) D(k_1) D(k_2) T_{\text{tree}}^{\text{D-wave}}(\tilde{k}_1, \tilde{k}_2; \tilde{q}_1, \tilde{q}_2) \,. \end{aligned} \tag{5.25}$$

Here, $D(k)$ denotes the free propagator, see Eq. (5.3).

Furthermore, since p_i, q_i are on the mass shell, $\tilde{p}_i^\mu = p_i^\mu$ and $\tilde{q}_i^\mu = q_i^\mu$. On the contrary, $\tilde{k}_i^\mu = k_i^\mu + v^\mu(w_v(k_i) - v k_i) \neq k_i^\mu$. The additional term cancels with the denominator in $D(k_i)$, leaving us, after performing the contour integral, with an integral over the low-energy polynomial that vanishes in the dimensional regularization. Hence, a replacement $\tilde{k}_i^\mu \to k_i^\mu$ in the numerator is justified. Next, using Eq. (5.8), we may rewrite the above equation as:

$$\begin{aligned} \text{second iteration} &= \int \frac{d^D k_1}{(2\pi)^D i} \frac{d^D k_2}{(2\pi)^D i} (2\pi)^D \delta^D(p_1 + p_2 - k_1 - k_2) \\ &\times \frac{T_{\text{tree}}^{\text{D-wave}}(p_1, p_2; k_1, k_2) T_{\text{tree}}^{\text{D-wave}}(k_1, k_2; q_1, q_2)}{(m^2 - k_1^2 - i\varepsilon)(m^2 - k_2^2 - i\varepsilon)} \,. \end{aligned} \tag{5.26}$$

It is seen that this integral is written down in a completely Lorentz-invariant form. In order to evaluate it, we perform the boost to the center-of-mass frame of two particles. In this system, the angular integral can be readily done, yielding the Legendre polynomial. Pulling again the numerator out from the integral, we finally get:

$$\text{second iteration} = (4 D_4 p^4(s))^2 \frac{1}{2} I(s)(2 \cdot 2 + 1) P_2(\cos\theta) \,. \tag{5.27}$$

Now, it is easy to write down the result for the D-wave amplitude, summing up the bubbles at all orders:

$$T_2(s) = \frac{p^4(s)}{(4D_4)^{-1} - \frac{1}{2} p^4(s) I(s)} \,. \tag{5.28}$$

Furthermore, it is already clear that, if higher-order terms are taken into account, the D-wave amplitude takes the form

$$T_2(s) = \frac{p^4(s)}{(T_{\text{tree}}^{\text{D-wave}})^{-1} - \frac{1}{2} p^4(s) I(s)} \,, \qquad T_{\text{tree}}^{\text{D-wave}} = 4D_4 + 4D_6(s - 4m^2) + \cdots \,. \tag{5.29}$$

The matching condition in the D-wave is given by:

$$16\pi\sqrt{s}\big((T_{\text{tree}}^{\text{D-wave}})^{-1} - \frac{1}{2} p^4(s) J(s)\big) = p^5(s) \cot\delta_2(s) \,. \tag{5.30}$$

We are now in a position to write down the expression of the complete amplitude:

$$T(s,t) = \sum_\ell (2\ell+1) P_\ell(\cos\theta) T_\ell(s), \qquad T_\ell(s) = \frac{p^{2\ell}(s)}{(T^\ell_{\text{tree}})^{-1} - \frac{1}{2}\, p^{2\ell}(s) I(s)}, \tag{5.31}$$

where T^ℓ_{tree} represents a low-energy polynomial in the variable $(s-4m^2)$. The matching condition

$$16\pi\sqrt{s}\big((T^\ell_{\text{tree}})^{-1} - \frac{1}{2}\, p^{2\ell}(s) J(s)\big) = p^{2\ell+1}(s)\cot\delta_\ell(s) \tag{5.32}$$

allows one to perform the matching of the couplings in the low-energy effective Lagrangian to the parameters of the effective-range expansion in all partial waves.

In conclusion, we would like to note that, albeit we have started with an explicitly non-covariant Lagrangian, the physical amplitudes are relativistic invariant, i.e., do not depend on the vector v^μ. This statement is by no means trivial[4]. The relativistic invariance could be achieved, because a) the interaction Lagrangian of four pions has a particularly simple form – it is a bunch of local vertices, and b) the threshold expansion has been applied in the calculation of Feynman integrals. In the three-particle sector, neither of these conditions hold. The result depends on v^μ and the relativistic invariance is achieved, when v^μ is fixed in terms of the external momenta. Below, in Sect. 5.3, we shall consider this issue in detail.

5.2.3 Introducing Dimers

As in Refs. [60, 61], we shall introduce dimer fields in the Lagrangian in order to trade four-particle interactions in favor of particle-dimer vertices. This will lead to a significant simplification in the description of the three-particle systems, since the bookkeeping of different diagrams is made much easier in the particle-dimer picture. Note also that, according to our philosophy, introducing a dimer does not necessarily mean that a physical dimer (two-particle bound state) should exist, albeit this may still be the case. Thus, the particle-dimer formalism is not an *approximation* – rather, it is a *different choice of variables* in the path integral, equivalent to the original formulation. Note also that, instead of a single dimer field, we in fact have to introduce an infinite bunch of dimer fields with different spin, corresponding to different angular momenta ℓ in the two-particle system.

Let us again start with the S-wave, and consider the Lagrangian

$$\begin{aligned} \mathcal{L}_{\text{S}} &= \phi^\dagger 2w_v(i(v\partial) - w_v)\phi + \sigma T^\dagger T \\ &+ \left(\frac{1}{2}\, T^\dagger\big(f_0\phi\phi + f_2\big((w_\mu\phi)(w^\mu\phi) - m^2\phi\phi\big) + \cdots\big) + \text{h.c.}\right) + \cdots . \end{aligned} \tag{5.33}$$

Here, T denotes a (scalar) dimer field which does not possess a kinetic term, and $\sigma = \pm 1$, depending on the sign of the coupling C_0. It is easily seen that, integrating out the dimer field in the path integral, we arrive at the four-particle local coupling one has started with. It is then a simple algebraic exercise to express the new couplings $f_0, f_2, \ldots$ through the $C_0, C_2, \ldots$ and σ.

The inclusion of the dimers with higher spins proceeds similarly – one has to merely reformulate the construction of Ref. [61] in the present relativistic setting. To this end, we introduce the tensor

[4] In Refs. [166, 167], the invariance was demonstrated for a particular choice $v^\mu = v_0^\mu$.

dimer fields $T_{\mu_1,\cdots,\mu_\ell}$, corresponding to the angular momentum ℓ. These fields are symmetric under the permutation of each pair of indices, traceless in each pair of indices and obey the constraints[5]:

$$v^{\mu_i} T_{\mu_1,\cdots,\mu_\ell} = 0\,, \qquad i = 1,\cdots,\ell\,. \tag{5.34}$$

These constraints leave the correct number of independent degrees of freedom, equal to $2\ell + 1$.. The Lagrangian in the two-particle sector can be written as:

$$\mathcal{L} = \phi^\dagger 2w_v(i(v\partial) - w_v)\phi + \sum_{\ell=0}^{\infty} \sigma_\ell T^\dagger_{\mu_1,\cdots,\mu_\ell} T^{\mu_1,\cdots,\mu_\ell} + \frac{1}{2}\sum_{\ell=0}^{\infty}\left(T^\dagger_{\mu_1,\cdots,\mu_\ell} O^{\mu_1,\cdots,\mu_\ell} + \text{h.c.}\right), \tag{5.35}$$

where $\sigma_\ell = \pm 1$ and $O^{\mu_1,\cdots,\mu_\ell}$ are the relativistic two-particle operators, corresponding to the orbital momentum ℓ. These operators can be easily constructed, based on the explicit expression of the spherical functions. For example, the lowest-order operator in the D-wave is given by:

$$\begin{aligned} O^{\mu\nu} &= g_0\Bigg(\frac{3}{2}\left(\phi(\bar{w}^\mu_\perp \bar{w}^\nu_\perp \phi) - (\bar{w}^\mu_\perp \phi)(\bar{w}^\nu_\perp \phi)\right) \\ &- \frac{1}{2}\left(g^{\mu\nu} - v^\mu v^\nu\right)\left(\phi(\bar{w}^\lambda_\perp \bar{w}_{\perp\lambda}\phi) - (\bar{w}^\lambda_\perp \phi)(\bar{w}_{\perp\lambda}\phi)\right)\Bigg), \end{aligned} \tag{5.36}$$

where $\bar{w}^\mu_\perp = \bar{w}^\mu - v^\mu(v\bar{w})$ and $\bar{w}^\mu$ denotes the operator w^μ which is boosted in the CM system of two particles *with respect to the vector* v^μ. Under this, we mean that the boosted total momentum of two particles on mass shell is parallel to the vector v^μ. Needless to say that, in a particular case $v^\mu = v^\mu_0$, we get the usual definition of the two-particle CM frame.

The transformation of w^μ to $\bar{w}^\mu$ is given through the matrix

$$\bar{w}^\mu = \Lambda^\mu_\nu w^\nu\,. \tag{5.37}$$

It is easier to work in the momentum space. Let $\tilde{p}_{1,2}$ be the on-mass shell momenta of individual particles. Then, $P = \tilde{p}_1 + \tilde{p}_2$ is the total on-mass shell momentum of the pair. The boost makes the vector P^μ parallel to v^μ, that is[6]

$$\bar{P}^\mu = \Lambda^\mu_\nu P^\nu = \sqrt{P^2} v^\mu\,, \qquad \Lambda^{-1\,\mu}_{\ \ \nu} v^\nu = \frac{1}{\sqrt{P^2}} P^\mu\,. \tag{5.38}$$

This leads to

$$\mathbf{v}^2 \bar{\mathbf{P}} = \mathbf{v}(\mathbf{v}\bar{\mathbf{P}})\,, \qquad |\mathbf{v}|\bar{P}^0 = v^0 |\bar{\mathbf{P}}|\,. \tag{5.39}$$

[5] It should be noted out that $T_{\mu_1,\cdots,\mu_\ell}$ does not correspond do the standard definition of a massive tensor field. For example, a massive vector field obeys a constraint $\partial^\mu T_\mu = 0$ instead of $v^\mu T_\mu = 0$. However, *on the mass shell,* these two definitions are related by the Lorentz boost that makes the four-momentum of the dimer parallel to v^μ.

[6] It is important to mention here that one can *always* find such a boost, because both particles are on mass shell, i.e., $P^2 \geq 4m^2$. This is different, e.g., in the RFT formalism [57, 58], where the square of the total momentum can have any sign. However, as mentioned in Refs. [233–235], there exists an ambiguity in the definition of Lorentz-transformed quantities for the off-shell amplitudes, and the possibility that was described above represents one of the options. In the context of the RFT formalism, this option was explored in detail in Ref. [201].

The above identities suffice to express the matrix elements of Λ^μ_ν in terms of the vectors v^μ, P^μ. Substituting back into the Lagrangian, one should replace the components of P^μ by the operators w^μ, acting on the ϕ fields. The resulting explicit expression is rather voluminous and non-local. It is always implicitly assumed that, in actual calculations, the pertinent expressions are expanded in the inverse powers of the mass m, the result is integrated in dimensional regularization and summed up back to all orders. Also, we do not display here the explicit expression of the matrix Λ^μ_ν, because it will never be needed.

In the momentum space, the lowest-order D-wave two-particle-dimer vertex is given by

$$\Gamma^{\mu\nu}(p) = -4g_0\left(\frac{3}{2}\,\bar{p}^\mu_\perp \bar{p}^\nu_\perp - \frac{1}{2}\,(g^{\mu\nu} - v^\mu v^\nu)(\bar{p}_\perp)^2\right), \tag{5.40}$$

where $\bar{p}^\mu = \frac{1}{2}\,(\bar{p}^\mu_1 - \bar{p}^\mu_2)$. Now, integrating out the dimer field $T^{\mu\nu}$, we arrive at

$$\Gamma^{\mu\nu}(p)\Gamma_{\mu\nu}(q) = 16g_0^2\left(\frac{9}{4}\,(\bar{p}_\perp \bar{q}_\perp)^2 - \frac{3}{4}\,(\bar{p}_\perp)^2(\bar{q}_\perp)^2\right). \tag{5.41}$$

Furthermore,

$$\bar{p}^\mu_\perp = \bar{p}^\mu - v^\mu(v\bar{p}) = \bar{p}^\mu - v^\mu(\Lambda^{-1}v)_\nu p^\nu = \bar{p}^\mu - \frac{1}{2\sqrt{P^2}}\,v^\mu((\tilde{p}_1+\tilde{p}_2)(\tilde{p}_1-\tilde{p}_2)) = \bar{p}^\mu\,. \tag{5.42}$$

Using Lorentz invariance, one can transform back to the laboratory frame:

$$\begin{aligned}\Gamma^{\mu\nu}(p)\Gamma_{\mu\nu}(q) &= 24g_0^2\left(\frac{3}{2}\,(pq)^2 - \frac{1}{2}\,p^2q^2\right) = \frac{3}{2}\,g_0^2\left(\frac{3}{2}\,(t-u)^2 - \frac{1}{2}\,(s-4m^2)^2\right)\\ &= 24g_0^2 p^4(s)P_2(\cos\theta)\,.\end{aligned} \tag{5.43}$$

This result is similar to Eq. (5.23) and gives a matching condition for the variable g_0. Inclusions of higher orders in the effective-range expansion, as well as higher partial waves is now straightforward and will not be written down in detail. The only difference to the "conventional" case with $v^\mu = v^\mu_0$ is that all momenta are boosted to the CM frame with respect to v^μ, i.e., the total momentum is parallel to v^μ after the boost. Further, instead of three-momenta in the boosted frame, the transverse components $p_\perp$ are considered, and the covariant expression $v^\mu v^\nu - g^{\mu\nu}$ replaces the three-dimensional Kronecker delta in the boosted frame. Last but not least, we wish to reiterate that, unlike the original formulation of the RFT formalism, the boost is always well defined in the NREFT framework. This happens because we work with the on-shell particles.

Finally note that the two-body on-shell amplitude, given in Eq. (5.31) can be rewritten in the following form

$$T(s,t) = 4\pi\sum_{\ell m}\mathscr{Y}_{\ell m}(\tilde{\mathbf{p}})\frac{1}{(T^\ell_{\text{tree}}(s))^{-1} - \frac{1}{2}\,p^{2\ell}(s)I(s)}\,\mathscr{Y}^*_{\ell m}(\tilde{\mathbf{q}}), \tag{5.44}$$

where

$$\tilde{\mathbf{p}} = \bar{\mathbf{p}} - \mathbf{v}\frac{\bar{\mathbf{p}}\mathbf{v}}{\mathbf{v}^2} + \mathbf{v}\frac{\bar{p}^0}{\mathbf{v}^2}, \qquad \tilde{\mathbf{q}} = \bar{\mathbf{q}} - \mathbf{v}\frac{\bar{\mathbf{q}}\mathbf{v}}{\mathbf{v}^2} + \mathbf{v}\frac{\bar{q}^0}{\mathbf{v}^2}, \qquad \tilde{\mathbf{p}}\tilde{\mathbf{q}} = -\bar{p}_\mu \bar{q}^\mu, \tag{5.45}$$

and

$$\mathscr{Y}_{\ell m}(\mathbf{k}) = |\mathbf{k}|^\ell Y_{\ell m}(\hat{k}), \qquad \hat{k} = \frac{\mathbf{k}}{|\mathbf{k}|}. \tag{5.46}$$

Note that, in case of $v^\mu = v_0^\mu$, the above definition of the boosted amplitude coincides with the boost introduced in [233–235]. Within this prescription the boosted three-momenta are always well-defined, even for $s < 0$.

5.3 Three-Body Sector

5.3.1 Particle-Dimer Lagrangian

The construction of the particle-dimer Lagrangian that describes short-range three-particle interactions, proceeds analogously to the case of the two-particle Lagrangian, except three differences. First, a dimer and ϕ are not identical particles and hence all (not only even) partial waves are allowed. Second, in difference with ϕ, dimers have spin. And third, in the particle-dimer system one cannot use equations of motion in order to reduce the number of the independent terms in the Lagrangian. The dimers, in general, are unphysical "particles" and do not have a fixed mass.

Let us again start with a scalar dimer. The tree-level particle-dimer scattering amplitude depends on the following kinematic variables:

$$s = (p+P)^2 = (q+Q)^2, \quad t = (p-q)^2 = (P-Q)^2, \quad \sigma_p^2 = P^2, \quad \sigma_q^2 = Q^2, \tag{5.47}$$

where p, q and P, Q are the momenta of incoming/outgoing particles and incoming/outgoing dimers, respectively. Consistent counting rules can be imposed, for example, assuming:

$$\begin{aligned} \Delta &= s - 9m^2 = O(\epsilon^2), \qquad t = O(\epsilon^2), \\ \Delta_p &= \sigma_p^2 - 4m^2 = O(\epsilon^2), \qquad \Delta_q = \sigma_q^2 - 4m^2 = O(\epsilon^2), \end{aligned} \tag{5.48}$$

where ϵ is a generic small parameter, and all transverse momenta count as $p_\perp = O(\epsilon)$.

Expanding the tree amplitude in Taylor series, we get:

$$T_d^{\text{tree}}(s,t,\sigma_p^2,\sigma_q^2) = x_0 + x_1(s-9m^2) + x_2 t + x_3(\sigma_p^2+\sigma_q^2-8m^2) + O(\epsilon^4). \tag{5.49}$$

Here, we have additionally used the invariance under time reversal that implies the interchange of the initial and final momenta. In the tree-level amplitude all coefficients $x_0, x_1, \ldots$ are real due to unitarity.

Furthermore, the couplings $x_0, x_1, \ldots$, *determined from the tree-level matching,* are not all independent. Indeed, the particle-dimer Lagrangian is used to calculate the three-particle amplitude, and the matching is performed for the latter. The couplings (or the linear combinations thereof), which do not contribute to the on-shell three-particle amplitude, are redundant and can be dropped. In order to

obtain the three-particle scattering amplitude from the particle-dimer scattering amplitude, one has to equip the external dimer legs with two-particle-dimer vertices and sum up over all permutations in the initial as well as final state. At order ϵ^2, it suffices to consider the vertex $f = f_0 + \frac{1}{2} f_2(\sigma^2 - 4m^2)$, see Eq. (5.33). Here, σ^2 stands for the four-momentum square of a dimer. Since any of the initial or final particles can be a spectator, one has to equip the quantities $\Delta_{p,q}$ and t by indices $i, j = 1, 2, 3$ that label spectator particles, and sum over these indices. Thus, one has to define:

$$\Delta_p^i = P_i^2 - 4m^2\,, \qquad \Delta_q^i = Q_i^2 - 4m^2\,, \qquad t^{ij} = (p_i - q_j)^2\,. \tag{5.50}$$

These obey the following kinematic identities on mass shell, see also Ref. [174]:

$$\sum_{i=1}^{3} \Delta_p^i = \sum_{i=1}^{3} \Delta_q^i = \Delta\,, \qquad \sum_{j=1}^{3} t^{ij} = \Delta_p^i - \Delta\,, \qquad \sum_{i=1}^{3} t^{ij} = \Delta_q^j - \Delta\,. \tag{5.51}$$

The three-particle amplitude is given by

$$T_3^{\text{tree}} = \sum_{i,j=1}^{3} f(\sigma_p^{i\,2}) T_d^{\text{tree}}(s, t^{ij}, \sigma_p^{i\,2}, \sigma_q^{j\,2}) f(\sigma_q^{j\,2}) + O(\epsilon^4)\,. \tag{5.52}$$

Taking into account the above identities, it is straightforward to ensure that only two independent terms survive in the tree-level three-particle amplitude at this order:

$$T_3^{\text{tree}} = z_0 + z_1 \Delta + O(\epsilon^2)\,. \tag{5.53}$$

This agrees with the result of Ref. [174]. Moreover, as shown in [236], in the particle-dimer formalism it is possible to trade the terms of the type $\Delta_p + \Delta_q$ and Δ for each other[7]. Thus our result confirms the findings of Ref. [236] as well. To summarize, only one coupling out of x_1, x_2, x_3 is independent and, without the loss of generality, one may assume, say, $x_2 = x_3 = 0$ (Note also that in Refs. [60, 61] we have written down an energy-independent next-to-leading order driving term containing $\mathbf{p}^2 + \mathbf{q}^2$. In the present context, it corresponds to the choice $x_1 = x_2 = 0$ and $x_3 \neq 0$.). Finally, note that a similar analysis can be carried out at higher orders. We do not consider here this rather straightforward exercise which, at order ϵ^4, again reproduces the result of Ref. [174].

Here one should however note that all the above analysis was limited to the case when a physical dimer does not exist. In case this is not true, the following line of reasoning can be applied. Let us go back to Eq. (5.49). In this case, σ_p^2 and σ_q^2 are not independent kinematic variables anymore, being fixed to the dimer mass squared. On the contrary, the derivative couplings x_1, x_2 can be independently matched to the S-wave effective range and the P-wave scattering length of the particle-dimer scattering.

Furthermore, note that all discussions up to now were restricted to the tree level. Owing to the fact that the use of the cutoff regularization in the Faddeev equation leads to the breakdown of naive counting rules that can be rectified only by adjusting the renormalization prescription, studying the independence of x_1, x_2, x_3 in general is a more subtle issue. In this case, we find it safe to include all couplings – after all, using (possibly) an overcomplete set of operators in the Lagrangian is certainly

[7] Ref. [236] considers the non-relativistic limit and the CM frame only. Hence, strictly speaking, this paper discusses the elimination of the next-to-leading contact interaction, proportional to $\mathbf{p}^2 + \mathbf{q}^2$, in favor of the linear function of the total CM energy E.

not a mistake.

A final remark here concerns the situation, where the low-lying three-particle resonances exist. In this case, the assumption that the short-range part of the particle-dimer interaction is a low-energy polynomial in $s - 9m^2$ might prove to be too restrictive, since the pertinent expansion has a very small radius of convergence, caused by a nearby resonance. A Laurent expansion of the short-range interaction, featuring a simple pole $\sim (s - s_0)^{-1}$ with an unknown parameter s_0, describes the system in a more adequate fashion in this case.

Next, let us briefly dwell on the partial-wave expansion of the particle-dimer short-range tree amplitude. As seen, the $O(\epsilon^2)$ amplitude contains only an S-wave contribution. At higher orders, one can define the scattering angle θ, according to

$$t - 2m^2 = \frac{(s + m^2 - \sigma_p^2)(s + m^2 - \sigma_q^2)}{4s} - \frac{\lambda^{1/2}(s, m^2, \sigma_p^2)\lambda^{1/2}(s, m^2, \sigma_q^2)}{4s} \cos\theta \,. \tag{5.54}$$

Then, the expansion of the tree particle-dimer amplitude in the series of Legendre polynomials can be written down straightforwardly. Note that, at a given order in ϵ, this expansion always contains a finite number of Legendre polynomials.

Having considered the scattering of a particle and a scalar dimer in a great detail, we now sketch the construction in case of a dimer with arbitrary integer spin. To this end, it is convenient to use a different basis for the dimer fields $T_{\mu_1,\cdots,\mu_\ell}$, removing the redundant components. In order to achieve this, consider first the Lorentz transformation[8]

$$\underline{\Lambda}^\mu_\nu v^\nu = v^\mu_0 \,, \qquad \underline{T}_{\mu_1,\cdots,\mu_\ell} = \underline{\Lambda}^{\nu_1}_{\mu_1} \cdots \underline{\Lambda}^{\nu_\ell}_{\mu_\ell} T_{\nu_1,\cdots,\nu_\ell} \,. \tag{5.55}$$

The transformed field $\underline{T}$ is zero, if one of the indices $\mu_1, \ldots, \mu_\ell$ is equal to zero, see Eq. (5.34). The space components can be directly related to the dimer field components $T_{\ell m}$ with $m = -\ell, \ldots, \ell$:

$$\underline{T}_{\mu_1,\cdots,\mu_\ell} = \sum_{m=-\ell}^{\ell} c^{\ell m}_{\mu_1,\cdots,\mu_\ell} T_{\ell m} \,. \tag{5.56}$$

The coefficients $c^{\ell m}_{\mu_1,\cdots,\mu_\ell}$ are pure numbers and can be read off from the explicit expressions of the spherical functions. They are zero, if one of the μ_i is equal to zero.

A generic matrix element can be also boosted to the rest frame:

$$\begin{aligned}\langle p, (P, \mu_1', \cdots, \mu_{\ell'}')|T_d^{\text{tree}}|q, (Q, \mu_1, \cdots, \mu_\ell)\rangle &= (\underline{\Lambda}^{-1})^{\nu_1'}_{\mu_1'} \cdots (\underline{\Lambda}^{-1})^{\nu_{\ell'}'}_{\mu_{\ell'}'} (\underline{\Lambda}^{-1})^{\nu_1}_{\mu_1} \cdots (\underline{\Lambda}^{-1})^{\nu_\ell}_{\mu_\ell} \\ &\times \sum_{m'=-\ell'}^{\ell'} \sum_{m=-\ell}^{\ell} c^{\ell' m'}_{\nu_1',\cdots,\nu_{\ell'}'} c^{\ell m}_{\nu_1,\cdots,\nu_\ell} \langle \underline{p}, (\ell' m')|T_d^{\text{tree}}|\underline{q}, (\ell m)\rangle \,,\end{aligned} \tag{5.57}$$

where $\underline{p}^\mu, \underline{q}^\mu$ are the Lorentz-transformed momenta:

$$\underline{p}^\mu = \underline{\Lambda}^\mu_\nu p^\nu \,, \qquad \underline{q}^\mu = \underline{\Lambda}^\mu_\nu q^\nu \,, \tag{5.58}$$

[8] Note that this transformation is different from Λ^μ_ν, considered in the previous section.

and we anticipated that the total momentum of the system K^μ is proportional to v^μ, so that the same Lorentz boost brings the considered matrix element to the CM frame.

The matrix element in the right-hand side can be expanded in partial waves:

$$\langle \underline{p}, (\ell' m') | T_d^{\text{tree}} | \underline{q}, (\ell m) \rangle = 4\pi \sum_{JM} \sum_{L'L} \mathscr{Y}_{JM}^{L'\ell'}(\underline{\mathbf{p}}, m') T_{JL'L}(\Delta, \Delta_p, \Delta_q) \left[\mathscr{Y}_{JM}^{L\ell}(\underline{\mathbf{q}}, m) \right]^* . \tag{5.59}$$

Here,

$$\mathscr{Y}_{JM}^{L\ell}(\underline{\mathbf{k}}, m) = \langle L(M-m), \ell m | JM \rangle \mathscr{Y}_{L(M-m)}(\underline{\mathbf{k}}) \tag{5.60}$$

is the spherical function with spin ℓ, which is given by an ordinary spherical function multiplied with the pertinent Clebsch-Gordan coefficient. Note that, for a generic v^μ, the above expansion has a more complicated form, since an additional boost is needed to bring the matrix element to the CM frame first[9]. Also, the above expressions show that in the partial-wave expansion of the three-particle amplitude one encounters two orbital momenta: 1) the orbital momentum of pairs which in the particle-dimer approach are represented by the dimer spin ℓ, and 2) the orbital momentum between a pair and a spectator, which corresponds to the quantum number L. The introduction of dimers allows one to neatly separate the partial-wave expansion in these two orbital momenta. The quantity J corresponds to a sum of these orbital momenta and is conserved.

Furthermore, the quantities $T_{JL'L}(\Delta, \Delta_p, \Delta_q)$ are the low-energy polynomials[10], expanded up to a given order in ϵ. Like in the case of a scalar dimer, some on-shell constraints will emerge between various low-energy couplings at a given order in ϵ. We shall make no attempt here to write down these constraints in a general form. When needed, this can be most easily done on the case-by-case basis.

A further remark is due at this place, concerning the expression of the most general Lorentz-invariant short-range amplitude. Namely, in the construction of the invariant kinematic structures we have never used the vector v^μ which should be also included on general grounds. The excuse is provided by the fact that, at the end, we shall relate v^μ to the external momenta (in particular, we shall take it parallel to the total momentum of the three-particle system). In this case, all invariants that can be constructed with the use of v^μ can be expressed in terms of the already considered ones. Anticipating this fact, we did not write down such invariants at all.

This concludes the construction of a short-range tree-level particle-dimer scattering amplitude with initial and final dimers having any spins ℓ, ℓ'. Construction of such an amplitude is equivalent to the construction of the particle-dimer Lagrangian. We do not make an attempt to display such a Lagrangian explicitly, because it is far more convenient to work directly with the momentum space amplitudes.

5.3.2 Faddeev Equation for the Particle-Dimer Amplitude

Now, we are ready to write down the Faddeev equation, describing the particle-dimer scattering, in an explicitly Lorentz-invariant form. In order to avoid cumbersome expressions that will only render the basic idea obscure, we shall first restrict ourselves to the S-wave interactions in both orbital momenta.

[9] The pertinent boost is given by $U(\tilde{\Lambda})|P\ell m\rangle = \sum_{m'=-\ell}^{\ell} D^{(\ell)}_{m'm}(W(\tilde{\Lambda}, P))|(\tilde{\Lambda}P)\ell m'\rangle$, where $W(\tilde{\Lambda}, P)$ denotes the corresponding Wigner rotation and $\tilde{\Lambda}$ is the transformation that brings the particle-dimer system to the rest frame.

[10] As already mentioned, the low-lying three-body resonances may lead to the poles in the variable Δ.

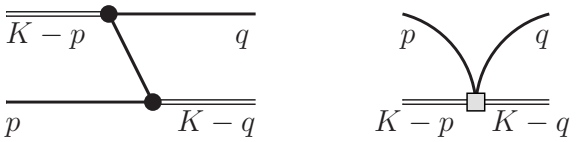

Figure 5.2: The kernel of the Faddeev equation. Double and single lines denote the dimers and particles, respectively. The dark blob describes a dimer-two-particle vertex, and a shaded box corresponds to the short-range part of the particle-dimer scattering.

As follows from the discussion above, including higher partial waves merely amounts to adding indices to some of the quantities in the expressions. This procedure can be readily carried out.

Let us start from the scalar dimer propagator:

$$i\langle 0|T[T(x)T^\dagger(y)]|0\rangle = \int \frac{d^4P}{(2\pi)^4}\, e^{-iP(x-y)} S(P^2), \tag{5.61}$$

where

$$S(P^2) = \left(-\frac{1}{\sigma}\right) + \left(-\frac{1}{\sigma}\right)^2 \Sigma(P^2) + \cdots = -\frac{1}{\sigma + \Sigma(P^2)}, \tag{5.62}$$

and

$$\Sigma(P^2) = \int \frac{d^D k}{(2\pi)^D i} \frac{\frac{1}{2} f^2(\bar{P}^2)}{2w_v(k)(w_v(k) - vk - i\varepsilon)\, 2w_v(P-k)(w_v(P-k) - v(P-k) + i\varepsilon)}, \tag{5.63}$$

with

$$\bar{P}^2 = (w_v(k) + w_v(P-k))^2 + P_\perp^2, \qquad f(u) = f_0 + \frac{1}{2} f_2 (u - 4m^2) + \cdots. \tag{5.64}$$

Performing the threshold expansion and evaluating the expression in dimensional regularization, one gets:

$$\Sigma = \frac{1}{2} f^2(P^2) I(P^2), \tag{5.65}$$

where $I(P^2)$ is given in Eq. (5.10).

Next, let us consider the tree-level particle-dimer scattering amplitude, which consists of two diagrams shown in Fig. 5.2. These are diagrams describing one-particle exchange and the local particle-dimer interaction. Furthermore, vertices in each diagram consist of an infinite number of terms, corresponding to the derivative operators in the Lagrangian. Thus, the tree-level amplitude is

given by[11]

$$T^{\text{tree}} = \frac{f(s_p)f(s_q)}{2w_v(K-p-q)(w_v(p)+w_v(q)+w_v(K-p-q)-vK-i\varepsilon)} + T_d^{\text{tree}}\,. \tag{5.66}$$

Here, p, q are the four-momenta of the external particles, and K is a total momentum of a particle-dimer pair. Hence, the four momenta of dimers are $P = K - p$ and $Q = K - q$. The short-range particle-dimer amplitude is given by Eq. (5.49). Furthermore, the kinematic variables s_p, s_q are given by

$$\begin{aligned} s_p &= (w_v(p) + w_v(K-p-q))^2 + (K-q)_\perp^2\,, \\ s_q &= (w_v(q) + w_v(K-p-q))^2 + (K-p)_\perp^2\,, \end{aligned} \tag{5.67}$$

and, for any vector a^μ, we have $a_\perp^\mu = a^\mu - v^\mu(va)$.

Furthermore, let us consider the difference:

$$\begin{aligned} s_p - \sigma_q^2 = s_p - (K-q)^2 = (w_v(p) + w_v(K-p-q))^2 - (w_v(p) - v(K-p-q))^2 \\ = (w_v(p) + w_v(K-p-q) + w_v(q) - vK)(w_v(p) + w_v(K-p-q) - w_v(q) + vK)\,. \end{aligned} \tag{5.68}$$

A similar relation holds for the $s_q - \sigma_p^2 = s_q - (K-p)^2$. Taking into account the fact that the function $f(u)$ is a low-energy polynomial in the variable $u - 4m^2$, it is seen that the arguments s_p, s_q in these functions can be replaced by σ_q^2, σ_p^2. In the difference, the denominator cancels and hence, it only modifies the regular part T_d^{tree}. The fact that the modified short-range part now depends on the vector v^μ, does not lead to any problem. One could merely ignore such v-dependent terms since, at the end, v^μ will be chosen proportional to K^μ. Thus, one could write

$$\tilde{T}^{\text{tree}} = \frac{f(\sigma_p^2)f(\sigma_q^2)}{2w_v(K-p-q)(w_v(p)+w_v(q)+w_v(K-p-q)-vK-i\varepsilon)} + \tilde{T}_d^{\text{tree}}\,. \tag{5.69}$$

Note that the separate terms in Eqs. (5.66) and (5.69) are manifestly invariant, *if the vector v^μ is also boosted along with all other vectors.* This is different from the standard formulation, where v^μ is chosen along v_0^μ and *does not transform* under Lorentz transformations.

Graphically, the Faddeev equation for the particle-dimer scattering amplitude is depicted in Fig. 5.3. Denoting this amplitude by $\tilde{T}$, we have:

$$\tilde{T}(p,q) = \tilde{T}^{\text{tree}}(p,q) + \int^{\Lambda_v} \frac{d^3k_\perp}{(2\pi)^3 2w_v(k)}\, \tilde{T}^{\text{tree}}(p,k) S((K-k)^2) \tilde{T}(k,q)\,, \tag{5.70}$$

[11] In the "rest system" $v^\mu = v_0^\mu$, this expression can be obtained with the use of the time-ordered perturbation theory. For arbitrary v^μ, one considers instead the evolution in direction of the vector v^μ. The role of the Hamiltonian in this case is played by $\mathbb{H} = v_\mu \mathbb{P}^\mu$, where $\mathbb{P}^\mu$ denotes the operator of the full four-momentum. The four-momentum of a free particle obeys the mass-shell condition $vk = w_v(k)$. It is then clear that, in the frame defined by the vector v^μ, the one-particle exchange diagram takes the form given in Eq. (5.66). An alternative derivation of the same expression starts from the Bethe-Salpeter equation and performs the "equal-time projection" of this equation by integrating over the component of the relative momentum, parallel to the vector v^μ.

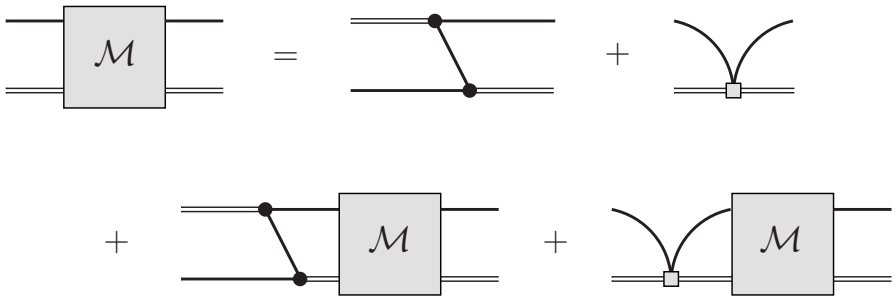

Figure 5.3: Faddeev equation for the particle-dimer scattering amplitude.

where

$$\int^{\Lambda_v} \frac{d^3k_\perp}{(2\pi)^3 2w_v(k)} F(k) = \int \frac{d^4k}{(2\pi)^3} \delta(k^2 - m^2)\theta(\Lambda^2 + k^2 - (vk)^2)F(k)\,. \tag{5.71}$$

Defining now

$$\begin{aligned} \tilde{T}(p,q) &= f(\sigma_p^2)\mathcal{M}(p,q)f(\sigma_q^2), \\ \tilde{T}^{\text{tree}}(p,q) &= f(\sigma_p^2)\mathcal{Z}(p,q)f(\sigma_q^2), \end{aligned} \tag{5.72}$$

we may finally rewrite the Faddeev equation as

$$\mathcal{M}(p,q) = \mathcal{Z}(p,q) + \int^{\Lambda_v} \frac{d^3k_\perp}{(2\pi)^3 2w_v(k)} \mathcal{Z}(p,k)\tau((K-k)^2)\mathcal{M}(k,q)\,. \tag{5.73}$$

Here, $\tau(z)$ is the physical two-body scattering matrix

$$\tau(z) = f^2(z)S(z) = \frac{1}{-\sigma f^{-2}(z) - \frac{1}{2} I(z)} = T_0(z), \tag{5.74}$$

with $T_0(z)$ defined in Eq. (5.19).

The three-particle amplitude can be expressed through the particle-dimer amplitude

$$\begin{aligned} T_3(p_1,p_2,p_3;q_1,q_2,q_3) &= T_3^{\text{disc}} + T_3^{\text{conn}}, \\ T_3^{\text{disc}} &= \sum_{i,j=1}^{3} (2\pi)^3 \delta^3(p_{i\perp} - q_{j\perp}) 2w_v(p_i)\tau((K-p_i)^2), \\ T_3^{\text{conn}} &= \sum_{i,j=1}^{3} \tau((K-p_i)^2)\mathcal{M}(p_i,q_j)\tau((K-q_j)^2)\,. \end{aligned} \tag{5.75}$$

Symbolically, this relation is depicted in Fig. 5.4.

Up to this point, all expressions are manifestly Lorentz invariant, if the vector v^μ is also Lorentz-

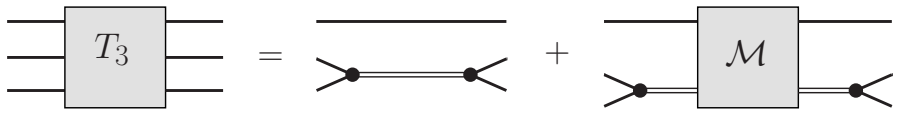

Figure 5.4: Expressing three-particle amplitude in terms of a particle-dimer amplitude. Summing up over all possible choices of spectator particles is implicit.

boosted along with other vectors. This means that, for instance, the particle-dimer amplitude $\mathcal{M}$, which implicitly depends on the choice of the quantization axis v^μ, is invariant under arbitrary Lorentz boosts

$$\mathcal{M}(\Lambda p; \Lambda q; \Lambda v) = \mathcal{M}(p; q; v)\,. \tag{5.76}$$

In other words, after fixing v^μ in terms of the external momenta p_i, q_j (the most natural choice is, as already mentioned above, to choose v^μ along the total four-momentum K^μ of the three-particle system), the particle-dimer amplitude becomes manifestly Lorentz-invariant. Thus, the goal stated in the beginning has been achieved. We would like to stress here that this happens because the two-particle scattering amplitude after using the threshold expansion depends only on the pertinent Mandelstam variable s for a given subsystem and does not depend on v^μ. If it were not the case, one would be forced to fix the direction of the quantization axis for each subsystem separately, as well as for the whole system, and this cannot be done simultaneously. It is also clear that this approach will face difficulties in the study of the four-particle system, which contains different three-particle subsystems.

In conclusion, note that if the dimers with higher spin are taken into account, both the dimer propagator S in Eq. (5.61) and the tree-level amplitude T^{tree} become matrices in the space of Lorentz indices, e.g., $S \to S_{\mu_1\ldots\mu_{\ell'},\nu_1\ldots\nu_\ell} \doteq S_{n_{\ell'}n_\ell}$ and $T^{\text{tree}} \to T^{\text{tree}}_{\mu_1\ldots\mu_{\ell'},\nu_1\ldots\nu_\ell} \doteq T^{\text{tree}}_{n_{\ell'}n_\ell}$. All further steps can be performed in a direct analogy to the case of the scalar dimer. Namely, replacing s_p by σ_q^2 and s_q by σ_p^2 is straightforward. This leads to a system of equations (cf. with Eq. (5.70)):

$$\begin{aligned}\tilde{T}_{n_{\ell'}n_\ell}(p,q) &= \tilde{T}^{\text{tree}}_{n_{\ell'}n_\ell}(p,q) \\ &+ \sum_{n_{\ell''}n_{\ell'''}} \int^{\Lambda_\nu} \frac{d^3k_\perp}{(2\pi)^3 2w_\nu(k)}\, \tilde{T}^{\text{tree}}_{n_{\ell'}n_{\ell''}}(p,k) S_{n_{\ell''}n_{\ell'''}}((K-k)^2) \tilde{T}_{n_{\ell'''}n_\ell}(k,q)\,.\end{aligned} \tag{5.77}$$

Note that the matrix S is diagonal in ℓ', ℓ in the infinite, but not in a finite volume. Furthermore,

$$\sum_{n_\ell}(\cdots) = \sum_{\ell=0}^{\ell_{max}} \sum_{\mu_1,\cdots,\mu_\ell} (\cdots)\,. \tag{5.78}$$

Next, one may define:

$$\begin{aligned}
\tilde{T}_{n_{\ell'}n_\ell}(p,q) &= f_{\ell'}(\sigma_p^2)\mathcal{M}_{n_{\ell'}n_\ell}(p,q)f_\ell(\sigma_q^2), \\
\tilde{T}^{\text{tree}}_{n_{\ell'}n_\ell}(p,q) &= f_{\ell'}(\sigma_p^2)\mathcal{Z}_{n_{\ell'}n_\ell}(p,q)f_\ell(\sigma_q^2), \\
\tau_{n_{\ell'}n_\ell}((K-k)^2) &= f_{\ell'}(\sigma_k^2)S_{n_{\ell'}n_\ell}((K-k)^2)f_\ell(\sigma_k^2), \\
\sigma_k^2 &= (K-k)^2 - 4m^2\,.
\end{aligned} \tag{5.79}$$

In the infinite volume, the matrix τ is also diagonal and contains the on-shell two-body partial-wave amplitudes.

The three-body amplitude is given by (cf. with Eq. (5.75)

$$\begin{aligned}
T_3(p_1,p_2,p_3;q_1,q_2,q_3) &= T_3^{\text{disc}} + T_3^{\text{conn}}\,, \\
T_3^{\text{disc}} &= \sum_{i,j=1}^{3}(2\pi)^3\delta^3(p_{i\perp}-q_{j\perp})2w_v(p_i) \\
&\times \sum_{n_{\ell'}n_\ell} Y_{n_{\ell'}}(\bar{p}^{(i)})(\tau_{n_{\ell'}n_\ell}((K-p_i)^2)Y_{n_\ell}(\bar{q}^{(j)})\,, \\
T_3^{\text{conn}} &= \sum_{i,j=1}^{3}\sum_{n_{\ell'''}n_{\ell''}n_{\ell'}n_\ell} Y_{n_{\ell'''}}(\bar{p}^{(i)})\tau_{n_{\ell'''}n_{\ell''}}((K-p_i)^2)\mathcal{M}_{n_{\ell''}n_{\ell'}}(p_i,q_j) \\
&\times \tau_{n_{\ell'}n_\ell}((K-q_j)^2)Y_{n_\ell}(\bar{q}^{(j)})\,.
\end{aligned} \tag{5.80}$$

The vectors $\bar{p}^{(i)}, \bar{q}^{(j)}$ are defined through the Lorentz boost similar to one in Eq. (5.38). Namely, say, p_3^μ is a four-momentum of a spectator in the final state. Define now the boost Λ_ν^μ, which brings the total on-shell momentum of a pair $P_{12}^\mu = \tilde{p}_1^\mu + \tilde{p}_2^\mu$ parallel to the vector v^μ. Then, $\bar{p}^{(3)\mu} = \frac{1}{2}\Lambda_\nu^\mu(\tilde{p}_1^\nu - \tilde{p}_2^\nu)$. It can be also shown that $\bar{p}^{(i)\mu} = \bar{p}_\perp^{(i)\mu} = \bar{p}^{(i)\mu} - v^\mu(v\bar{p}^{(i)})$. The quantity $\bar{q}^{(j)}$ is defined similarly. Finally,

$$Y_{n_\ell}(\bar{p}^{(i)}) \doteq Y_{\mu_1,\cdots,\mu_\ell}(\bar{p}^{(i)}) = \left(\frac{s}{4}-m^2\right)^{-\ell/2}\mathscr{Y}_{\mu_1,\cdots,\mu_\ell}(\bar{p}^{(i)}), \tag{5.81}$$

where the tensor $\mathscr{Y}_{\mu_1,\cdots,\mu_\ell}$ describes a particle with a spin ℓ:

$$\begin{aligned}
\mathscr{Y} &= 1\,, \\
\mathscr{Y}_\mu &= p^\mu\,, \\
\mathscr{Y}_{\mu\nu} &= \frac{3}{2}p_\mu p_\nu - \frac{1}{2}(g_{\mu\nu}-v_\mu v_\nu)p^2\,, \\
&\cdots
\end{aligned} \tag{5.82}$$

and $s = (\tilde{p}_1 + \tilde{p}_2)^2$.

5.3.3 Quantization Condition

In order to avoid the clutter of indices, we shall write down the quantization condition in case of the S-wave interactions only. We start by rewriting the Faddeev equation for the particle-dimer amplitude in a finite cubic box of size L with periodic boundary conditions, where it takes the form:[12]

$$\mathcal{M}_L(p,q) = \mathcal{Z}(p,q) + \frac{1}{L^3}\sum_{\mathbf{k}} \frac{1}{2w(\mathbf{k})}\,\theta(\Lambda^2 + m^2 - (vk)^2)\mathcal{Z}(p,k)\tau_L(K-k)\mathcal{M}_L(k,q)\,. \tag{5.83}$$

Here, $k^\mu = (w(\mathbf{k}), \mathbf{k})$ and $w(\mathbf{k}) = \sqrt{m^2 + \mathbf{k}^2}$, and the summation is carried out over the discrete values $\mathbf{k} = \frac{2\pi}{L}\,\mathbf{n},\ \mathbf{n} \in \mathbb{Z}^3$. Furthermore,

$$\tau_L(P) = \frac{16\pi\sqrt{s}}{p(s)\cot\delta_0(s) - \dfrac{2}{\sqrt{\pi}L\gamma}\,Z_{00}^{\mathbf{d}}(1;q_0^2)}\,, \tag{5.84}$$

where $s = P^2$, $\gamma = \left(1 - \dfrac{\mathbf{P}^2}{P_0^2}\right)^{-1/2}$, $\mathbf{d} = \dfrac{\mathbf{P}L}{2\pi}$, $q_0^2 = \dfrac{L^2}{4\pi^2}\left(\dfrac{s}{4} - m^2\right)$, and

$$\begin{aligned} Z_{00}^{\mathbf{d}}(1;q_0^2) &= \frac{1}{\sqrt{4\pi}}\sum_{\mathbf{r}\in P_d}\frac{1}{\mathbf{r}^2 - q_0^2}\,, \\ P_d &= \{\mathbf{r} = \mathbb{R}^3 | r_\parallel = \gamma^{-1}\left(n_\parallel - \frac{1}{2}\,|\mathbf{d}|\right),\ \mathbf{r}_\perp = \mathbf{n}_\perp\,,\ \mathbf{n}\in\mathbb{Z}^3\}\,. \end{aligned} \tag{5.85}$$

A crucial point in the above expressions is that the two-body amplitude τ_L does not depend on v^μ even in a finite volume. In order to see this, note first that the expression $p(s)\cot\delta_0(s)$ is the same in the infinite and in finite volume and is v^μ-independent. Furthermore, in the infinite volume, the loop is given by Eq. (5.10) and is explicitly Lorenz-invariant. In a finite volume, the three-momentum integral in this expression has to be replaced by a sum. The discretization is performed in the rest frame of a box. The result is given by the Lüscher zeta-function, which explicitly depends on the components of the vector P^μ (i.e., is not explicitly Lorentz-invariant) but not on v^μ, which does not appear at any stage. A detailed derivation of Eq. (5.84) along these lines can be found in appendix A.2.

Next, the above expression is written down in the assumption that $s > 0$. In case of $s < 0$, the $\tau_L(P)$ is replaced by $\tau(P^2)$ – as one knows, these two quantities below the two-particle threshold differ only by the exponentially suppressed terms. The latter is a perfectly well-defined Lorentz-invariant quantity and can be written down in terms of invariant kinematic variables, without performing any boost.

The quantization condition has the form $\det A = 0$, where

$$A_{\mathbf{pq}} = L^3 2w(\mathbf{p})\delta_{\mathbf{pq}}\tau_L^{-1}(K-p) - \mathcal{Z}(p,q)\,, \tag{5.86}$$

[12] Note that $w(\mathbf{k})$ appears in the denominator in Eq. (5.83). This happens because we carry out the discretization of the three-momenta in the rest frame of the box. To this end, first the Lorentz-invariant integration measure (in the infinite volume) $\dfrac{d^3k_\perp}{2w_v(k)}$ is rewritten as $\dfrac{d^3\mathbf{k}}{2w(\mathbf{k})}$ and the discretization is performed in the latter expression.

and the momenta p, q obey the condition $\Lambda^2 + m^2 - (vp)^2 \geq 0$, $\Lambda^2 + m^2 - (vq)^2 \geq 0$. The zeros of the determinant determine the finite-volume spectrum in an arbitrary reference frame.

As it is well known, the symmetries of a cubic box allow one to partially diagonalize the quantization condition. Below, we mainly follow the procedure described in [146] and generalize it to the case of the moving frame. In the CM frame, the rotational symmetry is reduced to the octahedral group O_h, containing 48 elements. In case of the moving frame, $\mathbf{K} \neq 0$, the symmetry is further reduced to different subgroups (little groups) of O_h, each element g of which leaves the vector $\mathbf{d} = \dfrac{L\mathbf{K}}{2\pi}$ invariant: $g\mathbf{d} = \mathbf{d}$. These symmetry groups and their irreps are described in Refs. [36, 148], where the matrices of the different irreps are explicitly given.

In order to carry out the diagonalization of the quantization condition into various irreps, one has first to introduce the notion of *shells* in the space of the discretized momenta $\mathbf{p} = \dfrac{2\pi}{L}\,\mathbf{n}$, $\mathbf{n} \in \mathbb{Z}^3$. In the CM frame, a shell is defined as a set of momenta that can be transformed into each other by the elements of the group O_h [146]. All the elements of a given shell have the same length $\mathbf{n}^2$ but not all vectors with the same length belong to the same shell. In case of a moving frame, the shells are defined by two invariants $\mathbf{n}^2$, $\mathbf{nd}$ instead of one.

Following Ref. [146], we may project the driving term in the quantization condition onto various irreps Γ, Γ':

$$\begin{aligned}
\mathcal{Z}^{\Gamma\Gamma'}_{\lambda\sigma,\rho\delta}(r,s) &= \sum_{g,g'\in\mathcal{G}} (T^{\Gamma}_{\sigma\lambda}(g))^* \mathcal{Z}(g\mathbf{p}_0(r), g'\mathbf{q}_0(s)) T^{\Gamma'}_{\delta\rho}(g') \\
&= \frac{G}{s_\Gamma}\,\delta_{\Gamma\Gamma'}\delta_{\sigma\delta} \sum_{g\in\mathcal{G}} (T^{\Gamma}_{\rho\lambda}(g))^* \mathcal{Z}(g\mathbf{p}_0(r), \mathbf{q}_0(s)) \\
&\doteq \frac{G}{s_\Gamma}\,\delta_{\Gamma\Gamma'}\delta_{\sigma\delta}\mathcal{Z}^{\Gamma}_{\lambda\rho}(r,s)\,. \qquad (5.87)
\end{aligned}$$

Here, r, s label various shells, $\mathbf{p}_0(r)$ and $\mathbf{q}_0(s)$ denote the pertinent *reference momenta*, and $T^{\Gamma}_{\sigma\lambda}(g)$ are the matrices of a given irrep of a group $\mathcal{G}$ (which coincides with the group O_h or one of its little groups). Furthermore, G is the number of the elements in this group, and s_Γ is the dimension of the irrep Γ.

The quantization condition can be diagonalized into various irreps. It has the form $\det A^{\Gamma} = 0$, where

$$A^{\Gamma}_{\rho\sigma}(r,s) = \delta_{rs} 2 w_r \delta_{\rho\sigma} \tau_L(s)^{-1} - \frac{\sqrt{\nu(r)\nu(s)}}{GL^3}\,\mathcal{Z}^{\Gamma}_{\sigma\rho}(r,s)\,, \qquad (5.88)$$

where $\nu(s)$ denotes the *multiplicity* of the shell s, i.e., the number of the independent vectors in it, and $w_r = w(\mathbf{p})$ with vector $\mathbf{p}$ belonging to the shell r. We have further used the fact that the quantity $\tau_L(K-k)$ is invariant under the group $\mathcal{G}$ and, hence, its projection onto an irrep Γ produces Kronecker symbols only.

5.3.4 Comparison with the RFT Approach

Below, we shall briefly compare the relativistic quantization condition, written down in the present paper, to the one known in the literature, see, for instance, Ref. [174]. Following the original derivation given in Refs. [57, 58], one ends up with an equation that closely resembles Eq. (5.83) with the quantization axis chosen at $v^\mu = v_0^\mu$. It is easy to see that a sole manifestly non-invariant ingredient of this equation is the one-particle exchange part contained in $\mathcal{Z}$ (in Refs. [57, 58, 174], this corresponds to the three-particle propagator G). In order to render the formalism Lorentz-invariant, the following approach was used. The three-particle propagator was replaced by

$$\begin{aligned} & \frac{1}{2w(\mathbf{l})}\,\frac{1}{w(\mathbf{p})+w(\mathbf{q})+w(\mathbf{l})-K^0} \\ \to\quad & \frac{1}{2w(\mathbf{l})}\,\frac{1}{w(\mathbf{p})+w(\mathbf{q})+w(\mathbf{l})-K^0} - \frac{1}{2w(\mathbf{l})}\,\frac{1}{w(\mathbf{p})+w(\mathbf{q})-w(\mathbf{l})-K^0} \\ =\quad & \frac{1}{m^2-b^2}\,, \end{aligned} \tag{5.89}$$

where $b^\mu = p^\mu + q^\mu - K^\mu$ and $\mathbf{l} = \mathbf{K} - \mathbf{p} - \mathbf{q}$. It can be easily seen that the added piece is a low-energy polynomial and it can be removed by adjusting the renormalization prescription in the short-range three-particle interaction.

This approach is, however, problematic if applied to any formalism in which the cutoff on loop momenta can be raised arbitrarily high. The problem arises because the additional term did not emerge from a Feynman integral and thus does not have correct analytic properties. In particular, it can be seen that the contribution, coming from the integration region where both momenta $\mathbf{p}$ and $\mathbf{q}$ are large (of order of m), violates the unitarity in the infinite volume *even in the low-energy region.* This can be easily verified looking for the zeros of the expression $w(\mathbf{p}) + w(\mathbf{q}) - w(\mathbf{l}) - K^0$ for $K^0 - 3m = E \ll m$. In other words, the decoupling of the low- and high-momentum regimes, which is intimately related to the analytic properties of the amplitudes does not occur. In a finite volume, by the same token, it can be straightforwardly verified that the above modification of the three-particle propagator will result in a bunch of spurious subthreshold energy levels which have nothing to do with the real spectrum of a system in question.

All the above effects emerge, if the integration momentum exceeds some critical value, of order of the particle mass itself. In all analysis carried out within the RFT approach so far, the cutoff is kept lower than this value and, hence, the above-mentioned deficiency did not surface. However, this also means that the cutoff cannot be made arbitrary large in a framework with the modified three-particle propagator. On physical grounds, one may consider such a purely kinematic restriction on the cutoff rather counter-intuitive, since a cutoff is usually associated with the massive degrees of freedom that one intends to shield away. Moreover, one might be concerned of the fact that the maximal allowed value of the cutoff turns out to be of order of the particle mass. It is however likely that, by adapting the methodology introduced here, the cutoff in the RFT approach could be raised arbitrarily high while maintaining relativistic invariance, and in particular the Lorentz invariance of the three-particle amplitude $K_{\mathrm{df},3}$.

In addition, we would like to mention that in the RFT approach[13], imposing a low cutoff can be also

[13] It should be noted that the similar arguments apply, with minor modifications, to the FVU approach as well.

justified by the necessity of staying above the cross-channel cut in the two-body amplitude, as well as avoiding the pseudothreshold singularity in the Källen function (in the equal-mass case which is considered here, both, this singularity, as well as the beginning of the left-hand cut, are located at $s = 0$, where s is the pertinent Mandelstam variable in the two-body system). Analogous singularities could lead to $K_{\text{df},3}$ becoming complex-valued if the definition were modified by allowing for a higher cutoff function. In short, both the additional pole in the relativistic analog of the three-particle propagator G and the cross-channel cut must be carefully considered in order to modify the cutoff function in the RFT method. This might be a formidable task in practice which the lower cutoff helps to avoid. The NREFT approach, in its turn, allows one to circumvent all these problems in a systematic fashion, since the two-body amplitudes constructed here possess the right-hand cut only, the three-body force, encoded in the effective couplings, is real by construction for all values of the cutoff function, and the three-particle propagator has only one pole. A simple physical explanation for this is that the antiparticle degrees of freedom, which are responsible for the additional (unwanted) singularities, are hidden in the couplings of the non-relativistic Lagrangian, both in the two- and three-particle sector. As one knows, this is justified only for momenta which are much smaller than the particle mass – for momenta of order of the mass both the two-body amplitude and the three-body potential are *modified* as compared to the relativistic theory. However, according to the decoupling theorem, the modification of the high-energy behavior of the amplitudes can be fully compensated at low energies by adjusting the renormalization prescription and thus does not lead to observable consequences. Loosely speaking, extending NREFT to describe amplitudes for momenta of order of the particle mass and beyond can be considered as a kind of a *regularization,* which consistently removes all singularities that emerge due to the presence of the antiparticles, and the cutoff is present solely to tame the ultraviolet behavior. Since all low-energy singularities are associated with particles only, the modified NREFT correctly reproduces the singularity structure of the amplitudes, and unitarity in the two- and three-particle sectors is obeyed at low energies. Furthermore, a finite-volume counterpart of this statement is that the quantization condition, based on the improved NREFT approach, neglects only exponentially suppressed volume effects at $mL \gg 1$, but makes no other approximations associated with the non-relativistic system. The choice to drop exponentially suppressed volume effects is common to all methods.

Last but not least, we would like to stress once more that the discussion of the distant singularities of different diagrams, which is given above, does not address the main question – namely, at which energies these singularities become physically important and cannot be brushed under the carpet anymore. This problem is common for all approaches since, as already mentioned, in order to derive the quantization condition, one is forced to restrict amplitudes on the mass shell and suppress explicit antiparticle degrees of freedom. At this moment, we do not have an answer to this very difficult question, which will also depend on a particular physical system considered. The perturbative studies might provide a clue on this issue. This, however forms a separate subject of investigations.

5.4 Exploring the Relativistic Invariant Quantization Condition in a Toy Model

We have used the relativistic invariant quantization condition, derived within the NREFT approach in the previous section, for producing synthetic data within a toy model. The aim of this investigation is to verify that the spectrum, obtained in this manner, indeed obeys the requirements, imposed by the

Table 5.1: Binding energies of the five deepest states for $\Lambda = 10^4$ and $H_0(\Lambda) = 0$ in the unitary limit.

n	B_n	$\sqrt{B_n/B_{n+1}}$
1	3.32333×10^{-1}	21.93
2	6.90973×10^{-4}	22.70
3	1.34132×10^{-6}	22.69
4	2.60432×10^{-9}	22.69
5	5.05640×10^{-12}	

Lorentz invariance. In this section, we shall always used the choice for the vector v^μ parallel to the total four-momentum of the three-particle system K^μ.

In the toy model, we consider the lowest-order S-wave interactions only, both in the two-particle as well as in the particle-dimer channels. This means that we have only two LECs: the non-derivative 4-particle coupling that is parameterized by the two-body scattering length a and the dimensionless non-derivative particle-dimer coupling $H_0 = H_0(\Lambda)$. The driving term in the Faddeev equation is written down as

$$\mathcal{Z}(p,q) = \frac{1}{2w_v(K-p-q)(w_v(p)+w_v(q)+w_v(K-p-q)-vK-i\varepsilon)} + \frac{H_0(\Lambda)}{\Lambda^2}, \tag{5.90}$$

and the two-body propagator is given by

$$\tau(s) = \frac{16\pi\sqrt{s}}{-\frac{1}{a} - 8\pi\sqrt{s}J(s) - ip(s)}. \tag{5.91}$$

In the non-relativistic limit, the first equation reduces to its non-relativistic counterpart displayed in Refs. [60, 61]. Furthermore, the finite-volume modification of the second equation, which enters the quantization condition, is defined according to Eq. (5.84). In addition to a, H_0, there are two more parameters in the model: the mass of the particle m and the cutoff Λ. In total, this yields three dimensionless parameters that describe the model completely – we measure all dimensionful parameters in the units of m and assume $m = 1$ in the following.

As the first quick check of our approach, we have calculated the spectrum of the so-called *Efimov states* in the infinite volume. An (infinite) tower of such shallow states, condensing towards the three-particle threshold, emerges in the non-relativistic theory in the unitary limit $a \to \infty$. Since in the vicinity of the threshold the particles should carry very low three-momenta, this non-relativistic result should be readily reproduced in the relativistic framework. Moreover, it is known that the binding energies of the neighboring Efimov states, $B_n = 3m - E_n$, fulfill the relation:

$$\sqrt{B_n/B_{n+1}} = \exp\left(\pi/s_0\right) \approx 22.69, \qquad s_0 = 1.00624. \tag{5.92}$$

This scaling has to be reproduced by the relativistic approach, providing a check for the latter.

In the relativistic theory, we have fixed the remaining parameters in the unitary limit as $\Lambda = 10^4$ and $H_0(\Lambda) = 0$. The results, listed in Table 5.1, are completely in line with our expectations and confirm that our approach possesses a correct non-relativistic limit in the infinite volume.

Next, the calculations in a finite volume are carried out where we go beyond the unitary limit. The scattering length and the cutoff in the toy model are chosen as $a = 5$ and $\Lambda = 3$, respectively (in the units of particle mass)[14]. For this value of the scattering length, a shallow dimer with the energy $E_d = 1.94725$ emerges in the infinite volume and the particle-dimer threshold lies at $E_{1d} = 2.94725$, close to the three-particle threshold. Furthermore, requiring the existence of a three-particle bound state at $E_1 = 2.6$ in the infinite volume fixes the value of the coupling $H_0 = -0.1182689$. Another shallow three-particle bound state is found in the infinite volume at $E_2 = 2.94671$, very close to the particle-dimer-threshold. All energies are given in the rest frame.

Figure 5.5 shows the volume dependence of the energy spectrum in the rest frame and moving frames, $\mathbf{d} = (0, 0, 1)$, $\mathbf{d} = (0, 1, 1)$ and $\mathbf{d} = (1, 1, 1)$, obtained for the above choice of the parameters, above and below the three-particle threshold. The energy spectra are given in terms of $M^{\mathbf{d}} = M^{\mathbf{d}}(L) = \sqrt{K_0^2 - (2\pi/L)^2\mathbf{d}^2}$, where $K_0 = K_0(L)$ are the energies in a finite volume that fulfill the quantization condition. The lowest two levels in these figures, shown in blue and red, correspond to the deep and shallow bound states, respectively. As seen from these figures, the shallow bound state converges to its infinite-volume limit very slowly, as expected. Namely, for smaller L, the finite-volume energy is larger than the exact infinite-volume value. With the increase of L it crosses the exact result and then approaches it from below very slowly, as $L \to \infty$. A similar behavior was observed in the non-relativistic case, see Ref. [146], so the present result does not come as a surprise. As we shall see, such an irregular behavior complicates the numerical study of the large-L limit of the shallow binding energy considerably, especially in the moving frames where the crossing emerges at larger values of L.

In order to check the relativistic invariance, we concentrate on the three-particle bound states. Indeed, it suffices to show that the quantity $M_i^{\mathbf{d}} - E_i$, $i = 1, 2$, where the quantity $M^{\mathbf{d}}$ was defined above, decreases exponentially for large values of L. In this case, it can be seen that the one-particle states, obtained by solving the quantization condition, obey the relativistic dispersion law up to the exponentially suppressed corrections. This is exactly the result one is looking for.

The result of the calculations is shown in Fig. 5.6. In case of the deep state, everything works fine. The logarithmic plot for the difference is almost a perfect straight line that is compatible with an exponential decrease $\sim \exp(-\kappa_{\text{deep}} L)$ and $\kappa_{\text{deep}} \simeq 0.7$ for all frames[15]. The situation with the shallow state is different. As mentioned above, the finite- and infinite-volume energies coincide at some L. This is manifested by the dips in the curves presented on the right panel. After the dip, it takes very large values of L for the curves to stabilize and show a linear behavior. In case of the rest frame, the curve becomes almost linear after $L \simeq 12 - 15$, see Fig. 5.7 (here, large values of L are shown). This behavior is consistent with the exponential decrease $\sim \exp(-\kappa_{\text{shallow}} L)$ and $\kappa_{\text{shallow}} \simeq 0.11, 0.03$ for the frames $\mathbf{d} = (0, 0, 0), (0, 0, 1)$. Note that the arguments of the exponent can be different in different frames, because the Lorentz symmetry is broken in a finite volume. Furthermore, the dips in the $\mathbf{d} = (0, 1, 1), (1, 1, 1)$ frames occur at much larger values of L. Since carrying out calculations on such large grids is very time-consuming, we display here the results for two reference frames only. Note

[14] It can be seen that this cutoff is high enough. At a lower cutoff, one may observe some small numerical irregularities (cusps) in the energy spectrum which represent cutoff artifacts. These irregularities are completely absent in the figures presented in this section. Also, we have checked that the low-energy spectrum is independent of Λ to a very good accuracy, if $H_0(\Lambda)$ is re-adjusted in the infinite volume to keep, e.g., the particle-dimer scattering length or the energy of the (shallow) bound state constant.

[15] The irregularities in the case $\mathbf{d} = (1, 1, 1)$ for large L are caused by the fact that the cutoff is not high enough. However, since increasing the cutoff becomes quite challenging, we have refrained from doing this. The exponential falloff of the corrections is anyway clearly observed for moderate values of L.

also that here we did not make an attempt to *predict* the values of κ in different frames. Albeit such a theoretical prediction is possible in principle, it is not relevant in the context of the problem considered in the present paper.

To summarize, in this section it was explicitly checked that the three-particle bound states, obtained from the solution of the quantization condition, obey the relativistic dispersion law up to the exponentially suppressed corrections. Recall now that the analysis of the lattice data in the three-particle sector proceeds in two steps. At the first step, the quantities having a short-range nature (like the coupling H_0) are extracted from data. These quantities, like the bound-state energies, can receive only exponentially suppressed corrections and, hence, up to such corrections, one may use the same values of these quantities in the fit of data coming from different moving frames. This is exactly the manifestation of the Lorentz-invariance in a finite box. At the end, as usual, one uses an explicitly Lorentz-invariant infinite-volume formalism to express physical observables through the couplings $H_0, \ldots$, extracted from data.

5.5 Conclusions

i) In this paper, we have proposed a manifestly relativistically invariant formulation of the three-particle quantization condition within the NREFT approach. It is shown that the higher partial waves can be consistently included in the formulation. The suggested framework can be readily used for the global analysis of lattice spectra, measured in different moving frames. This was already done in case of RFT and FVU approaches.

ii) The method, described in this paper, is very well known for decades in the literature and is based on the formulation of the three-particle problem with an arbitrary chosen quantization axis defined by a unit timelike vector v^μ (see, e.g., Ref. [202]). At the end, the vector v^μ is fixed in terms of the external momenta that renders the framework manifestly invariant. The most obvious choice is to take that vector parallel to the total three-momentum of the system, and we stick to this choice. It should be also mentioned that this construction relies on the fact that the scattering amplitudes in the various two-particle subsystems, which are calculated by using the dimensional regularization and threshold expansion, are explicitly invariant (i.e., do not depend in v^μ) even before fixing it in terms of the external momenta. For instance, this property is lost if the cutoff regularization is used for the two-particle subsystems as well. By the same token, a similar approach will encounter difficulties when applied to the four-particle problem, which features three-particle subsystems. This issue, however, lies beyond the scope of the present paper.

iii) The choice of the quantization axis along an arbitrary timelike vector v^μ does not affect the analytic properties of the non-relativistic amplitudes. Hence, there is no violation of unitarity in this approach, and spurious poles do not emerge from the quantization condition.

iv) The proposed framework has been tested within a toy model. It has been shown that the three-particle bound spectrum is explicitly Lorentz-invariant, i.e., the finite-volume corrections to the three-particle binding energies, obtained in different moving frames, are exponentially suppressed in L.

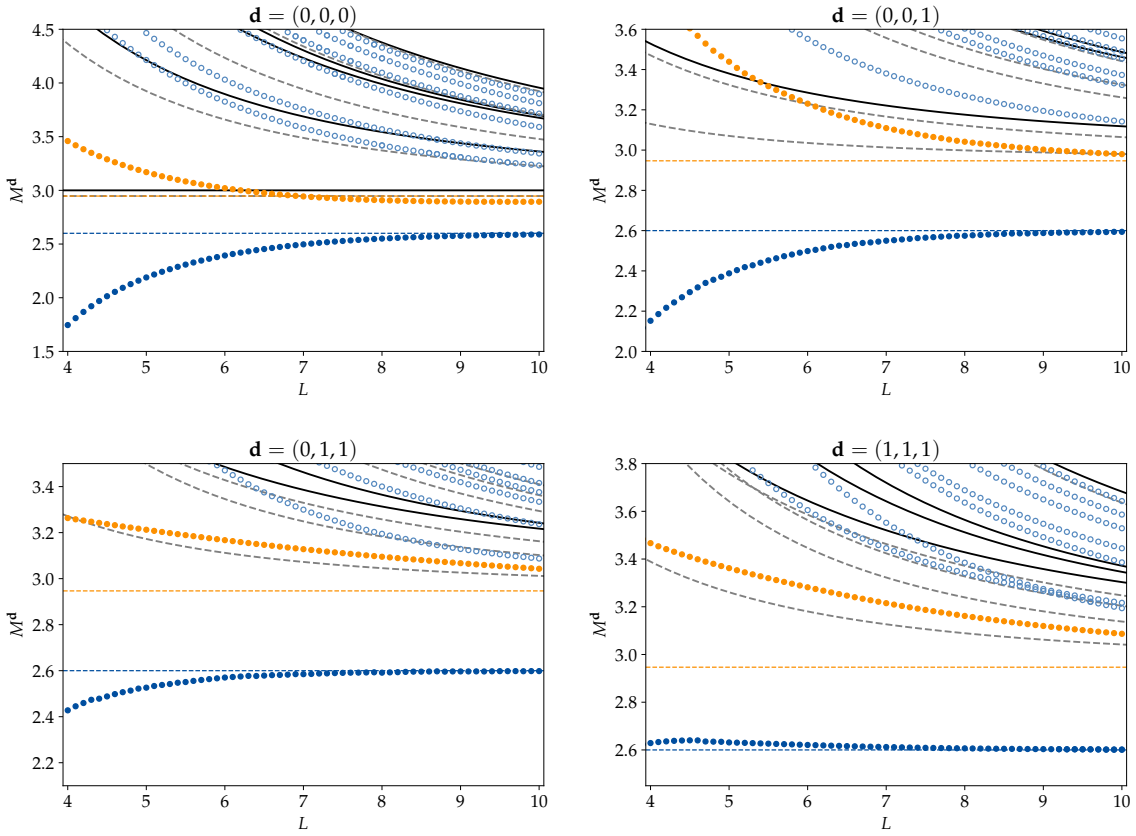

Figure 5.5: Dependence of the energy levels on the box size L in the rest frame and moving frames. Blue and red dotted curves correspond to the energy of the deep and shallow bound states, respectively, and the green dotted curves denote the so-called scattering states. The solid black lines and the gray dashed lines represent the energies of three free particles and a free particle-dimer system in a finite volume, respectively. Horizontal blue and red dashed lines indicate the energies of the infinite-volume deep and shallow bound states. One observes an avoided level crossing (related, presumably, to the crossing of the free particle-dimer levels) in the frame $\mathbf{d} = (1, 1, 1)$ but not in the other frames. Thus, this is a purely kinematic effect.

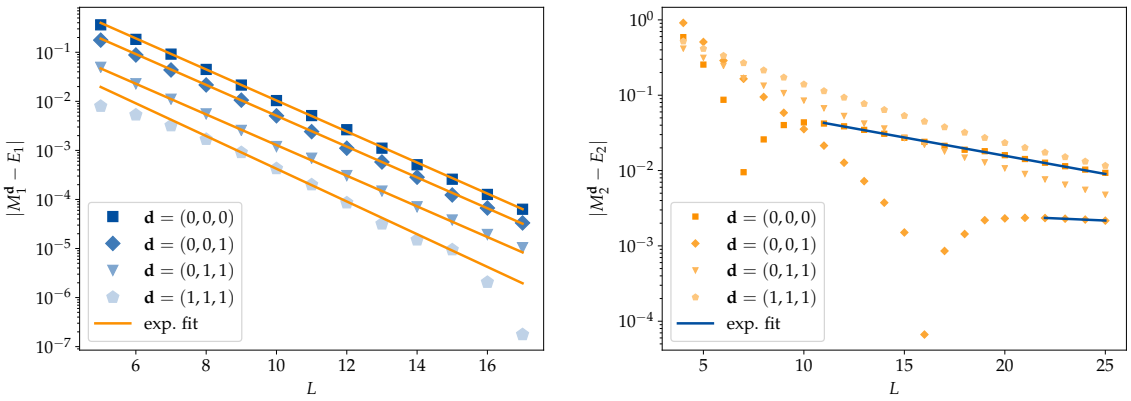

Figure 5.6: The difference between the finite- and infinite-volume binding energies for the deep (left panel) and shallow (right panel) bound states. Note that for a better visibility, we have divided the energy shift of the deep bound state, corresponding to $\mathbf{d} = (1, 1, 1)$, by a factor 25. Otherwise, the data for $\mathbf{d} = (0, 1, 1)$ and $\mathbf{d} = (1, 1, 1)$ would nearly overlap.

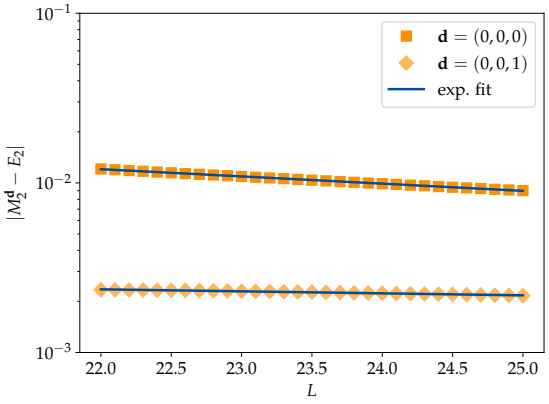

Figure 5.7: The differences between the finite- and infinite-volume binding energies for the shallow bound state at larger values of L. The straight lines show the results of the exponential fit.

v) In our opinion, it will be rather straightforward to adapt the proposed method for other approaches used in the literature (RFT and FVU). An alternative method, proposed within the RFT approach, can also be used. Within this method, a cutoff on the three-momenta cannot be moved beyond some maximal value of order of a particle mass, albeit all results obtained by using the cutoffs less than this value are still valid.

CHAPTER 6

Three-Particle Lellouch-Lüscher Formalism in Moving Frames

The content of this chapter following this prologue, including Appendices A.3 to A.6 is based on the publication

- F. Müller, J.-Y. Pang, A. Rusetsky and J.-J. Wu, *Three-particle Lellouch-Lüscher formalism in moving frames*, JHEP **02** (2023) 214, arXiv: 2211.10126 [hep-lat]

This chapter presents the generalization of the Lellouch-Lüscher equation for three-body decays which was derived in Chapter 4 at the leading order only. As stressed in the discussion of that chapter, including higher order decay couplings, the three-particle analogue of the Lellouch-Lüscher formula will turn into a matrix-like equation. Conceptually the infinite-volume decay amplitude is given by a linear combination of finite-volume decay matrix elements, where the pertinent LL factors account for an undetermined decay coupling each. The benefits of using an manifestly Lorentz-invariant formalism are obvious when working at higher orders since due to the invariance the number of these effective couplings can be reduced as compared to a non-covariant framework.

Another drawback of the formalism derived in Chapter 4 is its restriction to the rest frame. However, from a practical point of view, the use of a relativistic invariant setup might become inevitable. The reason is that, for a given frame, the box length L at which the finite-volume matrix elements are extracted, are fixed due to the condition that the three-particle states must have the energy of the decaying particle. Although there are higher exited states that satisfy this constraint in the same frame, the corresponding values of L might turn out to be impracticable for an actual calculation of the matrix element. Therefore a generalization valid to arbitrary frames is needed.

This chapter attempts to close this gap by proposing a manifestly relativistic-invariant Lellouch-Lüscher formalism for the decays into three spinless identical particles with no two-to-three transitions. Similarly to Chapter 4, the formalism is based on the use of the non-relativistic effective Lagrangians. Manifest Lorentz invariance is guaranteed, as in Chapter 5, by choosing the quantization axis along the total four-momentum of the three-particle system. A systematic inclusion of the higher-order derivative couplings, as well as higher partial waves is addressed.

In the first half of this chapter, the relativistic invariant formulation of the NREFT framework is revisited. For sake of notational simplicity, the quantization condition derived in Chapter 5 is restricted to S-wave interactions in the three- as well as in the two-body sector. In order to derive a

general quantization condition, incorporating the partial-wave mixing present in a finite volume, the dimer fields are preferably expressed in a basis of definite angular momentum rather then the tensor-representation used in Chapter 5. The author contributed a relation between these two bases. After including interactions of arbitrary angular momentum, the relativistic covariance of the particle-dimer Faddeev equations is shown explicitly. Finally the quantization condition is derived for dimer fields with arbitrary angular momentum and the partial diagonalization into the irreducible representations of the little groups in the moving frames is carried out.

In the second half, three-particle decays are described including higher derivative couplings. As discussed, the formalism developed in Chapter 5 provides a convenient framework to generalize the Lellouch-Lüscher equation to higher orders. The derivation conceptually follows the procedure outlined in Chapter 4. Here, the author of this thesis calculated the infinite-volume decay amplitude, as well as the finite-volume decay matrix elements within the NREFT perturbation theory. Again, the initial decay process and therefore the pertinent couplings are considered perturbatively while the final state rescattering is summed up to all orders. The dependence of the infinite-volume decay amplitude on the unknown decay couplings can be eliminated in favor of finite-volume decay matrix elements multiplied by LL factors if the number of these measured matrix elements matches the number of unknown decay coefficients. Applying the NREFT counting rules the author of this thesis derived a formula for these LL factors. These merely depend on the final state short-range interactions which can be determined by a fit to the two- and three-particle spectra.

6.1 Introduction

The study of the three-particle systems on the lattice has attracted much attention in the recent decade [2, 4, 28, 29, 55–61, 63–66, 68, 69, 101–104, 146, 157–163, 174, 178, 186–190, 200, 201, 206, 208–211, 213–226, 230–232, 237]. These studies imply, first and foremost, the measurement of the three-body spectrum which is further analyzed by using the quantization condition (an equation that connects the finite-volume energy spectrum with the infinite-volume observables in the three-particle system). The parameters, characterizing the three-body interactions in the infinite volume, could be extracted in a result of this analysis. In the literature, one finds three conceptually equivalent formulations of the three-body quantization condition: the so-called RFT [57, 58], NREFT [60, 61] and FVU [59, 206] approaches. Note that a Lorentz-invariant formulation of the NREFT approach was suggested recently [2]. We shall be using this approach in what follows. For more information on the subject, we refer the reader to the two recent reviews on the subject [30, 62].

Furthermore, a three-body analog of the Lellouch-Lüscher (LL) formula, which relates the three-body decay amplitudes, measured in a finite and in the infinite volume, has been derived [1, 191] in the NREFT and RFT settings, respectively. The Ref. [1] was more a proof of principle where the relation between the three-body decay amplitudes in a finite and in the infinite volume has been worked out only at the leading order in the EFT expansion. The technical details have been left for future work. The aim of the present paper is to complete the derivation, given in Ref. [1], in order to obtain a general three-body LL formula, and to carry out the comparison with the findings of Ref. [191]. A number of non-trivial issues have to be addressed to fill this gap. Namely,

i) Only S-wave contributions were allowed in the formula given in Ref. [1]. In some cases, the

contributions from higher partial waves may be essential.[1] A systematic inclusion of the higher partial waves has to be performed.

ii) The role of the derivative couplings could be substantial, especially if one considers decays into light particles (for example, pions). As already mentioned in [1], if the derivative vertices describing the three-particle decays are included, one does not end up with a single LL factor (in difference to the two-body case). Albeit a relatively straightforward task, an explicit form of the LL relation in this case should be still worked out.

iii) Even if the formula given in Ref. [1] has the relativistic appearance (for example, the single-particle energies are given by the relativistic expression $w(\mathbf{p}) = \sqrt{m^2 + \mathbf{p}^2}$), it is valid only in the center-of-mass (CM) frame and at the leading order in the EFT expansion. Including higher-dimensional operators in the Lagrangian leads to the proliferation of the number of the effective couplings that have to be determined from the fit to the lattice data. To this end, it would be useful to use data from the sectors with different total momenta. This is however possible, if and only if the approach is manifestly Lorentz-invariant.[2]

In order to achieve the goal stated above, we merge the NREFT derivation of the LL framework, given in Ref. [1], with the manifestly invariant three-particle setting of Ref. [2]. The layout of the paper is as follows. In Sect. 6.2 we list the main relations that define a Lorentz-invariant three-particle quantization condition. Here, we also display the effective Lagrangian that describes the three-particle decays at tree level in a relativistic-invariant fashion. We remind the reader that the decays are assumed to proceed via a different mechanism (e.g., through the weak or electromagnetic interactions) than the formation of the colorless bound states from quarks and gluons. For this reason, the masses of all particles (hadrons) are real, and the effective Lagrangian can be written down in terms of the fields of all hadrons, participating the reaction.[3] Furthermore, in Sect. 6.3 we give a detailed derivation of the LL framework in a manifestly Lorentz-invariant setting. Finally, Sect. 6.4 contains our main result and conclusions.

6.2 Relativistic Invariant Framework in the Three-Particle Sector

6.2.1 The Lagrangian

In the non-relativistic effective theory time and space coordinates are treated differently. For this reason, this theory is not manifestly Lorentz-invariant. In Ref. [2] the invariance was achieved by using the following trick. At the first stage, the quantization axis was chosen along the arbitrary unit four-vector v^μ. Using this vector, all expressions can be rewritten in a manifestly invariant form. This however does not suffice, since the presence of an "external" vector v^μ signals the breakdown of the

[1] An obvious example here is the decay $\omega \to 3\pi$. The decay width of this resonance is rather small, and the pole lies very close to the real axis. Hence, the formalism considered in this paper can be directly applied to this case.

[2] Here, we would like to mention that the manifest relativistic invariance of the RFT approach comes at the cost of imposing a cutoff on the spectator momentum in the three-body equation, which is of order of the particle mass. Increasing the cutoff beyond some critical value is not allowed as it would lead to the spurious singularities in the amplitude. For a more detailed discussion of the issue, we refer the reader to [2].

[3] Note that this differs from the case of the QCD resonances, like $a_1(1260)$ or the Roper resonance, which correspond to a pole in the complex energy plane.

Lorentz invariance. Only at the next stage, when v^μ is fixed in terms of the external momenta in a given process, the relativistic invariance is restored.[4]

Below, we shall briefly sketch the formalism of Ref. [2]. It is convenient to work in the particle-dimer picture, which has proven to be very useful for the derivation of the Faddeev equation in the infinite as well as in a finite volume. A dimer corresponds to an auxiliary field (an integration variable) introduced in this Lagrangian and, thus, not necessarily to a physical bound state of two particles, which may or may not exist in a channel with given quantum numbers. The Lagrangian that describes the three-particle system in question is written down in a following compact form (more details and derivation can be found in Ref. [2]):

$$\begin{aligned}\mathcal{L} &= \phi^\dagger 2w_v(i(v\partial) - w_v)\phi + \sum_{\ell m}\sigma_\ell T^\dagger_{\ell m}T_{\ell m} + \sum_{\ell m}(T^\dagger_{\ell m}O_{\ell m} + \text{h.c.}) \\ &+ 4\pi\sum_{\ell m}\sum_{\ell' m'}\sum_{LL'}\sum_{JM} T^\dagger_{\ell' m'}\left(\mathscr{Y}^{L'\ell'}_{JM}(\underline{\mathbf{w}}, m')\phi^\dagger\right) T^{\ell'\ell}_{JL'L}(\Delta, \overleftarrow{\Delta}_T, \overrightarrow{\Delta}_T)\left((\mathscr{Y}^{L\ell}_{JM}(\underline{\mathbf{w}}, m))^*\phi\right) T_{\ell m}\,.\end{aligned} \tag{6.1}$$

The notations in the above (rather compact) formula should be explained in detail. This is done in what follows. First, ϕ denotes a non-relativistic field operator for the scalar field with the mass m, and $\partial^\mu = (\partial_0, \boldsymbol{\nabla})$ (we remind the reader that in this paper we consider a system that consists of three identical spinless particles only and assume that the transitions between the sectors with a different number of particles are forbidden). The quantity $w_v = \sqrt{m^2 + \partial^2 - (v\partial)^2}$ corresponds to the on-shell energy of this particle in the quantization scheme defined by the vector v^μ and reduces to a familiar expression $w = \sqrt{m^2 - \boldsymbol{\nabla}^2}$ in the rest frame. For simplicity, we shall assume from the beginning that the unit vector v^μ is directed along the total four-vector K^μ of the three-particle system.

Furthermore, $T_{\ell m}$ is a dimer field with a spin ℓ and projection $m = -\ell, \cdots, \ell$. This field is constructed as follows. One starts from the tensor fields with ℓ indices $T_{\mu_1\cdots\mu_\ell}$. These fields are symmetric under a permutation of each two indices, traceless in each pair of indices and obey the constraint

$$v^{\mu_i}T_{\mu_1\cdots\mu_\ell} = 0\,, \qquad i = 1, \cdots, \ell\,. \tag{6.2}$$

Next, let $\underline{\Lambda}$ be a matrix of Lorentz transformation that transforms v^μ into v^μ_0:

$$\underline{\Lambda}(v)^{00} = v^0\,, \qquad \underline{\Lambda}(v)^{0i} = -\underline{\Lambda}(v)^{i0} = v^i\,, \qquad \underline{\Lambda}(v)^{ij} = -\delta^{ij} - \frac{v^i v^j}{v^0 + 1}\,, \tag{6.3}$$

or,

$$\underline{\Lambda}(v)^{\mu\nu} = g^{\mu\nu} - \frac{v^\mu v^\nu}{1 + (vv_0)} - \frac{v^\mu_0 v^\nu_0}{1 + (vv_0)} + \frac{v^\mu v^\nu_0 + v^\mu_0 v^\nu}{1 + (vv_0)}(vv_0) - (v^\mu v^\nu_0 - v^\mu_0 v^\nu)\,. \tag{6.4}$$

[4] With the choice of an arbitrary quantization axis v^μ, one has to define, what does one now mean under time and space coordinates. Let $\underline{\Lambda}$ be the Lorentz transformation $\underline{\Lambda}v = v_0$, where $v^\mu_0 = (1, \mathbf{0})$. Further, let $\underline{\Lambda}x = x'$. Then, x'^0 and $\mathbf{x}'$ are set to play the role of time and space coordinates.

Then,

$$T_{\ell m} = \sum_{\mu_1 \cdots \mu_\ell} (c^{-1})^{\ell m}_{\mu_1 \cdots \mu_\ell} \underline{\Lambda}^{\mu_1}_{\nu_1} \cdots \underline{\Lambda}^{\mu_\ell}_{\nu_\ell} T^{\nu_1 \cdots \nu_\ell}, \tag{6.5}$$

see Eqs. (3.9) and (3.10) of Ref. [2].[5] The matrix elements of c, which can be trivially derived, are purely of group-theoretical origin (see Appendix A.3). A general expression for an arbitrary ℓ is rather clumsy and will not be displayed in the main text. Note also that in Ref. [2] the Lagrangian was written down in terms of the tensor fields $T_{\mu_1 \cdots \mu_\ell}$. Owing to the orthogonality of the matrices c and Λ, the sum over the indices $\mu_1, \cdots, \mu_\ell$ in the Lagrangian can be readily rewritten as a sum over the indices ℓ, m.

The second term in the Lagrangian describes the "free dimer." The value of the parameter $\sigma_\ell = \pm 1$ is fixed by the sign of the two-body scattering length. The third term describes the interaction of a dimer with a spin ℓ coupled to a pair of particles in the state with an angular momentum ℓ (the sum over all ℓ is carried out at the end). The two-particle operators $O_{\ell m}$ take the form, similar to Eq. (6.5):

$$O_{\ell m} = \sum_{\mu_1 \cdots \mu_\ell} (c^{-1})^{\ell m}_{\mu_1 \cdots \mu_\ell} \underline{\Lambda}^{\mu_1}_{\nu_1} \cdots \underline{\Lambda}^{\mu_\ell}_{\nu_\ell} O^{\nu_1 \cdots \nu_\ell}. \tag{6.6}$$

Here, the fully symmetric operators $O^{\mu_1 \cdots \mu_\ell}$ are traceless in each of two indices and obey the relation

$$v^{\mu_i} O_{\mu_1 \cdots \mu_\ell} = 0, \qquad i = 1, \cdots, \ell. \tag{6.7}$$

These operators are constructed of two fields ϕ and the vector $\bar{w}^\mu_\perp = \bar{w}^\mu - v^\mu (v\bar{w})$, where $\bar{w}^\mu = \Lambda^\mu_\nu w^\nu$ and the differential operator w^μ is given by $w^\mu = v^\mu w_v + i\partial^\mu_\perp$, where $\partial^\mu_\perp = \partial^\mu - v^\mu (v\partial)$. Note also that the Λ^μ_ν differs from $\underline{\Lambda}^\mu_\nu$, which was introduced above. Namely, Λ^μ_ν is the Lorentz boost that renders the total four-momentum of the pair parallel to the vector v^μ. Thus, once one has chosen v^μ along the total four-momentum of the system, in the coordinate space Λ^μ_ν becomes a differential operator. For $\ell = 0, 2, \ldots$ the explicit form of the operator $O^{\mu_1 \cdots \mu_\ell}$ (up to an inessential overall normalization) is given by

$$\begin{aligned} O &= \frac{1}{2} \hat{f}_0 \phi^2 \\ O^{\mu\nu} &= \frac{3}{2} \hat{f}_2 (\phi(\bar{w}^\mu_\perp \bar{w}^\nu_\perp \phi) - (\bar{w}^\mu_\perp \phi)(\bar{w}^\nu_\perp \phi)) \\ &- \frac{1}{2} \hat{f}_2 (g^{\mu\nu} - v^\mu v^\nu)(\phi(\bar{w}^\lambda_\perp \bar{w}_{\perp\lambda} \phi) - (\bar{w}^\lambda_\perp \phi)(\bar{w}_{\perp\lambda} \phi)), \end{aligned} \tag{6.8}$$

and so on. Here, $\hat{f}_\ell$ is a differential operator which can be formally expanded in the Taylor series. For example, for $\ell = 0$,

$$\hat{f}_0 \phi^2 = f_0^{(0)} \phi^2 + \frac{1}{2} f_0^{(2)} (\phi(\bar{w}^\mu_\perp \bar{w}_{\perp\mu} \phi) - (\bar{w}^\mu_\perp \phi)(\bar{w}_{\perp\mu} \phi)) + \cdots. \tag{6.9}$$

[5] Note that, despite manifestly covariant notations used in Eq. (6.4), the quantity $\underline{\Lambda}$ is *not* a second-rank Lorentz tensor, since under the Lorentz transformations, the vector v_0 stays put.

The coefficients $f_\ell^{(0)}, f_\ell^{(2)}, \ldots$ are related to the effective-range expansion parameters in the two-body system (the scattering length, effective range and so on).

The construction for higher values of ℓ proceeds straightforwardly (for identical particles, only even values of ℓ are allowed). Namely, in the free field theory, the matrix element of the operator $O^{\mu_1\cdots\mu_\ell}$ between the vacuum and the two-particle state is given by

$$\begin{aligned}\langle 0|O^{\mu_1\cdots\mu_\ell}|p_1,p_2\rangle &= \frac{\sqrt{2\ell+1}f_\ell(-\bar{p}_\perp^2)}{N_\ell}\,\tilde{O}^{\mu_1\cdots\mu_\ell}(\bar{p}_\perp),\\ \frac{\sqrt{2\ell+1}f_\ell(-\bar{p}_\perp^2)}{N_\ell} &= f_\ell^{(0)} - f_\ell^{(2)}\bar{p}_\perp^2 + \cdots, \qquad N_\ell^{-1} = \frac{2^{\ell/2}\ell!}{A^-_{\ell,\ell-1}\cdots A^-_{\ell,0}}\,.\end{aligned} \tag{6.10}$$

where the quantities $A^-_{\ell,m}$ are defined in Appendix A.3. For $\ell = 0, 2, \ldots$, we have

$$\begin{aligned}\tilde{O}(\bar{p}_\perp) &= 1\,,\\ \tilde{O}^{\mu\nu}(\bar{p}_\perp) &= \frac{3}{2}\,\bar{p}_\perp^\mu\bar{p}_\perp^\nu - \frac{1}{2}\,(g^{\mu\nu}-v^\mu v^\nu)\bar{p}_\perp^2\,,\end{aligned} \tag{6.11}$$

and so on. Here, $\bar{p}_\perp^\mu = \bar{p}^\mu - v^\mu(v\bar{p})$ and $\bar{p}^\mu = \Lambda^\mu_\nu p^\nu = \frac{1}{2}\,\Lambda^\mu_\nu(p_1-p_2)^\nu$ (we remind the reader that $p_1^2 = p_2^2 = m^2$). Note also once more that Λ^μ_ν depends on the total momentum of the two-particle system $p_1 + p_2$. In order to write down the expression for a generic $O_{\mu_1\cdots\mu_\ell}(\bar{p}_\perp)$, one may define the tensors in the three-space (the Latin indices i_n run from 1 to 3):

$$P_{i_1\cdots i_\ell}(\mathbf{k}) = N_\ell\sqrt{\frac{4\pi}{2\ell+1}}\,c^{\ell m}_{i_1\cdots i_\ell}\left(\mathscr{Y}_{\ell m}(\mathbf{k})\right)^*\,. \tag{6.12}$$

Here, $\mathscr{Y}_{\ell m}(\mathbf{k}) = k^\ell Y_{\ell m}(\theta,\varphi)$, $Y_{\ell m}(\theta,\varphi)$ denotes the spherical function, and the coefficients c can be found in Appendix A.3. For $\ell = 0, 2$ one has

$$P(\mathbf{k}) = 1\,, \qquad P_{ij}(\mathbf{k}) = \frac{3}{2}\,k_ik_j - \frac{1}{2}\,\delta_{ij}\mathbf{k}^2\,, \quad \cdots \tag{6.13}$$

The general pattern is clear. The operators $\tilde{O}(\bar{p}_\perp)$, $\tilde{O}^{\mu\nu}(\bar{p}_\perp)$ are constructed in analogy with $P(\mathbf{k})$, $P_{ij}(\mathbf{k})$, and so on. Namely, one replaces k_i by $p_\perp^\mu$, $\mathbf{k}^2$ by $-p_\perp^\mu p_{\perp\mu}$ and δ_{ij} by $-g^{\mu\nu}+v^\mu v^\nu$. This prescription is valid for all values of ℓ. Finally, the operator $O^{\mu_1\cdots\mu_\ell}$ in the coordinate space can be immediately read off from the momentum-space expression. The prescription for the off-shell momenta is set by the replacement of a generic p^μ by the differential operator w^μ.

The last term of the Lagrangian describes the particle-dimer scattering at tree level. For any vector a^μ, we have $\underline{a}^\mu = \underline{\Lambda}^\mu_\nu a^\nu$. Next,

$$\mathscr{Y}^{JM}_{L\ell}(\mathbf{k},m) = \langle L(M-m),\ell m|JM\rangle\mathscr{Y}_{L(M-m)}(\mathbf{k})\,, \tag{6.14}$$

and $\langle L(M-m),\ell m|JM\rangle$ denotes the pertinent Clebsh-Gordan coefficient. Furthermore, the quantity $T^{\ell'\ell}_{JL'L}$ is a low-energy polynomial of its arguments, and the coefficients of the expansion are the low-energy couplings. The operator Δ_T is a differential operator acting on the dimer field (the arrow

shows, on which one it does act). In the momentum space,

$$\Delta_T T_{\ell m}(P) = (P^2 - 4m^2) T_{\ell m}(P), \tag{6.15}$$

where P denotes the four-momentum of the dimer. It can be expressed as $P = K - p$, where K is the total momentum of the particle-dimer system and p denotes the momentum of the spectator, which is assumed to be on shell, i.e., $p^2 = m^2$. Finally, in the momentum space, the operator Δ can be replaced by $K^2 - 9m^2$ and, thus, does not depend on the spectator momenta.

6.2.2 Matching of the Couplings Describing Particle-Dimer Scattering

Matching in the dimer framework is a very delicate issue. We have briefly touched on the issue in our previous paper [2], and here we would like to extend this discussion. This will hopefully help to avoid misunderstandings related to the above problem.

To start with, the dimer field in this framework is introduced as a dummy integration variable in the path integral. At the first glance, a one-to-one mapping of the effective couplings in the particle-dimer picture and the three-particle picture is guaranteed. Furthermore, carrying out a perturbative matching of the three-particle S-matrix elements imposes certain constraints on the independent effective couplings, as discussed in Ref. [2]: for example, at the next-to-leading order, as a consequence of the Bose-symmetry, only one independent coupling out of three survives in the local vertex that describes particle-dimer scattering. The number of independent couplings agrees with the findings of Refs. [174, 237], see also [163].

Does this result change, if a shallow physical bound state (a dimer) exists in some channel? On the one hand, it should not, because introducing a dummy field does not change the number of relevant parameters. On the other hand, one has more data to fit now: the S-matrix elements both in the three-particle sector *and* in the particle-dimer sector. If these two data sets are independent, there will be less constraints and more independent couplings in the Lagrangian, see again Ref. [2].

As can be seen from the above discussion, the difference boils down to a question, whether the data from three-particle scattering and particle-dimer scattering are independent from each other. This is a dynamical question, and one knows examples of either sort in Nature. For instance, the properties of a deuteron are very well determined by the low-energy NN scattering amplitude in the pertinent channel. In other words, the deuteron is a beautiful example of a *hadronic molecule* (One arrives at the same result, considering Weinberg's quantization condition [238].). In such a case, the particle-dimer scattering data are determined by the input from the three-particle sector and there is no need to consider them separately.

On the other hand, there are resonances, whose existence can be hardly attributed to the rescattering. Take the extreme case: if the weak interactions are turned on, the kaon will be seen as a (very narrow) resonance in the $\pi\pi$ scattering (for a full analogy with the deuteron, by adjusting quark masses one can even tune the kaon mass to be slightly below the two-pion threshold). However, the *formation* of the kaon has nothing to do with the rescattering of pions. The $\pi\pi$ scattering K-matrix will contain a pre-existing pole on the real axis, which will be eventually dressed by the pion loops. In such a case, the data from the three-particle sector and the particle-dimer sector are independent, and one needs more parameters in the Lagrangian to describe the S-matrix elements in all sectors. Expanding the pole term in the two-body K matrix will lead to the formulae that are *formally* the same as in the case of a molecule. The price to pay for this will be however a very small convergence radius. This case

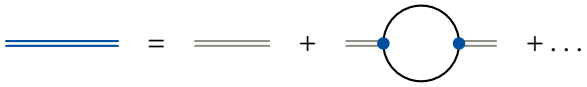

Figure 6.1: Full dimer propagator, obtained by summing up self-energy insertions to all orders. The double, dashed and single lines denote the full dimer propagator, the free dimer propagator given by $-\sigma_\ell^{-1}$, and the particle propagator.

resembles Chiral Perturbation Theory with/without the Δ-resonance – integrating out the Δ leads to the unnaturally large effective couplings that are almost saturated by the Δ-exchange.

To summarize, the particle-dimer picture provides a very flexible framework that can be used both in the presence or absence of physical dimers. Furthermore, when the (shallow) dimers are present, the case of molecular states should be distinguished from the one of tightly bound compounds (pre-existing resonances). In the particle-dimer picture, these two cases are merely described by a different number of the independent effective couplings, because additional parameters are needed to fix the position and the residue of the pre-existing pole in the two-body K-matrix. One could of course use the same (overcomplete) set of couplings in all cases, bearing in mind that if there are no dimers, or the dimers are predominantly molecules, flat directions emerge in the parameter space, when the fit to the finite-volume levels is performed.

Last but not least, the above discussion directly applies to the bound states in the three-particle channel (the trimers). These can also have either molecular nature, or represent tight compounds defined by a different dynamics. In the latter case, it could be again advantageous to introduce an elementary trimer field that will allow one to circumvent the problem with unnaturally large low-energy couplings.

6.2.3 Faddeev Equation

Now, we are in a position to write down the Faddeev equation for the particle-dimer scattering and derive the relativistic invariant quantization condition. We start from the infinite-volume case. After summation of the self-energy insertions (see Fig. 6.1), the dimer propagator can be written down as follows [2]:

$$i\langle 0|T[T_{\ell m}(x)T^\dagger_{\ell' m'}(y)]|0\rangle = \delta_{\ell\ell'}\delta_{mm'}\int \frac{d^4P}{(2\pi)^4}\, e^{-iP(x-y)} S_\ell(P^2)\,, \tag{6.16}$$

where

$$S_\ell(s) = -\frac{1}{\sigma_\ell - f_\ell^2(s)\frac{1}{2}p^{2\ell}(s)I(s)}\,, \qquad s = P^2 = 4(p^2(s)+m^2)\,. \tag{6.17}$$

Furthermore,

$$16\pi\sqrt{s}\left[\sigma_\ell f_\ell^{-2}(s) - \frac{1}{2}p^{2\ell}(s)J(s)\right] \;=\; p^{2\ell+1}(s)\cot\delta_\ell(s)\,, \tag{6.18}$$

and

$$
\begin{aligned}
I(s) &= \frac{\sigma(s)}{16\pi^2}\,\ln\frac{\sigma(s)-1}{\sigma(s)+1}\,, \qquad \sigma(s)=\left(1-\frac{4m^2}{s+i\varepsilon}\right)^{1/2}\,, \\
f_\ell(s) &= f_\ell^{(0)}+f_\ell^{(2)}\left(\frac{s}{4}-m^2\right)+\cdots\,,
\end{aligned}
\tag{6.19}
$$

and $\delta_\ell(s)$ denotes the phase shift in a given partial wave. Finally, if $s \geq 4m^2$,

$$
I(s) = J(s) + \frac{i\sigma(s)}{16\pi}\,. \tag{6.20}
$$

The scattering amplitude in a given partial wave $\mathcal{T}_\ell$ is obtained by equipping the dimer propagator with the endcaps corresponding to the decay of a dimer into a particle pair. For the process $p_1+p_2 \to p_3+p_4$ with the on-shell particles, the scattering amplitude is written as follows:

$$
\mathcal{T}(p_1,p_2;p_3,p_4) = 4\pi\sum_{\ell m}\frac{\mathcal{Y}_{\ell m}(\tilde{\mathbf{p}})\mathcal{Y}^*_{\ell m}(\tilde{\mathbf{q}})}{(T^\ell_{\text{tree}})^{-1}(s)-\frac{1}{2}\,p^{2\ell}(s)I(s)}\,, \tag{6.21}
$$

where [2]

$$
\tilde{\mathbf{p}} = \bar{\mathbf{p}} - \mathbf{v}\frac{\bar{\mathbf{p}}\mathbf{v}-\bar{p}^0}{\mathbf{v}^2}\,, \qquad \tilde{\mathbf{q}} = \bar{\mathbf{q}} - \mathbf{v}\frac{\bar{\mathbf{q}}\mathbf{v}-\bar{q}^0}{\mathbf{v}^2}\,, \tag{6.22}
$$

and

$$
\bar{p}^\mu = \frac{1}{2}\,\Lambda^\mu_\nu(v,u)(p_3-p_4)^\nu\,, \qquad \bar{q}^\mu = \frac{1}{2}\,\Lambda^\mu_\nu(v,u)(p_1-p_2)^\nu\,. \tag{6.23}
$$

Here, $\Lambda(v,u)$ takes the form:

$$
\Lambda(v,u)^{\mu\nu} = g^{\mu\nu} - \frac{u^\mu u^\nu}{1+(uv)} - \frac{v^\mu v^\nu}{1+(uv)} + \frac{u^\mu v^\nu + v^\mu u^\nu}{1+(uv)}\,(uv) - (u^\mu v^\nu - v^\mu u^\nu)\,. \tag{6.24}
$$

We remind the reader that $u^\mu = P^\mu/\sqrt{P^2}$ is the unit vector in the direction of the CM momentum of the pair. Also, the quantity $\Lambda(v,u)^{\mu\nu}$, in difference to $\underline{\Lambda}(v)^{\mu\nu}$, *is* a second-rank Lorentz-tensor, because both v^μ and u^μ transform like Lorentz-vectors. Note also that $\underline{\Lambda}(v)^{\mu\nu} = \Lambda(v_0,v)^{\mu\nu}$.

The expression (6.22) for the vectors $\tilde{\mathbf{p}}, \tilde{\mathbf{q}}$ looks very complicated but, in fact, have a very transparent physical meaning. In order to show this, note that $(v\bar{p}) = (v\bar{q}) = 0$. Taking this into account, it is easy to rewrite Eq. (6.22) in the following form:

$$
\tilde{\mathbf{p}} = \bar{\mathbf{p}} + \mathbf{v}\frac{\bar{\mathbf{p}}\mathbf{v}}{1+v^0} - \bar{p}^0\mathbf{v}\,, \qquad \tilde{\mathbf{q}} = \bar{\mathbf{q}} + \mathbf{v}\frac{\bar{\mathbf{q}}\mathbf{v}}{1+v^0} - \bar{q}^0\mathbf{v}\,. \tag{6.25}
$$

This gives $\tilde{p}_\mu = \underline{\Lambda}_{\mu\nu}(v)\bar{p}^\nu$ and $\tilde{q}_\mu = \underline{\Lambda}_{\mu\nu}(v)\bar{q}^\nu$. Furthermore, it can be straightforwardly checked that $\tilde{p}_0 = \tilde{q}_0 = 0$.

The full scattering amplitude is obtained by summing $\mathcal{T}_\ell$ over all ℓ. This summation renders the amplitude relativistic invariant – the result depends on the Mandelstam variables s, t only.

Next, let $T_{\ell' m', \ell m}(p, q)$ be the particle-dimer scattering amplitude. The indices $\ell m/\ell' m'$ denote the dimer spin and magnetic quantum number in the initial/final states, respectively. The Faddeev equation takes the matrix form:

$$\begin{aligned} T_{\ell' m', \ell m}(p, q) &= Z_{\ell' m', \ell m}(p, q) \\ &+ \sum_{\ell'' m''} \int^{\Lambda_v} \frac{d^3 k_\perp}{(2\pi)^3 2 w_v(k)} Z_{\ell' m', \ell'' m''}(p, k) S_{\ell''}((K-k)^2) T_{\ell'' m'', \ell m}(k, q) \,. \end{aligned} \tag{6.26}$$

Here, the "covariant" cutoff is defined as

$$\int^{\Lambda_v} \frac{d^3 k_\perp}{(2\pi)^3} F(k) = \int \frac{d^4 k}{(2\pi)^3} \delta(k^2 - m^2) \theta(\Lambda^2 + k^2 - (vk)^2) F(k) \,, \tag{6.27}$$

and

$$\begin{aligned} Z_{\ell' m', \ell m}(p, q) &= \frac{4\pi \left(\mathscr{Y}_{\ell' m'}(\tilde{\mathbf{p}})\right)^* f_{\ell'}(s_p) f_\ell(s_q) \mathscr{Y}_{\ell m}(\tilde{\mathbf{q}})}{2 w_v(K-p-q)(w_v(p) + w_v(q) + w_v(K-p-q) - vK - i\varepsilon)} \\ &+ 4\pi \sum_{LL'} \sum_{JM} \mathscr{Y}^{L'\ell'}_{JM}(\underline{\mathbf{p}}, m') T^{\ell'\ell}_{JL'L}(\Delta, \Delta_p, \Delta_q) \left(\mathscr{Y}^{L\ell}_{JM}(\underline{\mathbf{q}}, m)\right)^* \,. \end{aligned} \tag{6.28}$$

In the above expression, $\tilde{\mathbf{p}}, \tilde{\mathbf{q}}$ are defined as follows:

$$\begin{aligned} \tilde{p}^\mu &= \frac{1}{2} \underline{\Lambda}^{\mu\nu}(v) \Lambda_{\nu\alpha}(v, u_p)(\hat{q} - \hat{k})_\alpha \,, \qquad \tilde{q}^\mu = \frac{1}{2} \underline{\Lambda}^{\mu\nu}(v) \Lambda_{\nu\alpha}(v, u_q)(\hat{p} - \hat{k})^\alpha \,, \\ k^\mu &= K^\mu - p^\mu - q^\mu \,, \qquad s_p = (\hat{q} + \hat{k})^2 \,, \qquad s_q = (\hat{p} + \hat{k})^2 \,, \\ u_q^\mu &= (\hat{p} + \hat{k})^\mu / \sqrt{s_q} \,, \qquad u_p^\mu = (\hat{q} + \hat{k})^\mu / \sqrt{s_p} \,, \end{aligned} \tag{6.29}$$

and, for any four-vector a^μ, one has

$$\hat{a}^\mu = a^\mu - v^\mu (av) + v^\mu w_v(a) \,. \tag{6.30}$$

Furthermore,

$$\Delta = (K^2 - 9m^2) \,, \qquad \Delta_p = (K - \hat{p})^2 - 4m^2 \,, \qquad \Delta_q = (K - \hat{q})^2 - 4m^2 \,, \tag{6.31}$$

and the function $f_\ell(s)$ is related to the scattering phase, according to Eq. (6.18).

6.2.4 Relativistic Invariance

In order to establish the relativistic invariance of the above infinite-volume framework,[6] one has to perform an arbitrary Lorentz-boost on all external momenta: $p = p_\Omega \mapsto \Omega p$, $q = q_\Omega \mapsto \Omega q$,

[6] It is clear that the notion of relativistic invariance applies to the infinite-volume case only. In a finite volume, the invariance is broken by a box. Hence, in a finite volume, the statement boils down to a frame-independence of the couplings extracted from the fit to the energy levels, up to exponential corrections.

$K = K_\Omega \mapsto \Omega K$ and $v = v_\Omega \mapsto \Omega v$. The integration variable undergoes the same boost $k = k_\Omega \mapsto \Omega k$. All functions depending on Lorentz-scalars are, of course, manifestly Lorentz-invariant. Hence, the question boils down to the transformation of the three-vectors $\underline{\mathbf{p}}$, $\underline{\mathbf{q}}$ and $\tilde{\underline{\mathbf{p}}}$, $\tilde{\underline{\mathbf{q}}}$.

Let us first consider the four-vector $\underline{p} = \underline{\Lambda}(v)\hat{p}$, where $\underline{\Lambda}(v)$ is defined from the condition $\underline{\Lambda}(v)v = v_0$. In the boosted frame, one has $\underline{\Lambda}(v_\Omega)v_\Omega = v_0$. This gives

$$\underline{\Lambda}(v_\Omega) = R\underline{\Lambda}(v)\Omega^{-1}\,, \tag{6.32}$$

where R is a pure rotation that does not depend on the choice of the four-vector p. If Ω is a pure rotation itself, then $R = \Omega$. Hence,

$$\underline{p}_\Omega = \underline{\Lambda}(v_\Omega)\hat{p}_\Omega = R\underline{\Lambda}(v)\Omega^{-1}\Omega\hat{p} = R\underline{p}\,. \tag{6.33}$$

The same line of reasoning holds for the four-vector $\tilde{p} = \underline{\Lambda}(v)\Lambda(v,u)\hat{p}$, since the vector $\Lambda(v,u)\hat{p} \mapsto \Omega\Lambda(v,u)\hat{p}$ transforms exactly as the vector $\hat{p}$ (we remind the reader that $\Lambda(v,u)$, in difference of $\underline{\Lambda}(v)$, is the Lorentz-tensor). The transformation matrix $R = R(\Omega, v, u)$, which depends on the parameters of the Ω, as well as on the vectors v and u in a non-linear manner, is the same in both cases.[7]

To summarize, it is seen that the Lorentz transformations, acting on the three-vectors $\tilde{\underline{\mathbf{p}}}$, $\underline{\mathbf{p}}$, . . ., result in the $SO(3)$ transformations whose parameters can be expressed through the parameters of the initial Lorentz transformations as well as the vectors v and u. The transformation of the various quantities that enter the kernel of the Faddeev equation can be defined through the transformation properties of spherical functions, entering this expression:

$$\mathscr{Y}_{\ell m}(R\mathbf{p}) = \sum_{m'} \left(\mathscr{D}^{(\ell)}_{mm'}(R)\right)^* \mathscr{Y}_{\ell m'}(\mathbf{p})\,, \tag{6.34}$$

where $\mathscr{D}^{(l)}_{mm'}(R)$ denote Wigner D-functions. Furthermore, The kernel of the equation $Z = Z_{\text{ex}} + Z_{\text{loc}}$ consists of two parts, corresponding to the exchange diagram and the local particle-dimer interaction, see the first and the second terms in Eq. (6.28), respectively. The transformation of the first term is straightforwardly defined by Eq. (6.34):

$$\left(Z_{\text{ex}}\right)_{\ell' m', \ell m}(\Omega p, \Omega q) = \sum_{m''' m''} \mathscr{D}^{(\ell')}_{m' m'''}(R)\left(Z_{\text{ex}}\right)_{\ell' m''', \ell m''}(p,q)\left(\mathscr{D}^{(\ell)}_{mm''}(R)\right)^*\,. \tag{6.35}$$

Establishing the transformation properties of the local term is a bit trickier and will be considered in Appendix A.5. Here, we simply state that Z_{loc} transforms exactly in the same way as Z_{ex}. Hence, their sum has the same property. Furthermore, the propagator S_ℓ is invariant under the Lorentz transformations. From this, one finally concludes that the particle-dimer scattering amplitude, which is a solution of the Faddeev equation (6.26), has the same transformation property as the kernel Z:

$$T_{\ell' m', \ell m}(\Omega p, \Omega q) = \sum_{m''' m''} \mathscr{D}^{(\ell')}_{m' m'''}(R) T_{\ell' m''', \ell m''}(p,q)\left(\mathscr{D}^{(\ell)}_{mm''}(R)\right)^*\,. \tag{6.36}$$

This is nothing but the statement about the manifest Lorentz invariance of the framework.

[7] The rotation R is related to the Thomas-Wigner rotation [239, 240].

6.2.5 Faddeev Equation in a Finite Volume and the Quantization Condition

In a finite volume, the integration over three-momenta is replaced by the sums. In this course, the Faddeev equations, displayed above, undergo some modifications. As in the infinite volume, we start from the propagator of a dimer

$$i\langle 0|T[T_{\ell' m'}(x)T^{\dagger}_{\ell m}(y)]|0\rangle = \int \frac{dP^0}{2\pi}\frac{1}{L^3}\sum_{\mathbf{P}} e^{-iP(x-y)} S^L_{\ell' m',\ell m}(P)\,. \tag{6.37}$$

Here, the dimer three-momentum runs over the discrete values $\mathbf{P} = \dfrac{2\pi}{L}\mathbf{n}$, $\mathbf{n}\in\mathbb{Z}^3$. Note that, owing to the lack of the rotational invariance in a finite volume, the propagator is no more diagonal in the indices ℓm and $\ell' m'$. It obeys the Dyson-Schwinger equation

$$S^L_{\ell' m',\ell m}(P) = -\frac{1}{\sigma_{\ell'}}\delta_{\ell'\ell}\delta_{m' m} - \frac{1}{\sigma_{\ell'}}\sum_{\ell'' m''}\Sigma^L_{\ell' m',\ell'' m''}(P) S^L_{\ell'' m'',\ell m}(P), \tag{6.38}$$

where

$$\Sigma^L_{\ell' m',\ell m}(P) = f_{\ell'}(P^2) f_{\ell}(P^2)\int \frac{dq^0}{2\pi i}\frac{1}{2L^3}\sum_{\mathbf{q}}\frac{\left(\mathscr{Y}_{\ell' m'}(\tilde{\mathbf{q}})\right)^* \mathscr{Y}_{\ell m}(\tilde{\mathbf{q}})}{(m^2 - q^2 - i\varepsilon)(m^2 - (P-q)^2 - i\varepsilon)}, \tag{6.39}$$

where

$$\tilde{q}^{\mu} = \frac{1}{2}\underline{\Lambda}^{\mu\nu}(v)\Lambda_{\nu\alpha}(v,u)(\hat{q}-\hat{q}')^{\alpha}, \qquad u^{\mu} = \frac{(\hat{q}+\hat{q}')^{\mu}}{(\hat{q}+\hat{q}')^2}, \qquad q' = P - q\,. \tag{6.40}$$

Carrying out the integration over q^0 in Eq. (6.39), one obtains

$$\Sigma^L_{\ell' m',\ell m}(P) = f_{\ell'}(P^2) f_{\ell}(P^2)\frac{1}{2L^3}\sum_{\mathbf{q}}\frac{\left(\mathscr{Y}_{\ell' m'}(\tilde{\mathbf{q}})\right)^* \mathscr{Y}_{\ell m}(\tilde{\mathbf{q}})}{2w(\mathbf{q})2w(\mathbf{P}-\mathbf{q})(w(\mathbf{q})+w(\mathbf{P}-\mathbf{q})-P^0)}\,. \tag{6.41}$$

Note that the propagator still implicitly depends on v^{μ}, since v^{μ} enters the definition of any on-mass-shell vector $\hat{a}^{\mu}$. This dependence comes however only from the numerator and can be worked out explicitly. We relegate this task to Appendix A.4 where, in particular, it will be shown how does one systematically factor out this dependence. Moreover, already at this stage it is seen that the v-dependence disappears in the S-wave, as claimed in Ref. [2].

The Faddeev equation in a finite volume can be written as

$$\begin{aligned} T^L_{\ell' m',\ell m}(p,q) &= Z_{\ell' m',\ell m}(p,q) + \sum_{\ell''' m''',\ell'' m''}\frac{1}{L^3}\sum_{\mathbf{k}}^{\Lambda_v}\frac{1}{2w(\mathbf{k})} Z_{\ell' m',\ell''' m'''}(p,k) \\ &\times S^L_{\ell''' m''',\ell'' m''}(K-k) T^L_{\ell'' m'',\ell m}(k,q), \end{aligned} \tag{6.42}$$

where

$$\sum_{\mathbf{k}}^{\Lambda_v} f(k) \doteq \sum_{\mathbf{k}} \theta(\Lambda^2 + k^2 - (kv)^2) f(k)\,. \tag{6.43}$$

The three-body quantization condition takes the form $\det \mathscr{A} = 0$, where $\mathscr{A}$ is a matrix both in the spectator momenta p, q, as well as the partial-wave indices $\ell m, \ell' m'$:

$$\mathscr{A}_{\ell' m', \ell m}(p,q) = 2w(\mathbf{p})\delta_{\mathbf{pq}} \left(S^L_{\ell' m', \ell m}(K-p)\right)^{-1} - \frac{1}{L^3} Z_{\ell' m', \ell m}(p,q)\,. \tag{6.44}$$

Here,

$$\left(S^L_{\ell' m', \ell m}(K-p)\right)^{-1} = -\delta_{\ell'\ell}\delta_{m' m}\sigma_{\ell'} - \Sigma^L_{\ell' m', \ell m}(K-p)\,. \tag{6.45}$$

6.2.6 Reduction of the Quantization Condition

Using symmetry under the octahedral group (or the little groups thereof), one may achieve a partial diagonalization of the quantization condition. Namely, let $\mathcal{G}$ be a subgroup of the octahedral group O_h that leaves the vector $\mathbf{K}$ invariant. Since v^μ is chosen to be parallel to K^μ, the vector $\mathbf{v}$ is invariant under $\mathcal{G}$ as well. Hence, under the transformations from the group $\mathcal{G}$, the matrix $\mathscr{A}$ from Eq. (6.44) transforms as

$$\mathscr{A}_{\ell' m', \ell m}(gp, gq) = \sum_{m''' m''} \mathscr{D}^{(\ell')}_{m' m'''}(g) \mathscr{A}_{\ell' m''', \ell m''}(p,q) \left(\mathscr{D}^{(\ell)}_{m m''}(g)\right)^*, \qquad g \in \mathcal{G}\,. \tag{6.46}$$

It is well known that the linear space, in which the irreducible representation (irrep) of the $SO(3)$ group with the angular momentum ℓ is realized, falls into different orthogonal subspaces, corresponding to the irreducible representations of the octahedral group or the little groups thereof. The basis vectors of the irreps of two groups are related by a linear transformation

$$\mathscr{Y}^\ell_{\lambda(t\Delta)} = \sum_m c^{\ell m}_{\lambda(t\Delta)} \mathscr{Y}_{\ell m}\,. \tag{6.47}$$

Here, Δ denotes an irrep of the group $\mathcal{G}$, t labels different copies of the same irrep Δ, and λ is an index, corresponding to different basis vectors of a given irrep. The coefficients $c^{\ell m}_{\lambda t\Delta}$ are well known an, for small values of ℓ, are tabulated, e.g., in Ref. [36]. These coefficients obey the orthogonality conditions

$$\begin{aligned} \sum_m \left(c^{\ell m}_{\lambda'(t'\Delta')}\right)^* c^{\ell m}_{\lambda(t\Delta)} &= \delta_{t't}\delta_{\Delta'\Delta}\delta_{\lambda'\lambda}\,, \\ \sum_{t\Delta\lambda} \left(c^{\ell m'}_{\lambda(t\Delta)}\right)^* c^{\ell m}_{\lambda(t\Delta)} &= \delta_{mm'}\,. \end{aligned} \tag{6.48}$$

Besides this, we shall need to define the Clebsch-Gordan coefficients for the group $\mathcal{G}$. Note that the octahedral group O_h as well as the little groups C_{4v}, C_{2v}, C_{3v}, corresponding to a different choice of the center-of-mass momentum, are simply reducible. Since all the representations are unitary, these Clebsch-Gordan coefficients can be chosen to be real. The orthogonality condition for the

Clebsch-Gordan coefficients takes the form

$$\begin{aligned}\sum_{\Gamma\alpha}\langle\Sigma\rho,\Delta\lambda|\Gamma\alpha\rangle\langle\Sigma\rho',\Delta\lambda'|\Gamma\alpha\rangle &= \delta_{\rho\rho'}\delta_{\lambda\lambda'}\,,\\ \sum_{\rho\lambda}\langle\Sigma\rho,\Delta\lambda|\Gamma\alpha\rangle\langle\Sigma\rho,\Delta\lambda|\Gamma'\alpha'\rangle &= \delta_{\Gamma\Gamma'}\delta_{\alpha\alpha'}\,,\end{aligned} \tag{6.49}$$

where capital and small Greek letters label the irreps and the basis vectors in a given irrep, respectively.

Defining now

$$\mathscr{A}^{\ell'\ell}_{\lambda'(t'\Delta'),\lambda(t\Delta)}(p,q) = \sum_{m'm}\left(c^{\ell'm'}_{\lambda'(t'\delta')}\right)^{*}\mathscr{A}_{\ell'm',\ell m}(p,q)c^{\ell m}_{\lambda(t\Delta)}\,, \tag{6.50}$$

it is easy to show that this quantity transforms as

$$\mathscr{A}^{\ell'\ell}_{\lambda'(t'\Delta'),\lambda(t\Delta)}(gp,gq) = \sum_{\lambda'''\lambda''}T^{(\Delta')}_{\lambda'\lambda'''}(g)\mathscr{A}^{\ell'\ell}_{\lambda'''(t'\Delta'),\lambda''(t\Delta)}(p,q)T^{(\Delta)}_{\lambda''\lambda}(g^{-1})\,. \tag{6.51}$$

Here, $T^{(\Delta)}(g)$ denotes the matrix of an irreducible representation Δ.

At the next step, we define a projection

$$\begin{aligned}\mathscr{A}^{\ell'\Gamma'\alpha',\ell\Gamma\alpha}_{\sigma'(t'\Delta')\Sigma',\sigma(t\Delta)\Sigma}(p_r,q_s) &= \frac{s_{\sigma'}}{G}\frac{s_{\Sigma}}{G}\sum_{g',g\in\mathcal{G}}\sum_{\lambda'\rho',\lambda\rho}\langle\Sigma'\rho',\Delta'\lambda'|\Gamma'\alpha'\rangle T^{(\Sigma')}_{\rho'\sigma'}(g')\\ &\times \mathscr{A}^{\ell'\ell}_{\lambda'(t'\Delta'),\lambda(t\Delta)}(g'p_r,gq_s)\langle\Sigma\rho,\Delta\lambda|\Gamma\alpha\rangle\left(T^{(\Sigma)}_{\rho\sigma}(g)\right)^{*}\,.\end{aligned} \tag{6.52}$$

Here, p_r and q_s denote reference momenta in the shells r and s, respectively, s_Σ, $s_{\Sigma'}$ are the dimensions of the pertinent irreps, and G is the total number of the elements in the group $\mathcal{G}$ (for a detailed discussion, see, e.g., Ref. [146]). It can be seen (see Appendix A.6) that this matrix is diagonal in the irreps Γ,Γ':

$$\mathscr{A}^{\ell'\Gamma'\alpha',\ell\Gamma\alpha}_{\sigma'(t'\Delta')\Sigma',\sigma(t\Delta)\Sigma}(p_r,q_s) = \frac{s_{\Sigma'}s_{\Sigma}}{Gs_{\Gamma}}\delta_{\Gamma'\Gamma}\delta_{\alpha'\alpha}\mathscr{A}^{\ell'\ell;\Gamma}_{\sigma'(t'\Delta')\Sigma',\sigma(t\Delta)\Sigma}(p_r,q_s)\,, \tag{6.53}$$

where

$$\begin{aligned}\mathscr{A}^{\ell'\ell;\Gamma}_{\sigma'(t'\Delta')\Sigma',\sigma(t\Delta)\Sigma}(p_r,q_s) &= \sum_{g\in\mathcal{G}}\sum_{\lambda'\lambda}\sum_{\sigma''\gamma}\langle\Sigma'\sigma'',\Delta'\lambda'|\Gamma\gamma\rangle\langle\Sigma\sigma,\Delta\lambda|\Gamma\gamma\rangle\\ &\times T^{(\Sigma')}_{\sigma''\sigma'}(g)\mathscr{A}^{\ell'\ell}_{\lambda'(t'\Delta'),\lambda(t\Delta)}(gp_r,q_s)\,.\end{aligned} \tag{6.54}$$

This means that the quantization condition $\det\mathscr{A}=0$ diagonalizes in different irreps Γ, taking the form $\det\mathscr{A}^{\Gamma}=0$, where the matrix $\mathscr{A}^{\Gamma}$ is defined by Eq. (6.54).

6.2.7 Three-Particle Decays

In the following, for brevity, we shall refer to the heavy and light particles to as "kaons" and "pions," respectively, bearing in mind the weak decays of kaons into three pions (of course, this analogy is not full since it does not take into account the isospin.). The Lagrangian that describes the decay of the "kaon" into a "pion"-dimer pair can be written as

$$\mathscr{L}_G = \sqrt{4\pi} \sum_{\ell m} \frac{(-1)^\ell}{\sqrt{2\ell+1}} \left(K^\dagger G_\ell(\Delta_T) \left((\mathscr{Y}_{\ell,-m}(\underline{\mathbf{w}}))^* \phi \right) T_{\ell m} + \text{h.c.} \right) . \tag{6.55}$$

Here, G_ℓ is a low-energy polynomial

$$G_\ell(\Delta_T) = G_0^{(\ell)} + G_1^{(\ell)} \Delta_T + \cdots . \tag{6.56}$$

Here, Δ_T is defined in Eq. (6.15). The coefficients of the Taylor expansion $G_0^{(\ell)}, G_1^{(\ell)}, \ldots$ play the role of the effective couplings, and Δ_T is of order p^2 in the NREFT power counting. It is assumed that $G_0^{(\ell)}, G_1^{(\ell)}, \ldots$ are proportional to an intrinsically small coupling (an analog of the Fermi coupling in weak kaon decays). All terms in the decay amplitude at the second and higher orders in these couplings are neglected. Furthermore, integrating out the dimer field, one arrives at the Lagrangian that describes decays of "kaons" into three "pions" at tree level, analogous to the one displayed in Refs. [166, 167]. The Bose-symmetry in the final state imposes constraints on the couplings $G_0^{(\ell)}, G_1^{(\ell)}, \ldots$. An exact number of these constraints however depends on the details of the final-state interactions, see the discussion in Sect. 6.2.2.[8]

This Lagrangian should be supplemented by the Lagrangian describing the free "kaon"

$$\mathscr{L}_K = K^\dagger 2 w_v^K (iv\partial - w_v^K) K . \tag{6.57}$$

Here, $w_v^K = \sqrt{M^2 + \partial^2 - (v\partial)^2}$ and M denotes the mass of the "kaon". The full Lagrangian of the system is given by $\mathscr{L} + \mathscr{L}_G + \mathscr{L}_K$, where the individual terms are given by Eqs. (6.1), (6.55) and (6.56), respectively.

6.2.8 Convergence of the NREFT Approach

The convergence of the NREFT approach is a subtle issue which comprises several distinct aspects of the problem in question. Below, we wish to put this issue under scrutiny. To start with, a rule of thumb requiring $p/m \ll 1$, where p denotes the magnitude of a characteristic three-momentum in the process seems too restrictive, say, in kaon decays. From the point of view of kinematics, this restriction is not relevant: all low energy singularities in the amplitudes appear exactly at the right place [166, 167]. So, everything finally boils down to a question, whether the real part of the decay amplitude can be well approximated by a low-energy polynomial. Were this not the case, one would conclude that the contributions which are not explicitly taken into account in NREFT (say, all kinds of the t- and u-channel diagrams, multi-particle intermediate states and so on), play an important role and NREFT is not applicable. Fortunately, one can check this assumption experimentally in the

[8] The expansion Eq. (6.56) is an analog of the expansion of the quantity $A_{K3\pi}^{\text{PV}}$ from Ref. [191] in the particle-dimer formalism. The constraints imposed by the Bose-symmetry are already taken into account in that paper.

real kaon decays, since the decay amplitudes are measured very accurately. The experiment neatly confirms the conjecture: the real part of the amplitude can be indeed fitted by a polynomial in the Mandelstam variables s_i of a rather low order in the whole region of the Dalitz plot (see, e.g. [241]). This justifies the use of the NREFT approach for the description of the kaon decays into three pions, despite the fact that characteristic momenta of pions are of order of the pion mass itself.

Two remarks are in order. The first one concerns the choice of the expansion point. The "standard" version of the NREFT implies the expansion of the amplitudes in the external three-momenta. For example, in case of the two-particle scattering, this corresponds to the effective-range expansion which is performed around threshold. The convergence of such an expansion in some cases might be affected by the presence of the subthreshold singularities in the initial relativistic theory (for instance, effective-range expansion in the vicinity of the ρ-meson fails due to the left-hand cut in the $\pi\pi$ amplitude). In such cases, choosing the expansion point somewhere above threshold allows one to circumvent the problem, if the effect of the inelastic channels is still small. The NREFT framework is flexible enough and can be adapted to the change of the expansion point with a minor modification only. We do not display a modified Lagrangian here, because this issue is not directly related to the main problem considered in the present paper.

The second remark is general. One may ask, whether NREFT is applicable to study of the generic three-particle decays beyond $K \to 3\pi$. There exists no unique answer to this (very difficult) question. It should be therefore should be addressed on the case-to-case basis: for example, it would be conceivable that NREFT is still valid, if it is *a priori* known that the inelastic channels are not important for a process in question.

6.3 Derivation of the Three-Particle LL Formula in the Relativistic-Invariant Framework

6.3.1 The Wick Rotation

In the derivation of the 3-particle LL formula we closely follow the path outlined in Ref. [1]. There are, however, some differences caused by an explicit Lorentz invariance. These differences will be highlighted in the following.

We start with discussing the Wick rotation in case of a quantization axis chosen parallel to an arbitrary timelike unit vector v^μ. To be specific, we consider the simplest possible choice of the three-particle source/sink operator $\mathcal{O}(x) = \phi^3(x)$. As the first step in the derivation, we would like to extract the finite-volume matrix element $\langle 0|\mathcal{O}|n\rangle$, where $|n\rangle$ denotes a (discrete) eigenstate of the total Hamiltonian in a finite volume. To this end, we consider the two-point function

$$G(x-y) = \langle 0|T\mathcal{O}(x)\mathcal{O}^\dagger(y)|0\rangle \,. \tag{6.58}$$

Using the translational invariance and the closure relation, in the Minkowski space we get

$$G(x-y) = \sum_n e^{-iP_n(x-y)}\,|\langle 0|\mathcal{O}(0)|n\rangle|^2 \,. \tag{6.59}$$

The three-momentum of the intermediate state is quantized, $\mathbf{P}_n = \dfrac{2\pi}{L}\,\mathbf{n},\ \mathbf{n} \in \mathbb{Z}^3$. The time component

of the four vector is given by P_n^0, where it is assumed that $P_n^0 > |\mathbf{P}|$. In order to *define* the Wick rotation in the frame moving with the four-velocity v^μ, one defines the parallel and transverse components:

$$\begin{aligned} (x-y)_\parallel &= v(x-y), \qquad (x-y)_\perp^\mu = (x-y)^\mu - v^\mu (x-y)_\parallel , \\ P_{n,\parallel} &= vP_n , \qquad P_{n,\perp}^\mu = P_n^\mu - v^\mu P_{n,\parallel} , \end{aligned} \tag{6.60}$$

so that

$$P^\mu (x-y)_\mu = P_{n,\parallel}(x-y)_\parallel + P_{n,\perp}^\mu (x-y)_{\perp,\mu} . \tag{6.61}$$

The Wick rotation in the moving frame is defined through the analytic continuation

$$(x-y)_\parallel \to -i(x-y)_\parallel , \qquad (x-y)_\perp^\mu \to (x-y)_\perp^\mu . \tag{6.62}$$

Furthermore, since $P_n^0 > |\mathbf{P}_n|$, then

$$P_{n,\parallel} = v^0 P_n^0 - \mathbf{v}\mathbf{P}_n \geq v^0 P_n^0 - |\mathbf{v}|\,|\mathbf{P}_n| > 0 . \tag{6.63}$$

Thus, in the limit $(x-y)_\parallel \to \infty$, all exponentials are damping in the Euclidean space and one gets

$$G(x-y) = \sum_n e^{-P_{n,\parallel}(x-y)_\parallel - iP_{n,\perp}(x-y)_\perp} |\langle 0|\mathscr{O}(0)|n\rangle|^2 , \tag{6.64}$$

where *the same matrix elements* as in Eq. (6.59) appear in the right-hand side. It should be noted however that, on the lattice, one does not need calculate the Green functions, in which the continuation to the Euclidean space is performed in moving frames. This is a purely theoretical construction that will merely help us to derive 3-particle LL formula in all frames.

6.3.2 The Matrix Element

Next, let us evaluate the two-point function $G(x-y)$ in NREFT, starting from the infinite volume. It will be useful to use the components $(a_\parallel, a_\perp^\mu)$ instead of $(a^0, \mathbf{a})$ for all four vectors a^μ. For simplicity, we shall work in the Minkowski space and perform the Wick rotation only at the very end. The Feynman diagrams, contributing to the above two-point function, can be summed up, resulting in a compact expression

$$G(x-y) = 3^2 \int \frac{dK_\parallel}{2\pi i} \frac{d^3K_\perp}{(2\pi)^3} e^{-iK_\parallel (x-y)_\parallel - iK_\perp (x-y)_\perp} G(K), \tag{6.65}$$

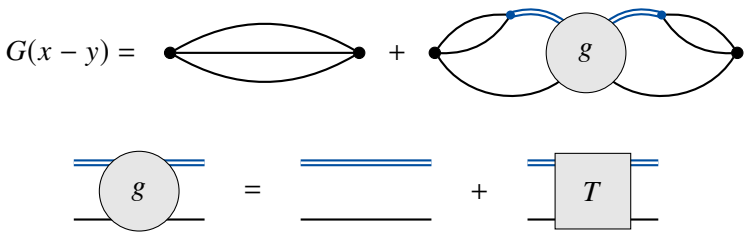

Figure 6.2: Two-point function, calculated in the effective field theory. The solid and double lines stand for the one-particle propagator and the full dimer propagator, respectively. The quantity T denotes the particle-dimer scattering amplitude.

where $G(k) = G_0(K) + G_1(k)$ and

$$\begin{aligned}
G_0(K) &= \frac{2}{3}\int \frac{d^3q_{1,\perp}}{(2\pi)^3 2w_v(q_1)}\,\frac{d^3q_{2,\perp}}{(2\pi)^3 2w_v(q_2)}\,\frac{1}{2w_v(K-q_1-q_2)} \\
&\times \frac{1}{\Big(w_v(q_1)+w_v(q_2)+w_v(K-q_1-q_2)-K_\parallel - i\varepsilon\Big)}\,, \\
G_1(K) &= 4\pi \sum_{\ell m,\ell' m'} \int \frac{d^3q_{1,\perp}}{(2\pi)^3 2w_v(q_1)}\,\frac{d^3q_{2,\perp}}{(2\pi)^3 2w_v(q_2)}\,\frac{d^3k_{1,\perp}}{(2\pi)^3 2w_v(k_1)}\,\frac{d^3k_{2,\perp}}{(2\pi)^3 2w_v(k_2)} \\
&\times \frac{\mathscr{Y}_{\ell' m'}(\tilde{\mathbf{q}}_1) f_{\ell'}((K-k_1)^2)}{2w_v(K-q_1-k_1)\Big(w_v(q_1)+w_v(k_1)+w_v(K-q_1-k_1)-K_\parallel - i\varepsilon\Big)} \\
&\times g_{\ell' m',\ell m}(k_1,k_2;K) \\
&\times \frac{f_\ell((K-k_2)^2)\left(\mathscr{Y}_{\ell m}(\tilde{\mathbf{q}}_2)\right)^*}{2w_v(K-q_2-k_2)\Big(w_v(q_2)+w_v(k_2)+w_v(K-q_2-k_2)-K_\parallel - i\varepsilon\Big)}\,.
\end{aligned} \tag{6.66}$$

Furthermore,

$$\begin{aligned}
g_{\ell' m',\ell m}(k_1,k_2;K) &= 2w_v(k_1)\delta^3(k_{1,\perp}-k_{2,\perp})\delta_{\ell\ell'}\delta_{mm'}S_\ell(K-k_1) \\
&+ S_{\ell'}(K-k_1)T_{\ell' m',\ell m}(k_1;k_2)S_\ell(K-k_2)\,.
\end{aligned} \tag{6.67}$$

Here, $\tilde{\mathbf{q}}_1$ and $\tilde{\mathbf{q}}_2$ are relative momenta of particle pairs, boosted to the CM frames of pertinent dimers. Graphically, the sum of all diagrams is displayed in Fig. 6.2.

The spectral representation of the particle-dimer scattering amplitude $T_{\ell' m',\ell m}(k_1,k_2)$ (again, in the infinite volume), can be written as follows

$$T_{\ell' m',\ell m}(k_1,k_2) = \sum_n \frac{\psi_n^{(\ell' m')}(k_1)\bar{\psi}_n^{(\ell m)}(k_2)}{P_{n,\parallel}-K_\parallel - i\varepsilon}\,. \tag{6.68}$$

Here, the index n labels the eigenvalues of the Hamiltonian in a given channel, and $\psi_n^{(\ell' m')}(k_1)$, $\bar{\psi}_n^{(\ell m)}(k_2)$ stand for the wave function and its conjugate, respectively.

In order to write down a finite-volume counterpart of the above equations, one has first to boost the integration momenta to the rest frame (because the discretization is done always in the rest frame). This can be achieved by using

$$\frac{d^3 q_{i,\perp}}{(2\pi)^3 2w_v(q_i)} = \frac{d^3\mathbf{q}_i}{(2\pi)^3 2w(\mathbf{k})}, \qquad \text{and similarly for } k_i \ , \tag{6.69}$$

while

$$\frac{d^3 K_\perp}{(2\pi)^3 2\sqrt{P_n^2 - K_\perp^2}} = \frac{d^3\mathbf{K}}{(2\pi)^3 2\sqrt{P_n^2 + \mathbf{K}^2}} \, . \tag{6.70}$$

Note also that one has adjusted the volume of the box so that $P_n^0 = \sqrt{M_K^2 + \mathbf{P}_n^2}$. Consequently, the four-momentum of the state $|n\rangle$ transforms similarly to the four-momentum of a single particle that is, generally, not the case for the multi-particle states in a finite volume.

Writing down Eq. (6.66) in a finite volume, using Eqs. (6.67) and (6.68), and carrying out the contour integration over $K_\parallel$, one arrives at

$$\begin{aligned}
G(x-y) \;=\; & 3^2 \sum_{\ell m, \ell' m', \ell'' m'', \ell''' m'''} \frac{4\pi}{L^{15}} \\
& \times \sum_{\mathbf{q}_1 \mathbf{q}_2 \mathbf{k}_1 \mathbf{k}_2} \frac{e^{-iP_{n,\parallel}(x-y)_\parallel - iK_\perp (x-y)_\perp} \sqrt{M_K^2 - K_\perp^2}}{2w(\mathbf{q}_1) 2w(\mathbf{q}_2) 2w(\mathbf{k}_1) 2w(\mathbf{k}_2) \sqrt{M_K^2 + \mathbf{K}^2}} \\
& \times \frac{\mathscr{Y}_{\ell' m'}(\tilde{\mathbf{q}}_1) f_{\ell'}((K-k_1)^2) S^L_{\ell' m', \ell''' m'''}(K-k_1) \psi_n^{(\ell''' m''')}(k_1)}{2w_v(K-q_1-k_1)\left(w_v(q_1) + w_v(k_1) + w_v(K-q_1-k_1) - P_{n,\parallel}\right)} \\
& \times \frac{\bar{\psi}^{(\ell'' m'')}(k_2) S^L_{\ell'' m'', \ell m}(K-k_2) f_\ell((K-k_2)^2) \left(\mathscr{Y}_{\ell m}(\tilde{\mathbf{q}}_2)\right)^*}{2w_v(K-q_2-k_2)\left(w_v(q_2) + w_v(k_2) + w_v(K-q_2-k_2) - P_{n,\parallel}\right)} + \ldots \, ,
\end{aligned} \tag{6.71}$$

where

$$K_\perp^0 = -\frac{\mathbf{v}^2}{v^0} P_{n,\parallel} + \frac{\mathbf{v}\mathbf{K}}{v^0}, \qquad \mathbf{K}_\perp = \mathbf{K} - \mathbf{v} P_{n,\parallel} \, . \tag{6.72}$$

In the equation above, we have explicitly singled out the contribution from a pole that emerges at $K_\parallel = P_{n,\parallel}$ with $P_n^2 = M_K^2$ for a given total three-momentum $\mathbf{K}$ (or, equivalently, for a fixed $\mathbf{K}_\perp$, as seen from Eq. (6.72)). The ellipsis stands for other single-pole contributions, $K_\parallel = P_{n,\parallel}$, emerging in the spectral decomposition of particle-dimer amplitude. The individual amplitudes feature many more singularities in this variable. However, we also take into account the fact that, in the rest frame, all these singularities cancel. This property should persist in moving frames as well, since the position of

the poles in our framework is Lorentz-invariant.

Now, continuing to the Euclidean space and comparing Eq. (6.64) with Eq. (6.71), one may finally read off the matrix element one is looking for:

$$\begin{aligned} |\langle 0|\mathscr{O}(0)|n\rangle| &= \frac{3\sqrt{4\pi}}{L^{3/2}}\left(\frac{M_K}{\sqrt{M_K^2+\mathbf{K}^2}}\right)^{1/2}\left|\sum_{\ell m,\ell' m'}\frac{1}{L^6}\sum_{\mathbf{qk}}^{\Lambda_v}\frac{\mathscr{Y}_{\ell' m'}(\tilde{\mathbf{q}})}{2w(\mathbf{q})2w(\mathbf{k})}\right. \\ &\times \left.\frac{f_{\ell'}((K-k)^2)S^L_{\ell' m',\ell m}(K-k)\psi_n^{(\ell m)}(k)}{2w_v(K-q-k)\left(w_v(q)+w_v(k)+w_v(K-q-k)-P_{n,\|}\right)}\right|. \end{aligned} \tag{6.73}$$

Here a cutoff on the momenta, which has been implicit in all previous expressions, is displayed. We also remind the reader that $|n\rangle$ denotes an eigenstate with the momentum $\mathbf{K}$ (no summation over $\mathbf{K}$). The components of the four-vector K^μ are:

$$K^\mu = \left(\frac{1}{v^0}(P_{n,\|}+\mathbf{vK}),\mathbf{K}\right). \tag{6.74}$$

Furthermore, since there is no more summation in $\mathbf{K}$, we may fix the vector v^μ along K^μ that leads to $K^\mu_\perp = 0$. Finally, in a finite volume, $|n\rangle$ is a basis vector of some irreducible representation Γ of some little group, or of an octahedral group (in case of $\mathbf{K}=0$). Particular values of ℓ,ℓ' contribute to this sum, if and only if Γ is contained in the pertinent irreducible representation of the rotation group.

6.3.3 Faddeev Equation for the Wave Function

The wave function, which was introduced in Eq. (6.68), obeys the homogeneous Faddeev equation both in the infinite and in a finite volume, which can be straightforwardly obtained by substituting the ansatz defined by Eq. (6.68) into the equation for the particle-dimer scattering amplitude (6.42) and identifying pole terms on the both sides of this equation. In a finite volume, this equation takes the form

$$\begin{aligned} \psi_n^{(\ell' m')}(p) &= \sum_{\ell m,\ell'' m''}\frac{1}{L^3}\sum_{\mathbf{k}}^{\Lambda_v}\frac{1}{2w(\mathbf{k})} \\ &\times Z_{\ell' m',\ell'' m''}(p,k)S^L_{\ell'' m'',\ell m}(K-k)\psi_n^{(\ell m)}(k)\,. \end{aligned} \tag{6.75}$$

The infinite-volume analog of the above equation can be written as

$$\psi_n^{(\ell' m')}(p) = \sum_{\ell m}\int^{\Lambda_v}\frac{d^3k_\perp}{(2\pi)^3 2w_v(k)}Z_{\ell' m',\ell m}(p,k)S_\ell(K-k)\psi_n^{(\ell m)}(k)\,. \tag{6.76}$$

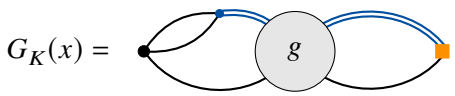

Figure 6.3: Contributions to the two-point function $G_K(x)$. The single and double lines denote the particle propagator and the full dimer propagator, respectively. The quantity T stands for the particle-dimer scattering amplitude. The difference between $G_K(x)$ and the two-point function $G(x-y)$, shown in Fig. 6.2, boils down to the different sink operators used (these correspond to the utmost right vertices in the pertinent diagrams).

Since these are inhomogeneous equations, the normalization of the wave function should be fixed independently. Using the standard technique (see, e.g., [242, 243]), in a finite volume one obtains

$$\begin{aligned} 1 &= \sum_{\ell' m', \ell m} \frac{1}{L^3} \sum_{\mathbf{p}}^{\Lambda_v} \frac{1}{2w(\mathbf{p})} \bar{\psi}_n^{(\ell' m')}(p) \left(\frac{d}{dK_\parallel} S^L_{\ell' m', \ell m}(K-p) \right) \psi_n^{(\ell m)}(p) \Big|_{K_\parallel = P_{n,\parallel}} \\ &+ \sum_{\ell m, \ell' m', \ell'' m'', \ell''' m'''} \frac{1}{L^6} \sum_{\mathbf{p},\mathbf{q}}^{\Lambda_v} \frac{1}{2w(\mathbf{p}) 2w(\mathbf{q})} \bar{\psi}_n^{(\ell' m')}(p) S^L_{\ell' m', \ell''' m'''}(K-p) \\ &\times \left(\frac{d}{dK_\parallel} Z_{\ell''' m''', \ell'' m''}(p,q) \right) S^L_{\ell'' m'', \ell m}(K-q) \psi_n^{(\ell m)}(q) \Big|_{K_\parallel = P_{n,\parallel}} . \end{aligned} \tag{6.77}$$

The infinite-volume counterpart of the above equation is

$$\begin{aligned} 1 &= \sum_{\ell m} \int^{\Lambda_v} \frac{d^3 p_\perp}{(2\pi)^3 2 w_v(p)} \bar{\psi}_n^{(\ell m)}(p) \left(\frac{d}{dK_\parallel} S_\ell(K-p) \right) \psi_n^{(\ell m)}(p) \Big|_{K_\parallel = P_{n,\parallel}} \\ &+ \sum_{\ell' m', \ell m} \int^{\Lambda_v} \frac{d^3 p_\perp}{(2\pi)^3 2 w_v(p)} \frac{d^3 q_\perp}{(2\pi)^3 2 w_v(q)} \bar{\psi}_n^{(\ell' m')}(p) S_{\ell'}(K-p) \\ &\times \left(\frac{d}{dK_\parallel} Z_{\ell' m', \ell m}(p,q) \right) S_\ell(K-q) \psi_n^{(\ell m)}(q) \Big|_{K_\parallel = P_{n,\parallel}} . \end{aligned} \tag{6.78}$$

6.3.4 The Decay Matrix Element

Let us now consider the two-point function $G_K(x) = \langle 0 | T \mathscr{O}(x) J_K^\dagger(0) | 0 \rangle$, where $J_K^\dagger(y) = \dfrac{\delta \mathscr{L}_G}{\delta K(y)}$ is a source operator for the field $K(y)$.

Applying the Feynman rules of the NREFT, in the infinite volume, the two-point function, shown in Fig. 6.3, can be expressed as

$$G_K(x) = 3 \int \frac{dK_\parallel}{2\pi i} \frac{d^3 K_\perp}{(2\pi)^3} e^{-iK_\parallel x_\parallel - iK_\perp x_\perp} G_K(K), \tag{6.79}$$

where

$$G_K(K) = 4\pi \sum_{\ell m,\ell' m'} \frac{(-1)^\ell}{\sqrt{2\ell+1}} \int \frac{d^3q_{1,\perp}}{(2\pi)^3 2w_v(q_1)} \frac{d^3k_{1,\perp}}{(2\pi)^3 2w_v(k_1)} \frac{d^3k_{2,\perp}}{(2\pi)^3 2w_v(k_2)}$$
$$\times \frac{f_{\ell'}((K-k_1)^2)\mathscr{Y}_{\ell' m'}(\tilde{\mathbf{k}}_1) g_{\ell' m',\ell m}(k_1,k_2;K)\mathscr{Y}_{\ell,-m}(\underline{\mathbf{k}}_2) G_\ell((K-k_2)^2)}{2w_v(K-q_1-k_1)\left(w_v(q_1)+w_v(k_1)+w_v(K-q_1-k_1)-K_\parallel - i\varepsilon\right)}, \tag{6.80}$$

with G_ℓ defined by Eq. (6.56). Again, the corresponding expression in the finite-volume is obtained by boosting the integration momenta into the rest frame of the box, according to Eq. (6.69). Using the spectral decomposition of the particle-dimer amplitude and carrying out the $K_\parallel$ integration:

$$G_K(x) = 3 \sum_{\ell m,\ell' m',\ell'' m'',\ell''' m'''} \frac{4\pi}{L^{12}} \frac{(-1)^\ell}{\sqrt{2\ell+1}} \sum_{\mathbf{q}_1\mathbf{k}_1\mathbf{k}_2} \frac{e^{-iP_{n,\parallel}x_\parallel} M_K}{2w(\mathbf{q}_1)2w(\mathbf{k}_1)2w(\mathbf{k}_2)\sqrt{M_K^2+\mathbf{K}^2}}$$
$$\times \frac{f_{\ell'}((K-k_1)^2)\mathscr{Y}_{\ell' m'}(\tilde{\mathbf{k}}_1) S^L_{\ell' m',\ell''' m'''}(K-k_1)\psi_n^{(\ell''' m''')}(k_1)}{2w_v(K-q_1-k_1)\left(w_v(q_1)+w_v(k_1)+w_v(K-q_1-k_1)-P_{n,\parallel}\right)}$$
$$\times \bar{\psi}_n^{(\ell'' m'')}(k_2) S^L_{\ell'' m'',\ell m}(K-k_2)\mathscr{Y}_{\ell,-m}(\underline{\mathbf{k}}_2) G_\ell((K-k_2)^2) + \dots . \tag{6.81}$$

Similar to Eq. (6.71), we only display the contribution of the pole that emerges at $K_\parallel = P_{n,\parallel}$ with $P_n^2 = M_K^2$ for a given three-momentum $\mathbf{K}$.

On the other hand, by inserting a full set of states, we obtain

$$G_K(x) = \sum_n e^{-iP_{n,\parallel}x_\parallel - iP_{n,\perp}x_\perp} \langle 0|\mathscr{O}(0)|n\rangle\langle n|J_K^\dagger(0)|0\rangle \ . \tag{6.82}$$

Comparing this expression for G_K with Eq. (6.81) and using the form of the matrix element in Eq. (6.73), we can read off

$$L^{3/2}\langle n|J_K^\dagger(0)|0\rangle = \pm\sqrt{4\pi}\left(\frac{M_K}{\sqrt{M_K^2+\mathbf{K}^2}}\right)^{1/2} \sum_{\ell m,\ell' m'} \frac{(-1)^\ell}{\sqrt{2\ell+1}}$$
$$\times \frac{1}{L^3}\sum_{\mathbf{k}}^{\Lambda_v} \frac{1}{2w(\mathbf{k})} \bar{\psi}_n^{(\ell' m')}(k) S^L_{\ell' m',\ell m}(K-k)\mathscr{Y}_{\ell,-m}(\underline{\mathbf{k}}) G_\ell((K-k)^2) \, . \tag{6.83}$$

Note that, due to the fact that the finite volume decay matrix element is real-valued, its phase is merely given by an undetermined sign. The choice of this sign is a delicate issue and is discussed in detail, say, in Ref. [191]. In brief, as argued in that paper, the phase of the eigenvector $|n\rangle$ is arbitrary, and one can always choose it in a way that the sign of the (real-valued) matrix element $\langle 0|\mathscr{O}(0)|n\rangle$ is positive. In the following we shall stick to this convention, which amounts to choosing "+" sign in the above

$$\langle \pi(\mathbf{k}_1)\pi(\mathbf{k}_2)\pi(\mathbf{k}_3); \text{out}|J_K^\dagger(0)|0\rangle =$$

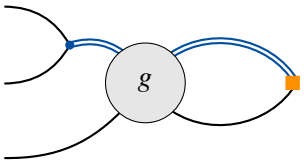

Figure 6.4: Contributions to the infinite volume decay matrix element. The single and double lines denote the particle propagator and the full dimer propagator, respectively.

equation.[9]

In the infinite volume the decay matrix element is given by, see Fig. 6.4:

$$\begin{aligned}
&\langle \pi(\mathbf{k}_1)\pi(\mathbf{k}_2)\pi(\mathbf{k}_3); \text{out}|J_K^\dagger(0)|0\rangle \\
&= 4\pi \sum_{\ell m,\ell' m'} \frac{(-1)^\ell}{\sqrt{2\ell+1}} \sum_{\alpha=1}^{3} \int \frac{d^3 k_\perp}{(2\pi)^3 2w_\nu(k)} \\
&\times f_{\ell'}((K-k_\alpha)^2)\mathscr{Y}_{\ell' m'}(\tilde{\mathbf{k}}_\alpha) g_{\ell' m',\ell m}(k_\alpha, k; K)\mathscr{Y}_{\ell,-m}(\underline{\mathbf{k}}) G_\ell((K-k)^2)\,.
\end{aligned} \tag{6.84}$$

Indeed this quantity is Lorentz invariant. The transformation property of $g_{\ell' m',\ell m}$ exactly cancels those of the spherical functions entering the expression.

6.3.5 The Three-Particle LL Formula

At a given order $O(\epsilon^{2n})$ in the NREFT power counting, where ϵ is a generic small parameter and $p_\perp = O(\epsilon)$, only a finite number of effective decay couplings $G_i^{(\ell)}$ have to be taken into account. Noting that $\mathscr{Y}_{\ell,-m}(\underline{\mathbf{k}}) = O(\epsilon^\ell)$ and $\Delta_T = O(\epsilon^2)$, for a given angular momentum ℓ (even only):

$$G_\ell(\Delta_T) = G_0^{(\ell)} + G_1^{(\ell)}\Delta_T + \cdots + G_{n-\ell/2}^{(\ell)}\Delta_T^{n-\ell/2} \tag{6.85}$$

Therefore, at order $O(\epsilon^{2n})$, there are $N = (n+1)(n+2)/2$ undetermined[10] couplings $G_i^{(\ell)}$.

Let x_α denote the finite volume decay matrix element extracted in some lattice setup α, with total momentum $\mathbf{K} = \mathbf{K}_\alpha$ and box length $L = L_\alpha$. Expanding the low-energy polynomial $G_\ell((K-k)^2)$, x_α

[9] In case of three weakly interacting particles in the final state, such a choice is a natural one, since the matrix element $\langle 0|\mathscr{O}(0)|n\rangle$, calculated in perturbation theory, starts with $3!\langle 0|\phi(0)|k\rangle^3$, where $|k\rangle$ denotes a state containing one free particle which is moving with a momentum k. Furthermore, the sign of the one-particle matrix element does not depend on L and k. Thus, if the perturbative corrections are small and do not exceed the leading term, the set of matrix elements $\langle 0|\mathscr{O}(0)|n\rangle$, corresponding to the different L, n and the total three-momentum $\mathbf{K}$, will have a positive relative sign. Note also that in the case of strong final-state interactions (i.e., when the two-particle resonances are present), the above argument is not *a priori* applicable and the question requires further scrutiny. We choose, however, not to elaborate further on this issue.

[10] Symmetry arguments could lower the number of independent couplings

can be written as a linear combination of the effective couplings:

$$x_\alpha = L_\alpha^{3/2}\langle n|J_K^\dagger(0)|0\rangle_\alpha = \sum_{\ell=0}^{2n}\sum_{i=0}^{n-\ell/2} a_i^{(\ell)}(K_\alpha, L_\alpha)G_i^{(\ell)} \equiv \sum_{I=1}^{N} a_{\alpha I}\, G_I\,, \tag{6.86}$$

where the amplitudes $a_i^{(\ell)}(K_\alpha, L_\alpha)$ can be read off from Eq. (6.83). A similar expression can be found for the infinite volume decay matrix element:

$$\langle\pi(\mathbf{k}_1)\pi(\mathbf{k}_2)\pi(\mathbf{k}_3);\text{out}|J_K^\dagger(0)|0\rangle = \sum_{\ell=0}^{2n}\sum_{i=0}^{n-\ell/2} A_i^{(\ell)}(K)G_i^{(\ell)} \equiv \sum_{I=1}^{N} A_I(K)\, G_I\,, \tag{6.87}$$

where $A_i^{(\ell)}(K)$ can be read off from Eq. (6.84) and K is the total momentum of the three-particle system. Measuring N finite volume decay matrix elements in different lattice setups and using Eq. (6.86), interpreted as a matrix equation, we can eliminate the dependence on the coupling constants G_i^ℓ of the infinite volume matrix element:

$$\langle\pi(\mathbf{k}_1)\pi(\mathbf{k}_2)\pi(\mathbf{k}_3);\text{out}|J_K^\dagger(0)|0\rangle = \sum_{\alpha=1}^{N}(\Phi_3)_\alpha \cdot L_\alpha^{3/2}|\langle n|J_K^\dagger(0)|0\rangle|_\alpha\,, \tag{6.88}$$

where the LL-factor $(\Phi_3)_\alpha$ is given by

$$(\Phi_3)_\alpha = \sum_{I=1}^{N} A_I(K)\,(a^{-1})_{I\alpha} \tag{6.89}$$

and a^{-1} is the inverse of the matrix

$$a = \begin{pmatrix} a_0^{(0)}(K_1,L_1) & a_1^{(0)}(K_1,L_1) & \dots & a_n^{(0)}(K_1,L_1) & \dots & a_0^{(2n)}(K_1,L_1) \\ \vdots & & \ddots & & & \vdots \\ a_0^{(0)}(K_N,L_N) & a_1^{(0)}(K_N,L_N) & \dots & a_n^{(0)}(K_N,L_N) & \dots & a_0^{(2n)}(K_N,L_N) \end{pmatrix}, \tag{6.90}$$

while

$$A_I(K) = \begin{pmatrix} A_0^{(0)}(K) & A_1^{(0)}(K) & \dots & A_n^{(0)}(K) & \dots & A_0^{(2n)}(K) \end{pmatrix}. \tag{6.91}$$

In the equations above it is assumed that the box sizes L_α were adjusted, such that $K^0 = \sqrt{M_K^2 + \mathbf{K}_\alpha^2}$, for each α.

The Eqs. (6.88)-(6.91) display our finial result, resembling the LL equation for the three-particle sector. As in the two-particle sector, the LL factors merely depend on the short-range pion interactions. Fixing the parameters of the two- and three-particle scattering sector by a fit to the corresponding energy-spectra by using the quantization conditions fully determines the amplitudes $A_i^{(\ell)}(K)$ and $a_i^{(\ell)}(K, L)$. One then extracts the finite volume decay matrix element in various different moving frames. Here one has to ensure that the energy of the three-particle eigenstate coincides with an energy level of the moving kaon. This is done by choosing the box length L appropriately. One can finally use Eqs. (6.88)-(6.91) to obtain the infinite volume decay amplitude. Note also that the above

expressions are very similar in form to the three-particle LL equation derived in the RFT formalism (see, e.g., Eq. (2.43) in Ref. [191]). For example, the eigenvector v in that paper can be related to the particle-dimer wave function $\psi_n^{(\ell m)}$ from our paper and so on. We did not attempt, however, to carry out a detailed comparison with Ref. [191].

Note that Eq. (6.88) is manifestly relativistic-invariant. The infinite volume decay amplitude is a linear combination of invariant amplitudes $A_i^{(\ell)}(K)$.

6.4 Conclusions

i) In the present paper we have derived a manifestly relativistic-invariant counterpart of the LL formula in the three-particle sector, describing the decay of a spinless particle into three likewise spinless, identical particles. Our result represents a generalization of the formula derived in Ref. [1], which is reproduced at the leading order and at a vanishing total three-momentum. The importance of having an explicitly invariant framework lies, first and foremost, in the possibility to use the data from different moving frames for performing a global fit. This possibility is extremely valuable, especially beyond the leading order.

ii) A major technical modification in this paper consisted in the inclusion of all partial waves in the pair interactions as well as in the particle-dimer interactions. This renders the proof of the Lorentz-invariance a highly non-trivial issue, due to the necessity to take into account the Thomas-Wigner rotation. A solution of this problem has been found in the present paper.

iii) Another technical complication was related to the necessity of the diagonalization of the quantization condition in various irreps of the octahedral group and various subgroups thereof. In this paper we explicitly write down the quantization condition, projected onto different irreps, in the presence of an arbitrary number of partial waves.

iv) The LL factors, relating the infinite volume decay matrix elements to its counterparts in various different moving frames, depend on the local two- and three-particle interactions that emerge due to the rescattering in the final state. The corresponding parameters in the three-particle sector can be fixed by a fit to the energy spectrum. Furthermore, as the quantization condition, derived in the present paper, is valid in an arbitrary moving frame, the energy spectra of the same lattice setups can be used, in which the finite volume decay amplitudes were determined.

v) The framework can be further generalized in a number of ways. Namely, in order to describe decays of particles with an arbitrary spin, the LL formula can be straightforwardly modified by an appropriate choice of source operators for the decaying particle and the three-particle final states, replacing $J_K^\dagger$ and $\mathcal{O}$ respectively. Furthermore, one may consider the case of the non-identical particles in the final state and include fermions (note that three pions carrying isospin have been already considered in Ref. [191]). It can be expected that all these actions are pretty straightforward and can be performed by using the same methods as in the present article.

CHAPTER 7

Conclusion and Outlook

Unraveling the complex nature of the strong force requires examining the spectrum of hadrons and their interactions. However, the non-perturbative aspects of quantum chromodynamics at the hadronic scale prevent the application of standard, i.e. perturbative, quantum field theoretic techniques. Nevertheless, lattice qunatum chromodynamics provides a method to study multi-hadron dynamics in the low-energy regime. Information about hadron interactions can be inferred from the finite-volume energy spectra, extracted from lattice simulations. One of the most remarkable features of the strong interactions is the intriguing abundance of resonances and bound states. However, especially in the presence of such hadronic resonances and bound states, the extraction of scattering and resonance properties is impeded, as simple perturbative calculations of the finite-volume energy spectra exhibit a poor convergence. In the two-body sector, the Lüscher formalism provides a framework that allows to map the finite-volume energy spectra to S-matrix elements, even in the case of resonant scattering. Applications of this framework and its various generalizations is a well-established praxis for hadron spectroscopy in the two-body sector nowadays.

In recent years the focus of lattice studies on multi-hadron systems has gradually shifted form two to three particles. This development is accompanied by a rapid progression in the generalization of the Lüscher formalism to the three-particle sector, which is essential in order to determine three-body observables from the finite-volume energy spectra. Utilizing the framework of non-relativistic effective field theories, the purpose of this thesis is to push the boundaries of the three-body finite-volume formalism further.

In that context, the formulation of a relativistic-invariant three-particle quantization condition, in the sense that it is valid in different moving frames at the same time, is of particular importance. Primarily, when determining scattering properties from finite-volume spectra, such a relativistic-invariant form of the quantization condition allows to avoid computational expensive simulations in big volumes. The number of data points used in the fitting procedure can be kept constant by including data of different total three-body momentum instead. Furthermore, the stringent constraints that are imposed by relativistic invariance effectively lower the number of couplings that are needed to describe the process under consideration. Within the non-relativistic effective field theory approach a generalization to a relativistic-invariant form of the three-particle quantization condition represents a highly non-trivial task due to the inherent explicit non-covariance of the framework. Thus, an important objective of the research project, that has been summarized in this thesis, is the implementation of a relativistic-covariant version of the non-relativistic effective field theory framework, enabling practical

applications of the non-relativistic effective field theory approach for the analysis of lattice QCD data in the three-body sector.

Furthermore, despite the considerable progress in the general treatment of the three-particle systems in a finite-volume, a framework that establishes a relation between finite-volume decay matrix elements and infinite-volume decay amplitudes was not available, such that studies of three-body decays from lattice QCD remained inaccessible. Another aspect of the research project was to derive such an analog of the Lellouch-Lüscher equation in the three-particle sector.

A first step towards the general description of three-particle decays in a finite-volume was presented in Chapter 4, where a three-body analog of the Lellouch-Lüscher formalism was derived in the rest frame at the leading order in the covariant form of non-relativistic effective field theory. At this order, the infinite-volume decay amplitude only depends on a single coupling that describes the decay of the initial particle, which can be eliminated by substituting the expression for the finite-volume decay matrix element, exhibiting the same dependence on that coupling. The resulting linear relation between these two quantities only depends on the rescattering of the particles in the final state, which is purely described by parameters that can be fixed by measurements of the two- and three-body spectra. While an explicitly Lorentz-invariant framework is favorable for the extraction of three-body decay amplitudes from lattice QCD in general, working at the leading order where the effective Lagrangian does not contain any derivative interactions, all issues related to the explicit non-covariance of the framework are irrelevant. The derivation in this chapter thus serves as a proof of concept.

The relativistic covariance of the non-relativistic effective field theory approach is addressed in Chapter 5. The explicit relativistic non-covariance of the infinite-volume particle-dimer scattering amplitude in the original framework can be primarily traced back to the three-particle propagators lack of invariance. Thus, a modified formalism has been developed in which the quantization axis in the non-relativistic effective Lagrangian is chosen according to the velocity of three-body system. This modification renders the three-particle propagator Lorentz-invariant and was used in order to derive a manifestly relativistic invariant three-particle quantization condition.

In contrast to the RFT approach, where invariance was achieved by explicitly altering the form of the three-particle propagator, the approach developed here is arguably advantageous: Due to the pole structure of the low-energy polynomial, representing the antiparticle contribution, that is added to the three-particle propagator in the RFT approach, the cutoff on the spectator-momenta can not be taken arbitrarily high, as this would lead to a violation of unitarity in the infinite- and emergence of spurious poles in the finite volume. In contrast, the antipartical degrees of freedom are integrated out systematically in the non-relativistic effective field theory approach, such that all singularities related to these are removed explicitly and only affect the actual values of the couplings entering the effective Lagrangian. Therefore, the cutoff function in the non-relativistic effective field theory approach only acts as an ultraviolet regulator.

The relativistic invariance of the quantization condition has been tested numerically in a toy model at the leading order, restricted to S-wave interactions, by elaborating the finite-volume energy spectra in various moving frames. As the implementation of a fitting routine possibly requires only little effort, the framework developed here can be applied for the global analysis of three-particle lattice simulations at different total three-body momenta in the foreseeable future.

The advances presented in Chapter 6 are twofold. First of all, the restriction to S-wave interactions in the derivation of the relativistic invariant quantization condition outlined in Chapter 5 was lifted by the

inclusion of dimer fields with arbitrary angular momentum. Despite the complicated transformation behavior of the interactions that arise due to the generalization to higher partial waves, explicit Lorentz-covariance of the particle-dimer scattering amplitude could be proven. Taking into account all partial waves, the framework fully describes a system of three identical spinless scalar bosons in a finite volume. Moreover, the quantization condition can be trivially adapted for the description of pseudoscalar mesons by taking into account their internal parity when projecting onto the several irreducible representations of the cubic group and its stabilizers in case of non-vanishing total three-body momentum. Therefore, the formalism established here, serves as a tool for the analysis of lattice QCD data of, e.g., the three-pion and three-kaon systems at maximal isospin.

Secondly, the leading order expression for the analog of the Lellouch-Lüscher formula derived in Chapter 4 was generalized to higher orders. No restrictions on the possible form of the Lagrangian, describing the initial decay of a scalar spinless boson into three identical likewise spinless bosons, was assumed. Most importantly, the derivation utilizes the relativistic-invariant formulation of the non-relativistic field theory approach. This does not only reduce the number of effective couplings needed to describe the initial decay, such that less finite-volume decay matrix elements have to be measured in the lattice simulation, it also enables to combine matrix elements that have been determined for different total three-body momentum.

With rising computational power and improved algorithms, simulations of three-body decays in lattice QCD are in prospect. Although a systematic strategy for the extraction of three-body decay amplitudes from lattice QCD has been established in this work, due to the restriction to identical particles, the framework is not yet applicable to real physical decays. Additional steps are required. Serving as test for CP-violation in the standard model, an obvious candidate for a lattice study of decays in the three-body sector is provided by the electroweak process of the positively charged kaon into three pions. In order to describe this decay that appears in the two channels, $K^+ \to \pi^+\pi^+\pi^-$ and $K^+ \to \pi^0\pi^0\pi^+$, the different isospin contributions for the system of three pions have to be included in the rescattering process. Due to the multi-channeled nature of the decay, even at the leading order where derivative couplings are absent, the Lellouch-Lüscher factor is not a solely described by a single number. This problem is covered in a current project [7].

Besides the progress in the non-relativistic effective field theory treatment of the three-particle sector that has been reported in this thesis, the research project has also contributed perturbative calculations of the energy shifts for the three-pion ground in the isopsin $I = 1$ channel [4], as well as the three-nucleon ground state [6], up-to-and-including effects of the order $O(L^{-6})$. The resulting expressions enable a convenient way to extract the three-body threshold amplitude, by performing a fit to the measured ground state energy levels. However, the applicability of perturbation theory for three-nucleon scattering is problematic. As expected, the perturbative expansion exhibits a poor convergence for physical values of the S-wave nucleon-nucleon scattering lengths, due to their unnatural large size. As discussed in the literature [244–247], it is possible that, in nature, the quark masses are close to a critical values where the scattering lengths diverge, corresponding to an infrared limit cycle of QCD in the three-nucleon sector [248, 249]. On the other hand, the perturbative calculation of the three-nucleon energy shift might be still valuable for the analysis of lattice simulations performed away from the physical quark masses.

Furthermore, the influence of unphysical singularities in the two-body amplitude that can emerge when using the effective range expansion to the three-particle energy spectrum has been investigated in [5]. Including effective-range effects, the two-particle scattering amplitude may develop a spurious

pole with negative residue, as described in 3.3.4. This unphysical singularity usually lies at large negative energies, well below the range of applicability of the effective field theory, so that such an inconsistent parametrization can be accepted when describing the low-energy two-body sector. However, in the Faddeev equation for the three-body amplitude, the center-of-mass energy of the two-body amplitude can take large negative values, such that an unphysical two-body singularity affects three-body unitarity even in the low-energy regime. Using a toy model, in [5] it was observed that, in the presence of such a spurious pole, the three-body energy spectrum exhibits an unphysical behavior with merging and disappearing energy levels. Furthermore, it was shown that a procedure to remove these spurious poles without imposing any restrictions on the spectator momentum cutoff, proposed in [183], can be adapted to the finite-volume calculations.

The research project has contributed to the further development of the three-body finite-volume formalism. These advances are not only restricted to the non-relativistic effective field theory approach. Problems that arise due to the modifications in order to render the RFT formulation relativistic invariant may be evaded by adapting the formalism established here, e.g. by making use of a covariant form of time-ordered perturbation theory. Furthermore, an three-body analogue of the Lellouch-Lüscher formula has been derived for the first time.

APPENDIX A

Appendix

A.1 Pinched Energy Levels in the Non-Relativistic Limit

This appendix discusses the role of "pinched" energy levels in the non-relativistic limit. As can be read off from Eq. (3.41), the Lüscher Zeta-function has poles at those energies, that correspond to the energy levels in the non-interacting case. Thus, in the vicinity of a "pinched" energy-level that lies in the narrow region in between two consecutive non-interacting energy levels, that are non-degenerate due to relativistic effects, the quantization condition for $\ell = 0$, Eq. (2.62), can be approximated by:

$$A(s;\mathbf{P}) = \cot\delta_0(s) - \frac{1}{\pi^{3/2}\gamma\eta} Z_{00}^{\mathbf{d}}(1,s) = c - \frac{r_1}{E_1' - E} - \frac{r_2}{E_2' - E} = 0\,, \tag{A.1}$$

where c is a constant and E_i' denote the free energy levels with $r_i > 0$ the corresponding residue of the Lüscher Zeta-function (multiplied by the prefactor). The non-interacting energies obey

$$E_i' = \sqrt{M^2 + \left(\frac{2\pi}{L}\mathbf{n}_i\right)^2} + \sqrt{M^2 + \left(\frac{2\pi}{L}\mathbf{m}_i\right)^2}\,, \tag{A.2}$$

with $\mathbf{n}_i \in \mathbb{Z}^3$, $\mathbf{m}_i = \mathbf{d} - \mathbf{n}_i$ and $\mathbf{n}_1^2 + \mathbf{m}_1^2 = \mathbf{n}_2^2 + \mathbf{m}_2^2$, such that

$$E_i' = E_{\text{nr}} - \delta E_i'\,, \tag{A.3}$$

where

$$E_{\text{nr}} = 2M - \left(\frac{2\pi}{L}\right)^2 \frac{1}{2M}\left(\mathbf{n}_i^2 + \mathbf{m}_i^2\right)\,, \tag{A.4}$$

corresponds to the (degenerate) non-interacting level in the non-relativistic case. The solutions to Eq. (A.1) are given by

$$E_{1/2} = E_{\text{nr}} - \frac{1}{2}(\delta E_1' + \delta E_2') - \frac{1}{2c}(r_1 + r_2) \pm \frac{1}{2c}\sqrt{4r_1r_2 + (r_1 - r_2 + c(\delta E_1' - \delta E_2'))^2}\,. \tag{A.5}$$

Taking the non-relativistic limit for which $\delta E_i' \to 0$:

$$E_1 \to E_{\rm nr}\,, \quad E_2 \to E_{\rm nr} - \frac{1}{2c}(r_1 + r_2)\,. \tag{A.6}$$

Obviously the solution at $E_1 = E_{\rm nr}$ does not correspond to a physical result.

In order to show that this is indeed the case, the two-body amplitude in the finite volume can be considered. For pure S-wave interactions it can be written as, see Eq. (3.40):

$$t(s;\mathbf{P}) = \frac{16\pi\sqrt{s}}{q^*}\, A(s;\mathbf{P})^{-1}\,. \tag{A.7}$$

The residues[1] at the energies $E_{1/2}$ that solve the quantization condition $A(s;\mathbf{P})$ are given by:

$$\text{res}_{1/2} = \frac{16\pi\sqrt{s_{1/2}}}{q^*_{1/2}}\,\frac{1}{2c^2}\left((r_1+r_2) \mp \frac{(r_1+r_2)^2 + c(r_1-r_2)(\delta E_1' - \delta E_2')}{\sqrt{4r_1r_2 + (r_1 - r_2 + c(\delta E_1' - \delta E_2'))^2}}\right), \tag{A.8}$$

where $s_i = E_i^2 - \mathbf{P}^2$ and $q_i^* = \sqrt{s_i/4 - M^2}$. It can be seen that in the non relativistic limit

$$\text{res}_1 \to 0\,, \quad \text{res}_2 \to \frac{16\pi\sqrt{s_1}}{q_1^*}\,\frac{r_1+r_2}{c^2}\,. \tag{A.9}$$

Thus, while the energy level at E_2 has a well behaved non-relativistic limit, the energy level that is pinched between the two consecutive non-interacting levels will disappear from the spectrum.

A.2 Two-Body Amplitude in a Finite Volume

This appendix proves the v^μ-independence of the finite volume two-body amplitude by providing an explicit derivation of Eq. (5.84). Calculating the two-particle scattering amplitude in a finite volume amounts to replacing the loop integral I defined in Eq. (5.7) by its finite volume counterpart I_L.

$$I_L = \frac{1}{L^3}\sum_{\mathbf{k}} \int \frac{dk_0}{2\pi i}\,\frac{1}{2w_v(k)(w_v(k) - vk - i\varepsilon)}\,\frac{1}{2w_v(P-k)(w_v(P-k) - v(P-k) - i\varepsilon)}\,. \tag{A.10}$$

At this stage, one uses Eq. (5.8). Adding and subtracting the real part of the same quantity, calculated in the infinite volume, one gets:

$$\begin{aligned} I_L &= \text{Re}(I(s)) + \left[\frac{1}{L^3}\sum_{\mathbf{k}} - \mathcal{P}\int \frac{d^3\mathbf{k}}{(2\pi)^3}\right] \\ &\times \int \frac{dk_0}{2\pi i}\left\{\frac{1}{(m^2 - k^2 - i\varepsilon)(m^2 - (P-k)^2 - i\varepsilon)} + \Delta\right\}. \end{aligned} \tag{A.11}$$

[1] Here the convention of the residue follows from $t(s;\mathbf{P}) = \text{res}_i/(E_i - E) + \text{regular}$.

Here, the quantity $I(s)$ and the real part thereof are given by Eqs. (5.10)-(5.12). Furthermore, the quantity Δ is equal to

$$\begin{aligned}\Delta &= \frac{1}{m^2-k^2-i\varepsilon}\,\frac{1}{2w_v(P-k)(w_v(P-k)+v(P-k)-i\varepsilon)} \\ &+ \frac{1}{m^2-(P-k)^2-i\varepsilon}\,\frac{1}{2w_v(k)(w_v(k)+vk-i\varepsilon)} \\ &+ \frac{1}{2w_v(k)(w_v(k)+vk-i\varepsilon)}\,\frac{1}{2w_v(P-k)(w_v(P-k)+v(P-k)-i\varepsilon)}\,. \end{aligned} \tag{A.12}$$

The energy denominators in the above expression can be expanded, according to Eq. (5.9). The last term turns then into a low-energy polynomial. The first two terms contain a single low-energy pole in k^0 each, at $k^0=\sqrt{m^2+\mathbf{k}^2}$ and $k^0=P^0-\sqrt{m^2+(\mathbf{P}-\mathbf{k})^2}$, respectively. Integrating over k^0 leads to a low-energy polynomial again[2]. In the infinite volume, such low-energy polynomials do not contribute to the integrals over spatial components of momenta in dimensional regularization. In a finite volume, the sum minus integral over spatial components of momenta gives a contribution that is exponentially suppressed in the box size L. Neglecting these exponential terms, it is seen that the contribution from Δ vanishes completely, and one can finally write:

$$I_L = J(s)+\left[\frac{1}{L^3}\sum_{\mathbf{k}}-\mathcal{P}\int\frac{d^3\mathbf{k}}{(2\pi)^3}\right]\int\frac{dk_0}{2\pi i}\,\frac{1}{(m^2-k^2-i\varepsilon)(m^2-(P-k)^2-i\varepsilon)}\,. \tag{A.13}$$

The explicit v^μ-dependence disappears already at this stage. The subsequent steps are pretty standard. Evaluating the integral over k^0 gives:

$$\begin{aligned} I_L &= J(s)+\left[\frac{1}{L^3}\sum_{\mathbf{k}}-\mathcal{P}\int\frac{d^3k}{(2\pi)^3}\right]\frac{1}{2w(\mathbf{k})w(\mathbf{P}-\mathbf{k})}\,\frac{w(\mathbf{k})+w(\mathbf{P}-\mathbf{k})}{(w(\mathbf{k})+w(\mathbf{P}-\mathbf{k}))^2-P_0^2} \\ &= J(s)+\left[\frac{1}{L^3}\sum_{\mathbf{k}}-\mathcal{P}\int\frac{d^3k}{(2\pi)^3}\right]\frac{1}{4w(\mathbf{k})w(\mathbf{P}-\mathbf{k})(w(\mathbf{k})+w(\mathbf{P}-\mathbf{k})-P_0)} \\ &= J(s)+\frac{1}{4\pi^{3/2}L\gamma\sqrt{s}}Z_{00}^{\mathbf{d}}(1;q_0^2)\,. \end{aligned} \tag{A.14}$$

The integrands in the first and second line differ by $\left[4w(\mathbf{k})w(\mathbf{P}-\mathbf{k})(w(\mathbf{k})+w(\mathbf{P}-\mathbf{k})+P_0)\right]^{-1}$. Since this is a low-energy polynomial in the three-momenta, it gives rise only to the exponentially suppressed corrections. Finally, following Ref. [148], the sum minus integral in the fourth line can be expressed through the Lüscher zeta-function, as defined in Eq. (5.85).

Noting that the tree-level amplitude is the same in the infinite and finite volume, the resulting

[2] Certain care should be taken carrying out integrations in k^0 over the low-energy polynomials. Strictly speaking, these integrals do not exist because of the divergence arising at $|k^0|\to\infty$. In the present papers, we consistently put all such integrals to zero that can be justified, for instance, by using split dimensional regularization [250].

two-body S-wave scattering amplitude in a finite volume reads as

$$\tau_L(P) = \frac{1}{(T_{\text{tree}}^{\text{S-wave}})^{-1} - \frac{1}{2} I_L(P)} = \frac{16\pi\sqrt{s}}{p(s)\cot\delta_0(s) - \frac{2}{\sqrt{\pi}L\gamma} Z_{00}^{\mathbf{d}}(1; q_0^2)}, \tag{A.15}$$

where $p(s)\cot\delta_0(s)$ is given by Eq. (5.21).

A.3 A Dimer Field with the Spin ℓ

We define a dimer field with the spin ℓ and projection $m = -\ell, \cdots, \ell$ from the tensor field $T_{\mu_1\cdots\mu_\ell}$. There are three constraints on $T_{\mu_1\cdots\mu_\ell}$:

- Permutation symmetry in all indices

$$T_{\mu_1\cdots\mu_i\cdots\mu_j\cdots\mu_\ell} = T_{\mu_1\cdots\mu_j\cdots\mu_i\cdots\mu_\ell}, \qquad \text{for all } i, j\,. \tag{A.16}$$

- The tensor $T_{\mu_1\cdots\mu_\ell}$ is traceless in each pair of indices

$$g^{\mu_i\mu_j} T_{\mu_1\cdots\mu_i\cdots\mu_j\cdots\mu_\ell} = 0, \qquad \text{for all } i, j\,. \tag{A.17}$$

- For all i, the field obeys the constraint (6.2).

By considering the Lorentz transformation $\underline{\Lambda}$ that boosts v^μ to $v_0^\mu = (1, \mathbf{0})$, one can define the "rest-frame" tensor $\underline{T}^{\mu_1\cdots\mu_\ell}$ as

$$\underline{T}^{\mu_1\cdots\mu_\ell} = \underline{\Lambda}^{\mu_1}_{\nu_1} \cdots \underline{\Lambda}^{\mu_\ell}_{\nu_\ell} T^{\nu_1\cdots\nu_\ell}. \tag{A.18}$$

Due to the constraint (6.2), the field $\underline{T}^{\mu_1\cdots\mu_\ell}$ vanishes, when any of the indices is equal to 0. For simplicity of the notations, we will use spatial indices, $i_1, \cdots, i_\ell$, instead of the Lorentz indices $\mu_1, \cdots, \mu_\ell$.

We begin with the case $\ell = 1$, and write down a transformation that relates the matrix $\underline{T}$ in the Cartesian and spherical bases

$$\underline{T}^i = c_{1m}^i T_{1m}, \qquad i = 1, 2, 3, \quad m = -1, 0, +1\,. \tag{A.19}$$

Here, c_{1m}^i is given by

$$c_{1,\pm1}^i = \frac{1}{\sqrt{2}} \begin{pmatrix} \mp 1 \\ -i \\ 0 \end{pmatrix}_i, \quad c_{1,0}^i = \begin{pmatrix} 0 \\ 0 \\ 1 \end{pmatrix}_i. \tag{A.20}$$

The above result is obtained by postulating

$$\langle 0|\underline{T}^i|j\rangle = \delta_{ij}, \qquad \langle 0|T_{1m}|1n\rangle = \delta_{mn}, \tag{A.21}$$

and using the known relation between the basis vectors $|j\rangle$ and $|1n\rangle$ (the Condon-Shortley phase convention is adopted throughout this paper).

Inversely, one can find that

$$T_{1m} = \left(c^{-1}\right)^{i}_{1m} \underline{T}_i, \tag{A.22}$$

where

$$\left(c^{-1}\right)^{i}_{1m} = \left(c^{i}_{1m}\right)^{*}. \tag{A.23}$$

The spin-ℓ field is build up by the direct product of ℓ spin-1 fields, i.e.,

$$\begin{aligned} T_{\ell m} = \mathscr{C}^{\ell m}_{m_1\cdots m_\ell} T_{1m_1} \otimes \cdots \otimes T_{1m_\ell} &= \mathscr{C}^{\ell m}_{m_1\cdots m_\ell} (c^{i_1}_{1m_1})^{*} \cdots (c^{i_\ell}_{1m_\ell})^{*} \underline{T}_{i_1} \otimes \cdots \otimes \underline{T}_{i_\ell} \\ &\equiv \left(c^{-1}\right)^{i_1\cdots i_\ell}_{\ell m} \underline{T}_{i_1\cdots i_\ell}. \end{aligned} \tag{A.24}$$

Here we are using the following notations:

$$\left(c^{-1}\right)^{i_1\cdots i_\ell}_{\ell m} = \mathscr{C}^{\ell m}_{m_1\cdots m_\ell} (c^{i_1}_{1m_1})^{*} \cdots (c^{i_\ell}_{1m_\ell})^{*}, \tag{A.25}$$

$$\underline{T}_{i_1\cdots i_\ell} = \underline{T}_{i_1} \otimes \cdots \otimes \underline{T}_{i_\ell}. \tag{A.26}$$

The coefficient $\mathscr{C}^{\ell m}_{m_1\cdots m_\ell}$ for $m_1 = \cdots = m_\ell = 1$ can be read off directly, since the highest-weight state takes the form

$$|\ell, \ell\rangle = \underbrace{|1, m_1 = 1\rangle \otimes \cdots \otimes |1, m_\ell = 1\rangle}_{\ell} \equiv |\underbrace{1, \cdots, 1}_{\ell}\rangle. \tag{A.27}$$

From the above equation it follows that $\mathscr{C}^{\ell\ell}_{1\cdots 1} = 1$. For the lower-weight states, we can use the ladder operator

$$J^{-}|j, m+1\rangle = A^{-}_{j,m}|j, m\rangle, \quad A^{-}_{j,m} = \sqrt{(j-m)(j+m+1)}. \tag{A.28}$$

Acting on the state with maximum weight, one gets

$$J^{-}|\ell, \ell\rangle = A^{-}_{\ell,\ell-1}|\ell, \ell-1\rangle. \tag{A.29}$$

At the same time, we have,

$$J^{-}|\underbrace{1, 1, \cdots, 1}_{\ell}\rangle = A_{1,0}|\underbrace{0, 1, \cdots, 1}_{\ell}\rangle + A_{1,0}|\underbrace{1, 0, \cdots, 1}_{\ell}\rangle + \cdots A_{1,0}|\underbrace{1, 1, \cdots, 0}_{\ell}\rangle\,. \tag{A.30}$$

This means that

$$\mathscr{C}^{\ell,\ell-1}_{0,1,\cdots,1} = \mathscr{C}^{\ell,\ell-1}_{1,0,\cdots,1} = \cdots = \mathscr{C}^{\ell,\ell-1}_{1,1,\cdots,0} = \frac{A^-_{1,0}}{A^-_{\ell,\ell-1}}\,. \tag{A.31}$$

Continuing to act with the ladder operator, one gets

$$(J^-)^2\,|\ell,\ell\rangle = A_{\ell,\ell-1}A_{\ell,\ell-2}|\ell,\ell-2\rangle. \tag{A.32}$$

On the other hand,

$$\begin{aligned}
&(J^-)^2\,|1,1,\cdots,1\rangle \\
&= J^-\left(A^-_{1,0}|0,1,\cdots,1\rangle + A^-_{1,0}|1,0,\cdots,1\rangle + \cdots + A^-_{1,0}|1,1,\cdots,0\rangle\right) \\
&= \underbrace{\frac{2!}{1!1!0!\cdots 0!}}_{\ell}\left(A^-_{1,0}\right)^2\left(|0,0,\cdots,1,1\rangle + \cdots + |1,1,\cdots,0,0\rangle\right) \\
&\quad + \underbrace{\frac{2!}{2!0!\cdots 0!}}_{\ell} A^-_{1,0}A^-_{1,-1}\left(|1,1,\cdots,-1\rangle + \cdots + |1,1,\cdots,-1\rangle\right)\,.
\end{aligned} \tag{A.33}$$

The first bracket in the above equation contains ℓ terms, in which -1 stands in the first position, in the second position, and so on. The second bracket contains $\frac{1}{2}\,\ell(\ell-1)$ terms, in which two zeros stand in arbitrary positions. Hence,

$$\begin{aligned}
|\ell,\ell-2\rangle =& \frac{1}{A_{\ell,\ell-1}A_{\ell,\ell-2}}\Bigg(\underbrace{\frac{2!}{1!1!0!\cdots 0!}}_{\ell}\left(A^-_{1,0}\right)^2\left[|0,0,1,\cdots,1,1\rangle + \cdots + |1,1,1,\cdots,0,0\rangle\right] \\
&+ \underbrace{\frac{2!}{2!0!\cdots 0!}}_{\ell}\left(A^-_{1,0}A^-_{1,-1}\right)\left[|-1,1,\cdots,1\rangle + \cdots + |1,1,\cdots,-1\rangle\right]\Bigg).
\end{aligned} \tag{A.34}$$

From this, we can read off that

$$\begin{aligned}
\mathscr{C}^{\ell,\ell-2}_{0,0,1,\cdots,1,1} = \mathscr{C}^{\ell,\ell-2}_{1,0,0,\cdots,1,1} = \cdots = \mathscr{C}^{\ell,\ell-2}_{1,1,\cdots,0,0} &= \underbrace{\frac{2!}{1!1!0!\cdots 0!}}_{\ell}\,\frac{\left(A^-_{1,0}\right)^2}{A_{\ell,\ell-1}A_{\ell,\ell-2}}\,, \\
\mathscr{C}^{\ell,\ell-2}_{-1,1,\cdots,1} = \mathscr{C}^{\ell,\ell-2}_{1,-1,\cdots,1} = \cdots = \mathscr{C}^{\ell,\ell-2}_{1,1,\cdots,-1} &= \underbrace{\frac{2!}{2!0!\cdots 0!}}_{\ell}\,\frac{A^-_{1,0}A^-_{1,-1}}{A_{\ell,\ell-1}A_{\ell,\ell-2}}\,.
\end{aligned} \tag{A.35}$$

This procedure can be continued in a straightforward manner. Recalling that $A^-_{1,-1} = A^-_{1,0} = \sqrt{2}$,

generic expression for the coefficients $\mathscr{C}$ is given by

$$\mathscr{C}^{\ell m}_{m_1\cdots m_\ell} = \frac{(\sqrt{2})^{\ell-m}}{A^-_{\ell,\ell-1}\cdots A^-_{\ell,m}} \frac{(\ell-m)!}{(1-m_1)!\cdots(1-m_\ell)!}\,. \tag{A.36}$$

To summarize, $T_{\ell m}$ and $\underline{T}^{\mu_1\cdots\mu_\ell}$ are related by

$$T_{\ell m} = \left(c^{-1}\right)^{\mu_1\cdots\mu_\ell}_{\ell m} \underline{T}_{\mu_1\cdots\mu_\ell}\,, \tag{A.37}$$

and, inversely,

$$\underline{T}^{\mu_1\cdots\mu_\ell} = c^{\mu_1\cdots\mu_\ell}_{\ell m} T_{\ell m}, \quad (\ell \text{ not summed}) \tag{A.38}$$

Here the matrix c matrix is given by

$$c^{\mu_1\cdots\mu_\ell}_{\ell m} = \begin{cases} \mathscr{C}^{\ell m}_{m_1\cdots m_\ell}(c^{i_1}_{1m_1})\cdots(c^{i_\ell}_{1m_\ell}), & (\mu_1 = i_1,\cdots,\mu_\ell = i_\ell)\,, \\ 0, & \text{if at least one of } \mu_i = 0\,. \end{cases} \tag{A.39}$$

The matrix c^{-1} is complex conjugate of c:

$$\left(c^{-1}\right)^{\mu_1\cdots\mu_\ell}_{\ell m} = \left(c^{\mu_1\cdots\mu_\ell}_{\ell m}\right)^*\,. \tag{A.40}$$

Moreover, it obeys the constraints that are imposed by Eqs. (A.16)-(A.17), namely

$$c^{\mu_1\cdots\mu_i\cdots\mu_j\cdots\mu_\ell}_{\ell m} = c^{\mu_1\cdots\mu_j\cdots\mu_i\cdots\mu_\ell}_{\ell m}, \tag{A.41}$$

$$g_{\mu_i\mu_j} c^{\mu_1\cdots\mu_i\cdots\mu_j\cdots\mu_\ell}_{\ell m} = 0. \tag{A.42}$$

The constraint from Eq. (6.2) is obeyed automatically, owing to Eq. (A.39).

A.4 The Dimer Propagator in a Finite Volume

In this appendix, we briefly sketch the calculation of the finite-volume self energy, displayed in Eq. (6.39). The on-shell momenta in Eq. (6.40) are defined as

$$\hat{q}_\mu = q_\mu - v_\mu(vq - w_v(q))\,, \qquad \hat{q}'_\mu = (P-q)_\mu - v_\mu(v(P-q) - w_v(P-q))\,. \tag{A.43}$$

Furthermore, for any four-momentum,

$$\tilde{p} = \Lambda(v_0,v)\Lambda(v,u)\hat{p} = \left(\Lambda(v_0,v)\Lambda(v,u)\Lambda^{-1}(v_0,u)\right)\Lambda(v_o,u)\hat{p}\,. \tag{A.44}$$

The product of three matrices in the brackets is a pure rotation:

$$\left(\Lambda(v_0,v)\Lambda(v,u)\Lambda^{-1}(v_0,u)\right)^{\mu\nu} = R^{\mu\nu}(v,u)\,, \tag{A.45}$$

where

$$\begin{aligned} R^{00} &= 1\,, \qquad R^{0i} = R^{i0} = 0\,, \\ R^{ij} &= -\delta^{ij} - \frac{(1-v^0)u^i u^j}{(1+(uv))(1+u^0)} - \frac{(1-u^0)v^i v^j}{(1+(uv))(1+v^0)} - \frac{\mathbf{uv}(v^i u^j + u^i v^j)}{(1+(uv))(1+u^0)(1+v^0)} \\ &+ \frac{(1+u^0+v^0+uv)(v^i u^j - u^i v^j)}{(1+(uv))(1+u^0)(1+v^0)}\,. \end{aligned} \tag{A.46}$$

Below the elastic threshold $P^2 < 4m^2$, one can merely replace the sum by an integral in Eq. (A.48) – the corrections to the infinite-volume limit are exponentially suppressed. Therefore, we concentrate on the case $P^2 \geq 4m^2$ here. In this case, the expression for the self-energy can be further simplified. Namely, the quantities $\hat{q}, \hat{q}'$ in the numerator in Eq. (6.39) can be expanded in Taylor series in $(vq - w_v(q))$ and $(v(P-q) - w_v(P-q))$. All terms, except the first one, obviously vanish in this expansion, since after the integration over q^0 one gets a low-energy polynomial and the sum vanishes, if the dimensional regularization is used (we remind the reader that, by implicit convention, the infinite-volume limit is already subtracted in this sum). This expansion, in particular, leads to the replacement $u^\mu \to P^\mu/\sqrt{s}$, where $P^\mu = (\sqrt{s+\mathbf{P}^2}, \mathbf{P})$. Hence, u^μ becomes independent of the summation momentum and, after integration over q^0, the expression of the self-energy simplifies to

$$\Sigma^L_{\ell' m', \ell m}(P) = \sum_{m''' m''} \mathscr{D}^{(\ell')}_{m' m'''}(R(u,v)) \bar{\Sigma}^L_{\ell' m''', \ell m''}(P) \left(\mathscr{D}^{(\ell')}_{m m''}(R(u,v))\right)^* . \tag{A.47}$$

where

$$\bar{\Sigma}^L_{\ell' m', \ell m}(P) = f_{\ell'}(P^2) f_\ell(P^2) \frac{1}{2L^3} \sum_{\mathbf{q}} \frac{\left(\mathscr{Y}_{\ell' m'}(\mathbf{k})\right)^* \mathscr{Y}_{\ell m}(\mathbf{k})}{2w(\mathbf{q}) 2w(\mathbf{P}-\mathbf{q})(w(\mathbf{q}) + w(\mathbf{P}-\mathbf{q}) - P^0)}\,, \tag{A.48}$$

where

$$\mathbf{k} = \mathbf{l} - \mathbf{u}\frac{\mathbf{lu}}{u^0(u^0+1)}\,, \qquad \mathbf{l} = \mathbf{q} - \frac{1}{2}\mathbf{P}\,, \tag{A.49}$$

At this point it is seen that the dependence of v^μ is trivially factored out and is contained in the Wigner D-functions only.

Next, we shall use the well-known addition property of the spherical functions

$$\begin{aligned} \mathscr{Y}^*_{\ell' m'}(\mathbf{k}) \mathscr{Y}_{\ell m}(\mathbf{k}) &= (-1)^{m'} \sqrt{\frac{(2\ell'+1)(2\ell+1)}{4\pi}} \\ &\times \sum_{js} (-1)^j \sqrt{2j+1} |\mathbf{k}|^{\ell'+\ell-j} \begin{pmatrix} \ell' & \ell & j \\ -m' & m & -s \end{pmatrix} \begin{pmatrix} \ell' & \ell & j \\ 0 & 0 & 0 \end{pmatrix} \mathscr{Y}_{js}(\mathbf{k})\,. \end{aligned} \tag{A.50}$$

Here, $\begin{pmatrix} \ell' & \ell & j \\ -m' & m & -s \end{pmatrix}$ and $\begin{pmatrix} \ell' & \ell & j \\ 0 & 0 & 0 \end{pmatrix}$ denote the Wigner $3j$ symbols. Note that $\ell' + \ell - j$ should be an even integer – otherwise, the second of the $3j$ symbols would vanish.

Furthermore, we shall use the following identity (see, e.g., [50]):

$$\frac{1}{2w(\mathbf{q})2w(\mathbf{P}-\mathbf{q})(w(\mathbf{q})+w(\mathbf{P}-\mathbf{q})-P^0)} = \frac{1}{2P^0}\,\frac{1}{\mathbf{l}^2-\dfrac{(\mathbf{lP})^2}{P^{0\,2}}-q_0^2}+\cdots, \tag{A.51}$$

where $q_0^2=\sqrt{\dfrac{s}{4}-m^2}$ and the ellipses stand for the terms that are low-energy polynomials and thus do not contribute.

It is immediately seen that the denominator in the r.h.s of the above relation is equal to $\mathbf{k}^2-q_0^2$. Taking into account that $\ell'+\ell-j$ is even, Eq. (A.48) can be rewritten as follows

$$\begin{aligned}\bar{\Sigma}^L_{\ell' m',\ell m}(P) &= \frac{\pi^2}{LP^0}\,f_{\ell'}(P^2)f_\ell(P^2)q_0^{\ell'+\ell-j}\sqrt{\frac{(2\ell'+1)(2\ell+1)}{4\pi}}\\ &\times \sum_{js}(-1)^{j+m}\sqrt{2j+1}\begin{pmatrix}\ell' & \ell & j\\ -m' & m & -s\end{pmatrix}\begin{pmatrix}\ell' & \ell & j\\ 0 & 0 & 0\end{pmatrix}Z^{\mathbf{d}}_{js}(1;s),\end{aligned} \tag{A.52}$$

where

$$\begin{aligned}Z^{\mathbf{d}}_{js}(1;s) &= \sum_{\mathbf{r}\in P_d}\frac{\mathscr{Y}_{js}(\mathbf{r})}{\mathbf{r}^2-\eta^2}\qquad,\\ P_d &= \left\{\mathbf{r}\in\mathbb{R}^3|r_\parallel=\gamma^{-1}(n_\parallel-\frac{1}{2}\,|\mathbf{d}|),\ \mathbf{r}_\perp=\mathbf{n}_\perp,\ \mathbf{n}\in\mathbb{Z}^3\right\},\end{aligned} \tag{A.53}$$

and

$$\mathbf{d}=\frac{L}{2\pi}\,\mathbf{P},\qquad \eta=\frac{L}{2\pi}\,q_0,\qquad \gamma=\frac{P^0}{\sqrt{s}}\,. \tag{A.54}$$

Final remark is in order. As mentioned already, our calculations concern the finite-volume corrections only. The infinite-volume part has to be added by hand at the end of the day. In our case, the real part of the loop function $J(s)$ should be added, see Eq. (6.20). Once this is done, the finite-volume loop function below threshold smoothly converges to the infinite-volume result, when $L\to\infty$.

A.5 Lorentz Transformations for Z_{loc}

In order to establish the properties of Z_{loc} under Lorentz transformations, we shall use the following well-known properties of the Wigner functions:

$$\begin{aligned}\mathscr{D}^{(j)}_{mn}(R)\mathscr{D}^{(j')}_{m'n'}(R) &= \sum_{J=|j-j'|}^{j+j'}\langle jm,j'm'|J(m+m')\rangle\langle jn,j'n'|J(n+n')\rangle\mathscr{D}^{(J)}_{(m+m')(n+n')}(R),\\ \mathscr{D}^{(j)}_{mm'}(R) &= (-1)^{m-m'}\left(\mathscr{D}^{(j)}_{(-m)(-m')}(R)\right)^*.\end{aligned} \tag{A.55}$$

Now, taking into account the fact that $T_{JL'L}$ are invariant under Lorentz transformations, one may write

$$\begin{aligned}\left(Z_{\text{loc}}\right)_{\ell' m', \ell m}(\Omega p, \Omega q) &= 4\pi \sum_{JLL'} \sum_{MM'} T_{JLL'} \delta_{M'M} \langle L'(M'-m'), \ell' m' | JM' \rangle \mathscr{Y}_{L'(M'-m')}(R\underline{\mathbf{p}}) \\ &\times \langle L(M-m), \ell m | JM \rangle \left(\mathscr{Y}_{L(M-m)}(R\underline{\mathbf{q}})\right)^* . \end{aligned} \tag{A.56}$$

In the above equation, one may use the transformation law, given in Eq. (6.34). In addition, one may replace the Kronecker-delta $\delta_{M'M}$ by

$$\delta_{M'M} = \sum_N \mathscr{D}^{(J)}_{M'N}(R) \left(\mathscr{D}^{(J)}_{MN}(R)\right)^* . \tag{A.57}$$

Using now the second equation in (A.55), the local contribution can be rewritten as follows

$$\begin{aligned}\left(Z_{\text{loc}}\right)_{\ell' m', \ell m}(\Omega p, \Omega q) &= 4\pi \sum_{JLL'} \sum_{MM'} T_{JLL'} \sum_N \sum_{nn'} \mathscr{D}^{(J)}_{M'N}(R) \left(\mathscr{D}^{(J)}_{MN}(R)\right)^* \\ &\times \langle L'(M'-m'), \ell' m' | JM' \rangle \mathscr{Y}_{L'n'}(\underline{\mathbf{p}}) (-1)^{M'-m'-n'} \mathscr{D}^{(L')}_{(m'-M')(-n')}(R) \\ &\times \langle L(M-m), \ell m | JM \rangle \left(\mathscr{Y}_{Ln}(\underline{\mathbf{q}})\right)^* (-1)^{M-m-n} \left(\mathscr{D}^{(L)}_{(m-M)(-n)}(R)\right)^* . \end{aligned} \tag{A.58}$$

Next, one uses addition theorem, given in Eq. (A.55) and performs the sum over M', M afterwards. The addition theorem gives

$$\begin{aligned}&\mathscr{D}^{(L')}_{(m'-M')(-n')}(R) \mathscr{D}^{(J)}_{M'N}(R) \\ &\quad = \sum_{j'} \langle L'(m'-M'), JM' | j'm' \rangle \langle L'(-n'), JN | j'(N-n') \rangle \mathscr{D}^{(j')}_{m'(N-n')}(R) , \end{aligned} \tag{A.59}$$

and the same for the "unprimed" indices. Furthermore, the summation with M', M is carried out by using the symmetry properties for the Clebsch-Gordan coefficients. For example,

$$\begin{aligned}&\sum_{M'} (-1)^{M'-m'-n'} \langle L'(m'-M'), JM' | j'm' \rangle \langle L'(M'-m'), \ell m' | JM' \rangle \\ &= \sum_{M'} (-1)^{J-n'-\ell'} \sqrt{\frac{2J+1}{2\ell'+1}} \langle L'(m'-M'), JM' | j'm' \rangle \langle L'(m'-M'), JM' | \ell m' \rangle \\ &= (-1)^{J-n'-\ell'} \sqrt{\frac{2J+1}{2\ell'+1}} \delta_{j'\ell'} , \end{aligned} \tag{A.60}$$

and, similarly, for the "unprimed" indices. Substituting this expression into the original formula gives

$$\begin{aligned}\left(Z_{\mathsf{loc}}\right)_{\ell' m',\ell m}(\Omega p,\Omega q) \;=\; & 4\pi \sum_{JLL'} \sum_{n'n} \sum_{j'j} \sum_{N} T_{JLL'} \\ & \times (-1)^{-n'+J-\ell'} \sqrt{\frac{2J+1}{2\ell'+1}} \delta_{j'\ell'} \langle L'(-n'), JN | j'(N-n') \rangle \mathscr{Y}_{L'n'}(\underline{\mathbf{p}}) \mathscr{D}^{(j')}_{m'(N-n')}(R) \\ & \times (-1)^{-n+J-\ell} \sqrt{\frac{2J+1}{2\ell+1}} \delta_{j\ell} \langle L(-n), JN | j(N-n) \rangle \left(\mathscr{Y}_{Ln}(\underline{\mathbf{q}})\right)^* \left(\mathscr{D}^{(j)}_{m(N-n)}(R)\right)^* . \end{aligned} \tag{A.61}$$

Using the symmetries of the Clebsch-Gordan coefficients again, we get:

$$\begin{aligned}\left(Z_{\mathsf{loc}}\right)_{\ell' m',\ell m}(\Omega p,\Omega q) \;=\; & 4\pi \sum_{JLL'} \sum_{n'n} \sum_{N} T_{JLL'} \\ & \times \langle L'n', \ell'(N-n') | JN \rangle \mathscr{Y}_{L'n'}(\underline{\mathbf{p}}) \mathscr{D}^{(j')}_{m'(N-n')}(R) \\ & \times \langle Ln, \ell(N-n) | JN \rangle \left(\mathscr{Y}_{Ln}(\underline{\mathbf{q}})\right)^* \left(\mathscr{D}^{(j)}_{m(N-n)}(R)\right)^* . \end{aligned} \tag{A.62}$$

Finally, one arrives at

$$\left(Z_{\mathsf{loc}}\right)_{\ell' m',\ell m}(\Omega p,\Omega q) = \sum_{m'''m''} \mathscr{D}^{(\ell')}_{m'm'''}(R) \left(Z_{\mathsf{loc}}\right)_{\ell' m''',\ell m''}(p,q) \left(\mathscr{D}^{(\ell)}_{mm''}(R)\right)^* . \tag{A.63}$$

A.6 Projection Onto the Various Irreps

In this appendix, we give a detailed derivation of Eqs. (6.53) and (6.54). To this end, we shall transform Eq. (6.52) by using the transformation property of $\mathscr{A}$, manifested in Eq. (6.51):

$$\begin{aligned}\mathscr{A}^{\ell'\Gamma'\alpha',\ell\Gamma\alpha}_{\sigma'(t'\Delta')\Sigma',\sigma(t\Delta)\Sigma}(p_r,q_s) \;=\; & \frac{s_{\sigma'}}{G} \frac{s_{\Sigma}}{G} \sum_{g',g\in\mathcal{G}} \sum_{\lambda'\rho',\lambda\rho} \sum_{\lambda'''\lambda''} \langle \Sigma'\rho', \Delta'\lambda' | \Gamma'\alpha' \rangle T^{(\Sigma')}_{\rho'\sigma'}(g') T^{(\Delta')}_{\lambda'\lambda'''}(g) \\ & \times \mathscr{A}^{\ell'\ell}_{\lambda'''(t'\Delta'),\lambda''(t\Delta)}(\underbrace{g^{-1}g'}_{=g''} p_r, q_s) T^{(\Delta)}_{\lambda''\lambda}(g^{-1}) T^{(\Sigma)}_{\sigma\rho}(g^{-1}) \langle \Sigma\rho, \Delta\lambda | \Gamma\alpha \rangle \\ = \; & \frac{s_{\Sigma'}}{G} \frac{s_{\Sigma}}{G} \sum_{g,g''\in\mathcal{G}} \sum_{\lambda'\rho',\lambda\rho} \sum_{\lambda'''\lambda''\sigma''} \langle \Sigma'\rho', \Delta'\lambda' | \Gamma'\alpha' \rangle T^{(\Sigma')}_{\rho'\sigma''}(g) T^{(\Sigma')}_{\sigma''\sigma'}(g'') T^{(\Delta')}_{\lambda'\lambda'''}(g) \\ & \times \mathscr{A}^{\ell'\ell}_{\lambda'''(t'\Delta'),\lambda''(t\Delta)}(g'' p_r, q_s) T^{(\Delta)}_{\lambda''\lambda}(g^{-1}) T^{(\Sigma)}_{\sigma\rho}(g^{-1}) \langle \Sigma\rho, \Delta\lambda | \Gamma\alpha \rangle . \end{aligned} \tag{A.64}$$

In what follows, we shall use the relation

$$\begin{aligned}
&\sum_{\rho'\lambda'} \langle \Sigma'\rho', \Delta'\lambda' | \Gamma'\alpha' \rangle T^{(\Sigma')}_{\rho'\sigma''}(g) T^{(\Delta')}_{\lambda'\lambda'''}(g) \\
&\quad = \sum_{\rho'\lambda'} \langle \Sigma'\rho', \Delta'\lambda' | \Gamma'\alpha' \rangle \sum_{\Xi\beta'\gamma'} \langle \Sigma'\rho', \Delta'\lambda' | \Xi'\beta' \rangle \langle \Sigma'\sigma'', \Delta'\lambda''' | \Xi'\gamma' \rangle T^{(\Xi')}_{\beta'\gamma'}(g) \\
&\quad = \sum_{\gamma'} \langle \Sigma'\sigma'', \Delta'\lambda''' | \Gamma'\gamma' \rangle T^{(\Gamma')}_{\alpha'\gamma'}(g) \,. \qquad \text{(A.65)}
\end{aligned}$$

A similar relation holds also for the product $T^{(\Sigma)}(g^{-1}) \times T^{(\Delta)}(g^{-1})$. With the use of these relations, the original expression simplifies to

$$\begin{aligned}
\mathscr{A}^{\ell'\Gamma'\alpha',\ell\Gamma\alpha}_{\sigma'(t'\Delta')\Sigma',\sigma(t\Delta)\Sigma}(p_r, q_s) \;=\; \frac{s_{\sigma'}}{G} \frac{s_\Sigma}{G} \sum_{g,g''\in\mathcal{G}} \sum_{\gamma\gamma'} \sum_{\lambda'''\lambda''\sigma''} \langle \Sigma'\sigma'', \Delta'\lambda''' | \Gamma'\gamma' \rangle T^{(\Gamma')}_{\alpha'\gamma'}(g) \\
\times T^{(\Sigma')}_{\sigma''\sigma'}(g'') \mathscr{A}^{\ell'\ell}_{\lambda'''(t'\Delta'),\lambda''(t\Delta)}(g'' p_r, q_s) \langle \Sigma\sigma, \Delta\lambda'' | \Gamma\gamma \rangle T^{(\Gamma)}_{\gamma\alpha}(g^{-1}) \,. \qquad \text{(A.66)}
\end{aligned}$$

Carrying out the summation over g with the use of the orthogonality condition of the matrices of the irreps, we finally arrive at Eqs. (6.53) and (6.54).

Bibliography

[1] F. Müller and A. Rusetsky, *On the three-particle analog of the Lellouch-Lüscher formula*, JHEP **03** (2021) 152, arXiv: 2012.13957 [hep-lat]
(cit. on pp. iv, 61, 76, 108, 109, 122, 131).

[2] F. Müller, J.-Y. Pang, A. Rusetsky and J.-J. Wu,
Relativistic-invariant formulation of the NREFT three-particle quantization condition,
JHEP **02** (2022) 158, arXiv: 2110.09351 [hep-lat]
(cit. on pp. iv, 75, 108–111, 113–115, 118).

[3] F. Müller, J.-Y. Pang, A. Rusetsky and J.-J. Wu,
Three-particle Lellouch-Lüscher formalism in moving frames, JHEP **02** (2023) 214,
arXiv: 2211.10126 [hep-lat] (cit. on pp. iv, 107).

[4] F. Müller, T. Yu and A. Rusetsky, *Finite-volume energy shift of the three-pion ground state*,
Phys. Rev. D **103** (2021) 054506, arXiv: 2011.14178 [hep-lat]
(cit. on pp. iv, 31, 63, 76, 108, 135).

[5] J.-Y. Pang et al., *Spurious poles in a finite volume*, JHEP **07** (2022) 019,
arXiv: 2204.04807 [hep-lat] (cit. on pp. iv, 57, 135, 136).

[6] R. Bubna, F. Müller and A. Rusetsky,
Finite-volume energy shift of the three-nucleon ground state, Phys. Rev. D **108** (2023) 014518,
arXiv: 2304.13635 [hep-lat] (cit. on pp. iv, 31, 135).

[7] J.-Y. Pang, R. Bubna, F. Müller, A. Rusetsky and J.-J. Wu,
Lellouch-Lüscher factor for the $K \to 3\pi$ decays, (2023), arXiv: 2312.04391 [hep-lat]
(cit. on pp. iv, 135).

[8] R. Bubna et al., *Lüscher equation with the long-range forces*, (in preparation) (cit. on p. iv).

[9] Y. Ne'eman, *Derivation of strong interactions from a gauge invariance*,
Nucl. Phys. **26** (1961) 222, ed. by R. Ruffini and Y. Verbin (cit. on p. 1).

[10] M. Gell-Mann, *Symmetries of baryons and mesons*, Phys. Rev. **125** (1962) 1067
(cit. on pp. 1, 9).

[11] S. Okubo, *Note on unitary symmetry in strong interactions*, Prog. Theor. Phys. **27** (1962) 949
(cit. on pp. 1, 9).

[12] V. E. Barnes et al., *Confirmation of the existence of the Ω^- hyperon*, Phys. Lett. **12** (1964) 134
(cit. on p. 1).

[13] M. Gell-Mann, *A Schematic Model of Baryons and Mesons*, Phys. Lett. **8** (1964) 214
(cit. on p. 1).

[14] G. Zweig, "An SU(3) model for strong interaction symmetry and its breaking. Version 2", *DEVELOPMENTS IN THE QUARK THEORY OF HADRONS. VOL. 1. 1964 - 1978*, ed. by D. B. Lichtenberg and S. P. Rosen, 1964 22 (cit. on p. 1).

[15] E. D. Bloom et al., *High-Energy Inelastic e p Scattering at 6-Degrees and 10-Degrees*, Phys. Rev. Lett. **23** (1969) 930 (cit. on p. 1).

[16] M. Breidenbach et al., *Observed behavior of highly inelastic electron-proton scattering*, Phys. Rev. Lett. **23** (1969) 935 (cit. on p. 1).

[17] D. H. Perkins, *Neutrino interactions*, eConf **C720906V4** (1972) 189, ed. by J. D. Jackson and A. Roberts (cit. on p. 1).

[18] J. D. Bjorken, *Asymptotic Sum Rules at Infinite Momentum*, Phys. Rev. **179** (1969) 1547 (cit. on p. 1).

[19] E. M. Riordan et al., *Extraction of $R = \frac{\sigma_L}{\sigma_T}$ from Deep Inelastic $e - p$ and $e - d$ Cross Sections*, Phys. Rev. Lett. **33** (9 1974) 561, URL: https://link.aps.org/doi/10.1103/PhysRevLett.33.561 (cit. on p. 1).

[20] M. Haguenauer, ""Gargamelle" Experiment", *17th International Conference on High-Energy Physics*, 1974 IV.95 (cit. on p. 1).

[21] J. Kuti and V. F. Weisskopf, *Inelastic Lepton-Nucleon Scattering and Lepton Pair Production in the Relativistic Quark-Parton Model*, Phys. Rev. D **4** (11 1971) 3418, URL: https://link.aps.org/doi/10.1103/PhysRevD.4.3418 (cit. on p. 1).

[22] H. D. Politzer, *Reliable Perturbative Results for Strong Interactions?*, Phys. Rev. Lett. **30** (26 1973) 1346, URL: https://link.aps.org/doi/10.1103/PhysRevLett.30.1346 (cit. on p. 1).

[23] D. J. Gross and F. Wilczek, *Ultraviolet Behavior of Non-Abelian Gauge Theories*, Phys. Rev. Lett. **30** (26 1973) 1343, URL: https://link.aps.org/doi/10.1103/PhysRevLett.30.1343 (cit. on p. 1).

[24] H. Fritzsch, M. Gell-Mann and H. Leutwyler, *Advantages of the color octet gluon picture*, Physics Letters B **47** (1973) 365, ISSN: 0370-2693, URL: https://www.sciencedirect.com/science/article/pii/0370269373906254 (cit. on p. 2).

[25] M. Y. Han and Y. Nambu, *Three Triplet Model with Double SU(3) Symmetry*, Phys. Rev. **139** (1965) B1006, ed. by T. Eguchi (cit. on p. 2).

[26] Y. Nambu, "A systematics of hadrons in subnuclear physics", *Preludes in theoretical physics*, ed. by H. Feshbach and L. C. P. Van Hove, Amsterdam: North-Holland, 1966 133 (cit. on p. 2).

[27] G. Altarelli, *Experimental tests of perturbative QCD*, Annu. Rev. Nucl. Part. Sci. **39** (1989) 357, URL: https://cds.cern.ch/record/197024 (cit. on p. 2).

[28] M. Fischer et al., *Scattering of two and three physical pions at maximal isospin from lattice QCD*, Eur. Phys. J. C **81** (2021) 436, arXiv: 2008.03035 [hep-lat] (cit. on pp. 2, 3, 63, 76, 108).

[29] A. Alexandru et al., *Finite-volume energy spectrum of the $K^-K^-K^-$ system*, Phys. Rev. D **102** (2020) 114523, arXiv: 2009.12358 [hep-lat] (cit. on pp. 2, 3, 63, 76, 108).

[30] M. Mai, M. Döring and A. Rusetsky, *Multi-particle systems on the lattice and chiral extrapolations: a brief review*, Eur. Phys. J. ST **230** (2021) 1623, arXiv: 2103.00577 [hep-lat] (cit. on pp. 2, 76, 108).

[31] L. Maiani and M. Testa, *Final state interactions from euclidean correlation functions*, Physics Letters B **245** (1990) 585, ISSN: 0370-2693, URL: https://www.sciencedirect.com/science/article/pii/0370269390906953 (cit. on pp. 2, 19).

[32] M. Lüscher, *Volume Dependence of the Energy Spectrum in Massive Quantum Field Theories. 2. Scattering States*, Commun. Math. Phys. **105** (1986) 153 (cit. on pp. 3, 18, 20).

[33] M. Lüscher, *Two particle states on a torus and their relation to the scattering matrix*, Nucl. Phys. B **354** (1991) 531 (cit. on pp. 3, 20).

[34] K. Rummukainen and S. A. Gottlieb, *Resonance scattering phase shifts on a nonrest frame lattice*, Nucl. Phys. B **450** (1995) 397, arXiv: hep-lat/9503028 (cit. on p. 3).

[35] C. h. Kim, C. T. Sachrajda and S. R. Sharpe, *Finite-volume effects for two-hadron states in moving frames*, Nucl. Phys. B **727** (2005) 218, arXiv: hep-lat/0507006 (cit. on pp. 3, 28, 62).

[36] M. Göckeler et al., *Scattering phases for meson and baryon resonances on general moving-frame lattices*, Phys. Rev. D **86** (2012) 094513, arXiv: 1206.4141 [hep-lat] (cit. on pp. 3, 22, 24, 27, 98, 119).

[37] R. A. Briceño, *Two-particle multichannel systems in a finite volume with arbitrary spin*, Physical Review D **89** (2014), URL: https://doi.org/10.1103%2Fphysrevd.89.074507 (cit. on pp. 3, 21).

[38] F. Romero-López, A. Rusetsky and C. Urbach, *Vector particle scattering on the lattice*, Phys. Rev. D **98** (2018) 014503, arXiv: 1802.03458 [hep-lat] (cit. on p. 3).

[39] S. He, X. Feng and C. Liu, *Two particle states and the S-matrix elements in multi-channel scattering*, Journal of High Energy Physics **2005** (2005) 011, URL: https://dx.doi.org/10.1088/1126-6708/2005/07/011 (cit. on pp. 3, 21).

[40] M. Lage, U.-G. Meißner and A. Rusetsky, *A method to measure the antikaon–nucleon scattering length in lattice QCD*, Physics Letters B **681** (2009) 439, URL: https://doi.org/10.1016%2Fj.physletb.2009.10.055 (cit. on pp. 3, 21).

[41] M. T. Hansen and S. R. Sharpe, *Multiple-channel generalization of Lellouch-Lüscher formula*, Physical Review D **86** (2012), URL: https://doi.org/10.1103%2Fphysrevd.86.016007 (cit. on pp. 3, 21, 28, 62).

[42] R. A. Briceño and Z. Davoudi,
Moving multichannel systems in a finite volume with application to proton-proton fusion,
Physical Review D **88** (2013),
URL: https://doi.org/10.1103%2Fphysrevd.88.094507 (cit. on pp. 3, 21).

[43] R. A. Briceño, J. J. Dudek and R. D. Young,
Scattering processes and resonances from lattice QCD, Rev. Mod. Phys. **90** (2018) 025001,
arXiv: 1706.06223 [hep-lat] (cit. on pp. 3, 26).

[44] M. Mai, U.-G. Meißner and C. Urbach, *Towards a theory of hadron resonances*,
Phys. Rept. **1001** (2023) 1, arXiv: 2206.01477 [hep-ph] (cit. on p. 3).

[45] L. Lellouch and M. Lüscher,
Weak Transition Matrix Elements from Finite-Volume Correlation Functions,
Communications in Mathematical Physics **219** (2001) 31,
URL: https://doi.org/10.1007%2Fs002200100410 (cit. on pp. 3, 28, 62, 76).

[46] N. H. Christ, C. Kim and T. Yamazaki,
Finite volume corrections to the two-particle decay of states with non-zero momentum,
Phys. Rev. D **72** (2005) 114506, arXiv: hep-lat/0507009 (cit. on pp. 3, 28, 62).

[47] R. A. Briceño, M. T. Hansen and A. Walker-Loud,
Multichannel $1 \to 2$ transition amplitudes in a finite volume, Phys. Rev. D **91** (2015) 034501,
arXiv: 1406.5965 [hep-lat] (cit. on pp. 3, 62).

[48] R. A. Briceño and M. T. Hansen,
Relativistic, model-independent, multichannel $2 \to 2$ transition amplitudes in a finite volume,
Phys. Rev. D **94** (2016) 013008, arXiv: 1509.08507 [hep-lat] (cit. on p. 3).

[49] W. Detmold and M. J. Savage,
Electroweak matrix elements in the two-nucleon sector from lattice QCD,
Nuclear Physics A **743** (2004) 170, ISSN: 0375-9474, URL:
https://www.sciencedirect.com/science/article/pii/S0375947404008152
(cit. on p. 3).

[50] V. Bernard, D. Hoja, U.-G. Meißner and A. Rusetsky, *Matrix elements of unstable states*,
JHEP **09** (2012) 023, arXiv: 1205.4642 [hep-lat] (cit. on pp. 3, 42, 45, 62, 64, 69, 145).

[51] A. Agadjanov, V. Bernard, U.-G. Meißner and A. Rusetsky,
A framework for the calculation of the $\Delta N\gamma^*$ transition form factors on the lattice,
Nucl. Phys. B **886** (2014) 1199, arXiv: 1405.3476 [hep-lat] (cit. on pp. 3, 64).

[52] A. Baroni, R. A. Briceño, M. T. Hansen and F. G. Ortega-Gama,
Form factors of two-hadron states from a covariant finite-volume formalism,
Phys. Rev. D **100** (3 2019) 034511,
URL: https://link.aps.org/doi/10.1103/PhysRevD.100.034511 (cit. on p. 3).

[53] J. Lozano, U.-G. Meißner, F. Romero-López, A. Rusetsky and G. Schierholz,
Resonance form factors from finite-volume correlation functions with the external field method,
JHEP **10** (2022) 106, arXiv: 2205.11316 [hep-lat] (cit. on p. 3).

[54] K. H. Sherman, F. G. Ortega-Gama, R. Briceño and A. W. Jackura,
Two-current transition amplitudes with two-body final states, Physical Review D (2022)
(cit. on p. 3).

[55] K. Polejaeva and A. Rusetsky, *Three particles in a finite volume*,
The European Physical Journal A **48** (2012),
URL: https://doi.org/10.1140%2Fepja%2Fi2012-12067-8
(cit. on pp. 3, 31, 58, 63, 70, 76, 108).

[56] R. A. Briceño and Z. Davoudi,
Three-particle scattering amplitudes from a finite volume formalism,
Phys. Rev. D **87** (9 2013) 094507,
URL: https://link.aps.org/doi/10.1103/PhysRevD.87.094507
(cit. on pp. 3, 58, 76, 108).

[57] M. T. Hansen and S. R. Sharpe,
Relativistic, model-independent, three-particle quantization condition,
Phys. Rev. D **90** (11 2014) 116003,
URL: https://link.aps.org/doi/10.1103/PhysRevD.90.116003
(cit. on pp. 3, 31, 76, 86, 99, 108).

[58] M. T. Hansen and S. R. Sharpe, *Expressing the three-particle finite-volume spectrum in terms of the three-to-three scattering amplitude*, Phys. Rev. D **92** (11 2015) 114509,
URL: https://link.aps.org/doi/10.1103/PhysRevD.92.114509
(cit. on pp. 3, 31, 54, 63, 76, 86, 99, 108).

[59] M. Mai and M. Döring, *Three-body Unitarity in the Finite Volume*,
Eur. Phys. J. A **53** (2017) 240, arXiv: 1709.08222 [hep-lat]
(cit. on pp. 3, 31, 58, 63, 76, 108).

[60] H.-W. Hammer, J.-Y. Pang and A. Rusetsky,
Three-particle quantization condition in a finite volume: 1. The role of the three-particle force,
JHEP **09** (2017) 109, arXiv: 1706.07700 [hep-lat]
(cit. on pp. 3, 31, 63, 66–68, 76, 85, 89, 101, 108).

[61] H.-W. Hammer, J.-Y. Pang and A. Rusetsky, *Three particle quantization condition in a finite volume: 2. general formalism and the analysis of data*, JHEP **10** (2017) 115,
arXiv: 1707.02176 [hep-lat] (cit. on pp. 3, 31, 63, 66–68, 76, 85, 89, 101, 108).

[62] M. T. Hansen and S. R. Sharpe, *Lattice QCD and Three-particle Decays of Resonances*,
Ann. Rev. Nucl. Part. Sci. **69** (2019) 65, arXiv: 1901.00483 [hep-lat]
(cit. on pp. 3, 76, 108).

[63] T. D. Blanton and S. R. Sharpe,
Equivalence of relativistic three-particle quantization conditions,
Phys. Rev. D **102** (5 2020) 054515,
URL: https://link.aps.org/doi/10.1103/PhysRevD.102.054515
(cit. on pp. 3, 76, 108).

[64] A. W. Jackura et al., *Equivalence of three-particle scattering formalisms*,
Phys. Rev. D **100** (2019) 034508, arXiv: 1905.12007 [hep-ph] (cit. on pp. 3, 76, 108).

[65] T. D. Blanton, F. Romero-López and S. R. Sharpe,
$I = 3$ Three-Pion Scattering Amplitude from Lattice QCD,
Phys. Rev. Lett. **124** (3 2020) 032001,
URL: https://link.aps.org/doi/10.1103/PhysRevLett.124.032001
(cit. on pp. 3, 63, 76, 77, 108).

[66] R. Brett et al., *Three-body interactions from the finite-volume QCD spectrum*,
Phys. Rev. D **104** (2021) 014501, arXiv: 2101.06144 [hep-lat] (cit. on pp. 3, 76, 108).

[67] Z. T. Draper et al.,
Interactions of πK, $\pi\pi K$ and $KK\pi$ systems at maximal isospin from lattice QCD,
JHEP **05** (2023) 137, arXiv: 2302.13587 [hep-lat] (cit. on p. 3).

[68] M. Mai et al., *Three-Body Dynamics of the a1(1260) Resonance from Lattice QCD*,
Phys. Rev. Lett. **127** (2021) 222001, arXiv: 2107.03973 [hep-lat] (cit. on pp. 3, 108).

[69] M. Garofalo, M. Mai, F. Romero-López, A. Rusetsky and C. Urbach,
Three-body resonances in the φ^4 theory, JHEP **02** (2023) 252,
arXiv: 2211.05605 [hep-lat] (cit. on pp. 3, 108).

[70] U.-G. Meißner and A. Rusetsky, *Effective Field Theories*, Cambridge University Press, 2022,
ISBN: 978-1-108-68903-8 (cit. on pp. 4, 34, 42).

[71] S. Weinberg, *Phenomenological Lagrangians*,
Physica A: Statistical Mechanics and its Applications **96** (1979) 327, ISSN: 0378-4371,
URL: https://www.sciencedirect.com/science/article/pii/0378437179902231
(cit. on p. 4).

[72] J. Gasser and H. Leutwyler, *Chiral perturbation theory to one loop*,
Annals of Physics **158** (1984) 142, ISSN: 0003-4916,
URL: https://www.sciencedirect.com/science/article/pii/0003491684902422
(cit. on p. 4).

[73] J. Gasser and H. Leutwyler,
Chiral perturbation theory: Expansions in the mass of the strange quark,
Nuclear Physics B **250** (1985) 465, ISSN: 0550-3213,
URL: https://www.sciencedirect.com/science/article/pii/0550321385904924
(cit. on p. 4).

[74] C. Vafa and E. Witten, *Restrictions on symmetry breaking in vector-like gauge theories*,
Nuclear Physics B **234** (1984) 173, ISSN: 0550-3213,
URL: https://www.sciencedirect.com/science/article/pii/055032138490230X
(cit. on pp. 4, 9).

[75] J. Goldstone, *Field Theories with Superconductor Solutions*, Nuovo Cim. **19** (1961) 154
(cit. on p. 4).

[76] J. Goldstone, A. Salam and S. Weinberg, *Broken Symmetries*, Phys. Rev. **127** (3 1962) 965,
URL: https://link.aps.org/doi/10.1103/PhysRev.127.965 (cit. on p. 4).

[77] M. Gell-Mann, R. J. Oakes and B. Renner,
Behavior of Current Divergences under $SU_3 \times SU_3$, Phys. Rev. **175** (5 1968) 2195,
URL: https://link.aps.org/doi/10.1103/PhysRev.175.2195 (cit. on p. 4).

[78] S. Coleman, J. Wess and B. Zumino, *Structure of Phenomenological Lagrangians. I*, Phys. Rev. **177** (5 1969) 2239, URL: https://link.aps.org/doi/10.1103/PhysRev.177.2239 (cit. on p. 4).

[79] C. G. Callan, S. Coleman, J. Wess and B. Zumino, *Structure of Phenomenological Lagrangians. II*, Phys. Rev. **177** (5 1969) 2247, URL: https://link.aps.org/doi/10.1103/PhysRev.177.2247 (cit. on p. 4).

[80] E. Jenkins and A. V. Manohar, *Baryon chiral perturbation theory using a heavy fermion lagrangian*, Physics Letters B **255** (1991) 558, ISSN: 0370-2693, URL: https://www.sciencedirect.com/science/article/pii/037026939190266S (cit. on p. 4).

[81] V. Bernard, N. Kaiser, J. Kambor and U.-G. Meißner, *Chiral structure of the nucleon*, Nucl. Phys. B **388** (1992) 315 (cit. on pp. 4, 34).

[82] T. Becher and H. Leutwyler, *Baryon chiral perturbation theory in manifestly Lorentz invariant form*, Eur. Phys. J. C **9** (1999) 643, arXiv: hep-ph/9901384 (cit. on p. 5).

[83] J. Gegelia and G. Japaridze, *Matching heavy particle approach to relativistic theory*, Phys. Rev. D **60** (1999) 114038, arXiv: hep-ph/9908377 (cit. on p. 5).

[84] T. Fuchs, J. Gegelia, G. Japaridze and S. Scherer, *Renormalization of relativistic baryon chiral perturbation theory and power counting*, Phys. Rev. D **68** (2003) 056005, arXiv: hep-ph/0302117 (cit. on p. 5).

[85] S. Myint and C. Rebbi, *Chiral perturbation theory on the lattice: Strong coupling expansion*, Nuclear Physics B **421** (1994) 241, ISSN: 0550-3213, URL: https://www.sciencedirect.com/science/article/pii/055032139490233X (cit. on p. 5).

[86] S. Sharpe and R. Singleton, *Spontaneous flavor and parity breaking with Wilson fermions*, Phys. Rev. D **58** (7 1998) 074501, URL: https://link.aps.org/doi/10.1103/PhysRevD.58.074501 (cit. on p. 5).

[87] W. Lee and S. R. Sharpe, *Partial flavor symmetry restoration for chiral staggered fermions*, Phys. Rev. D **60** (11 1999) 114503, URL: https://link.aps.org/doi/10.1103/PhysRevD.60.114503 (cit. on p. 5).

[88] J. Gasser and H. Leutwyler, *Light quarks at low temperatures*, Physics Letters B **184** (1987) 83, ISSN: 0370-2693, URL: https://www.sciencedirect.com/science/article/pii/0370269387904928 (cit. on p. 5).

[89] H. Leutwyler, *Energy levels of light quarks confined to a box*, Physics Letters B **189** (1987) 197, ISSN: 0370-2693, URL: https://www.sciencedirect.com/science/article/pii/0370269387912962 (cit. on p. 5).

[90] J. Gasser and H. Leutwyler,
Spontaneously broken symmetries: Effective lagrangians at finite volume,
Nuclear Physics B **307** (1988) 763, ISSN: 0550-3213,
URL: https://www.sciencedirect.com/science/article/pii/0550321388901071
(cit. on p. 5).

[91] Y. Aoki et al., *FLAG Review 2021*, Eur. Phys. J. C **82** (2022) 869,
arXiv: 2111.09849 [hep-lat] (cit. on p. 5).

[92] S. Weinberg, *Nuclear forces from chiral lagrangians*, Physics Letters B **251** (1990) 288,
ISSN: 0370-2693,
URL: https://www.sciencedirect.com/science/article/pii/0370269390909383
(cit. on p. 5).

[93] U. van Kolck, *Few-nucleon forces from chiral Lagrangians*, Phys. Rev. C **49** (6 1994) 2932,
URL: https://link.aps.org/doi/10.1103/PhysRevC.49.2932 (cit. on p. 5).

[94] D. B. Kaplan, M. J. Savage and M. B. Wise,
Nucleon-nucleon scattering from effective field theory, Nuclear Physics B **478** (1996) 629,
ISSN: 0550-3213,
URL: https://www.sciencedirect.com/science/article/pii/0550321396003574
(cit. on p. 5).

[95] D. B. Kaplan, *More effective field theory for non-relativistic scattering*,
Nuclear Physics B **494** (1997) 471, ISSN: 0550-3213, URL:
https://www.sciencedirect.com/science/article/pii/S0550321397001788
(cit. on pp. 5, 65).

[96] D. B. Kaplan, M. J. Savage and M. B. Wise,
A New expansion for nucleon-nucleon interactions, Phys. Lett. B **424** (1998) 390,
arXiv: nucl-th/9801034 (cit. on p. 5).

[97] P. Bedaque and U. van Kolck, *Nucleon-deuteron scattering from an effective field theory*,
Physics Letters B **428** (1998) 221, ISSN: 0370-2693, URL:
https://www.sciencedirect.com/science/article/pii/S0370269398004304
(cit. on p. 5).

[98] P. F. Bedaque, H. W. Hammer and U. van Kolck,
The Three boson system with short range interactions, Nucl. Phys. A **646** (1999) 444,
arXiv: nucl-th/9811046 (cit. on pp. 5, 45, 65).

[99] P. F. Bedaque, H.-W. Hammer and U. L. van Kolck, *Effective theory of the triton*,
Nuclear Physics **676** (2000) 357 (cit. on p. 5).

[100] E. Epelbaum, H.-W. Hammer and U.-G. Meißner, *Modern Theory of Nuclear Forces*,
Rev. Mod. Phys. **81** (2009) 1773, arXiv: 0811.1338 [nucl-th] (cit. on p. 5).

[101] S. Kreuzer and H.-W. Hammer, *Efimov physics in a finite volume*,
Physics Letters B **673** (2009) 260, ISSN: 0370-2693, URL:
https://www.sciencedirect.com/science/article/pii/S0370269309002135
(cit. on pp. 5, 68, 76, 108).

[102] S. Kreuzer and H. .-.-W. Hammer,
On the modification of the Efimov spectrum in a finite cubic box,
Eur. Phys. J. A **43** (2010) 229, arXiv: 0910.2191 [nucl-th] (cit. on pp. 5, 68, 76, 108).

[103] S. Kreuzer and H. .-.-W. Hammer, *The Triton in a finite volume*, Phys. Lett. B **694** (2011) 424, arXiv: 1008.4499 [hep-lat] (cit. on pp. 5, 68, 76, 108).

[104] S. Kreuzer and H. W. Grießhammer,
Three particles in a finite volume: The breakdown of spherical symmetry,
Eur. Phys. J. A **48** (2012) 93, arXiv: 1205.0277 [nucl-th] (cit. on pp. 5, 68, 76, 108).

[105] M. Tanabashi et al., *Review of Particle Physics*, Phys. Rev. D **98** (2018) 030001 (cit. on pp. 8, 18).

[106] K. Osterwalder and R. Schrader, *Axioms for Euclidean Green's Functions*, Commun. Math. Phys. **31** (1973) 83 (cit. on p. 10).

[107] K. Osterwalder and R. Schrader, *Axioms for Euclidean Green's Functions. 2.*, Commun. Math. Phys. **42** (1975) 281 (cit. on p. 10).

[108] K. G. Wilson, *Confinement of Quarks*, Phys. Rev. D **10** (1974) 2445, ed. by J. C. Taylor (cit. on p. 13).

[109] H. B. Nielsen and M. Ninomiya,
Absence of Neutrinos on a Lattice. 1. Proof by Homotopy Theory, Nucl. Phys. B **185** (1981) 20, ed. by J. Julve and M. Ramón-Medrano, [Erratum: Nucl.Phys.B 195, 541 (1982)] (cit. on p. 13).

[110] J. B. Kogut and L. Susskind, *Hamiltonian Formulation of Wilson's Lattice Gauge Theories*, Phys. Rev. D **11** (1975) 395 (cit. on p. 14).

[111] L. Susskind, *Lattice Fermions*, Phys. Rev. D **16** (1977) 3031 (cit. on p. 14).

[112] H. Neuberger, *Exactly massless quarks on the lattice*, Phys. Lett. B **417** (1998) 141, arXiv: hep-lat/9707022 (cit. on p. 14).

[113] H. Neuberger, *More about exactly massless quarks on the lattice*, Phys. Lett. B **427** (1998) 353, arXiv: hep-lat/9801031 (cit. on p. 14).

[114] D. B. Kaplan, *A Method for simulating chiral fermions on the lattice*, Phys. Lett. B **288** (1992) 342, arXiv: hep-lat/9206013 (cit. on p. 14).

[115] V. Furman and Y. Shamir, *Axial symmetries in lattice QCD with Kaplan fermions*, Nucl. Phys. B **439** (1995) 54, arXiv: hep-lat/9405004 (cit. on p. 14).

[116] M. Lüscher, *Exact chiral symmetry on the lattice and the Ginsparg-Wilson relation*, Phys. Lett. B **428** (1998) 342, arXiv: hep-lat/9802011 (cit. on p. 14).

[117] K. Symanzik,
*Continuum Limit and Improved Action in Lattice Theories. 1. Principles and phi**4 Theory*, Nucl. Phys. B **226** (1983) 187 (cit. on p. 14).

[118] K. Symanzik, *Continuum Limit and Improved Action in Lattice Theories. 2. O(N) Nonlinear Sigma Model in Perturbation Theory*, Nucl. Phys. B **226** (1983) 205 (cit. on p. 14).

[119] B. Sheikholeslami and R. Wohlert,
Improved Continuum Limit Lattice Action for QCD with Wilson Fermions,
Nucl. Phys. B **259** (1985) 572 (cit. on p. 14).

[120] M. Lüscher, S. Sint, R. Sommer and P. Weisz,
Chiral symmetry and O(a) improvement in lattice QCD, Nucl. Phys. B **478** (1996) 365,
arXiv: hep-lat/9605038 (cit. on p. 14).

[121] M. Lüscher, S. Sint, R. Sommer, P. Weisz and U. Wolff,
Nonperturbative O(a) improvement of lattice QCD, Nucl. Phys. B **491** (1997) 323,
arXiv: hep-lat/9609035 (cit. on p. 14).

[122] K. Jansen and R. Sommer,
O(a) improvement of lattice QCD with two flavors of Wilson quarks,
Nucl. Phys. B **530** (1998) 185, [Erratum: Nucl.Phys.B 643, 517–518 (2002)],
arXiv: hep-lat/9803017 (cit. on p. 14).

[123] P. Weisz, *Continuum Limit Improved Lattice Action for Pure Yang-Mills Theory. 1.*,
Nucl. Phys. B **212** (1983) 1 (cit. on p. 15).

[124] P. Weisz and R. Wohlert,
Continuum Limit Improved Lattice Action for Pure Yang-Mills Theory. 2.,
Nucl. Phys. B **236** (1984) 397, [Erratum: Nucl.Phys.B 247, 544 (1984)] (cit. on p. 15).

[125] M. Lüscher and P. Weisz, *On-Shell Improved Lattice Gauge Theories*,
Commun. Math. Phys. **97** (1985) 59, [Erratum: Commun.Math.Phys. 98, 433 (1985)]
(cit. on p. 15).

[126] T. Takaishi, *Heavy quark potential and effective actions on blocked configurations*,
Phys. Rev. D **54** (1996) 1050 (cit. on p. 15).

[127] S. Duane, A. D. Kennedy, B. J. Pendleton and D. Roweth, *Hybrid Monte Carlo*,
Phys. Lett. B **195** (1987) 216 (cit. on p. 16).

[128] N. Metropolis, A. W. Rosenbluth, M. N. Rosenbluth, A. H. Teller and E. Teller,
Equation of state calculations by fast computing machines, J. Chem. Phys. **21** (1953) 1087
(cit. on p. 16).

[129] W. K. Hastings,
Monte Carlo Sampling Methods Using Markov Chains and Their Applications,
Biometrika **57** (1970) 97 (cit. on p. 16).

[130] X. Feng, K. Jansen and D. B. Renner,
The pi+ pi+ scattering length from maximally twisted mass lattice QCD,
Phys. Lett. B **684** (2010) 268, arXiv: 0909.3255 [hep-lat] (cit. on p. 17).

[131] G. Parisi, *The Strategy for Computing the Hadronic Mass Spectrum*,
Phys. Rept. **103** (1984) 203, ed. by C. Itzykson, Y. Pomeau and N. Sourlas (cit. on p. 17).

[132] G. P. Lepage, "The Analysis of Algorithms for Lattice Field Theory",
Theoretical Advanced Study Institute in Elementary Particle Physics, 1989 (cit. on p. 17).

[133] S. Güsken et al., *Nonsinglet Axial Vector Couplings of the Baryon Octet in Lattice QCD*,
Phys. Lett. B **227** (1989) 266 (cit. on p. 17).

[134] C. Alexandrou, F. Jegerlehner, S. Güsken, K. Schilling and R. Sommer, *B meson properties from lattice QCD*, Phys. Lett. B **256** (1991) 60 (cit. on p. 17).

[135] C. R. Allton et al., *Gauge invariant smearing and matrix correlators using Wilson fermions at Beta = 6.2*, Phys. Rev. D **47** (1993) 5128, arXiv: hep-lat/9303009 (cit. on p. 17).

[136] M. Albanese et al., *Glueball Masses and String Tension in Lattice QCD*, Phys. Lett. B **192** (1987) 163 (cit. on p. 17).

[137] A. Hasenfratz and F. Knechtli, *Flavor symmetry and the static potential with hypercubic blocking*, Phys. Rev. D **64** (2001) 034504, arXiv: hep-lat/0103029 (cit. on p. 17).

[138] C. Morningstar and M. J. Peardon, *Analytic smearing of SU(3) link variables in lattice QCD*, Phys. Rev. D **69** (2004) 054501, arXiv: hep-lat/0311018 (cit. on p. 17).

[139] M. Lüscher and U. Wolff, *How to Calculate the Elastic Scattering Matrix in Two-dimensional Quantum Field Theories by Numerical Simulation*, Nucl. Phys. B **339** (1990) 222 (cit. on p. 18).

[140] S. Dürr et al., *Ab-Initio Determination of Light Hadron Masses*, Science **322** (2008) 1224, arXiv: 0906.3599 [hep-lat] (cit. on p. 18).

[141] M. Lüscher, *Volume Dependence of the Energy Spectrum in Massive Quantum Field Theories. 1. Stable Particle States*, Commun. Math. Phys. **104** (1986) 177 (cit. on p. 18).

[142] M. Bruno and M. T. Hansen, *Variations on the Maiani-Testa approach and the inverse problem*, JHEP **06** (2021) 043, arXiv: 2012.11488 [hep-lat] (cit. on p. 20).

[143] K. Huang and C. N. Yang, *Quantum-mechanical many-body problem with hard-sphere interaction*, Phys. Rev. **105** (1957) 767 (cit. on pp. 20, 31, 76).

[144] T. D. Lee, K. Huang and C. N. Yang, *Eigenvalues and Eigenfunctions of a Bose System of Hard Spheres and Its Low-Temperature Properties*, Phys. Rev. **106** (1957) 1135 (cit. on pp. 20, 31, 76).

[145] H. A. Bethe, *Theory of the Effective Range in Nuclear Scattering*, Phys. Rev. **76** (1949) 38 (cit. on p. 22).

[146] M. Döring et al., *Three-body spectrum in a finite volume: the role of cubic symmetry*, Phys. Rev. D **97** (2018) 114508, arXiv: 1802.03362 [hep-lat] (cit. on pp. 22, 58, 67, 68, 76, 98, 102, 108, 120).

[147] F. Lee, A. Alexandru and R. Brett, *Higher order quantization conditions for two spinless particles*, PoS **LATTICE2021** (2022) 235, arXiv: 2110.03750 [hep-lat] (cit. on pp. 22, 24).

[148] V. Bernard, M. Lage, U.-G. Meißner and A. Rusetsky, *Resonance properties from the finite-volume energy spectrum*, JHEP **08** (2008) 024, arXiv: 0806.4495 [hep-lat] (cit. on pp. 24, 37, 98, 139).

[149] U. J. Wiese,
Identification of Resonance Parameters From the Finite Volume Energy Spectrum,
Nucl. Phys. B Proc. Suppl. **9** (1989) 609, ed. by A. S. Kronfeld and P. B. Mackenzie
(cit. on p. 25).

[150] C. Culver, M. Mai, A. Alexandru, M. Döring and F. X. Lee,
Pion scattering in the isospin $I = 2$ channel from elongated lattices,
Phys. Rev. D **100** (2019) 034509, arXiv: 1905.10202 [hep-lat] (cit. on p. 26).

[151] Z. Bai et al., *Standard Model Prediction for Direct CP Violation in $K \to \pi\pi$ Decay*,
Phys. Rev. Lett. **115** (2015) 212001, arXiv: 1505.07863 [hep-lat] (cit. on p. 30).

[152] R. Abbott et al.,
Direct CP violation and the $\Delta I = 1/2$ rule in $K \to \pi\pi$ decay from the standard model,
Phys. Rev. D **102** (2020) 054509, arXiv: 2004.09440 [hep-lat] (cit. on pp. 30, 62).

[153] T. Blum et al., *$\Delta I = 3/2$ and $\Delta I = 1/2$ channels of $K \to \pi\pi$ decay at the physical point with periodic boundary conditions*, (2023), arXiv: 2306.06781 [hep-lat] (cit. on p. 30).

[154] S. R. Beane, W. Detmold and M. J. Savage,
n-Boson Energies at Finite Volume and Three-Boson Interactions,
Phys. Rev. D **76** (2007) 074507, arXiv: 0707.1670 [hep-lat] (cit. on pp. 31, 76).

[155] W. Detmold and M. J. Savage,
*The Energy of n Identical Bosons in a Finite Volume at O(L**-7)*,
Phys. Rev. D **77** (2008) 057502, arXiv: 0801.0763 [hep-lat] (cit. on pp. 31, 76).

[156] S. R. Beane et al., *Charged multihadron systems in lattice QCD+QED*,
Phys. Rev. D **103** (2021) 054504, arXiv: 2003.12130 [hep-lat] (cit. on p. 31).

[157] F. Romero-López, A. Rusetsky, N. Schlage and C. Urbach,
Relativistic N-particle energy shift in finite volume, JHEP **02** (2021) 060,
arXiv: 2010.11715 [hep-lat] (cit. on pp. 31, 63, 76, 108).

[158] P. Guo and V. Gasparian, *A solvable three-body model in finite volume*,
Phys. Lett. B **774** (2017) 441, arXiv: 1701.00438 [hep-lat] (cit. on pp. 31, 76, 108).

[159] R. A. Briceño, M. T. Hansen and S. R. Sharpe, *Relating the finite-volume spectrum and the two-and-three-particle S matrix for relativistic systems of identical scalar particles*,
Phys. Rev. D **95** (2017) 074510, arXiv: 1701.07465 [hep-lat]
(cit. on pp. 31, 54, 72, 76, 108).

[160] R. A. Briceño, M. T. Hansen and S. R. Sharpe,
Three-particle systems with resonant subprocesses in a finite volume,
Phys. Rev. D **99** (2019) 014516, arXiv: 1810.01429 [hep-lat] (cit. on pp. 31, 54, 76, 108).

[161] M. T. Hansen, F. Romero-López and S. R. Sharpe,
Generalizing the relativistic quantization condition to include all three-pion isospin channels,
JHEP **07** (2020) 047, [Erratum: JHEP 02, 014 (2021)], arXiv: 2003.10974 [hep-lat]
(cit. on pp. 31, 63, 76, 108).

[162] T. D. Blanton and S. R. Sharpe,
Relativistic three-particle quantization condition for nondegenerate scalars,
Phys. Rev. D **103** (2021) 054503, arXiv: 2011.05520 [hep-lat] (cit. on pp. 31, 76, 108).

[163] T. D. Blanton and S. R. Sharpe,
Three-particle finite-volume formalism for $\pi^+\pi^+K^+$ and related systems,
Phys. Rev. D **104** (2021) 034509, arXiv: 2105.12094 [hep-lat]
(cit. on pp. 31, 76, 108, 113).

[164] Z. T. Draper, M. T. Hansen, F. Romero-López and S. R. Sharpe,
Three relativistic neutrons in a finite volume, JHEP **07** (2023) 226,
arXiv: 2303.10219 [hep-lat] (cit. on p. 31).

[165] M. E. Luke and A. V. Manohar,
Reparametrization invariance constraints on heavy particle effective field theories,
Phys. Lett. B **286** (1992) 348, arXiv: hep-ph/9205228 (cit. on p. 34).

[166] G. Colangelo, J. Gasser, B. Kubis and A. Rusetsky, *Cusps in K —> 3 pi decays*,
Phys. Lett. B **638** (2006) 187, arXiv: hep-ph/0604084
(cit. on pp. 37, 61, 64, 78–81, 83, 85, 121).

[167] J. Gasser, B. Kubis and A. Rusetsky, *Cusps in K –> 3pi decays: a theoretical framework*,
Nucl. Phys. B **850** (2011) 96, arXiv: 1103.4273 [hep-ph]
(cit. on pp. 37, 61, 64, 78–81, 83, 85, 121).

[168] R. Haag, *On quantum field theories*, Kong. Dan. Vid. Sel. Mat. Fys. Med. **29N12** (1955) 1
(cit. on p. 37).

[169] J. S. R. Chisholm, *Change of variables in quantum field theories*, Nucl. Phys. **26** (1961) 469
(cit. on p. 37).

[170] S. Kamefuchi, L. O'Raifeartaigh and A. Salam,
Change of variables and equivalence theorems in quantum field theories,
Nucl. Phys. **28** (1961) 529 (cit. on p. 37).

[171] A. V. Manohar, *Introduction to Effective Field Theories*,
(2018), ed. by S. Davidson, P. Gambino, M. Laine, M. Neubert and C. Salomon,
arXiv: 1804.05863 [hep-ph] (cit. on p. 37).

[172] M. Beneke and V. A. Smirnov, *Asymptotic expansion of Feynman integrals near threshold*,
Nucl. Phys. B **522** (1998) 321, arXiv: hep-ph/9711391 (cit. on pp. 37, 80).

[173] P. F. Bedaque, H. W. Hammer and U. van Kolck,
Renormalization of the three-body system with short range interactions,
Phys. Rev. Lett. **82** (1999) 463, arXiv: nucl-th/9809025 (cit. on pp. 45, 65, 76).

[174] T. D. Blanton, F. Romero-López and S. R. Sharpe,
Implementing the three-particle quantization condition including higher partial waves,
JHEP **03** (2019) 106, arXiv: 1901.07095 [hep-lat]
(cit. on pp. 50, 51, 72, 76, 77, 89, 99, 108, 113).

[175] S. M. Dawid, M. H. E. Islam and R. A. Briceño,
Analytic continuation of the relativistic three-particle scattering amplitudes,
Phys. Rev. D **108** (2023) 034016, arXiv: 2303.04394 [nucl-th] (cit. on p. 54).

[176] S. M. Dawid, M. H. E. Islam, R. A. Briceño and A. W. Jackura, *Evolution of Efimov States*,
(2023), arXiv: 2309.01732 [nucl-th] (cit. on pp. 54, 76).

[177] M. Mai, B. Hu, M. Döring, A. Pilloni and A. Szczepaniak,
Three-body Unitarity with Isobars Revisited, Eur. Phys. J. A **53** (2017) 177,
arXiv: 1706.06118 [nucl-th] (cit. on pp. 54, 77).

[178] D. Sadasivan et al.,
Pole position of the a1(1260) resonance in a three-body unitary framework,
Phys. Rev. D **105** (2022) 054020, arXiv: 2112.03355 [hep-ph] (cit. on pp. 54, 108).

[179] M. Mikhasenko et al., *Three-body scattering: Ladders and Resonances*, JHEP **08** (2019) 080,
arXiv: 1904.11894 [hep-ph] (cit. on p. 54).

[180] A. Jackura et al.,
Phenomenology of Relativistic $\mathbf{3} \to \mathbf{3}$ *Reaction Amplitudes within the Isobar Approximation*,
Eur. Phys. J. C **79** (2019) 56, arXiv: 1809.10523 [hep-ph] (cit. on p. 54).

[181] S. M. Dawid and A. P. Szczepaniak,
Bound states in the B-matrix formalism for the three-body scattering,
Phys. Rev. D **103** (2021) 014009, arXiv: 2010.08084 [nucl-th] (cit. on p. 54).

[182] L. D. Faddeev, *Scattering theory for a three particle system*,
Zh. Eksp. Teor. Fiz. **39** (1960) 1459 (cit. on p. 54).

[183] M. Ebert, H. .-.-W. Hammer and A. Rusetsky,
An alternative scheme for effective range corrections in pionless EFT,
Eur. Phys. J. A **57** (2021) 332, arXiv: 2109.11982 [hep-ph] (cit. on pp. 57, 136).

[184] R. A. Briceño and M. T. Hansen, *Multichannel* $0 \to 2$ *and* $1 \to 2$ *transition amplitudes for arbitrary spin particles in a finite volume*, Phys. Rev. D **92** (2015) 074509,
arXiv: 1502.04314 [hep-lat] (cit. on p. 62).

[185] H. B. Meyer, *Lattice QCD and the Timelike Pion Form Factor*,
Phys. Rev. Lett. **107** (2011) 072002, arXiv: 1105.1892 [hep-lat] (cit. on p. 62).

[186] S. R. Beane et al., *Multi-Pion Systems in Lattice QCD and the Three-Pion Interaction*,
Phys. Rev. Lett. **100** (2008) 082004, arXiv: 0710.1827 [hep-lat] (cit. on pp. 63, 76, 108).

[187] B. Hörz and A. Hanlon,
Two- and three-pion finite-volume spectra at maximal isospin from lattice QCD,
Phys. Rev. Lett. **123** (2019) 142002, arXiv: 1905.04277 [hep-lat]
(cit. on pp. 63, 76, 108).

[188] C. Culver, M. Mai, R. Brett, A. Alexandru and M. Döring,
Three pion spectrum in the $I = 3$ *channel from lattice QCD*, Phys. Rev. D **101** (2020) 114507,
arXiv: 1911.09047 [hep-lat] (cit. on pp. 63, 76, 108).

[189] M. T. Hansen, R. A. Briceño, R. G. Edwards, C. E. Thomas and D. J. Wilson,
Energy-Dependent $\pi^+\pi^+\pi^+$ *Scattering Amplitude from QCD*,
Phys. Rev. Lett. **126** (2021) 012001, arXiv: 2009.04931 [hep-lat]
(cit. on pp. 63, 76, 108).

[190] F. Romero-López, A. Rusetsky and C. Urbach,
Two- and three-body interactions in φ^4 *theory from lattice simulations*,
Eur. Phys. J. C **78** (2018) 846, arXiv: 1806.02367 [hep-lat] (cit. on pp. 63, 76, 108).

[191] M. T. Hansen, F. Romero-López and S. R. Sharpe,
Decay amplitudes to three hadrons from finite-volume matrix elements, JHEP **04** (2021) 113, arXiv: 2101.10246 [hep-lat] (cit. on pp. 63, 76, 108, 121, 128, 131).

[192] A. Agadjanov, V. Bernard, U.-G. Meißner and A. Rusetsky,
The $B \to K^*$ form factors on the lattice, Nucl. Phys. B **910** (2016) 387, arXiv: 1605.03386 [hep-lat] (cit. on p. 64).

[193] R. A. Briceño et al., *The resonant $\pi^+\gamma \to \pi^+\pi^0$ amplitude from Quantum Chromodynamics*, Phys. Rev. Lett. **115** (2015) 242001, arXiv: 1507.06622 [hep-ph] (cit. on p. 64).

[194] R. A. Briceño et al.,
The $\pi\pi \to \pi\gamma^\star$ amplitude and the resonant $\rho \to \pi\gamma^\star$ transition from lattice QCD, Phys. Rev. D **93** (2016) 114508, [Erratum: Phys.Rev.D 105, 079902 (2022)], arXiv: 1604.03530 [hep-ph] (cit. on p. 64).

[195] M. Bissegger, A. Fuhrer, J. Gasser, B. Kubis and A. Rusetsky,
Radiative corrections in K —> 3 pi decays, Nucl. Phys. B **806** (2009) 178, arXiv: 0807.0515 [hep-ph] (cit. on pp. 64, 78, 81).

[196] M. Bissegger, A. Fuhrer, J. Gasser, B. Kubis and A. Rusetsky, *Cusps in K(L) —> 3 pi decays*, Phys. Lett. B **659** (2008) 576, arXiv: 0710.4456 [hep-ph] (cit. on pp. 64, 78, 81).

[197] C. .-.-O. Gullstrom, A. Kupsc and A. Rusetsky,
Predictions for the cusp in eta —> 3pi0 decay, Phys. Rev. C **79** (2009) 028201, arXiv: 0812.2371 [hep-ph] (cit. on pp. 64, 78, 81).

[198] S. P. Schneider, B. Kubis and C. Ditsche, *Rescattering effects in eta –> 3pi decays*, JHEP **02** (2011) 028, arXiv: 1010.3946 [hep-ph] (cit. on p. 64).

[199] B. Kubis and S. P. Schneider, *The Cusp effect in eta-prime —> eta pi pi decays*, Eur. Phys. J. C **62** (2009) 511, arXiv: 0904.1320 [hep-ph] (cit. on p. 64).

[200] F. Romero-López, S. R. Sharpe, T. D. Blanton, R. A. Briceño and M. T. Hansen,
Numerical exploration of three relativistic particles in a finite volume including two-particle resonances and bound states, JHEP **10** (2019) 007, arXiv: 1908.02411 [hep-lat] (cit. on pp. 72, 76, 108).

[201] T. D. Blanton and S. R. Sharpe,
Alternative derivation of the relativistic three-particle quantization condition, Phys. Rev. D **102** (2020) 054520, arXiv: 2007.16188 [hep-lat] (cit. on pp. 72, 76, 86, 108).

[202] V. G. Kadyshevsky, *Quasipotential type equation for the relativistic scattering amplitude*, Nucl. Phys. B **6** (1968) 125 (cit. on pp. 75, 103).

[203] V. G. Kadyshevsky, *Relativistic equation for the S matrix in the p representation, I. Unitarity and causality conditions*, Sov. Phys. **19** (1964) 443 (cit. on p. 75).

[204] V. Efimov, *Energy levels arising form the resonant two-body forces in a three-body system*, Phys. Lett. B **33** (1970) 563 (cit. on p. 76).

[205] V. Efimov, *Low-energy Properties of Three Resonantly Interacting Particles*, Sov. J. Nucl. Phys. **29** (1979) 546 (cit. on p. 76).

[206] M. Mai and M. Döring, *Finite-Volume Spectrum of $\pi^+\pi^+$ and $\pi^+\pi^+\pi^+$ Systems*, Phys. Rev. Lett. **122** (2019) 062503, arXiv: 1807.04746 [hep-lat] (cit. on pp. 76, 108).

[207] U.-G. Meißner, G. Ríos and A. Rusetsky, *Spectrum of three-body bound states in a finite volume*, Phys. Rev. Lett. **114** (2015) 091602, [Erratum: Phys.Rev.Lett. 117, 069902 (2016)], arXiv: 1412.4969 [hep-lat] (cit. on p. 76).

[208] M. Jansen, H. .-.-W. Hammer and Y. Jia, *Finite volume corrections to the binding energy of the X(3872)*, Phys. Rev. D **92** (2015) 114031, arXiv: 1505.04099 [hep-ph] (cit. on pp. 76, 108).

[209] M. T. Hansen and S. R. Sharpe, *Perturbative results for two and three particle threshold energies in finite volume*, Phys. Rev. D **93** (2016) 014506, arXiv: 1509.07929 [hep-lat] (cit. on pp. 76, 108).

[210] M. T. Hansen and S. R. Sharpe, *Threshold expansion of the three-particle quantization condition*, Phys. Rev. D **93** (2016) 096006, [Erratum: Phys.Rev.D 96, 039901 (2017)], arXiv: 1602.00324 [hep-lat] (cit. on pp. 76, 108).

[211] P. Guo, *One spatial dimensional finite volume three-body interaction for a short-range potential*, Phys. Rev. D **95** (2017) 054508, arXiv: 1607.03184 [hep-lat] (cit. on pp. 76, 108).

[212] S. König and D. Lee, *Volume Dependence of N-Body Bound States*, Phys. Lett. B **779** (2018) 9, arXiv: 1701.00279 [hep-lat] (cit. on p. 76).

[213] S. R. Sharpe, *Testing the threshold expansion for three-particle energies at fourth order in ϕ^4 theory*, Phys. Rev. D **96** (2017) 054515, [Erratum: Phys.Rev.D 98, 099901 (2018)], arXiv: 1707.04279 [hep-lat] (cit. on pp. 76, 108).

[214] P. Guo and V. Gasparian, *Numerical approach for finite volume three-body interaction*, Phys. Rev. D **97** (2018) 014504, arXiv: 1709.08255 [hep-lat] (cit. on pp. 76, 108).

[215] Y. Meng, C. Liu, U.-G. Meißner and A. Rusetsky, *Three-particle bound states in a finite volume: unequal masses and higher partial waves*, Phys. Rev. D **98** (2018) 014508, arXiv: 1712.08464 [hep-lat] (cit. on pp. 76, 108).

[216] P. Guo, M. Döring and A. P. Szczepaniak, *Variational approach to N-body interactions in finite volume*, Phys. Rev. D **98** (2018) 094502, arXiv: 1810.01261 [hep-lat] (cit. on pp. 76, 108).

[217] P. Guo and T. Morris, *Multiple-particle interaction in (1+1)-dimensional lattice model*, Phys. Rev. D **99** (2019) 014501, arXiv: 1808.07397 [hep-lat] (cit. on pp. 76, 108).

[218] P. Klos, S. König, H. W. Hammer, J. E. Lynn and A. Schwenk, *Signatures of few-body resonances in finite volume*, Phys. Rev. C **98** (2018) 034004, arXiv: 1805.02029 [nucl-th] (cit. on pp. 76, 108).

[219] R. A. Briceño, M. T. Hansen and S. R. Sharpe, *Numerical study of the relativistic three-body quantization condition in the isotropic approximation*, Phys. Rev. D **98** (2018) 014506, arXiv: 1803.04169 [hep-lat] (cit. on pp. 76, 108).

[220] M. Mai, M. Döring, C. Culver and A. Alexandru,
Three-body unitarity versus finite-volume $\pi^+\pi^+\pi^+$ spectrum from lattice QCD,
Phys. Rev. D **101** (2020) 054510, arXiv: 1909.05749 [hep-lat] (cit. on pp. 76, 108).

[221] R. A. Briceño, M. T. Hansen, S. R. Sharpe and A. P. Szczepaniak, *Unitarity of the infinite-volume three-particle scattering amplitude arising from a finite-volume formalism*,
Phys. Rev. D **100** (2019) 054508, arXiv: 1905.11188 [hep-lat] (cit. on pp. 76, 108).

[222] J.-Y. Pang, J.-J. Wu, H. .-.-W. Hammer, U.-G. Meißner and A. Rusetsky,
Energy shift of the three-particle system in a finite volume, Phys. Rev. D **99** (2019) 074513,
arXiv: 1902.01111 [hep-lat] (cit. on pp. 76, 108).

[223] P. Guo and M. Döring, *Lattice model of heavy-light three-body system*,
Phys. Rev. D **101** (2020) 034501, arXiv: 1910.08624 [hep-lat] (cit. on pp. 76, 108).

[224] J.-Y. Pang, J.-J. Wu and L.-S. Geng, *DDK system in finite volume*,
Phys. Rev. D **102** (2020) 114515, arXiv: 2008.13014 [hep-lat] (cit. on pp. 76, 108).

[225] P. Guo, *Modeling few-body resonances in finite volume*, Phys. Rev. D **102** (2020) 054514,
arXiv: 2007.12790 [hep-lat] (cit. on pp. 76, 108).

[226] S. König, *Few-body bound states and resonances in finite volume*,
Few Body Syst. **61** (2020) 20, arXiv: 2005.01478 [hep-lat] (cit. on pp. 76, 108).

[227] T. T. Wu, *Ground State of a Bose System of Hard Spheres*, Phys. Rev. **115** (1959) 1390
(cit. on p. 76).

[228] S. Tan,
Three-boson problem at low energy and implications for dilute Bose-Einstein condensates,
Phys. Rev. A **78** (2008) 013636, arXiv: 0709.2530 [cond-mat.stat-mech] (cit. on p. 76).

[229] S. R. Beane et al., *Charged multihadron systems in lattice QCD+QED*,
Phys. Rev. D **103** (2021) 054504, arXiv: 2003.12130 [hep-lat] (cit. on p. 76).

[230] W. Detmold et al., *Multi-Pion States in Lattice QCD and the Charged-Pion Condensate*,
Phys. Rev. D **78** (2008) 014507, arXiv: 0803.2728 [hep-lat] (cit. on pp. 76, 108).

[231] W. Detmold, K. Orginos, M. J. Savage and A. Walker-Loud,
Kaon Condensation with Lattice QCD, Phys. Rev. D **78** (2008) 054514,
arXiv: 0807.1856 [hep-lat] (cit. on pp. 76, 108).

[232] T. D. Blanton et al.,
Interactions of two and three mesons including higher partial waves from lattice QCD,
JHEP **10** (2021) 023, arXiv: 2106.05590 [hep-lat] (cit. on pp. 76, 108).

[233] J.-J. Wu, T. .-.-S. H. Lee, D. B. Leinweber, A. W. Thomas and R. D. Young,
Finite-volume Hamiltonian method for $\pi\pi$ scattering in lattice QCD,
JPS Conf. Proc. **10** (2016) 062002, arXiv: 1512.02771 [hep-lat] (cit. on pp. 86, 88).

[234] Y. Li, J.-J. Wu, D. B. Leinweber and A. W. Thomas,
Hamiltonian effective field theory in elongated or moving finite volume,
Phys. Rev. D **103** (2021) 094518, arXiv: 2103.12260 [hep-lat] (cit. on pp. 86, 88).

[235] Y. Li, J. J. Wu, R. D. Young and T. S. H. Lee, *in preparation* (cit. on pp. 86, 88).

[236] P. F. Bedaque, G. Rupak, H. W. Grießhammer and H.-W. Hammer, *Low-energy expansion in the three-body system to all orders and the triton channel*, Nucl. Phys. A **714** (2003) 589, arXiv: nucl-th/0207034 (cit. on p. 89).

[237] T. D. Blanton, F. Romero-López and S. R. Sharpe, *Implementing the three-particle quantization condition for $\pi^+\pi^+K^+$ and related systems*, JHEP **02** (2022) 098, arXiv: 2111.12734 [hep-lat] (cit. on pp. 108, 113).

[238] S. Weinberg, *Evidence That the Deuteron Is Not an Elementary Particle*, Phys. Rev. **137** (1965) B672 (cit. on p. 113).

[239] L. H. Thomas, *The motion of a spinning electron*, Nature **117** (1926) 514 (cit. on p. 117).

[240] E. P. Wigner, *On Unitary Representations of the Inhomogeneous Lorentz Group*, Annals Math. **40** (1939) 149, ed. by Y. S. Kim and W. W. Zachary (cit. on p. 117).

[241] J. R. Batley et al., *Determination of the S-wave pi pi scattering lengths from a study of K+- —> pi+- pi0 pi0 decays*, Eur. Phys. J. C **64** (2009) 589, arXiv: 0912.2165 [hep-ex] (cit. on p. 122).

[242] V. K. Agrawala, J. G. Belinfante and G. H. Renninger, *On the Cutkosky-Leon normalization condition*, Nuovo Cim. A **44** (1966) 740 (cit. on p. 127).

[243] S. König, *Effective quantum theories with short- and long-range forces*, PhD thesis: U. Bonn (main), 2013 (cit. on p. 127).

[244] S. R. Beane, P. F. Bedaque, M. J. Savage and U. van Kolck, *Towards a perturbative theory of nuclear forces*, Nucl. Phys. A **700** (2002) 377, arXiv: nucl-th/0104030 (cit. on p. 135).

[245] S. R. Beane and M. J. Savage, *Variation of fundamental couplings and nuclear forces*, Nucl. Phys. A **713** (2003) 148, arXiv: hep-ph/0206113 (cit. on p. 135).

[246] S. R. Beane and M. J. Savage, *The Quark mass dependence of two nucleon systems*, Nucl. Phys. A **717** (2003) 91, arXiv: nucl-th/0208021 (cit. on p. 135).

[247] E. Epelbaum, U.-G. Meißner and W. Gloeckle, *Nuclear forces in the chiral limit*, Nucl. Phys. A **714** (2003) 535, arXiv: nucl-th/0207089 (cit. on p. 135).

[248] E. Braaten and H. W. Hammer, "An Infrared renormalization group limit cycle in QCD", *17th International IUPAP Conference on Few-Body Problems in Physics*, 2003, arXiv: nucl-th/0309030 (cit. on p. 135).

[249] E. Epelbaum, H. .-.-W. Hammer, U.-G. Meißner and A. Nogga, *More on the infrared renormalization group limit cycle in QCD*, Eur. Phys. J. C **48** (2006) 169, arXiv: hep-ph/0602225 (cit. on p. 135).

[250] G. Leibbrandt and J. Williams, *Split dimensional regularization for the Coulomb gauge*, Nucl. Phys. B **475** (1996) 469, arXiv: hep-th/9601046 (cit. on p. 139).

List of Figures

List of Tables

Acknowledgements

First of all, I would like to thank my supervisor Akaki Rusetsky. Already early during my Master studies his excellent lectures provided me insights into effective field theory and hadron physics, which finally led me to work in this intriguing area of research. I appreciate his enormous support, especially his willingness to discuss problems and work on solutions together at any time. His advice was always helpful. Moreover I could rely on his ability for proposing many new interesting projects. Being part of his research group for all these years has been an enriching experience not only professionally but also personally. I am grateful that I could work in such a pleasant atmosphere. Similarly, I thank Ulf-G. Meißner who made my PhD position possible. Moreover, I have to thank my collaborators Rishabh Bubna, Jia-Jun Wu, Jin-Yi Pang, Hans-Werner Hammer and Martin Ebert. Our weekly meeting have always been very inspiring and productive.

I am thankful to Stephen Sharpe for his great hospitality during my stay at the Institute for Nuclear Theory and for offering an inspiring environment there. I also thank Sebastian Dawid for all the interesting conversations during that time and the helpful discussion about the analytic continuation of the three-body amplitude in particular.

I want to thank Barbara Kraus, Christa Börsch and Heike Frömbgen-Penkert for the help on organisational matters, especially during the coordination of assistants at the Lattice Conference 2022. Next, I need to thank Maxim Mai. It was really pleasant to share the office with him and I was able to learn a lot about actual applications of the finite-volume formalism to LQCD data. Furthermore, I want to thank the members of the HISKP who accompanied me during my time there. Especially the discussions during the, occasionally surprisingly long, coffee breaks with Marvin Zanke, Simon Holz, Gio Chanturia, Hannah Schäfer and Jonathan Lozano de la Parra have certainly created a delightful atmosphere. Likewise, the regular social evenings organized by Christiane Gross and Daniel Severt have guaranteed a lively exchange between different research groups.

Finally, I want to thank my parents for their unconditional support. They have been encouraging my curiosity from a young age on and allowed me to study, due to their financial assistance. My deepest gratitude belongs to Amélie. You helped me in so many things that are unrelated to this project, but definitely have contributed to its success.